

**ASPECTS OF IRON METABOLISM IN THE BLOOD-BRAIN
BARRIER**

**A STUDY IN PRIMARY CULTURES OF PORCINE BLOOD-BRAIN
BARRIER ENDOTHELIAL CELLS**

W. van Gelder

Promotie-commissie.

Promotor: Prof. Dr. H.G. van Eijk
(Erasmus Universiteit Rotterdam)

Co-promotor: Dr. M.I. Cleton-Soeteman
(Erasmus Universiteit Rotterdam)

Overige leden: Prof. Dr. J.F. Koster
(Erasmus Universiteit Rotterdam)

Prof. Dr. J.J.M. Marx
(Rijks Universiteit Utrecht)

Prof. J.H.P. Wilson
(Erasmus Universiteit Rotterdam)

Het onderzoek, zoals beschreven in dit proefschrift, werd verricht bij de Vakgroep Biochemie, afdeling Chemische Pathologie van de Erasmus Universiteit te Rotterdam en het George M. Leader Family Laboratory for Alzheimer's disease research, Department of Neuroscience and Anatomy, Milton S. Hershey Medical Center, Pennsylvania State University, Hershey, PA, USA.

**ASPECTS OF IRON METABOLISM IN THE BLOOD-BRAIN
BARRIER**

A STUDY IN PRIMARY CULTURES OF PORCINE BLOOD-BRAIN
BARRIER ENDOTHELIAL CELLS

**ASPECTEN VAN HET IJZERMETABOLISME IN DE
BLOED-HERSEN BARRIERE**

EEN STUDIE IN PRIMAIRE CULTURES VAN VARKENS BLOED-HERSEN
BARRIERE ENDOTHEELCELLEN

PROEFSCHRIFT

Ter verkrijging van de graad van doctor
aan de Erasmus Universiteit Rotterdam
op gezag van de Rector Magnificus
Prof. Dr. P.W.C. Akkermans M.A.
en volgens besluit van het College van Dekanen.
De openbare verdediging zal plaatsvinden op
woensdag 1 November 1995 om 15.45 uur.

door

Warntje van Gelder
geboren te Valkenburg-Houthem.

"...and they shall beat their swords into plowshares, and their spears into pruninghooks..."

Micah: chapter 4, vs 3.

Aan Wilma, Jasper en Bart

Contents:

Page:

Abbreviations

7 - 8

Chapter 1:

Introduction.

9 - 50

Chapter 2:

Materials and methods.

51 - 79

Chapter 3:

Isolation, purification and characterization of porcine serum transferrin and hemopexin.

80 - 97

Chapter 4:

Isolation and partial characterization of a 440 kDa and a 660kDa porcine spleen ferritin fraction.

98 - 115

Chapter 5:

Quantification of different transferrin receptor pools in primary cultures of porcine blood-brain barrier endothelial cells.

116 - 133

Chapter 6:

Regulatory aspects of iron uptake in blood-brain barrier endothelial cells cultured in either iron-enriched or iron-depleted media.

134 - 150

Chapter 7:

Transcytosis of 6.6 nm gold-labeled transferrin: an ultrastructural study in blood-brain barrier endothelial cells.

151 - 171

Chapter 8:

A new approach to visualize and quantify the susceptibility to oxidative stress in cultured blood-brain barrier endothelial cells. A 2,4 dinitrophenyl hydrazine assay in iron-enriched and iron-depleted cultures.

172 - 191

Chapter 9:

Effects of aging on the regional distribution of iron, transferrin, ferritin, and oxidatively modified proteins in rat brains.

192 - 210

Chapter 10:

General discussion and conclusions.

211 - 220

Chapter 11:

Summary / samenvatting.

221 - 229

Publications.

230 - 231

Dankwoord / acknowledgements.

232 - 233

Curriculum vitae.

234

Abbreviations:

Au:	gold
Au-Tf:	gold labeled transferrin
BBB:	blood-brain barrier
BBB-EC:	blood-brain barrier endothelial cell
B _{max} :	maximal amount of ligand binding sites
BSA:	bovine serum albumin
B _{tot} :	maximal amount of ligand bound to the cell
CNS:	central nervous system
CPM:	counts per minute
CURL:	compartment of uncoupling of receptor and ligand
DFx:	desferrioxamine
DNPH:	2,4 dinitrophenyl hydrazine
EDTA:	ethylenediaminetetraacetic acid
EPMA:	electron probe microanalysis
ESI:	electron spectroscopic imaging
FCS:	fetal calf serum
Fe ⁺ :	iron suppleted
Fe ⁻ :	iron depleted
FITC:	fluorescein isothiocyanate
HBSS:	Hanks' balanced salt solution
HEPES:	N-2-hydroxyethylpiperazine-N'-2-ethanesulphonic acid
HRP:	horse radish peroxidase
HTAB:	hexadecyltrimethylammonium bromide
IEF:	isoelectric focussing
IEP:	isoelectric point
IRE:	iron responsive element
IRE-BP:	iron responsive element-binding protein
K _d :	ligand-receptor dissociation constant
kDa:	unit of molecular mass
K _{in} :	internalization rate constant
K _{out} :	externalization rate constant
LDL:	low density lipoproteins
LMW:	low molecular weight
NTA:	nitrilotriacetate
NO:	nitrous oxygen
P ₀ :	primary culture of BBB-EC's
P ₁ :	first passage culture of BBB-EC's
PAGE:	polyacrylamide gelelectrophoresis
PBS:	phosphate buffered saline
PMSF:	phenylmethanesulphonyl fluoride
PUFA:	poly unsaturated fatty acids
SDS:	sodium dodecyl sulfate
TBS:	Tris buffered saline
TEM:	transmission electron microscopy
Tf:	transferrin
TfR:	transferrin receptor

T_{in} : TfR internalization time
 T_{out} : TfR externalization time
Tris: tris(hydroxymethyl)aminomethane
v/v: volume/volume
w/v: weight/volume
w/w: weight/weight

CHAPTER 1

Introduction.

Introduction.

§ 1.0 Contents.

§ 1.1: Introduction.

§ 1.2: The role of iron in biological processes.

§ 1.3: Iron intake, absorption and distribution in the human body.

§ 1.3.1: Cellular iron uptake: mechanism and regulation.

§ 1.3.1.1: Transferrin.

§ 1.3.1.2: Ferritin.

§ 1.3.1.3: Transferrin receptor.

§ 1.3.1.4: Cellular iron uptake.

§ 1.3.1.5: Regulation of cellular iron homeostasis.

§ 1.3.1.5.1: The IRE concept.

§ 1.3.1.5.2: Modulation of transferrin targeting and transferrin-transferrin receptor interaction through carbohydrate chain variations.

§ 1.4: Blood-brain barrier: structure and function.

§ 1.5: Iron homeostasis in the brain.

§ 1.6: Iron toxicity.

§ 1.7: Aims of the thesis.

§ 1.1 Introduction.

Iron is a trace element essential to every life form (4,139), with the possible exception of a few microorganisms (e.g. *Lactobacillus plantarum*) (11). Iron is the sixth most abundant element in the universe, the fourth most abundant element in the earth's crust and as a metal only second to aluminium (176,211).

Despite its overwhelming presence in the environment, the biological availability of iron is seriously impeded by the fact that, at neutral pH, iron is nearly insoluble (solubility product $\text{Fe}(\text{OH})_3 \approx 4 \times 10^{-38}$). In order to meet their needs, micro-organisms and plants secrete for iron transport a variety of high-affinity iron binding compounds (siderophores), capable of chelating iron (139). Iron-loaded siderophores either (re-)enter the cell by means of a receptor mediated process, or release their iron to a "membrane-associated iron shuttle" (139).

Humans, on the other hand, do not possess such a highly specialized iron sequestering system and their metabolic needs can only be met by dietary intake. However, iron uptake in the digestive tract is rather inefficient, due to: (i) the low solubility of inorganic iron, (ii) the preferential mucosal uptake of iron in its ferrous state, and (iii) insufficient iron absorption from vegetable proteins. Furthermore, (iv) a major part of the world population has limited access to animal proteins (19,31,35,177). Clearly, these factors contribute to the

Chapter 1

global problem of nutritional iron deficiency. It is estimated that between 500 and 600 million people (mainly in developing countries) suffer from iron deficiency anaemia and this is probably a very conservative estimate (19,175).

Although iron is essential to life, the opposite might also be true (128). There is an ever increasing number of publications on the subject of iron and its catalytic role in the formation of oxygen free radicals (46,88,91,128). These radicals are capable of damaging DNA, proteins and lipids alike (98) and there is a growing list of diseases in which the involvement of oxygen free radicals is proven, suspected or hypothesized (see § 1.6).

§ 1.2 The role of iron in biological processes.

Iron, as an element essential to life, is ubiquitous in the mammalian physiology. In each cell a variety of iron containing proteins and enzymes can be found, especially at the inner membrane of mitochondria, where they have key-functions in the process known as oxidative phosphorylation. The iron containing proteins and enzymes can be divided in three groups (130,211):

-1- Iron-tetrapyrrole complexes (haem proteins):

these proteins characteristically consist of a protein linked to a porphyrin group. Major mammalian constituents of this group are: haemoglobin, myoglobin, cytochromes, catalase and peroxidase.

-2- Iron-sulphur proteins:

in these proteins iron is complexed to sulphur, more specifically to the sulfhydryl groups of cysteine residues. Examples of these iron-sulphur proteins are: aconitase, xanthine oxidase and ferredoxins (e.g. adrenodoxin).

-3- Iron proteins (nonhaem, nonsulphur):

a heterogeneous group of proteins, in which iron is linked neither to sulphur nor porphyrin. Examples are: transferrin, ferritin, lactoferrin, superoxide dismutase, proline hydroxylase and ribonucleotide reductase.

Albeit far from complete, this list gives an impression of the multitude of biological processes that are in one way or another dependent on iron.

§ 1.3 Iron intake, absorption and distribution in the human body.

Introduction.

As mentioned before (§ 1.1), inorganic iron is nearly insoluble under aerobic conditions at neutral pH, and can therefore not be absorbed from food products. Looking at the process of iron uptake into the mucosal cells, one has to make a distinction between haem and non-haem iron compounds. Haem iron in food, which is hardly degraded in the digestive tract, is rapidly taken up in the mucosal cell by means of a specific haem receptor (32,177,199). Non-haem iron compounds are not so readily absorbed from our daily food, as several factors affect their uptake: (i) pH of the gastric juice (necessary to solubilize non-haem iron), (ii) the iron valency (ferrous iron is more readily absorbed), (iii) the presence of enhancers (e.g. ascorbic acid, animal proteins) and (iv) inhibitors of iron absorption (e.g. phytate, polyphenols, calcium). The mechanisms by which non-haem iron enters the mucosal cell have not been clearly established. The proposed systems range from simple diffusion to uptake by high affinity iron receptors, and it is likely that more than one system is involved. Neither transcellular transport of iron, nor the mechanism by which iron enters the blood compartment at the basolateral side of the mucosal cell have been clarified yet (9).

Regulation of iron uptake occurs at the mucosal cell lining and depends on: (i) the iron content of the mucosal cell (159), (ii) the degree of iron accumulation in the iron storage sites (9,32,138,177) and (iii) the rate of erythropoiesis (32,177).

		mg iron/75 kg (male)	mg iron/kg
functional components	Haemoglobin	2300	31
	Myoglobin	320	4
	haem enzymes	80	1
	non-haem enzymes	100	1
	Transferrin	4	0.05
storage components	Ferritin	700	9
	Hemosiderin	300	4
total		3800	50

Table 1:

Average overall distribution of iron in the human (male) body.

Chapter 1

Once iron enters the circulation it will bind to transferrin, a ± 80 kDa glycoprotein (60,199), which regulates the iron flux between the locations of absorption, utilization and storage (33,95,199).

On average, the adult male human body contains 4 g iron. Nearly two third of it is incorporated in haemoglobin and myoglobin (*Table 1*) (30,198,199).

§ 1.3.1 Cellular iron uptake: mechanism and regulation.

Three proteins play a major role in the transport, cellular uptake and processing of iron: transferrin, transferrin receptor and ferritin.

§ 1.3.1.1 Transferrin.

Transferrin is a monomeric glycoprotein of circa 80 kDa capable of binding two Fe(III) ions. Transferrins from different mammalian species vary in amino acid and carbohydrate composition (reviewed in 4,210, and 212), which is reflected in (minor) variations in iron release at acidic pH and interspecies transferrin binding by transferrin receptors (75,210).

Transferrin (*Fig. 1*) consists of a single polypeptide chain with either one or two (depending on the species) N-linked complex type glycan chains (210) (see also § 3.5).

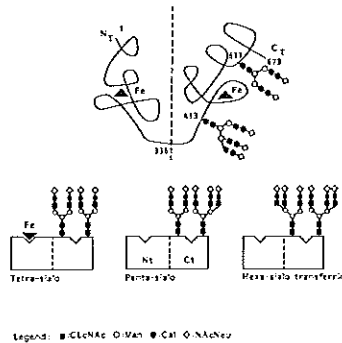


Fig. 1:

Schematic representation of the human transferrin molecule. Note the difference between C- and N-terminal regions. Three examples of variations in the C-terminal carbohydrate moieties are depicted.

The molecule can be divided in a N-terminal and C-terminal domain, each containing one iron binding site. In fact, one could better refer to these sites as "metal binding sites", for

Introduction.

transferrin specifically binds a large number of metals ranging from aluminium to platinum and even elements like plutonium and curium (213). The physiological significance of this interaction may be questioned for most metals, but possibly transferrin participates in the accumulation and therefore toxicity of certain metals, e.g. aluminium, manganese and plutonium (54,76,140,148,178,213).

The two iron binding sites of transferrin act virtually independent of each other and the affinity constants of the N- and C-terminal lobe (at pH \approx 7.4) are 1×10^{22} and 6×10^{22} respectively (60). To bind iron specifically to one of either binding sites, the concomitant binding of a synergistic anion (e.g. bicarbonate (HCO_3^-) or carbonate (CO_3^{2-})) is essential (212). This anion is needed to stabilize the metal complex at the binding site. Without it, the affinity of the binding site is lowered to such extent that either hydrolysis of iron or nonspecific binding to other parts of the protein may prevail.

The release of iron from transferrin can be induced by acidification. In this respect both binding sites behave differently, for the release of iron from the N-lobe binding site occurs more readily upon acidification, whereas the C-lobe binding site releases its iron more gradually and at a lower pH (68,69,136). Both the presence of an additional iron chelator and the reduction of Fe(III) to Fe(II) facilitate the release of iron from transferrin (71,151, 164).

Transferrin synthesis is mainly -although not exclusively- located within the hepatocytes of the liver. A number of other tissues have been shown to produce (limited) amounts of transferrin, including brain tissue, Sertoli cells, mammary gland and so on (7,29,48,60,132, 214). This extrahepatic production will hardly affect the overall concentration of transferrin in plasma, but could at a local level be of significant importance, especially when a specific compartment cannot be reached by plasma transferrin due to physiological barriers (e.g. blood-brain barrier) (214). Transferrin displays a rather complex electrophoretic behaviour, due to variations in three structural determinants: (i) genetic polymorphism, (ii) iron content and (iii) degree of branching and/or sialylation of the N-linked glycoproteins, also known as microheterogeneity of transferrin (60,61). Variations in either (i) or (ii) can affect the interaction between transferrin and its receptor. The effect of transferrin microheterogeneity in the transferrin transferrin receptor interaction is less clear. Preliminary data indicate that variations in the N-linked glycan chains could modulate transferrin-

Chapter 1

receptor interaction (61).

§ 1.3.1.2 Ferritin.

The dualism of iron, being both essential to life and toxic in its free form, could well explain the highly efficient way in which its cellular uptake, transport and storage are organized. To cope with this dualism, an iron storage system should be able to: (i) store efficiently varying quantities of iron, in a way that (ii) iron cannot exert its toxic effects, but (iii) without reducing the bio-availability of iron. The iron storage protein ferritin fulfills these requirements (95).

All prokaryotic and eukaryotic cells contain ferritin as their major iron storage protein (130). Ferritin protein is composed of 24 subunits of two types: the H-type of circa 21 kDa and the L-type of circa 19 kDa amounting to a total mass of circa 450 kDa (2,55,66,103,1-05,167). Inter- and intraspecies heterogeneity is explained by the various proportions in which the subunits assemble. Arranged with 4:3:2 symmetry (*Fig. 2*) the subunits form a hollow shell, in which up to 5000 iron atoms can be stored (55,105,167).

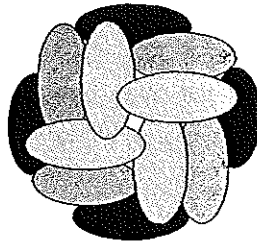


Fig. 2:

A schematic representation of a ferritin molecule. Ferritin consists of 24 subunits, forming a hollow shell in which iron can be stored. Iron may enter or leave the molecule via channels in between these subunits. Courtesy Dr. J.S. Starreveld

Due to the arrangement of the subunits, the hollow shell displays 14 channels through which iron can enter the ferritin core. The process of iron uptake in ferritin is not completely clear (56,131). Iron is almost exclusively taken up in its ferrous (Fe^{2+}) state. At the outer surface of the ferritin shell ferrous iron is oxidized to its ferric (Fe^{3+}) state by a ferroxidase centre located on the ferritin H-chains (18,95,129). Fe^{3+} then enters the shell and is stored in a complex with oxygen and phosphorus: $(\text{FeOOH})_8(\text{FeO-OPO}_3\text{H}_2)$.

Introduction.

Although ferritin can store up to 5000 iron atoms, *in vivo* it rarely contains more than 2500 iron atoms (see also chapter 4).

Iron release from ferritin is similar to iron uptake with respect to the obscurity of the process *in vivo* (56). *In vitro* experiments showed that reducing agents, free radicals and chelators can bring about the release of iron from ferritin (34,95,103,105,207) and this process can be enhanced by an increase in temperature (207) or a decrease in pH (207). Lysosomes or acidic endosomes are the most likely places for iron release from ferritin *in vivo* (95).

Since ferroxidase seems to be exclusively located on the H-chain, a difference in subunit composition could lead to functional differences between ferritins (12,56,104,131). In response to iron uptake, there appears to be a preferential synthesis of L-subunits, and it would seem that ferritin rich in L-subunits is used for long term iron storage (65,95,104,-158). H-subunit rich ferritin can take up free iron more readily than L-subunit rich ferritin. The production of H-subunit enriched ferritin is stimulated during inflammation, and this will rapidly reduce the intracellular (free) iron concentration, thus protecting the cell against oxygen free radical formation (see § 1.6) (102,171).

§ 1.3.1.3 Transferrin receptor.

Under normal (physiological) conditions most, though not all, plasma iron is bound to transferrin. A combination of a high transferrin plasma concentration (50 - 110 $\mu\text{mol/l}$) and two high affinity binding sites for iron per transferrin molecule (see § 1.3.1.1) will effectively prevent serious competition by other molecules. However, there are a number of plasma proteins capable of either binding iron (e.g. lactoferrin, ferritin) or carrying an iron containing compound (e.g. haemopexin, haptoglobin) (3). Furthermore, plasma iron can be bound by low molecular weight compounds (e.g. citrate, ascorbate), especially in those circumstances where transferrin is fully saturated with iron (iron overload). The non-transferrin plasma iron pool is discussed to some extent by Baker and Morgan (15) and a number of transferrin-independent iron transport pathways are currently under investigation (53,112,117).

The transfer of transferrin bound iron to the interior of a cell is mediated by the transferrin receptor. The transferrin receptor is a circa 180 kDa class II transmembrane glycopro-

Chapter 1

tein (192). It is a dimer, composed of two homologous subunits linked by two disulphide bridges and each subunit is capable of binding one transferrin molecule (110,150,192,215). The large C-terminal domain (*Fig. 3*) of the transferrin receptor subunit protrudes in the extracellular space, a 26 amino acid hydrophobic part spans the plasma membrane and the small N-terminal domain ends in the cytoplasm (192,215).

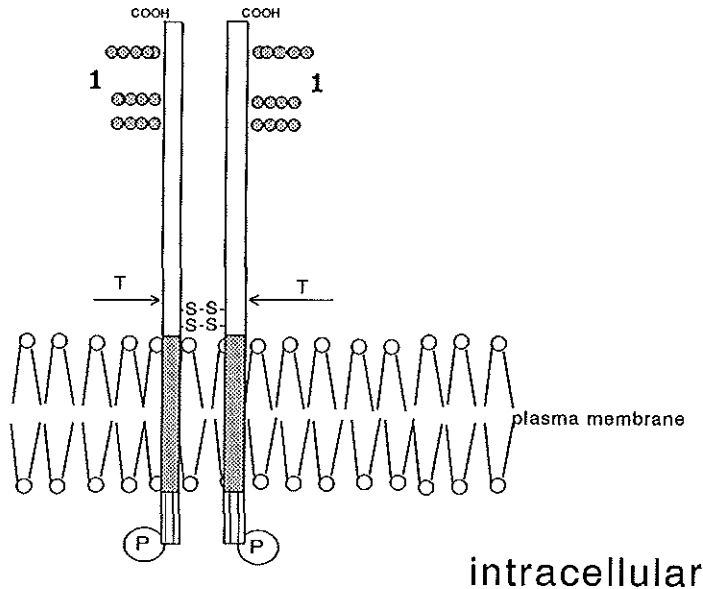


Fig. 3:

The transferrin receptor is a dimer consisting of two identical 95 kDa polypeptide structures. Each monomer can be divided in (i) large extracellular region (empty box) with a number of sugar residues (1) attached to the C-terminal end, (ii) a small and hydrophobic intermediate segment (gray box) that spans the plasma membrane, and (iii) a short cytoplasmic "tail" harbouring a phosphorylation site (P).

The distribution of transferrin receptors in the cell can be studied by: (i) ligand (i.e. transferrin) binding at low temperature, or (ii) using monoclonal antibodies (e.g. OKT9). With either technique transferrin receptors can be detected on a large number of tissues, ranging from bone marrow to endothelial cells of the blood-brain barrier (3,113,192,215). In fact, the transferrin receptor is considered to be the most important mechanism for iron uptake in the majority of mammalian cells (3,60).

Considering the transferrin receptor distribution at a cellular level, at least two and most

Introduction.

likely three different transferrin receptor pools may be discerned (see also chapter 5): (i) transferrin receptors located on the cell surface, and (ii) transferrin receptors within the cell, either (iia) actively taking part in the endocytic cycle, or (iib) apparently non-functional transferrin receptors possibly in storage pools (110,184,185,208,209).

The affinity of the transferrin receptor for transferrin depends on two interdependent parameters: pH and transferrin iron saturation. At a pH of circa 7.4, comparable to that of the extracellular space, the transferrin receptor displays a high affinity for diferric (i.e. both iron binding sites occupied) transferrin, with association constant estimates ranging from $2-7 \times 10^9$ (109,110). Under these circumstances the affinity of the transferrin receptor for apo-transferrin (i.e. devoid of iron) is nearly two orders of magnitude less (220). However, when the pH decreases to about 5.5, comparable to that of the endosomes (see § 1.3.1.4), the transferrin receptor affinity for apo-transferrin increases, whereas the affinity for diferric transferrin decreases (15,84,192,215). In this way, transferrin and transferrin receptor remain coupled during the endocytic cycle (see § 1.3.1.4).

§ 1.3.1.4 Cellular iron uptake.

As has been discussed in the previous paragraph, transferrin is the primary source of iron for mammalian cells. However, there is evidence that other iron containing proteins (e.g. ferritin) can deliver iron to the cell by means of receptor mediated or receptor independent mechanisms (17,165, reviewed in 3 and 15). Whether these mechanisms significantly contribute to the iron influx *in vivo* is still a matter of debate (15, 215).

The initial step in cellular iron uptake from transferrin, is the coupling of transferrin to its receptor. Next, either one of two mechanisms can result in the intracellular release of transferrin bound iron.

(i) In the "redox model" (194), which has been described for hepatocytes, a NADH:ferri-cyanide oxidoreductase will bring reducing equivalents near the transferrin receptor bound transferrin. Concomitantly, protons are released in that same area through Na^+/H^+ pumping. This combination will trigger the release of Fe^{2+} from transferrin. Fe^{2+} will then be bound by, and transferred to the cytosol by means of a Fe^{2+} specific membrane binder/carrier (15,194,215).

(ii) The second, and probably most important, mechanism is that of "receptor mediated

Chapter 1

endocytosis". The internalization sequence starts with the coupling of transferrin to the transferrin receptor. The short cytoplasmic tail of transferrin receptors (see § 1.3.1.3) contains an internalization sequence (84,101,195), that promotes the concentration of transferrin receptors in coated pits to nearly eight times the concentration of these receptors in non-coated plasma membranes. Coated pits are small indentations in the cell surface coated with clathrin, a protein that is both involved in (i) selection of sequestered receptor type, and (ii) formation and internalization of coated vesicles into the cytoplasm (84,186,193). Whether the internalization sequence is actually triggered by the coupling of transferrin to its receptor is still a matter of debate (5,21,122).

Once the coated vesicle has entered the cytosol, it will shed its clathrin coating and an ATP-dependent proton pump (217) will lower the pH to about 5-6.5 (3,15,60,186,192,202,-215,218). As discussed by de Jong et al (60), lowering of the pH has three important effects: (i) a conformation-transition of the transferrin receptor facilitating segregation from other receptors (CURL), (ii) a promotion of the release of iron from transferrin, and (iii) an increase in the affinity of the transferrin receptor for apo-transferrin (see § 1.3.1.1). Apo-transferrin will therefore remain complexed to the transferrin receptor and thus evade lysosomal degradation. The complex will remain intact until it has returned to, and fused with the cell membrane. There, the transferrin-transferrin receptor complex will be exposed to extracellular pH levels and thereupon release apo-transferrin into the circulation.

A complete cycle may take between 3 min (15) for reticulocytes and 90 min (162) for bovine blood-brain barrier endothelial cells (60,185). These cycle times point to a major flaw in the proposed mechanism. Even if the pH in the endosome would drop to about 5.5 (202,218) it would take hours before transferrin releases both iron atoms (see § 1.3.1.1) (56,60). A number of additional mechanisms have been proposed to promote the iron release from transferrin: (i) a change in the conformation of the transferrin receptor at a pH of 5.6 which will accelerate the iron release from transferrin (3,16), (ii) a reduction of transferrin bound iron to its ferrous state, possibly by a transmembrane ferrireductase (see above) or ascorbate (71,151) and (iii) the chelation of iron by low molecular weight chelators derived from the cytosol. If true, the latter could also add to a better understanding of what will happen to iron after release from transferrin. Unfortunately, to date there is no evidence for the existence of these chelators (15,164,194,206).

Introduction.

§ 1.3.1.5 Regulation of cellular iron homeostasis.

§ 1.3.1.5.1 The IRE concept.

The duality of iron, both being essential to life and toxic in certain conditions (see § 1.6), requires a regulatory system within each cell that will respond quickly and adequately to changes in intra- and extracellular iron concentrations.

Recently, a new and fascinating concept of iron regulation at a molecular level was discovered: the "iron responsive element" (IRE) (160, reviewed in 102,141,171). IRE's are short sequences in mRNA of the transferrin receptor, ferritin and erythroid 5-aminolevulinate synthase (eALAS). The IRE sequence consists of a short double stranded stem of variable length and capped by an unpaired loop of six nucleotides (*Fig. 4*), located either at the 5' untranslated region (UTR) of ferritin H- and L-subunit mRNA and eALAS, or the 3' UTR of transferrin receptor mRNA.

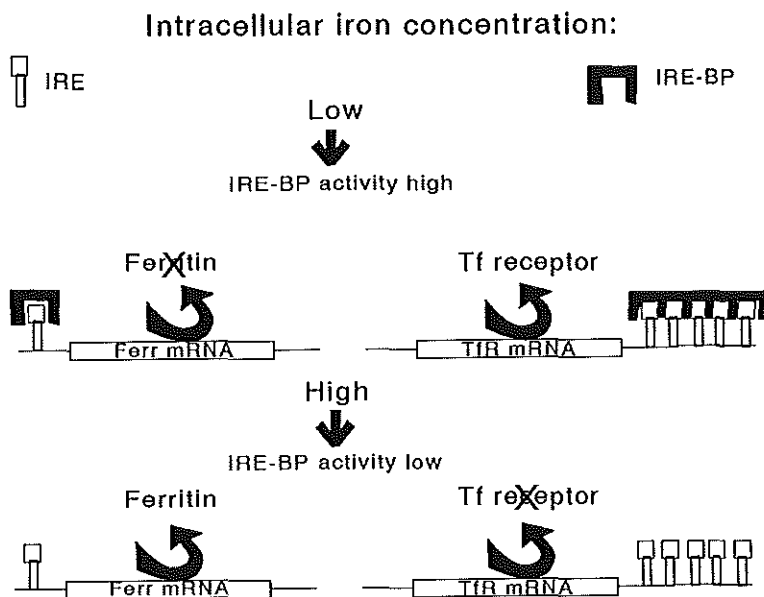


Fig. 4:

Schematic representation of the interaction between the iron responsive element (IRE) and the iron-binding protein (IRE-BP) and the effects of this interaction.

Chapter 1

This IRE-sequence is the target of an IRE-binding protein (IRE-BP), also known as iron regulatory factor (IRF) (141). The IRF is an iron sulphur protein with a deep cleft, in structure similar to aconitase (citric acid cycle). The 4Fe-4S cluster, essential for its enzymatic (aconitase) function, is located within this cleft.

When the cellular iron concentration is sufficient (or more), the iron-sulphur cluster will contain four iron atoms (4Fe-4S). The enzyme will then function as a cytoplasmic aconitase and not be able to bind an IRE. On the other hand, if the cellular iron concentration is low, the iron-sulphur cluster will lose its fourth iron. Although this is sufficient to inactivate the aconitase function of the protein, it will still be unable to bind an IRE (141,154). It is proposed (154) that nitric oxide (NO) participates in the interaction between IRF and IRE, either through assistance in the complete removal of the iron-sulphur cluster, or by inducing a conformational change in IRF, resulting in an coupling of IRE and IRF.

When IRF is activated (reduced cellular iron), it will bind to the IRE at the 5' UTR of H- and L-subunit mRNA and inhibit translation of this mRNA (157,173). At the same time, IRF will bind to the 3' UTR-IRE's of transferrin receptor mRNA and stimulate receptor synthesis, by blocking rapid degradation of this transferrin receptor mRNA (125,149). Ergo: the iron storage capacity is reduced, while the capacity for iron uptake is increased. The process is reversed when the cellular iron concentration is increased.

§ 1.3.1.5.2 Modulation of transferrin targeting and transferrin-transferrin receptor interaction through carbohydrate chain variations.

Both transferrin and transferrin receptor are glycoproteins. However, despite recent advances in the field of glycoproteins (8), the role of carbohydrate moieties in transferrin and transferrin receptor are still obscure. As discussed by de Jong et al (60), certain conditions (e.g.pregnancy) can modulate transferrin microheterogeneity and therefore possibly affect interaction with the transferrin receptor (see § 1.3.1.1). Likewise, variations in the carbohydrate moiety of the transferrin receptor could influence the interaction with its ligand (61).

Experimental data on this subject are scarce, however, it is conceivable that a systemic modulation of carbohydrates moieties on glycoproteins like transferrin and its receptor

Introduction.

could affect iron fluxes within the body (201).

§ 1.4 Blood-brain barrier: structure and function.

The survival of complex organisms depends on their ability to maintain a constant "milieu interieure". This process, known as homeostasis, should at least have the following properties: (i) a barrier that shields the interior of the organism from its (hostile) surroundings, (ii) system(s) (active/passive) to take up nutrients to maintain a proper function of the organism, (iii) excretory system(s) to loose toxic or excess amounts of metabolites, and (iv) a metabolic system that is capable of converting nutrients and metabolites (e.g. for energy supply).

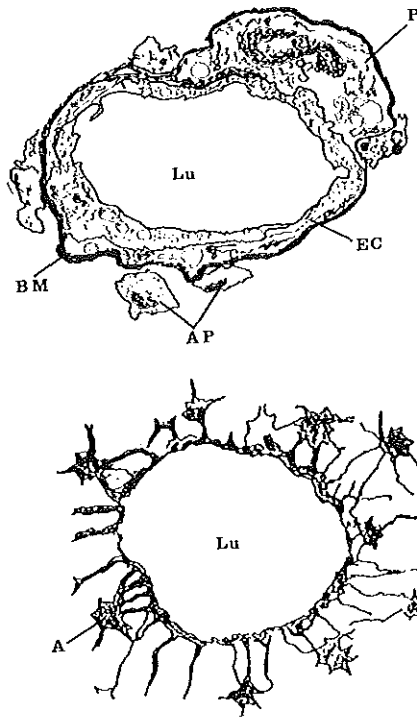


Fig. 5:

Cross-section through a brain capillary. Note the basal membrane that surrounds both endothelial cells (EC) and pericytes (P). Astrocytic endfeet (AP) of adjacent astrocytes (A) are in close contact with the basal membrane and cover most of the exterior surface of the capillary. Lu = lumen.

Chapter 1

In man, brain tissue critically depends on a proper function of homeostasis. A number of (known) plasma constituents like hormones (e.g. noradrenaline), amino acids (e.g. glycine) and ions (e.g. K^+) can affect brain function. For instance glycine, an neurotransmitter with inhibitory effects throughout the brain and spinal chord, must be kept at a much lower concentration within the brain than in plasma (36,87,168). A variation in these plasma constituents due to meals, exercise or disease could (without homeostasis) disturb normal cerebral functioning. On the other hand, the effects of locally produced neurotransmitters in the brain would be severely reduced, should these compounds be able to leak away freely into the main blood stream. It is therefore essential that brain tissue is separated, but not completely isolated, from the circulation.

Homeostasis within brain tissue is maintained by the endothelial cells lining the capillaries that penetrate the brain (*Fig. 5*). It is still a matter of debate whether only endothelial cells are responsible for the blood-brain barrier. Astrocytic endfeet are in close contact with the endothelial cells, and in vivo as well as in vitro experiments have shown that interactions between both cell types do occur (41,45,116,168). However, there is also evidence that endothelial cells not in contact with astrocytes are still capable of maintaining a barrier function (41,45). To maintain a stable "milieu interieure" within the central nervous system (CNS), brain capillaries with a surface area of circa 240 cm^2/g brain tissue (161), display all four properties as mentioned above:

(ad i) The barrier function of the blood-brain barrier endothelial cells is amongst others a result of tight junctions (zonula occludens) connecting adjacent endothelial cells (40,41,10-6,163). These organelles are missing in endothelial cells lining capillaries of most non-neural tissues. These cells are far less tightly interconnected and display fenestrations (holes or channels) that allow free passage of plasma solutes. The tight junctions between blood-brain barrier endothelial cells impose a twofold barrier: (a) passive, due to their non-selective obstruction of intercellular passage of polar compounds, (b) active, as they prohibit the lateral diffusion of plasma membrane components (e.g. transporters). This morphological phenomenon leads to a functional polarity of the endothelial cell with respect to membrane constituents (e.g. receptor proteins) (26,41,86).

(ad ii) Systems responsible for the transport of compounds into the brain via the endothelial cells of the blood-brain barrier are only partially understood. In general, at least four

Introduction.

(a-d) different mechanisms can be discriminated (161).

(a) Passive diffusion through (or between) the endothelial cells of the blood-brain barrier: this process is limited to either lipid-soluble molecules (e.g. ethanol), which readily pass the lipid bilayer of the plasma membrane, or small solutes (water, urea) capable of trafficking the plasma membrane and/or intercellular spaces barred by tight junctions (82,-197). Inorganic ions cannot readily pass a lipid bilayer, and their passage depends mainly on the presence of active transport processes (see below under (c)).

(b) Facilitated diffusion: this process consists of the passage of substrates through pores, channels or "passive uniporters". Characteristics of this system are: "downhill" transport of substrate (which does not require energy), high permeability, stereospecificity in selection (e.g. D-glucose versus L-glucose), and saturable kinetics (83,161). A major example of this type of transport across the blood-brain barrier is glucose transport. Glucose is the main energy source for brain cells and the presence of a stereospecific glucose transporter in the plasma membranes of the blood-brain barrier endothelial cells has long since been established (25,87). This transporter, identical to the glucose transporter type I (GLUT1) of human erythrocytes (127), is a circa 55 kDa glycoprotein, in vivo probably present as a dimer (83).

(c) Active transport: this type of transport features the transport of solutes against a concentration gradient (uphill) at the cost of energy. Active transporters can be subdivided in primary and secondary active transporters. The primary active transporters are mainly "ion pumps", creating an ion and/or voltage gradient across a membrane. Their activity is coupled to and dependent on an energy liberating reaction (e.g. hydrolysis of ATP). Secondary active transporters use these ion gradients as an energy source for "uphill" solute transport (83).

An example of a primary active transporter is the Na/K-ATPase transporter located in the abluminal (brainside) membrane of the BBB endothelial cell (26,87,127). Tight control of the intracerebral potassium concentration is essential for proper neurotransmission, as potassium affects the excitatory threshold of neurons.

Amino acid transport across the BBB is regulated by three different transporters: the L-, A-, and ASC-system, each displaying a high affinity for a select group of amino acids. Both the A- and ASC-system are sodium dependent secondary active transporters, located

Chapter 1

exclusively in the abluminal membrane, capable of pumping small amino acids (e.g. glycine) uphill into the endothelial cell. The L-system on the other hand, is present on both the luminal and abluminal membrane. It is a sodium independent system and mediates an active diffusive process of the larger amino acids (24,26,87,127). The distribution of the various amino acid transporters illustrates the fact that -for synthesis of neurotransmitters- the brain has to import the larger amino acids, whereas the smaller amino acids can be synthesized by the brain cells themselves.

(d) Endocytosis: a process that leads to the intracellular uptake of smaller solutes and macromolecules. Basically, the cell internalizes a piece of its own plasma membrane and associated molecules, replacing it by another piece. Endocytosis can be subdivided into three different processes: fluid phase endocytosis, adsorptive endocytosis and receptor mediated endocytosis.

Fluid phase endocytosis is mainly a membrane recycling process, replacing old and rigid plasma membrane sections by freshly synthesized plasma membranes. Concomitantly, nearby molecules, although not associated with the membrane, will be involuntary taken up (43). Membrane fragments and other compounds within these vesicles will eventually be degraded. Horse-radish peroxidase (HRP) does not bind to the plasma membrane but is readily taken up in fluid phase endocytosis. Reese and Karnovsky (40,163) used HRP to prove that the endothelial cells lining the capillaries in fact constitute the blood-brain barrier.

Adsorptive endocytosis involves the binding of positively charged molecules to oppositely charged membrane constituents, or the binding of lectins to carbohydrates associated with the cell surface.

Receptor mediated endocytosis has been discussed in some detail in § 1.3.1.4. With respect to the blood-brain barrier, specific receptors for transferrin, insulin and low density lipoprotein (LDL) have been found on the luminal side of the BBB endothelial cells (23,43,80,113). Following endocytosis, a number of alternative routes have been described for the endocytic vesicle: degradation, uncoupling of ligand (with or without receptor recycling), ligand modification, and transcytosis (43,80,187). The concept of transcytosis has aroused a lot of controversy, in part due to pitfalls in the interpretation of experimental results (42,43). However, should transcytosis exist, it would offer a possibility to transfer

Introduction.

drugs across the blood-brain barrier while circumventing the metabolic system of the endothelial cell (see below at (iv)) (43,120).

(ad iii) The excretory capacity of the blood-brain barrier is probably limited. There are a number of transporters (active and passive) located in the abluminal membrane of the BBB endothelial cell (see above) that are capable of removal of specific compounds. However, endocytic activity is reported to be virtually absent in the abluminal membrane of the BBB endothelial cell (43).

The two major pathways involved in the secretion of cerebrospinal fluid, (macro)molecules, and waste products into the circulation are in fact the arachnoid villi (and granulations), and the choroid plexus (161,183,216).

(ad iv) Metabolic barrier: The BBB endothelial cells contain several important enzymes capable of modification, inactivation, or even degradation of molecules after uptake (13,14,26,59,87,116,142). A well known example of this metabolic barrier is the presence of both monoamine oxidase and L-Dopa decarboxylase in BBB endothelial cells. These enzymes impede the cerebral uptake of L-Dopa, and high systemic concentrations of L-Dopa in combination with a L-Dopa decarboxylase inhibitor are necessary to overcome this blockade (26,87). The function of a number of enzymes in the endothelial cell are reviewed by J6o (116). Next to these enzymes, endothelial lysosomes probably contribute to the metabolic barrier (14). The active metabolic processes in the BBB endothelial cells impose an effective barrier to a number of substances (e.g. drugs), thereby -unfortunately-restricting the therapeutic accessibility of brain tissue.

Despite all the sophisticated transport mechanisms and barriers that warrant a highly selective passage of compounds across the blood-brain barrier, there are a number of ways to circumvent the blood-brain barrier: (a) fenestrated bloodvessels of the circumventricular organs (e.g. pineal body, neurohypophysis), (b) choroid plexus epithelium involved in two-way transcytosis, (c) leaky superficial cortical blood vessels and (d) retrograde axoplasmic transport through neurons (43,58,183). It is difficult to assess the contribution of these pathways to the passage of compounds into the brain, however, they should not be underestimated (43).

§ 1.5 Iron homeostasis in the brain.

Iron is an essential element in the metabolic system of the cell (see § 1.1 and 1.2), and the cells that constitute the brain tissue are no exception to that rule. Apart from its crucial role in oxidative phosphorylation, it is also a cofactor in several enzymes required in the synthesis and degradation of neurotransmitters (overview in 20). Moreover, there is some evidence that iron deficiency affects cognitive functions (19,20,219).

The presence of iron in brain tissue was already recognized by Spatz (182) in the early part of this century. Recently, more detailed studies on the distribution of (non-haem) iron in the brain appeared in literature (20,22,28,107, reviewed in 52). Basal ganglia, substantia nigra, red nucleus and subfornical organ are the regions with the highest levels of iron in the brain, but in general white matter of frontal, temporal and motor cortex have quantitatively more iron than their gray matter counterparts (50). Hallgren and Sourander (94) estimated that the level of iron (per gram tissue weight) in basal ganglia was comparable to that in liver tissue. To date, there is no explanation for the high concentrations of iron in those areas. In fact, Morris et al (144) were unable to match this distribution pattern of iron with that of known neurotransmitter systems (e.g. GABA). The high level of iron in the subfornical organ however, could be explained by the fact that the capillary endothelial cells in that area are of a fenestrated type (see § 1.4) and do not display the normal characteristics of a BBB endothelial cell.

At the cellular level, the distribution pattern of iron becomes more complex (52). In all brain regions iron is predominantly found in oligodendrocytes, which are responsible for the production of myelin (49,52,72,133,137). Interestingly, there seems to be a "patchwork" distribution of iron-positive cells in the white matter, as if some cells accumulate iron, whereas others do not (49). Results on the detection of iron in neurons and endothelial cells are inconclusive, but seem to depend on the tissue fixation procedure and sensitivity of the iron staining technique (49,52,143,144).

The distribution pattern of ferritin, the iron storage protein, coincides with that of iron and is also mainly found in oligodendrocytes. Furthermore, ferritin could be detected in microglial cells, which have a phagocytic function in brain tissue (49,119). It is also reported that, with age, astrocytes (especially around the basal ganglia) are capable of accumulating iron (52). A possible explanation for this finding could be the presumed alteration in

Introduction.

blood-brain barrier function with age or disease (6,49,70,118).

Transferrin in brain tissue is predominantly located in oligodendrocytes as well (47,48,49,-145) and in the endothelial cells of cerebral microvessels (80,113,156). Besides, some transferrin could be detected within astrocytes, and this amount increased with age (49,145). Transferrin cannot routinely be detected in neurons. Connor (49) and Morris (145) were able to detect transferrin in some neurons (e.g. in the amygdala), however, there seemed to be no consistency in this staining pattern and it was concluded that transferrin staining in neurons was either the result of problems with tissue fixation, or transferrin uptake due to neuronal cell damage or stress. Generally, the overall cellular distribution of transferrin appears to differ from that of iron and ferritin, as transferrin positive cells in the white matter do not occur in patches (49).

The question why oligodendrocytes contain so much iron has not been solved yet. Speculations point either to the active metabolic requirements of the oligodendrocyte in the fatty acid synthesis (52), or to an active iron distributing role (85), for oligodendrocytes in vitro are capable of transferrin synthesis (73).

The distribution of iron in brain tissue is a dynamic process and changes in cellular and regional iron distribution occur in: (i) neonatal development (67,132), (ii) aging (1,49,52,-172), (iii) peripheral iron accumulation (e.g. hemochromatosis) (115), (iv) iron deficiency (20,219), (v) neurological diseases e.g. Parkinson's disease and Alzheimer's disease (AD) (50,51,63,64,114,115,135,180,181). The cause for changes in the distribution of cerebral iron is not very clear in most of these circumstances.

During neonatal development there is a strong increase in cerebral iron (20,189,190), which could partially be the result of an increased metabolic need, but also to a still under-developed blood-brain barrier (168).

With age, there is a predominantly cellular shift in iron localization. Astrocytes and microglia, especially in basal ganglia, amygdala and cerebral cortex, show an increase in iron and ferritin content (49). To date, there is no explanation for this redistribution of iron (191).

In hemochromatosis, there is an increase in cerebral hemorrhages; iron depositions in those areas that have capillaries with fenestrated endothelial cells; and sometimes an increase in iron in certain brain areas (e.g. globus pallidus) (115). The high iron concentra-

Chapter 1

tion in the peripheral circulation could well explain these (abundant) iron depositions, especially in those areas that are devoid of a normal blood-brain barrier.

In Alzheimer's disease, there is a marked increase in iron levels of the hippocampus, nucleus basalis of Meynert and in and around senile plaques (typical cerebral lesions in Alzheimer's disease) (52,114). There is sparse (and far from convincing) evidence of changes in blood-brain barrier permeability in Alzheimer's disease (6,70,118), which still leaves the question whether permeability changes cause or are a result of iron accumulation.

In general, results of morphological, histochemical and biochemical assessments of iron distribution in the brain all show that there is a steady increase in iron with age, and this process appears to be exacerbated in certain pathological circumstances. Some fundamental questions, however, remain to be solved. One of the issues that has not been clarified yet, is the question of how iron crosses the blood-brain barrier, i.e. the blood-brain barrier endothelial cell.

In 1984, Jeffries (113) was the first to describe transferrin receptors on the luminal side of the blood-brain barrier endothelial cells. Naturally, this finding supported the concept of receptor mediated endocytosis of transferrin at the blood-brain barrier endothelial cell (see § 1.3.1.4 and § 1.4). Other results confirmed this model of receptor mediated endocytosis, followed by receptor-ligand uncoupling and recycling of transferrin to the luminal membrane (57,80,169,170,187). This is a well established concept of iron uptake, despite the still enigmatic nature of the transport of iron after its release from transferrin.

On the other hand, there is also some direct evidence (with $^{125}\text{I-Tf-}^{59}\text{Fe}$) to support a model of receptor mediated transcytosis (42,43,77,156,162). However, pitfalls in the interpretation of transcytotic transport do exist and are reported on by Broadwell (42). Recently, a number of reports appeared in which compounds conjugated to a transferrin receptor antibody (OX-26) were able to pass the blood-brain barrier (27,81,120,124). However, the latter should not be interpreted as a direct proof of receptor mediated transcytosis. To my knowledge, transferrin receptors have never been detected on the abluminal side of the BBB endothelial cells (113), and the OX-26 conjugate transport over this membrane could well be due to the involvement of other transport mechanisms. Furthermore, the concept of transcytosis will not explain the differences in the degree of sialylation of serum transferrin

Introduction.

as compared to cerebrospinal fluid transferrin (61).

A third possibility, as proposed by Ueda et al (196), would be a receptor independent iron transport across the BBB. The authors concluded that, although a major portion of the iron transport is receptor mediated, non-transferrin bound iron can also cross the BBB. In my opinion, this could also support the relative importance of those routes that circumvent the blood-brain barrier (see § 1.4).

The regulation of iron transport across the blood-brain barrier is another issue that remains to be solved (52). There are a few reports on the effect of peripheral iron status on iron transport across the BBB (23,115,147,190). In iron overloaded rats, high iron levels in brain tissue appear to downregulate receptor mediated endocytosis of iron across the BBB, without however, diminishing the increase in brain iron (147). Another hypothesis proposes a (temporary) increase in BBB permeability due to either iron deficiency (23), or iron overload (147).

Considering the existence of a mobile intracerebral iron pool, one would expect the transferrin receptor distribution to coincide with those regions that accumulate iron. However, results with monoclonal antibodies against the transferrin receptor (e.g. OX-26) only partially confirmed this pattern in one study (52), while another study could not show any relation with stored iron at all (108).

§ 1.6 Iron toxicity.

Although iron is vital to and present in all mammalian cells, there are multiple regulatory mechanisms in each cell to restrict the amount of "free" or, better still, low molecular weight (LMW) iron (88,205). LMW iron is iron weakly bound to intracellular compounds of low molecular weight e.g.: ATP, ADP, GTP and citrate (78,100,174,204,205). Considering the abundance of high affinity iron binding sites, it is difficult to imagine the concept of LMW iron. However, our knowledge of intracellular iron metabolism is far from complete, especially where it concerns the transition of iron from one carrier to another (e.g. transferrin to ferritin). One of the hypotheses (see § 1.3.1.4) proposes that LMW iron is involved in these transfers (15,164,200).

Iron is a transition metal, capable of participating in single electron transfer reactions, and

Chapter 1

therefore a potential (Fig. 4) catalyst in the generation of highly reactive oxygen free radicals. Due to the nature of the iron binding sites, iron in ferritin and transferrin can not directly function as a catalyst (39,100,126). On the other hand, iron in LMW iron compounds may readily catalyze the formation of OH (39,44,78,89,126,174,204).

Reactive oxygen species, e.g. hydroxyl radical and ferryl species are capable of donating a single electron to target compounds like DNA, RNA, proteins, lipids, thereby altering the structure and function of these compounds (44,46,79,91,98,99,100,153,205). Numerous ways exist to generate (or induce the generation of) oxygen free radical species; a few of those pathways are depicted in Fig. 6.

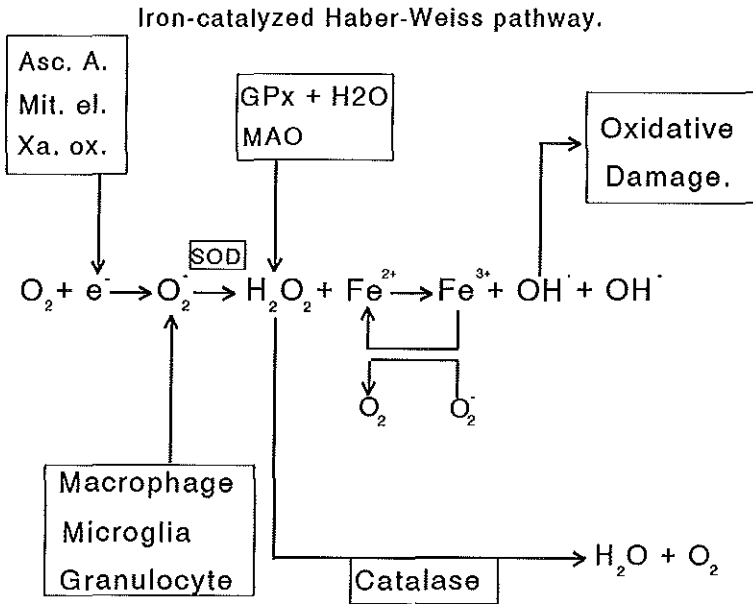


Fig. 6:

This diagram depicts a few of the enzymes and cell types that could be involved in the synthesis of reactive oxygen species (e.g. OH). Asc.A.= ascorbic acid; Mit.el.= electron "leakage" from mitochondrial electron carriers; Xa.ox.= xanthine oxidase; GPx = glutathione peroxidase; MAO = monoamine oxidase; SOD = superoxide dismutase.

Considering the presence of iron in brain tissue, there are at least two reasons to take the catalytic role of iron into further consideration. (i) As mentioned in § 1.5, certain regions

Introduction.

in the brain contain high amounts of iron and, even more important, the distribution of iron in the brain changes under certain conditions (e.g. aging). Iron uptake and redistribution imply transition of iron and therefore (possibly) an increase in LMW iron (200). (ii) Brain tissue is highly susceptible to oxydative damage, because of a high rate of oxidative metabolic activity, and low levels of antioxidant enzymes (e.g. catalase). Moreover, brain tissue contains high concentrations of readily oxidizable unsaturated fatty acids (PUFA's) e.g. in plasma membranes (74,92,93,96,97). These plasma membranes are essential for proper neuronal functioning and interneuronal communication. Moreover, neuronal cells are not capable of replication.

There is a growing list of publications that link the process of oxidative damage to central nervous system damage in aging (10,79,179,203), Alzheimer's disease (74,134,155,166,-188), Parkinson's disease (62,152), trauma and stroke (37,38), and on a cellular level in oligodendrocytes (90,121).

Research in this field is, however, hampered by the inaccessibility of the brain compartment and the evidence presented is therefore mainly indirect. Nevertheless, a better understanding of brain iron metabolism in conjunction with extended research on oxidative damage in neurological disorders could increase our understanding of the pathogenesis of certain diseases, in casu Alzheimer's disease and Parkinson's disease (74).

§ 1.7 Aims of the thesis.

The intriguing duality of iron, being both essential for cellular metabolism and noxious in certain conditions, can be clearly discerned in the central nervous system. A decrease in cerebral iron concentration will affect cognitive functions, whereas certain neurological diseases are accompanied by an increase in intracerebral iron concentration. These extreme conditions imply that the distribution of iron in brain tissue is subject to changes, and suggest that iron may continuously enter or leave the brain. Mechanism and regulation of iron transport into the brain are, however, largely unknown.

To further investigate the transport of iron into the brain, the following issues were addressed:

- (i) Development of techniques to isolate blood-brain barrier microvascular endothelial

Chapter 1

cells, and to grow these cells on various supports.

- (ii) Isolation and purification of the iron transport and storage proteins transferrin and ferritin.
- (iii) Quantification of transferrin receptor distribution in the BBB-EC's.
- (iv) Quantification of transferrin receptor kinetics, iron uptake and release in the BBB-EC's
- (v) Ultrastructural morphology of the BBB-EC's.
- (vi) Visualization of transferrin uptake and its cellular pathway.
- (vii) Investigation on the possible adverse effects of iron on the BBB-EC's exposed to oxidative stress.

Introduction.

References:

- (1) Adrian G.S., Herbert D.C., Robinson L.K., Walter C.A., Buchanan J.M., Adrian E.K., Weaker F.J., Eddy C.A., Yang F. and Bowman B.H. (1992) Expression of a human chimeric transferrin gene in senescent transgenic mice reflects the decrease of transferrin levels in aging humans. *Biochim. Biophys. Acta* 1132: 168-176.
- (2) Aisen Ph. (1980) Iron transport and storage proteins. *Annual Review of Biochemistry*, 49, 357-393.
- (3) Aisen P. (1992) Entry of iron into cells: a new role for the transferrin receptor in modulating iron release from transferrin. *Ann. Neurol.* 32: S62-68.
- (4) Aisen P. (1994) Iron metabolism: an evolutionary perspective. In: *Iron metabolism in health and disease* (eds: Brock J.H., Halliday J.W., Pippard M.J. and Powell L.W.), pp 1-30. Saunders company Ltd, London, Uk.
- (5) Ajioka R.S. and Kaplan J. (1986) Intracellular pools of transferrin receptors result from constitutive internalization of unoccupied receptors. *Proc. Natl. Acad. Sci. USA* 83: 6445-6449.
- (6) Alafuzoff L, Adolfsson R., Grundke-Iqbal I. and Winblad B. (1987) Blood-brain barrier in Alzheimer dementia and in non-demented elderly. *Acta Neuropathol.* 73: 160-166.
- (7) Aldred A.R., Dickson P.W., Marley P.D. and Schreiber G. (1987) Distribution of transferrin synthesis in brain and other tissues in the rat. *J. Biol. Chem.* 262: 5293-5297.
- (8) Allen H.J. and Kisailus E.C. (Eds.) (1992) *Glycoconjugates. Composition, structure, and function.* Marcel Dekker, Inc, New York, USA.
- (9) Alvarez-Hernandez X., Smith M. and Glass J. (1994) Regulation of iron uptake and transport by transferrin in Caco-2 cells, an intestinal cell line. *Biochim. Biophys. Acta* 1192: 215-222.
- (10) Ames B. (1989) Endogenous DNA damage as related to cancer and aging. *Mut. Res.* 214: 41-46.
- (11) Archibald F.S. and Fridovich I. (1981) Manganese, superoxide dismutase, and oxygen tolerance in some lactic acid bacteria. *J. Bacteriol.* 146: 928-936.
- (12) Arosio P., Levi S., Santambrogio P., Cozzi A., Luzzago A., Cesareni G. and Albertini A. (1991) Structural and functional studies of human ferritin H and L chains. *Curr. Stud. Hematol. Blood Transfus.* 58: 127-131.
- (13) Audus K.L. and Borchardt R.T. (1986) Characterization of an in vitro blood-brain barrier model system for studying drug transport and metabolism. *Pharmac. Res.* 3: 81-87.

Chapter 1

- (14) Audus K.L. Raub T. (1993) Lysosomes of brain and other vascular endothelia. In: *The blood-brain barrier.* (ed: Partridge W.M.), pp 201-227.
- (15) Baker E. and Morgan E.H. (1994) Iron transport. In: *Iron metabolism in health and disease* (eds: Brock J.H., Halliday J.W., Pippard M.J. and Powell L.W.), pp 63-95. Saunders company Ltd, London, UK.
- (16) Baker E.N. and Lindley P.F. (1992) New perspectives on the structure and function of transferrins. *J. Inorg. Biochem.* 47: 147-160.
- (17) Bakoy O.E. and Thorstensen K. (1994) The process of cellular uptake of iron from transferrin. A computer simulation program. *Eur. J. Biochem.* 222: 105-112.
- (18) Bauminger E.R., Harrison P.M., Hechel D., Hodson N.W., Nowik I., Treffry A. and Yewdall S.J. (1993) Iron (II) oxidation and early intermediates of iron-core formation in recombinant human H-chain ferritin. *Biochem. J.* 296: 709-719.
- (19) Baynes R.D. (1994) Iron deficiency. In: *Iron metabolism in health and disease* (eds: Brock J.H., Halliday J.W., Pippard M.J. and Powell L.W.), pp 189-225. Saunders company Ltd, London, UK.
- (20) Beard J.L., Connor J.R. and Jones B.C. (1993) Iron in the brain. *Nutr. Rev.* 51: 157-170.
- (21) Beauchamp J.R. and Woodman P.G. (1994) Regulation of transferrin receptor recycling by protein phosphorylation. *Biochem. J.* 303: 647-655.
- (22) Benkovic S.A. and Connor J.R. (1993) Ferritin, transferrin, and iron in selected regions of the adult and aged rat brain. *J. Comp. Neurol.* 337: 1-17.
- (23) Ben-Shachar D., Yehuda S., Finberg J.P.M., Spanier I. and Youdim M.B.H. (1988) Selective alteration in blood-brain barrier and insulin transport in iron-deficient rats. *J. Neurochem.* 50: 1434-1437.
- (24) Betz A.L. and Goldstein G.W. (1978) Polarity of the blood-brain barrier: neutral amino acid transport into isolated brain capillaries. *Science* 202: 225-227.
- (25) Betz A.L., Csejtey J. and Goldstein G.W. (1979) Hexose transport and phosphorylation by capillaries isolated from rat brain. *Am. J. Physiol* 236: 96-102.
- (26) Betz A.L., Firth J.A. and Goldstein G.W. (1980) Polarity of the blood-brain barrier: distribution of enzymes between the luminal and antiluminal membranes of brain capillary endothelial cells. *Brain Res.* 192: 17-28.
- (27) Bickel U., Yoshikawa T., Landaw E.M., Faull K.F. and Partridge W.M. (1993) Pharmacological effects in vivo in brain by vector-mediated peptide drug delivery. *Proc.*

Introduction.

Natl. Acad. Sci. USA 90: 2618-2622.

(28) Blijenberg B.G. (1973) Thesis: Enkele aspecten van de ijzerstofwisseling met betrekking tot de hersenen.

(29) Bloch B., Popovici T., Chouham S., Levin M.J., Tuil D. and Kahn A. (1987) Transferrin gene expression in choroid plexus of the adult rat brain. *Brain Res. Bull.* 18: 573-576.

(30) Bothwell T.H., Charlton R.W., Cook J.D. and Finch C.A. (1979) Introduction. In: *Iron metabolism in man* (Au: Bothwell T.H., Charlton R.W., Cook J.D. and Finch C.A.), pp 1-4. Blackwell Scientific Publications, Oxford, Uk.

(31) Bothwell T.H., Charlton R.W., Cook J.D. and Finch C.A. (1979) Iron nutrition. In: *Iron metabolism in man* (Au: Bothwell T.H., Charlton R.W., Cook J.D. and Finch C.A.), pp 7-43. Blackwell Scientific Publications, Oxford, Uk.

(32) Bothwell T.H., Charlton R.W., Cook J.D. and Finch C.A. (1979) Iron absorption. In: *Iron metabolism in man* (Au: Bothwell T.H., Charlton R.W., Cook J.D. and Finch C.A.), pp 256-283. Blackwell Scientific Publications, Oxford, Uk.

(33) Bothwell T.H., Charlton R.W., Cook J.D. and Finch C.A. (1979) Plasma iron. In: *Iron metabolism in man* (Au: Bothwell T.H., Charlton R.W., Cook J.D. and Finch C.A.), pp 284-310. Blackwell Scientific Publications, Oxford, Uk.

(34) Bothwell T.H., Charlton R.W., Cook J.D. and Finch C.A. (1979) Storage iron. In: *Iron metabolism in man* (Au: Bothwell T.H., Charlton R.W., Cook J.D. and Finch C.A.), pp 311-326. Blackwell Scientific Publications, Oxford, Uk.

(35) Bothwell T.H. and Charlton R.W. (1982) Nutritional aspects of iron deficiency. In: *The biochemistry and physiology of iron* (eds: Saltman P. and Hegener J.), pp 749-766. Elsevier Science Publishing Co., Inc., New York, USA.

(36) Bradbury M. (1979) Why a blood-brain barrier? *TINS* 3: 36-38.

(37) Braughler J.M. and Hall E.D. (1989) Central nervous system trauma and stroke. I Biochemical considerations for oxygen radical formation and lipid peroxidation. *Free Rad. Biol. Med.* 6: 289-301.

(38) Braughler J.M. and Hall E.D. (1989) Central nervous system trauma and stroke. II Physiological and pharmacological evidence for involvement of oxygen radicals and lipid peroxidation. *Free Rad. Biol. Med.* 6: 303-313.

(39) Brieland J.K., Clarke S.J., Karmioli S., Phan S.H. and Fantone J.C. (1992) Transferrin: a potential source of iron for oxygen free radical-mediated endothelial cell injury. *Arch. Biochem. Biophys.* 294: 265-270.

Chapter 1

- (40) Brightman M.W. and Reese T.S. (1969) Junctions between intimately apposed cell membranes in the vertebrate brain. *J. Cell Biol.* 40: 648-677.
- (41) Brightman M.W. and Tao-Cheng J.H. (1993) Tight junctions of brain endothelium and epithelium. In: *The blood-brain barrier.* (ed: Pardridge W.M.), pp 107-125.
- (42) Broadwell R.D. (1989) Transcytosis of macromolecules through the blood-brain barrier: a cell biological perspective and critical appraisal. *Acta Neuropathol.* 79: 117-128.
- (43) Broadwell R.D. Banks W.A. (1993) Cell biological perspective for the transcytosis of peptides and proteins through the mammalian blood-brain fluid barrier. In: *The blood-brain barrier.* (ed: Pardridge W.M.), pp 165-199.
- (44) Cadenas E. (1989) Biochemistry of oxygen toxicity. *Ann. Rev. Biochem.* 58: 79-110.
- (45) Cancilla P.A., Bready J. and Berliner J. (1993) Brain endothelial-astrocyte interactions. In: *The blood-brain barrier.* (ed: Pardridge W.M.), pp 25-46.
- (46) Cheeseman K.H. and Slater T.F. (1993) An introduction to free radical biochemistry. In: *Free radicals in medicine* (eds: Cheeseman K.H. and Slater T.F.), pp 481-493. Churchill Livingstone, London, UK.
- (47) Connor J.R. and Fine R.E. (1986) The distribution of transferrin immunoreactivity in the rat central nervous system. *Brain Res.* 368: 319-328.
- (48) Connor J.R. and Fine R.E. (1987) Development of transferrin-positive oligodendrocytes in the rat central nervous system. *J. Neurosci. Res.* 17: 51-59.
- (49) Connor J.R., Menzies S.L., St. Martin S.M. and Mufson E.J. (1990) Cellular distribution of transferrin, ferritin, and iron in normal and aged human brains. *J. Neurosci. Res.* 27: 595-611.
- (50) Connor J.R. (1992) Proteins of iron regulation in the brain in Alzheimer's disease. In: *Iron and human disease.* (ed: Lauffer R.B.), pp. 365-393. CRC Press Inc., Florida, USA.
- (51) Connor J.R., Menzies S.L., St. Martin S.M. and Mufson E.J. (1992) A histochemical study of iron, transferrin, and ferritin in Alzheimer's diseased brains. *J. Neurosci. Res.* 31: 75-83.
- (52) Connor J.R. (1993) Cellular and regional maintenance of iron homeostasis in the brain: normal and diseased states. In: *Iron in central nervous system disorders.* (eds: Riederer P. and Youdim M.B.H.), pp 1-18. Springer-Verlag, New York, USA.
- (53) Conrad M.E., Umbreit J.N., Moore E.G., Uzel C. Berry M.R. (1994) Alternate iron transport pathway. Mobilferrin and integrin in K562 cells. *J. Biol. Chem.* 269: 7169-7173.

Introduction.

- (54) Corrigan F.M., Crichton J.S., van Rijn A.G., Skinner E.R. and Ward N.I. (1992) Transferrin, cholesterol and aluminium in Alzheimer's disease. *Clin. Chim. Acta* 211: 121-123.
- (55) Crichton R.R. (1983) Primary structure of horse and human apoferritins. *Structure and Function of Iron Storage and Transport Proteins*. (ed. by Urushizaki I., Aisen P., Listowski J. & Drysdale J.W.), pp. 3-10. Elsevier Science, Amsterdam.
- (56) Crichton R.R. and Ward R.J. (1992) Structure and molecular biology of iron binding proteins and the regulation of "free" iron pools. In: *Iron and human disease* (ed: Lauffer R.B.), pp 23-75. CRC Press, Inc., Florida, USA.
- (57) Crowe A. and Morgan E.H. (1992) Iron and transferrin uptake by brain and cerebrospinal fluid in the rat. *Brain Res.* 592: 8-16.
- (58) Cserr H.F. (1971) Physiology of the choroid plexus. *Physiol. Rev.* 51: 273-311.
- (59) Dehouck M.P., Jolliet-Riant P., Brée F., Fruchart J.C., Cecchelli R. and Tillement J.P. (1992) Drug transfer across the blood-brain barrier: correlation between in vitro and in vivo models. *J. Neurochem.* 58: 1790-1797.
- (60) de Jong G., van Dijk J.P. and van Eijk H.G. (1990) The biology of transferrins. *Clin. Chim. Acta* 190: 1-46.
- (61) de Jong G. (1993) Thesis: The physiological significance of transferrin microheterogeneity. An interpretation of the role of N-linked glycans in transferrin and iron metabolism.
- (62) Dexter D.T., Carter C.J., Wells F.R., Javoy-Agid F., Agid Y., Lees A., Jenner P. and Marsden C.D. (1989) Basal lipid peroxidation in substantia nigra is increased in Parkinson's disease. *J. Neurochem.* 52: 381-389.
- (63) Dexter D.T., Carayon A., Vidailhet M., Ruberg M., Agid F., Agid Y., Lees A.J., Wells F.R., Jenner P. and Marsden C.D. (1990) Decreased ferritin levels in brain in parkinson's disease. *J. Neurochem.* 55: 16-20.
- (64) Dexter D.T., Jenner P., Schapira A.H.V. and Marsden C.D. (1992) Alterations in levels of iron, ferritin, and other trace metals in neurodegenerative diseases affecting the basal ganglia. *Ann. Neurol.* 32: S94-100.
- (65) Dickey L.F., Sreedharan S., Theil E.C., Didsbury J.R., Wang Y.H. and Kaufman R.E. (1987) Differences in the regulation of messenger RNA for housekeeping and specialized-cell ferritin. *J. Biol. Chem.* 262: 7901-7909.
- (66) Drysdale JW (1977) Ferritin phenotypes: structure and metabolism. *Ciba Foundation Symposium* 71. *Iron Metabolism*. pp 41-57.

Chapter 1

- (67) Dwork A.J., Lawler G., Zybert P.A., Durkin M., Osman M., Willson N. and Barkai A.I. (1990) An autoradiographic study of the uptake and distribution of iron by the brain of the young rat. *Brain Res.* 518: 31-39.
- (68) Egan T.J., Ross D.C. and Langley R.P. (1994) Iron and the transferrins: mechanisms of iron binding and release. *South Afr. J. Sci.* 90: 539-543.
- (69) El Hage Chahine J.M. and Fain D. (1994) The mechanism of iron release from transferrin. Slow-proton-transfer-induced loss of nitrilotriacetatoiron(III) complex in acidic media. *Eur. J. Biochem.* 223: 581-587.
- (70) Elovaara I., Icen A., Palo J. and Erkinjuntti T. (1985) CSF in Alzheimer's disease. Studies on blood-brain barrier function and intrathecal protein synthesis. *J. Neurol. Sci.* 70: 73-80.
- (71) Escobar A., Gaete V. and Nunez M.T. (1992) Effect of ascorbate in the reduction of transferrin-associated iron in endocytic vesicles. *J. Bioenerg. Biomembr.* 24: 227-233.
- (72) Espinosa de los Monteros A. and de Vellis J. (1988) Myelin basic protein and transferrin characterize different subpopulations of oligodendrocytes in rat primary glial cultures. *J. Neurosci. Res.* 21: 181-187.
- (73) Espinosa de los Monteros A., Kumar S., Scully S, Cole R. and de Vellis J. (1990) Transferrin gene expression and secretion by rat brain cells in vitro. *J. neurosci. Res.* 18: 299-304.
- (74) Evans P.H. (1993) Free radicals in brain metabolism and pathology. *Brit. Med. Bull.* 49: 577-587.
- (75) Evans R.W., Crawley J.B., Garrat R.C., Grossmann J.G., Neu M., Aitken A., Patel K.J., Meilak A., Wong C., Singh J., Bomford A. and Hasnain S.S. (1994) Characterization and structural analysis of a functional human serum transferrin variant and implications for receptor recognition. *Biochem.* 33: 12512-12520.
- (76) Farrar G., Altmann P., Welch S.G. Wychrij O., Ghose B., Lejeune J., Corbett J., Prasher V. and Blair J.A. (1990) Defective gallium-transferrin binding in Alzheimer disease and Down syndrome: possible mechanism for accumulation of aluminium in brain. *Lancet* 335: 747-750.
- (77) Fishman J.B., Rubin J.B., Handrahan J.V., Connor J.R. and Fine R.E. (1987) Receptor-mediated transcytosis of transferrin across the blood-brain barrier. *J. Neurosci. Res.* 18: 299-304.
- (78) Floyd R.A. and Lewis C.A. (1983) Hydroxyl free radical formation from hydrogen peroxide by ferrous iron-nucleotide complexes. *Biochem.* 22: 2645-2649.

Introduction.

- (79) Floyd R.A. and Carney J.M. (1992) Free radical damage to protein and DNA: mechanisms involved and relevant observations on brain undergoing oxidative stress. *Ann. Neurol.* 32: S22-27.
- (80) Friden P.M. (1993) Receptor-mediated transport of peptides and proteins across the blood-brain barrier. In: *The blood-brain barrier.* (ed: Pardridge W.M.), pp 229-247.
- (81) Friden P.M., Walus L.R., Watson P., Doctrow S.R., Kozarich J.W., Backman C., Bergman H., Hoffer B., Bloom F. and Granholm A.C. (1993) Blood-brain barrier penetration and in vivo activity of an NGF conjugate. *Science* 259: 373-377.
- (82) Gennis R.B. (1989) Interactions of small molecules with membranes: partitioning, permeability, and electrical effects. In: *Biomembranes. Molecular structure and function* (Au:Gennis R.B.), pp 235-269.
- (83) Gennis R.B. (1989) Pores, channels and transporters. In: *Biomembranes. Molecular structure and function* (Au:Gennis R.B.), pp 270-322.
- (84) Gennis R.B. (1989) The cell surface: receptors, membrane recycling and signal transduction. In: *Biomembranes. Molecular structure and function* (Au:Gennis R.B.), pp 323-369.
- (85) Gerber M.R. and Connor J.R. (1989) Do oligodendrocytes mediate iron regulation in the human brain? *Neurol.* 26: 95-98.
- (86) Goldstein G.W. (1979) Relation of potassium transport to oxidative metabolism in isolated brain capillaries. *J. Physiol.* 286: 185-195.
- (87) Goldstein G.W. and Betz A.L. (1986) The blood-brain barrier. *Sci. Am.* 255: 74-83.
- (88) Götz M.E., Dirr A., Gsell W., Burger R., Freyberger A. and Riederer P. (1993) Some reflections on iron dependent free radical damage in the central nervous system. In: *Iron in central nervous system disorders.* (eds: Riederer P. and Youdim M.B.H.), pp 45-54. Springer-Verlag, Wien, Austria.
- (89) Graf E., Mahoney J.R., Bryant R.G. and Eaton J.W. (1984) Iron-catalyzed hydroxyl radical formation. Stringent requirement for free iron coordination site. *J. Biol. Chem.* 259: 3620-3624.
- (90) Griot C., Vandeveld M., Richard A., Peterhans E. and Stocker R. (1990) Selective degeneration of oligodendrocytes mediated by reactive oxygen species. *Free Rad. Res. Comms.* 11: 181-193.
- (91) Gutteridge J.M.C. and Halliwell B. (1989) Iron toxicity and oxygen radicals. In: *Ballière's Clinical Hematology*, vol 2: pp 195-256.

Chapter 1

- (92) Gutteridge J.M.C. (1992) Iron and oxygen radicals in brain. *Ann. Neurol.* 32: S16-21.
- (93) Gutteridge J.M.C. (1992) Hydroxyl radicals, iron, oxidative stress, and neurodegeneration. *Ann. N.Y. Acad. Sci.* 738: 201-213.
- (94) Hallgren B. and Sourander P. (1958) The effect of age on the non-haemin iron in the human brain. *J. Neurochem.* 3: 41-51.
- (95) Halliday J.W., Ramm G.A. and Powell L.W. (1994) Cellular iron processing and storage: the role of ferritin. In: *Iron metabolism in health and disease* (eds: Brock J.H., Halliday J.W., Pippard M.J. and Powell L.W.), pp 97-121. Saunders company Ltd, London, Uk.
- (96) Halliwell B. (1989) Oxidants and the central nervous system: some fundamental questions. *Acta Neurol. Scand.* 126: 23-33.
- (97) Halliwell B. (1992) Oxygen radicals as key mediators in neuronal disease: fact or fiction? *Ann. Neurol.* 32: S10-15.
- (98) Halliwell B., Gutteridge J.M.C. and Cross C.E. (1992) Free radicals, antioxidants, and human disease: where are we now? *J. Lab. Clin. Med.* 119:598-620.
- (99) Halliwell B. and Gutteridge J.M.C. (1992) Biologically relevant metal ion-dependent hydroxyl radical generation. An update. *FEBS Lett.* 307: 108-112.
- (100) Halliwell B. (1993) Iron and damage to biomolecules. In: *Iron and human disease* (ed: Lauffer R.B.), pp 209-236. CRC Press, Inc., Florida, USA.
- (101) Hansen S.H., Sandvig K. and van Deurs B. (1992) Internalization efficiency of the transferrin receptor. *Exp. Cell Res.* 199: 19-28.
- (102) Harford J.B., Rouault T.A. and Klausner R.D. (1994) The control of cellular iron homeostasis. In: *Iron metabolism in health and disease* (eds: Brock J.H., Halliday J.W., Pippard M.J. and Powell L.W.), pp 123-149. Saunders company Ltd, London, Uk.
- (103) Harrison P.M., Hoare R.J., Hoy T.G. & Macara I.G. (1974) Ferritin and haemosiderin: structure and function. *Iron in biochemistry and medicine.* (ed. by Jacobs A. & Worwood M.), pp. 73-114. Academic Press, London.
- (104) Harrison P.M., Clegg G.A. and May K. (1980) Ferritin structure and function. In : *Iron in biochemistry and medicine* (eds: Jacobs A. and Worwood M.), pp 131-171. Academic Press, London, Uk.
- (105) Harrison P.M. and Lilley T.H. (1989) Ferritin. In: *Iron carriers and iron proteins* (ed: Loehr T.M.), pp 125-238. VCH Publishers, Inc, New York, USA.

Introduction.

- (106) Heimark R.L. (1993) Cell-cell adhesion molecules of the blood-brain barrier. In: The blood-brain barrier. (ed: Pardridge W.M.), pp 87-106.
- (107) Hill J.M. and Switzer R.C. (1984) The regional distribution and cellular localization of iron in the rat brain. *Neurosci.* 11: 595-603.
- (108) Hill J.M., Ruff M.R., Weber R.J. and Pert C.B. (1985) Transferrin receptors in rat brain: neuropeptide-like pattern and relationship to iron distribution. *Proc. Natl. Acad. Sci. USA* 82: 4553-4557.
- (109) Huebers H.A., Csiba E., Huebers E. and Finch C.A. (1983) Competitive advantage of diferric transferrin in delivering iron to reticulocytes. *Proc. Natl. Acad. Sci. USA* 80: 300-304.
- (110) Huebers H.A. and Finch C.A. (1987) Transferrin receptors. *Physiol. Rev.* 67: 532-542.
- (111) Hunt C.R., Riegler R. and Davis A.A. (1989) Changes in glycosylation after the affinity of the human transferrin receptor for its ligand. *J. Biol. Chem.* 264: 9643-9648.
- (112) Inman R.S., Coughlan M.M. and Wessling-Resnick M. (1994) Extracellular ferrireductase activity of K562 cells is coupled to transferrin-independent iron transport. *Biochem.* 33: 11850-11857.
- (113) Jeffries W.A., Brandon M.R., Hunt S.V., Williams A.F., Gatter K.C. and Mason D.Y. (1984) Transferrin receptor on endothelium of brain capillaries. *Nature* 312: 162-163.
- (114) Jellinger K., Paulus W., Grundke-Iqbal I., Riederer P. and Youdim M.B.H. (1990) Brain iron and ferritin in Parkinson's and Alzheimer's diseases. *J. Neural. Transm. [P-D Sect]* 2: 327-340.
- (115) Jellinger K. and Kienzl E. (1993) Iron deposits in brain disorders. In: *Iron in central nervous system disorders.* (eds: Riederer P. and Youdim M.B.H.), pp 19-36. Springer-Verlag, New York, USA.
- (116) Joó F. (1992) The cerebral microvessels in culture, an update. *J. Neurochem.* 58: 1-17.
- (117) Jordan I. and Kaplan J. (1994) The mammalian transferrin-independent iron transport system may involve a surface ferrireductase activity. *Biochem J.* 302: 875-879.
- (118) Kalaria R.N., Sromek S.M., Grahovac I. and Harik S.I. (1992) Transferrin receptors of rat and human brain and cerebral microvessels and their status in Alzheimer's disease. *Brain Res.* 585: 87-93.
- (119) Kaneko Y., Kitamoto T., Tateishi J. and Yamaguchi K. (1989) Ferritin immunohisto-

Chapter 1

chemistry as a marker for microglia. *Acta Neuropathol.* 79: 129-136.

(120) Kang Y.S., Bickel U. and Pardridge W.M. (1994) Pharmacokinetics and saturable blood-brain barrier transport of biotin bound to a conjugate of avidin and a monoclonal antibody to the transferrin receptor. *Drug Metab. Disp.* 22: 99-105.

(121) Kim Y.S. and Kim S.U. (1991) Oligodendroglial cell death induced by oxygen radicals and its protection by catalase. *J. Neurosci. Res.* 29: 100-106.

(122) Klausner R.D., Harford J and van Renswoude J. (1984) Rapid internalization of the transferrin receptor in K562 cells is triggered by ligand binding or treatment with phorbol ester. *Proc. Natl. Acad. Sci. USA* 81: 3005-3009.

(123) Koeppen A.H. and Dentinger M.P. (1988) Brain hemosiderin and superficial siderosis of the central nervous system. *J. Neuropathol. Exp. Neurol.* 47: 249-270.

(124) Kordower J.H., Charles V., Bayer R., Bartus R.T., Putney S., Walus L.R. and Friden P.M. (1994) Intravenous administration of a transferrin receptor antibody-nerve growth factor conjugate prevents the degeneration of cholinergic striatal neurons in a model of Huntington disease. *Proc. Natl. Acad. Sci. USA* 91: 9077-9080.

(125) Kühn L.C. and Hentze M.W. (1992) Coordination of cellular iron metabolism by post-transcriptional gene regulation. *J. inorg. Biochem.* 47: 183-195.

(126) Lamb D.J. and Leake D.S. (1994) Iron released from transferrin at acidic pH can catalyze the oxidation of low density lipoprotein. *FEBS Lett.* 352: 15-18.

(127) Lattera J. and Goldstein G.W. (1993) Brain microvessels and microvascular cells in vitro. In: *The blood-brain barrier.* (ed: Pardridge W.M.), pp 1-24.

(128) Lauffer R.B. (1992) Iron, aging and human disease: historical background and new hypotheses. In: *Iron and human disease* (ed: Lauffer R.B.), pp 1-20. CRC Press, Inc., Florida, USA.

(129) Lawson D.M., Treffry A., Arymiuk P.J., Harrison P.M., Yewdale S.J., Luzzago A., Cesarani G., Levi S. and Arioso P. (1989) Identification of the ferroxidase centre in ferritin. *FEBS Lett.* 254: 207-210.

(130) Leigh J.G., Moore G.R. and Wilson M.T. (1993) Biological iron. In: *Chemistry of iron* (ed: Silver J.), pp 181-243. Blackie Academic & Professional, London, UK.

(131) Levi S., Yewdall S.J., Harrison P.M., Santambrogio P., Cozzi A., Rovida E., Albertini A. and Arioso P. (1992) Evidence that H- and L-chains have cooperative roles in the iron-uptake mechanism of human ferritin. *Biochem. J.* 288: 591-596.

(132) Levin M.J., Tuil D., Uzan G., Dreyfus J.C. and Kahn A. (1984) Expression of the

Introduction.

transferrin gene during development of non-hepatic tissues: high level of transferrin mRNA in fetal muscle and adult brain. *Biochem. Biophys. Res. Comm.* 122: 212-217.

(133) LeVine S.M. and Macklin W.B. (1990) Iron-enriched oligodendrocytes: a reexamination of their spatial distribution. *J. Neurosci. Res.* 26: 508-512.

(134) Lohr J.B. (1991) Oxygen radicals and neuropsychiatric illness. *Arch. Gen. Psychiatry* 48: 1097-1106.

(135) Maes M., Meltzer H.Y., Buckley P. and Bosmans E. (1995) Plasma-soluble interleukin-2 and transferrin receptor in schizophrenia and major depression. *Eur. Arch. Psychiatry Clin. Neurosci.* 244: 325-329.

(136) Marques H.M., Walton T. and Egan T.J. (1995) Release of iron from C-terminal monoferric transferrin to phosphate and pyrophosphate at pH 5.5 proceeds through two pathways. *J. Inorg. Biochem.* 57: 11-21.

(137) Martín S.M., Landel H.B., Lansing A.J. and Vijayan V.K. (1991) Immunocytochemical double labeling of glial fibrillary acidic protein and transferrin permits the identification of astrocytes and oligodendrocytes in the rat brain. *J. Neuropathol. Exp. Neurol.* 50: 161-170.

(138) Marx J.J.M. (1982) Ferrokinetic regulation of iron absorption in man. In: *The biochemistry and physiology of iron* (eds: Saltman P. and Hegenauer J.), pp 245-247. Elsevier Science Publishing Co., Inc., New York, USA.

(139) Matzanke B.F., Müller-Matzanke G. and Raymond K.N. (1989) Siderophore-mediated iron transport. In: *Iron carriers and iron proteins* (ed: Loehr T.M.), pp 1-121. VCH Publishers, Inc, New York, USA.

(140) McGregor S.J., Brown D. and Brock J.H. (1991) Transferrin-gallium binding in Alzheimer's disease. *Lancet* 338: 1394-1395.

(141) Melefors Ö. and Hentze M.W. (1993) Iron regulatory factor - the conductor of cellular iron regulation. *Blood Rev.* 7:251-258.

(142) Méresse S., Dehouck M.P., Delorme P., Bensaïd M., Tauber J.P., Delbart C., Fruchart J.C. and Cecchelli R. (1989) Bovine brain endothelial cells express tight junctions and monoamine oxidase activity in long-term culture. *J. Neurochem.* 53: 1363-1371.

(143) Moos T. and Mollgard K. (1993) A sensitive post-DAB enhancement technique for demonstration of iron in the central nervous system. *Histochem.* 99: 471-475.

(144) Morris C.M., Candy J.M., Oakley A.E., Bloxham C.A. and Edwardson J.A. (1992) Histochemical distribution of non-haem iron in the human brain. *Acta Anat.* 144: 235-257.

Chapter 1

- (145) Morris C.M., Candy J.M., Bloxham C.A. and Edwardson J.A. (1992) Immunocytochemical localisation of transferrin in the human brain. *Acta Anat.* 143: 14-18.
- (146) Morris C.M., Candy J.M., Bloxham C.A. and Edwardson J.A. (1992) Distribution of transferrin receptors in relation to cytochrome oxidase activity in the human spinal chord, lower brainstem and cerebellum. *J. Neurol. Sci.* 111: 158-172.
- (147) Morris C.M., Keith A.B., Edwardson J.A. and Pullen R.G.L. (1992) Brain iron uptake and brain iron levels in chronic iron overload. *Neurosci. Res. Comm.* 10: 45-51.
- (148) Morris C.M., Candy J.M., Kerwin J.M. and Edwardson J.A. (1994) Transferrin receptors in the normal human hippocampus and in Alzheimer's disease. *Neuropath. Appl. Neurobiol.* 20: 473-477.
- (149) Müllner E.W., Neupert B. and Kühn L.C. (1989) A specific mRNA binding factor regulates the iron-dependent stability of cytoplasmic transferrin receptor mRNA. *Cell* 58: 373-382.
- (150) Newman R., Schneider C., Sutherland R., Vodinelich L. and Greaves M. (1982) The transferrin receptor. *TIBS*
- (151) Nunez M.T., Pinto I. and Glass J. (1989) Assay and characteristics of the iron binding moiety of reticulocyte endocytic vesicles. *J. Membr. Biol.* 107: 129-135.
- (152) Olanow C.W. (1990) Oxidation reactions in Parkinson's disease. *Neurology* 40: 32-37.
- (153) Pacifici R.E. and Davies K.J.A. (1991) Protein, lipid and DNA repair systems in oxidative stress: the free radical theory of aging revisited. *Gerontology* 37: 166-180.
- (154) Pantopoulos K., Weiss G. and Hentze M.W. (1994) Nitric oxide and the posttranscriptional control of cellular iron traffic. *Trends Cell Biol.* 4:82-86.
- (155) Pappolla M.A., Omar R.A., Kim K.S. and Robakis N.K. (1992) Immunohistochemical evidence of antioxidant stress in Alzheimer's disease. *Am. J. Pathol.* 140: 621-628.
- (156) Pardridge W.M., Eisenberg J. and Yang J. (1987) Human blood-brain barrier transferrin receptor. *Metabolism* 9: 892-895.
- (157) Patino M.M. and Walden W.E. (1992) Cloning of a functional cDNA for the rabbit ferritin mRNA repressor protein. *J. Biol. Chem.* 267: 19011-19016.
- (158) Pietrangelo A., Rocchi E., Ferrari A., Ventura E. and Cairo G. (1991) Regulation of hepatic transferrin, transferrin receptor and ferritin genes in human siderosis. *Hepatology* 14: 1083-1089.

Introduction.

- (159) Pietrangelo A., Rocchi E., Ferrari A., Perini M., Ventura E. and Cairo G. (1992) Regulation of transferrin, transferrin receptor and ferritin genes in human duodenum. *Gastroenterology* 102: 802-809.
- (160) Rao K., Harford J.B., Rouault T., McClelland A., Ruddle F.H. and Klausner R.D. (1986) Transcriptional regulation by iron of the gene for the transferrin receptor. *Molec. Cell. Biol.* 6: 236-240.
- (161) Rapoport S.I. (1976) *Blood-brain barrier in physiology and medicine.* Raven Press, New York, USA.
- (162) Raub T.J. and Newton C.R. (1991) Recycling kinetics and transcytosis of transferrin in primary cultures of bovine brain microvessel endothelial cells. *J. Cell. Physiol.* 149: 141-151.
- (163) Reese T.S. and Karnovsky M.J. (1967) Fine structural localization of a blood-brain barrier to exogenous peroxidase. *J. Cell Biol.* 34: 207-217.
- (164) Richardson D.R. and Baker E. (1992) Intermediate steps in cellular iron uptake from transferrin. Detection of a cytoplasmic pool of iron, free of transferrin. *J. Biol. Chem.* 267: 21384-21389.
- (165) Richardson D.R. and Baker E. (1994) Two saturable mechanisms of iron uptake from transferrin in human melanoma cells: the effect of transferrin concentration, chelators, and metabolic probes on transferrin and iron uptake. *J. Cell Physiol.* 161: 160-168.
- (166) Richardson J.S., Subbarao K.V. and Ang L.C. (1992) On the possible role of iron-induced free radical peroxidation in neuronal degeneration in Alzheimer's disease. *Ann. N.Y. Acad. Sci* 648: 326-327.
- (167) Ringeling P.L. (1991) Thesis: Rat liver ferritin biochemical and microanalytical aspects.
- (168) Risau W. and Wolburg H. (1990) Development of the blood-brain barrier. *TINS* 13: 174-178.
- (169) Roberts R., Sandra A., Siek G.C., Lucas J.J. and Fine R.E. (1992) Studies of the mechanism of iron transport across the blood-brain barrier. *Ann. Neurol.* 32: S43-50.
- (170) Roberts R.L., Fine R.E. and Sandra A. (1993) Receptor-mediated endocytosis of transferrin at the blood-brain barrier. *J. Cell Sci.* 104: 521-532.
- (171) Rogers J.T. (1992) Genetic regulation of the iron transport and storage genes: links with the acute phase response. In: *Iron and human disease* (ed: Lauffer R.B.), pp 77-104. CRC Press, Inc., Florida, USA.

Chapter 1

- (172) Roskams A.J.I. and Connor J.R. (1994) Iron, transferrin, and ferritin in the rat brain during development and aging. *J. Neurochem.* 63: 709-716.
- (173) Rouault T.A., Hentze M.W., Gaughman W., Harford J.B. and Klausner R.D. (1988) Binding of a cytosolic protein to the iron-responsive element of human ferritin messenger RNA. *Science* 241: 1207-1210.
- (174) Rush J.D., Maskos Z. and Koppenol W.H. (1990) Reactions of iron(II) nucleotide complexes with hydrogen peroxide. *FEBS Lett.* 261: 121-123.
- (175) Scrimshaw N.S. (1991) Iron deficiency. *Scient. American* october, 24-30.
- (176) Silver J. (1993) Introduction to iron chemistry. In: *Chemistry of iron* (ed: Silver J.), pp 1-29. Blackie Academic & Professional, London, Uk.
- (177) Skikne B. and Baynes R.D. (1994) Iron absorption. In: *Iron metabolism in health and disease* (eds: Brock J.H., Halliday J.W., Pippard M.J. and Powell L.W.), pp 152-187. Saunders company Ltd, London, Uk.
- (178) Sloot W.N., van der Sluijs-Gelling A.J. and Gramsbergen J.B.P. (1994) Selective lesions by manganese and extensive damage by iron after injection into rat striatum or hippocampus. *J. Neurochem.* 62: 205-216.
- (179) Smith C.D., Carney J.M., Tatsumo T., Stadtman E.R., Floyd R.A. and Markesbery W.R. (1992) Protein oxidation in aging brain. *Ann. N.Y. Acad. Sci.* 663: 110-119.
- (180) Sofic E., Riederer P., Heinsen H., Beckmann H., Reynolds G.P., Hebenstreit G. and Youdim M.B.H. (1988) Increased iron (III) and total iron content in post mortem substantia nigra of parkinsonian brain. *J. Neural. Transm.* 74: 199-205.
- (181) Sofic E., Jellinger K., Riederer P. and Youdim M.B.H. (1991) Selective increase of iron in substantia nigra zona compacta of parkinsonian brains. *J. Neurochem.* 56: 978-982.
- (182) Spatz H. (1922) Über denn Eisennachweis im Gehirn, besonders in Zentren des extrapyramidalen-motorischen Systems. *Z. Ges. Neurol. Psychiatr.* 77: 261-290.
- (183) Spector R. and Johanson C.E. (1989) The mammalian choroid plexus. *Sci. Am. Nov:* 48-53.
- (184) Starreveld J.S., van Dijk H.P., Kroos M.J. and van Eijk H.G. (1993) Regulation of transferrin receptor expression and distribution in in vitro cultured human cytotrophoblasts. *Clin. Chim. Acta* 220: 47-60.
- (185) Starreveld J.S. (1994) Thesis: Iron metabolism in cultured cytotrophoblasts. A model of the maternal-fetal interphase.

Introduction.

- (186) Stoorvogel W., Strous G.J., Ciechanover A. and Schwartz A.L. (1991) Trafficking of the transferrin receptor. In: Liver diseases. Targeted diagnosis and therapy using specific receptors and ligands (eds: Wu G.Y. and Wu C.H.), pp 267-304.
- (187) Strahan M.E., Crowe A. and Morgan E.H. (1992) Iron uptake in relation to transferrin degradation in brain and other tissues of rats. *Am. J. Physiol.* 263: R924-R929.
- (188) Subbarao K.V., Richardson J.S. and Ang L.C. (1990) Autopsy samples of Alzheimer's cortex show increased peroxidation in vitro. *J. Neurochem.* 55: 342-345.
- (189) Taylor E.M. and Morgan E.H. (1990) Developmental changes in transferrin and iron uptake by the brain in the rat. *Dev. Brain Res.* 55: 35-42.
- (190) Taylor E.M., Crowe A. and Morgan E.H. (1991) Transferrin and iron uptake by the brain: effects of altered iron status. *J. Neurochem.* 57: 1584-1592.
- (191) Taylor E.M. and Morgan E.H. (1991) Role of transferrin in iron uptake by the brain: a comparative study. *J. Comp. Physiol.* 161: 521-524.
- (192) Testa U., Pelosi E. and Peschle C. (1993) The transferrin receptor. *Crit. Rev. Oncogen.* 4: 241-276.
- (193) Thatte H.S., Bridges K.R. and Golan D.E. (1994) Microtubule inhibitors differentially affect translational movement, cell surface expression, and endocytosis of transferrin receptors in K562 cells. *J. Cell. Physiol.* 160: 345-357.
- (194) Thorstensen K. and Romslo I. (1990) The role of transferrin in the mechanism of cellular iron uptake. *Biochem. J.* 271: 1-10.
- (195) Trowbridge I.S. and Collawn J.F. (1992) Structural requirements for high efficiency endocytosis of the human transferrin receptor. *J. Inorg. Biochem.* 47: 209-217.
- (196) Ueda F., Raja K.B., Simpson R.J., Trowbridge I.S. and Bradbury M.W.B. (1993) Rate of ⁵⁹Fe uptake into brain and cerebrospinal fluid and the influence thereon of antibodies against the transferrin receptor. *J. Neurochem* 60: 106-113.
- (197) van Bree J.B.M.M., de Boer A.G., Danhof M., Ginsel L.A. and Breimer D.D. (1988) Characterization of an "in vitro" blood-brain barrier: effects of molecular size and lipophilicity on cerebrovascular endothelial transport rates of drugs. *J. Pharmacol. Exp. Ther.* 247: 1233-1239.
- (198) van Dijk J.P. and van Eijk H.G. (1995) Ontwikkelingen in het onderzoek van het ijzermetabolisme. *Ned. Tijdschr. Klin. Chem.* 20: 9-13.
- (199) van Eijk H.G. and van der Heul C. (1993) IJzerstofwisseling. *Tijdschr. NVKC* 18: 3-17.

Chapter 1

- (200) van Gelder W., Siersema P.D., Voogd A., de Jeu-Jaspars N.C.M., Koster J.F., de Rooij F.W.M. and Wilson J.H.P. (1993) The effect of desferrioxamine on iron metabolism and lipid peroxidation in hepatocytes of C57/BL10 mice in experimental uroporphyrin. *Biochem. Pharmacol.* 46: 221-228.
- (201) van Kamp G.J., Mulder K., Kuiper M. and Wolters E.Ch. (1995) Changed transferrin sialylation in Parkinson's disease. *Clin. Chim. Acta* 235: 159-167.
- (202) van Renswoude J., Bridges K.R., Harford J.B. and Klausner R.D. (1982) Receptor mediated endocytosis of transferrin and uptake of iron in K562 cells. Identification of a non-lysosomal compartment. *Proc Natl. Acad. Sci. USA* 79: 6186-6190.
- (203) Viani P., Cervato G., Fiorilli A. and Cestaro B. (1991) Age-related differences in synaptosomal peroxidative damage and membrane properties. *J. Neurochem.* 56: 253-258.
- (204) Voogd A., Sluiter W., van Eijk H.G. and Koster J.F. (1992) Low molecular weight iron and the oxygen paradox in isolated rat hearts. *J. Clin. Invest.* 90: 2050-2055.
- (205) Voogd A. (1993) Thesis: Iron and the oxygen paradox in ischaemic hearts.
- (206) Vyoral D., Hradilek A. and Neuwirt J. (1992) Transferrin and iron distribution in subcellular fractions of K562 cells in the early stages of transferrin endocytosis. *Biochim. Biophys. Acta* 137: 148-154.
- (207) Wagstaff M. and Jacobs A. (1982) Iron release from human ferritins. In: *The biochemistry and physiology of iron* (eds: Saltman P. and Hegenauer J.), pp 463-471. Elsevier Science Publishing Co., Inc., New York, USA.
- (208) Ward D.M. and Kaplan J. (1986) Mitogenic agents induce redistribution of transferrin from internal pools to the cell surface *Biochem J.* 238: 721-728.
- (209) Weigel P.H. (1992) Mechanisms and control of glycoconjugate turnover. In: *Glycoconjugates. Composition, structure, and function.* (Eds: Allen H.J. and Kisailus E.C.), pp 421-497. Marcel Dekker, Inc, New York, USA.
- (210) Welch S.G. (1990) A comparison of the structure and properties of serum transferrin from 17 animal species. *Comp. Biochem. Physiol.* 97B: 417-427.
- (211) Welch S. (1992) The chemistry and biology of iron. In: *Transferrin: the iron carrier* (Au: Welch S.), pp 2-23. CRC Press Inc, Florida, USA.
- (212) Welch S.G. (1992) Transferrin structure and iron binding. In: *Transferrin: the iron carrier* (Au: Welch S.), pp 61-108. CRC Press Inc, Florida, USA.
- (213) Welch S.G. (1992) Transferrin binding of elements other than iron. In: *Transferrin: the iron carrier* (Au: Welch S.), pp 109-127. CRC Press Inc, Florida, USA.

Introduction.

- (214) Welch S. (1992) The transferrin gene. In: *Transferrin: the iron carrier* (Au: Welch S.), pp 129-158. CRC Press Inc, Florida, USA.
- (215) Welch S. (1992) The transferrin receptor and the cellular uptake of iron. In: *Transferrin: the iron carrier* (Au: Welch S.), pp 159-185. CRC Press Inc, Florida, USA.
- (216) Wolfson L.I., Katman R. and Escriva A. (1974) Clearance of amine metabolites from the cerebrospinal fluid: the brain as a "sink". *Neurol* 24: 772-779.
- (217) Yamashiro D.J., Flus S.R. and Maxfield F.R. (1983) Acidification of endocytic vesicles by an ATP-dependent proton pump. *J. Cell. Biol.* 97: 929-934.
- (218) Yamashiro D.J., Tycko B., Fluss S.R. and Maxfield F.R. (1984) Segregation of transferrin to a mildly acidic (pH 6.5) para-golgi compartment in the recycling pathway. *Cell* 37: 789-800.
- (219) Youdim M.B.H. and Ben-Shachar D. (1987) Minimal brain damage induced by early iron deficiency: modified dopaminergic neurotransmission. *Isr. J. Med. Sci.* 23: 19-25.
- (220) Young S.P., Bomford A. and Williams R. (1984) The effect of iron saturation of transferrin on its binding and uptake by rabbit reticulocytes. *Biochem. J.* 219: 505-510.

CHAPTER 2

Materials and methods.

Materials and methods.

§ 2.0 Contents.

§ 2.1: Introduction.

§ 2.2: Procedures for the isolation, culturing and treatment of porcine blood-brain barrier microvascular endothelial cells.

§ 2.3: Morphological techniques.

§ 2.4: Semiquantitative immunochemical procedures.

§ 2.5: Analytical and quantitative techniques.

§ 2.6: Protein isolation and purification procedures.

§ 2.7: Statistical analyses and curve fittings.

§ 2.8: Transferrin receptor quantitation and kinetics.

§ 2.9: Rat brain dissection.

§ 2.10 Fixation, embedding and transmission electron microscopy.

§ 2.1 Introduction.

This chapter gives an overview of all experimental procedures that, in one way or another, contributed to the results described in this thesis.

A list of specific chemicals and techniques is included in each chapter.

§ 2.2 Procedures for the isolation and culturing of porcine blood-brain barrier microvascular endothelial cells.

§ 2.2.1 Blood-brain barrier microvessel endothelial cell isolation and culturing.

Microvascular endothelial cells were isolated from fresh porcine brain using a method adapted from Mischeck (16) and Méresse (15). Within 20 min after bleeding the animal, brain tissue was rinsed with HBSS (4 °C) and homogenized after careful removal of cerebellum, meninges and choroid plexus. The homogenate was resuspended in 50 ml per brain culture medium (M 199, containing 20 mM HEPES, 4mM L-Glutamine, 2.5 mg/L Fungizone and 50 mg/L Gentamycin). Dispase (4 g/L) was added and the homogenate was gently shaken for 3 hrs at 37°C. Following filtration through a nylon mesh (150 µm), the filtrate was centrifuged (1800 g, 12 min). Supernatant and top layer of the pellet (consisting of white matter) were removed. The bottom layer of the pellet (reddish in color) was resuspended in culture medium with 20 % (v/v) Fetal Calf Serum. This procedure was repeated 3 times and cells were plated on gelatine coated (0.2% gelatine (w/v) in PBS) petri dishes. After 30 min culture medium was replaced, removing most non-attached cells. The next day, cells were washed briefly with PBS and incubated with culture medium with

Chapter 2

10 % (v/v) Fetal Calf Serum). Culture medium was changed every other day.

§ 2.2.2 *Blood-brain barrier microvessel endothelial cell culturing in iron-enriched and iron-depleted media.*

Following isolation, all cells were cultured according to the standard procedure for 3 days (see § 2.2.1). Subsequently, cells designated to be "iron loaded", were incubated with culture medium containing 300 μM diferric transferrin (= Fe^+ medium). Fe^+ medium was changed every other day and experiments were performed when cultures were nearly confluent.

Cells designated to be "iron deficient" were treated according to the standard procedure until two days before the actual experiment. At that time, Deferoxamine (50 $\mu\text{g}/\text{ml}$) was added to the culture medium (= Fe^- medium) and this was repeated on the day before the experiment.

§ 2.2.3 *Culturing of blood-brain barrier endothelial cells on semiporous membranes.*

A detailed description of the BBB-EC isolation procedure can be found in § 2.2.1. Briefly, brain tissue was homogenized after careful removal of cerebellum, meninges and choroid plexus. The homogenate was resuspended in culture medium containing Dispase and gently shaken for 3 hours. Following filtration and centrifugation (4x), cells were resuspended in culture medium containing Penicilline (100 U/ml) and Streptomycine (100 $\mu\text{g}/\text{ml}$) (instead of Gentamycine) and 20% fetal calf serum.

Cells designated to be "primary cultures" (P_0) were plated on membranes, and left to stand for 1 h before culture medium was replaced. After 24 h culture medium was renewed and this was repeated every 48 h. From day 3 on, culture medium contained only 10% fetal calf serum.

"First passage cells" (P_1) were seeded in gelatin coated plastic culture flasks, grown to confluency (see § 2.2.1) and then harvested with a mixture of 0.25% (w/v) trypsin and 0.01% (w/v) EDTA in PBS. Following resuspension in culture medium and centrifugation, cells were plated on membranes according to the procedure described above.

Before plating, membranes were preconditioned for 2 h at 37 °C with culture medium containing 20% fetal calf serum.

Materials and methods.

§ 2.2.4 Incubations under hypoxic conditions.

Primary cultures of blood-brain barrier endothelial cells, grown either in iron-enriched or iron-depleted medium, were exposed to hypoxic conditions as described by Pietersma et al (20). Briefly, when cultures reached confluency, they were placed in a incubator equipped with a conducting surface to maintain a temperature of 37 °C. The incubator was completely sealed and could only be accessed by gloves sealed to the cabinet wall. A continuous flow of 95% N₂ and 5% CO₂, humidified and heated to 37 °C was maintained throughout the incubation period. Together, these measurements warranted a continuous low oxygen pressure of ± 7.5 mm Hg, as monitored by an oxygen analyzer at the cabinet outlet. Prior to use, buffers were gassed with 95% N₂ and 5% CO₂ and kept in the cabinet to equilibrate to hypoxic conditions.

§ 2.2.5 Oxidizing system.

To test the relative susceptibility of BBB-EC's to oxidative damage and the effect thereon of iron-enriched and iron-depleted culturing, cells were exposed to an oxidizing system composed of vitamin C and H₂O₂.

Prior to exposing cells to the oxidizing system, culture dishes (or cover slides) were rinsed twice with PBS at room temperature. Next cells were incubated with M199 culture medium containing 2 mM vitamin C at stored at 37 °C under normoxic circumstances (5% CO₂ and 20% O₂). After 15 min H₂O₂ (2 mM) was added to the medium and mixed.

Cover slides for DNPH immunofluorescence experiments (see § 2.3.4) were kept at 37 °C for 1 h, rinsed 3 times with PBS, followed by immediate fixation in methanol (-20 °C).

Petri dishes for the carbonyl assay (see § 2.5.2.10) were kept at 37 °C for either 1, 2 or 3 h. At the end of the incubation period cells were placed on ice, rinsed twice with icecold PBS and processed.

§ 2.3 Morphological techniques.

§ 2.3.1 Anti-Von Willebrand Factor immunocytochemistry.

Glass coverslides, stored in acid bichromate, were coated with 0.2% gelatine (w/v) in PBS (as described in § 2.3.5) and cells were grown for 4 to 6 days. After fixation for 5 min in

Chapter 2

methanol (-20°C), cells were incubated with 5% Blotto (Sigma, USA) for 30 min, rinsed 3 times with PBS and incubated with mouse anti-human Von Willebrand Factor. Finally, cells were incubated with fluorescein labeled goat anti-mouse IgG for 30 min, rinsed with PBS and examined in a Leitz Aristoplan fluorescence microscope.

§ 2.3.2 *Coupling of 6.6 nm gold to transferrin.*

According to manufacturers instructions, coupling of protein to the gold particles critically depends on the pH of the mixture. Coupling conditions are considered optimal when the mixture has a pH equal to or slightly above (≤ 0.5 pH units) the iso electric point of the protein that is to be labeled. Therefore, diferric porcine transferrin (IEP ± 5.9 , see chapter 3) was dialyzed for 24 h against 0.5 mM NaHCO₃ buffer of pH 6.4. Next, the minimal concentration of protein needed to prevent the gold particles from aggregating in a 1% sodium chloride solution, was assessed spectrophotometrically at 580 nm. Based on the results of this titration, an aliquot of the 6.6 nm gold sol was brought to pH 6.5 and mixed with Tf (18.75 μ g Tf/ml gold sol solution) under continuous stirring. This solution was left to stand for 15 min. To further stabilize the Au-Tf mixture and block the remaining free surface area on the gold particles, BSA (10%, pH 9.0) was added to a final concentration of 1% (w/v).

To remove both unbound transferrin and gold-aggregates, the transferrin-gold (Au-Tf) suspension was centrifuged (45000 x g, 45 min, 4 °C). Supernatant and solid pellet were discarded, whereas the "slurry pellet" was collected and loaded on a linear (10-30%) sucrose gradient and centrifuged (80000 x g, 90 min, 4 °C). Supernatant was carefully removed and the upper one third of the gradient was collected. Following dialyzation against PBS containing 1% (w/v) BSA and 20 mM NaN₃, the protein-gold mixture was stored at 4 °C.

§ 2.3.3 *Incubation procedure of membrane-grown endothelial cells with gold-labeled transferrin.*

P₀ and P₁ cells were grown on membranes until confluent (as described in § 2.2.3. Prior to incubation, membranes were gently washed with icecold PBS (2x) and placed on ice. The luminal sides of the cells (upper chamber) were then incubated with 1 ml M199, containing

Materials and methods.

HEPES, L-glutamine, and $\pm 1 \mu\text{g/ml}$ Au-Tf for 2 h at 4 °C. The lower compartment was filled with 1.5 ml M199 containing HEPES and L-glutamine. Next, membranes were washed twice with icecold PBS to remove unbound Au-Tf. Endocytosis of Au-Tf was started by placing the membranes in 1.5 ml M199 of 37 °C, simultaneously replacing the icecold medium in the upper chamber for M199 (37 °C) containing 100 ng/ml unlabeled diferric Tf. Endocytosis was stopped at 1, 5 or 10 min by placing the membranes on ice and rinsing the cells twice with icecold PBS. Membranes were then submerged in fixation fluid (see § 2.10.1) and left to stand overnight at 4 °C.

§ 2.3.4 2,4 Dinitrophenol hydrazine immunocytochemistry.

Primary isolates of BBB-EC's were grown on glass cover slides, coated with 3-aminopropyltriethoxysilane according to the procedure described in § 2.3.5. From day 3 on, 50% of the cultures were exposed to iron-enriched medium as described in § 2.2.2, whereas the remaining 50% were treated according to normal culture conditions (see § 2.2.1). After 10 days, cells were rinsed with PBS, and either fixed directly or fixed following exposure to the oxidizing system (see § 2.2.5). Cells were fixed in methanol (-20 °C) for 5 min, and thereupon immediately immersed in a solution of 10 mM 2,4 DNP dissolved in a mixture (9:5, v/v) of methanol and sodium phosphate buffer, pH = 3. After 10 min, cells were washed by repeated dipping in a 1:1 (v/v) mixture of ethanol and ethyl acetate. Following removal of unbound DNP, cells were incubated for 1 h at room temperature in 5% (w/v) Blotto to block nonspecific binding. Cells were then rinsed 3 times 5 min with PBS and incubated for 1 h at room temperature with rabbit anti-dinitrophenol (diluted 1:100). Next, cells were rinsed again (3 times) with PBS and incubated for 1 h in the dark with Swine anti-rabbit Fluorescein (diluted 1:200). Coverslips were then washed with PBS and distilled water, mounted on glass slides and viewed with a Zeiss Axioskop fluorescence microscope. This microscope was equipped with a triple pass filter set for simultaneous viewing of FITC, Texas Red, and DAPI. Images were taken with Fugicolor Super G400 ASA film.

§ 2.3.5 Coverslide coating procedures for immunocytochemistry.

Glass coverslips were stored in acid bichromate for prolonged periods of time (weeks)

Chapter 2

prior to use. Immediately before coating cover slides were extensively rinsed, first with 96% ethanol and then followed by distilled water.

Gelatine coating: cover slides were placed in small petri dishes and 0.2% gelatine (w/v) in PBS (± 90 °C) was added. The cover slides were then stored overnight under sterile conditions in a breeding cabinet at 37 °C. Prior to use, cover slides were rinsed once with PBS.

3-Aminopropyltriethoxysilane coating: cover slides were air dried prior to use, then immersed for 15 sec in a mixture of acetone and 3-aminopropyltriethoxysilane (50:1, v/v). Next, slides were repeatedly dipped in acetone, followed by dipping in regular tap water and air dried overnight under sterile conditions in a breeding cabinet at 37 °C.

§ 2.4 Semiquantitative immunochemical procedures.

§ 2.4.1 *Crossed immunoelectrophoresis.*

Samples from transferrin and hemopexin containing fractions were subjected to crossed immunoelectrophoresis (7) to assess their purity. Briefly, 1 g Agarose was dissolved in 100 ml of a 0.1 mol/l tris-barbiturate buffer (pH 8.6) heated to 90 °C under continuous stirring. After pouring and cooling of the gel, a well was punched and filled with 2 μ l sample. The gel was mounted on a LKB 2117 Multiphor System (LKB, Sweden) and electrophoresis in the first dimension was performed at 10 V/cm for 30 min (1.5 h for hemopexin) at 15 °C. The sample containing lane was cut out and transferred to another glass plate with agarose gel containing rabbit anti-porcine serum protein antibodies (courtesy W.L. van Noort). Electrophoresis in the second dimension was performed for 20 hrs at 2.5 V/cm (2 V/cm for hemopexin). The gel was washed for 48 h in 0.15 mol/l NaCl repeatedly changing the washing solution. The gel was then air dried and stained with Coomassie Brilliant Blue R-250 (0.1%, w/v) in ethanol/acetic acid/water (4.5:1:4.5, v/v/v). Similar experiments were performed with goat anti-swine total serum protein antibodies.

§ 2.4.2 *Alpha-2-macroglobulin and 440 and 660 kDa assays.*

Ouchterlony double immunodiffusion was accomplished in sodium barbiturate buffered 1% Agarose (ICN, The Netherlands) and stained with amido black.

Materials and methods.

Rabbit anti-porcine-serum protein antibodies (obtained from Nordic, The Netherlands) were used, because neither porcine alpha-2-macroglobulin nor its antibody, are commercially available. As alpha-2-macroglobulin is a serum protein, one would expect a cross reaction between alpha-2-macroglobulin and anti-serum protein antibodies.

The 440 and 660 kDa ferritin Ouchterlony assays were performed with polyclonal antibodies raised against both purified fractions (see chapter 4).

§ 2.4.3 Transferrin and ferritin immunosorbent assays.

Standards (either rat transferrin diluted between 1-15 ng/50 μ l TBS, or type I horse ferritin diluted between 0.25-15 ng/50 μ l TBS; Sigma Chemical Co., St. Louis, MO) and homogenates (diluted to approximately 1 mg protein/50 μ l TBS) were applied in triplicate onto nitrocellulose membranes (MSI, Westboro, MA) presoaked in TBS, using a Manifold II vacuum slot blot device (Schleicher and Schuell Inc., Kene, NH), as described by Roskams and Connor (22). Briefly, the membranes were blocked for 1 h at room temperature with Blotto (5% w/v, Carnation instant nonfat dried milk in TBS), rinsed for 5 min (3x) with TBS, and incubated overnight at 4 °C with primary antibody: either rabbit anti-rat transferrin (1:1000) (courtesy Dr. R. Fine, Boston University, MA); or rabbit anti-horse ferritin (1:3000) (Jackson ImmunoResearch Lab. Inc.). Membranes were then rinsed and incubated in secondary antibody 125 I-goat anti-rabbit IgG (NEN Research Products, Wilmington, DE), 4 μ Ci per blot for 1 h at room temperature. Membranes were then rinsed, dried, and packed with film for approximately 15 h.

Developed films were analyzed using a Molecular Dynamics Model 100A Densitometer (Molecular Dynamics, Sunnyvale, CA) and *pdi*Quantity one software (*pdi*, Huntington Station, NY). Regression analysis of the optical densities measured for the rat standards was used to determine sample ferritin and transferrin concentrations. Each slot blot contained its own standard curve and data were only analyzed from slot blots with standard curve correlation coefficients ≥ 0.95 . All samples were run on three separate blots and averaged to report the final value.

Chapter 2

§ 2.5 Analytical and quantitative procedures.

§ 2.5.1 Analytical techniques.

§ 2.5.1.1 Native and SDS polyacrylamide gel electrophoresis.

Native polyacrylamide gel electrophoresis (PAGE) and sodium dodecyl sulfate (SDS) PAGE were performed on a PhastSystem (Pharmacia LKB, Sweden) using either 8-25%, 10-15%, or 4-15% gradient gels depending on the mass of the protein under study. Typical settings of the PhastSystem are summarized in *Table 1*.

Native PAGE Gel type:	Temp.	Pre-run	Sample application	Separation
Gradient 4 - 15%	15 °C	400 V 10 mA 2.5 W 20 Vh	400 V 1 mA 2.5 W 5 Vh	400 V 10 mA 2.5 W 300 Vh
Gradient 10 - 15%	15 °C	0 V 0 mA 0 W 0 Vh	250 V 10 mA 3.0 W 10 Vh	250 V 10 mA 3.0 W 65 Vh
Gradient 8 - 25%	15 °C	0 V 0 mA 0 W 0 Vh	250 V 10 mA 3.0 W 10 Vh	250 V 10 mA 3.0 W 65 Vh

Table 1:

Parameter values of the PhastSystem used in native and SDS PAGE of porcine transferrin, hemopexin and ferritin.

Native (non-denaturing) polyacrylamide gel electrophoresis (PAGE) and sodium dodecyl sulfate (SDS)-PAGE were also performed on a mini protean system 2 (Bio Rad, the Netherlands) according to manufacturer's instructions.

Gels were stained for protein according to manufacturer's instructions. Iron staining was performed according to Chung (5). Gels were analyzed and quantitated using an Ultrosan XL enhanced laser densitometer (LKB, the Netherlands).

Materials and methods.

§ 2.5.1.2 *Tricine-SDS Polyacrylamide gel electrophoresis.*

Analyses of L and H subunit ratios in the porcine spleen ferritin fractions were performed on Tricine-PAGE (16.5% T and 3% C) gels according to Schägger & Jagow (23). The 16.5% Tricine SDS-PAGE (as compared to standard SDS-PAGE) resulted in a more distinct separation between both the 19 and 21 kDa subunits and allowed a better densitometric analysis of the subunit ratio.

§ 2.5.1.3 *Isoelectric focussing.*

Isoelectric focussing of porcine spleen ferritin was performed on 1% agarose gels (pH 4-6) using a Pharmacia PhastSystem (for details see *Table 2*).

Isoelectric focussing of porcine transferrin and hemopexin was performed on a PhastSystem using PhastGel IEF (pH 4-6.5) gels (30). Typical settings are summarized in *Table 2*.

Isoelectric focussing Gel type:	Temp.	Pre-focussing	Sample application	Separation
1% Agarose pH: 4 - 6	15 °C	1000 V 2.5 mA 3.5 W 60 Vh	200 V 2.5 mA 3.5 W 15 Vh	1000 V 2.5 mA 3.5 W 205 Vh
PhastGel IEF pH: 4- 6.5	15 °C	2000 V 2.0 mA 3.5 W 15 Vh	200 V 2.0 mA 3.5 W 15 Vh	2000 V 5.0 mA 3.5 W 1000 Vh

Table 2:

Parameter values of the PhastSystem used in isoelectric focussing of porcine transferrin, hemopexin and ferritin.

§ 2.5.1.4 *Sepharose-concanavalin A chromatography.*

Prior to amino acid and carbohydrate analyses, porcine transferrin was applied to a column packed with Sepharose-linked concanavalin A according to a procedure described by Hatton et al (11).

Chapter 2

§ 2.5.1.5 *Determination of the iron to phosphorus ratio with Electron Probe Microanalysis (EPMA).*

EPMA was carried out (8) with a Transmission Electron Microscope (TEM) JEOL 2000 FX at 80 kV, with the use of an anticontamination device. The TEM was equipped with an X-ray detector with a high purity germanium crystal and ultrathin window. The detector was coupled to a Tracor Northern 5500 System. The specimen (ferritin) was observed in a single tilt holder with a graphite specimen retainer at a take-off angle of 35°. Nylon grids (60 mesh) were covered with a pyoloform film with multiple holes and coated with carbon. Ferritin suspensions were placed directly on these grids and air dried. Multiple analyses were performed during 100 sec (irradiated area: 0.75 μm^2) on that part of the ferritin suspension that covered the holes in the pyoloform film. Another set of analyses was performed under the same instrumental conditions on that part of the ferritin suspension that was covering the pyoloform film. Horse spleen ferritin served as a calibration standard. Of each fraction electron micrographs were made at $M = 500,000$.

§ 2.5.1.6 *Protein carbonyl staining in Western Blots.*

For Western blots, sonicates of 4 rats per group were pooled in order to obtain sufficient protein to load 50 μg protein per lane and treated as outlined in (§ 2.5.2.10). Control lanes consisted of pooled samples that were treated in the same manner, but did not undergo initial hydrazone derivitization. Resulting precipitates were solubilized in SDS running buffer and loaded onto a 10% polyacrylamide gel. Each gel contained a lane of Rainbow protein molecular weight markers (Amersham, Arlington Heights, IL). Gels were run at 155 V (constant voltage) for approximately 4 to 5 h. Proteins were transferred to nitrocellulose electrophoretically, using a semi-dry transfer apparatus. Blots were incubated for 2 h at room temperature with rabbit anti-dinitrophenyl antisera (Dakopatts, Denmark), diluted 1:1000 (v/v). Blots were rinsed and incubated for 1.5 h in mouse anti-rabbit IgG conjugated to alkaline phosphatase (Jackson Laboratories, West Grove, PA) and developed with the NBT/BCIP (USB) color substrate system.

Materials and methods.

§ 2.5.2 Quantitative procedures.

§ 2.5.2.1 Protein concentration measurements.

Protein concentrations were determined according to Bradford (3) using different concentrations of BSA as a standard.

§ 2.5.2.2 Cellular protein measurements.

Cells were washed with PBS (4°C), 250 µl distilled water was added and cells were harvested. Next, dishes were rinsed 3 times with 250 µl distilled water containing 0.1% Triton X-100. These rinses were added to the cell suspension. Following sonication of the suspension (10 sec, 0°C), 100 µl samples were taken (in duplicate) and protein concentrations were measured according to Bradford (3), using BSA as a standard.

§ 2.5.2.3 Cellular DNA measurements.

Cells were harvested as described in the previous section (§ 2.5.2.2). Samples were taken for protein measurements and the DNA content of each sample was assessed using a Nucleosan DNA kit (Sanbio, the Netherlands) according to manufacturer's instructions. Results from three separate experiments, each performed in 6-fold, are expressed in number of cells per mg protein.

§ 2.5.2.4 Carbohydrate analyses.

Carbohydrate analyses of transferrin fractions (obtained from the Sepharose-concanavalin A column) and hemopexin were performed on a LKB Alpha Plus 4151 (LKB, U.K.), equipped with a 60 cm column (2.4 mm) packed with Ultropac 11 resin (31).

§ 2.5.2.5 Amino acid and N-acetylglucosamine analyses.

Analyses of N-acetylglucosamine and amino acids were performed using a method described by van Eijk (29) on a Pharmacia Biochrom 20 (Pharmacia, U.K.) equipped with a 20 cm column (4.6 mm) packed with Ultropac 8 resin.

In both techniques, results of duplicate runs varied less than 3% within one sample. Human 4 sialo transferrin (with two bi-antennary glycan chains) was used as an internal

Chapter 2

standard in both carbohydrate- and amino acid analyses.

§ 2.5.2.6 *Sialic acid quantification.*

Following carbohydrate analysis, the amount of sialic acid in porcine transferrin and hemopexin was assessed according to a technique described by Horgan (13). Both 4 sialo transferrin (with two bi-antennary glycan chains) and N-acetylneuraminic acid were used as standards.

§ 2.5.2.7 *Ferritin iron determination.*

Ferritin iron was determined according to a method adapted from Harris (10) using Ferrozine (Sigma, USA). To 100 μ l sample an equal amount of 37% (w/v) HCl was added, mixed and left to stand for 15 min. Next, 100 μ l L-ascorbic acid (0.14 M), 0.5 ml sodium acetate (saturated) and Ferrozine (10 mM) were added to this mixture. After 10 min the absorbance at 562 nm was measured and compared to a range of standard Fe(III) solutions.

§ 2.5.2.8 *Total iron determination (flame atomic absorption spectrophotometry).*

Iron determinations in rat brain homogenates were made using atomic absorption spectrophotometry. Aliquots (30 μ l) of rat brain homogenates were digested in polypropylene tubes by adding 30 μ l of nitric acid and incubating at 37 °C for one week in a hot water bath. Three tubes containing 30 μ l sample buffer (0.25 M sucrose + 10 mM PMSF) underwent the same procedure and served as controls. Standard curves ranging from 0 to 1.00 μ g iron/ml were prepared by diluting iron standard (1 mg iron/ml, Alpha Products, Danvers, MA) in 5% nitric acid. Standards and digested samples were read in triplicate by injecting 20 μ l aliquots into a teflon cup, attached to a Instrument Laboratories Video 11 atomic absorption spectrophotometer (Allied Analytical Systems, Waltham, MA). Absorbance readings were recorded and used for analysis.

§ 2.5.2.9 *Phosphorus determination.*

Biochemical assessment of the amount of phosphorus in ferritin was performed according to Ames (1). Briefly: a ferritin containing sample is mixed with 30 μ l of a solution of 10% (w/v) $\text{Mg}(\text{NO}_3)_2 \cdot 6\text{H}_2\text{O}$ dissolved in 95% ethanol and subsequently dried and ashed. After

Materials and methods.

cooling, 0.3 ml HCl (0.5 mol/l) is added, and this is incubated for 15 min at 100 °C. The tube is cooled again and 0.7 ml of a (1:6) mixture of 0.57 mol/l ascorbic acid and 3.4 mmol ammonium molybdate.4H₂O dissolved in 1 mol/l H₂SO₄ is added. This mixture is stirred and incubated for 20 min at 45 °C. Samples are read spectrophotometrically at 820 nm and compared to standards of inorganic phosphate treated identically.

§ 2.5.2.10 Protein carbonyl determination.

Protein carbonyl concentration was determined by forming protein hydrazone derivatives using 2,4 dinitrophenylhydrazine (2,4 DNPH).

For brain tissue, we used a technique adapted from Smith et al (24). Brain samples were sonicated on ice in 0.01 M sodium phosphate containing 0.1% Triton X-100 (pH = 7.4). Sonicates were then centrifuged (10 min, 40000 x g, 4 °C) and supernatants were incubated with equal volumes of 10 mM 2,4 DNPH in 2 M HCl (15 min). The protein hydrazone derivatives were extracted in 10% trichloroacetic acid and centrifuged (10 min, 20000 x g, 4 °C). Pellets were washed 3 times with 1:1 v/v ethanol/ethyl acetate and solubilized in 6 M guanidine hydrochloride. Samples and blanks of guanidine HCl were read spectrophotometrically at 367 nm. Protein carbonyl concentrations were calculated with an reference absorptivity ϵ of 21.0 mM⁻¹ cm⁻¹ and expressed in nmol of 2,4,DNPH incorporated per mg of protein.

For cell cultures: blood-brain barrier endothelial cells were grown to near confluency in either iron-enriched or iron-depleted culture medium. Following exposure to an oxidizing system (see § 2.2.5), cell were placed on ice and washed twice with icecold PBS. Cells were then incubated for 10 min with 1 ml of a 10 mM sodium phosphate buffer (pH = 7.4) containing 0.1% Triton X-100. Cells were harvested, then sonication on melting ice and centrifuged (20000 x g, 10 min, 4 °C). An 1 ml aliquot of supernatant was incubated with an equal volume of 2,4 DNPH and left to stand for 15 min. An additional aliquot of each sample was incubated with 2 M HCl instead of DNPH (blank). The remaining part of the procedure was as described above. Carbonyl concentration were measured directly, as samples were read spectrophotometrically at 367 nm and corrected for blanks (with 2 M HCl instead of DNPH) and guanidine HCl. Protein carbonyl concentrations are expressed in nmol/mg protein.

Chapter 2

§ 2.5.2.11 Myeloperoxidase activity assay.

Myeloperoxidase activity was measured to assess the number of adherent granulocytes in the granulocyte adherence assay (see § 2.5.2.12) (20). Briefly, following incubation and adherence of granulocytes to blood-brain barrier endothelial cells, myeloperoxidase was extracted for 15 min in 5% hexadecyltrimethylammonium bromide (HTAB) (Merck, Germany). To 50 µl of this HTAB extraction solution 100 µl of a mixture of o-dianisidine hydrochloride (0.2 mg/ml) and 0.4 mM H₂O₂ was added and the reaction was monitored at 450 nm. The measured maximum reaction rate was compared to a standard curve obtained from different concentration of granulocytes incubated in HTAB, to estimate the number of adherent granulocytes.

In general, porcine granulocytes showed low myeloperoxidase activity.

§ 2.5.2.12 Granulocyte adherence assay.

Primary cultures of blood-brain barrier endothelial cells were grown either in iron-enriched or iron-depleted medium until reaching confluency. Cells were then placed in a airtight incubator (see § 2.2.4) and exposed for 2 h to hypoxic conditions as described by Pietersma et al (20) prior to incubation with granulocytes. Briefly, immediately upon exposure to hypoxic conditions, medium was removed and replaced by Krebs-Ringer bicarbonate buffer (= 118 mM NaCl, 4.7 mM KCl, 1.0 mM CaCl₂, 1.2 mM KH₂PO₄, 1.2 mM MgSO₄·7H₂O, 25 mM NaHCO₃, 5.5 mM glucose and 2.3 mg/ml HEPES) of pH = 7.4. After 2 h, hypoxic buffer was removed and replaced by Hanks' balanced salt solution (normoxic). This buffer was replaced after 5 min by granulocytes resuspended in Hanks' balanced salt solution. Cells were incubated with 1, 2, 3 or 4 x 10⁶ granulocytes/cm², then left to stand for 5 min to allow adherence. Next, cells were washed once with 1 ml Hanks' balanced salt solution and incubated for 15 min with HTAB to extract myeloperoxidase and assess the number of adherent granulocytes (see § 2.5.2.11).

Materials and methods.

§ 2.6 Protein isolation and purification procedures.

§ 2.6.1 Isolation of porcine transferrin.

§ 2.6.1.1 Serum pretreatment.

The technique used is a modification of the procedure described by Baumstark (2). Fresh porcine blood was obtained from the local abattoir, where citrate was added to prevent clotting during transport to our laboratory. Upon arrival, blood was immediately centrifuged (1000 g, 10 min). The resulting plasma was saturated with excess iron (400 μmol FeCl_3/l plasma) under continuous gentle stirring during 30 min at 37 °C. Aliquots of plasma were then dialyzed against a 20-fold excess of a 0.14 mol/l NaCl/0.01 mol/l CaCl_2 solution (overnight, 4 °C) to precipitate fibrin. The resulting semi-elastic coagulate was left to stand for two hours at room temperature and the fluid oozing from this coagulate was collected for further processing. This solution was brought to 50% saturation with $(\text{NH}_4)_2\text{SO}_4$, left to stand for 1 h at 4 °C and centrifuged (4000 g, 20 min, 4 °C). The clear supernatant was then brought to 70% saturation with $(\text{NH}_4)_2\text{SO}_4$, centrifuged (4000 g, 20 min, 4 °C) and the pellet dissolved in distilled water containing 1.54 mmol/l NaN_3 . Subsequently, this solution was rapidly dialyzed and concentrated on a Mini Ultrasette (Filtron, The Netherlands). Aliquots of this solution were stored at -20 °C until further use.

§ 2.6.1.2 Column preparation.

The column preparation, as described by Baumstark (2) was followed with some minor alterations. Briefly, Bio-Gel A 1.5m was coupled to Cibacron Blue 3GA (12): 3 g Cibacron Blue 3GA, dissolved in 150 ml 0.47 mol/l Na_2CO_3 , was mixed with 450 ml Bio-Gel A 1.5m and incubated for 42 h at 45 °C. Following removal of the unbound dye on a glass bed filter, the gel was loaded on a column (2.1 x 95 cm) and packed under 60 cm H_2O pressure. The gel was then washed with 3 column volumes 1.54 mmol/l NaN_3 , followed by 1 column volume 0.5 mol/l phosphate buffer ($\text{KH}_2\text{PO}_4/\text{K}_2\text{HPO}_4$, molar ratio 1:2, pH 7.1) and finally with 500 ml 0.5 mol/l KCNS before sealing the column fitting. It is recommended to use an adjustable end fitting, because the gel volume will change during column operation.

Chapter 2

The column was equilibrated with 1.54 mmol/l NaN_3 until a stable absorbance baseline was reached and pH and conductivity of the effluent matched those of the NaN_3 solution.

§ 2.6.1.3 Separation procedure.

Upon thawing, a sample of the pretreated serum (± 400 mg protein) was loaded onto the column, followed by circa 3 column volumes 1.54 mmol/l NaN_3 until the absorbance (at 280 nm) had returned to its baseline level. Hereafter, a linear phosphate buffer gradient was started to elute transferrin. The gradient consisted of 500 ml 0.1 mol/l $\text{KH}_2\text{PO}_4/\text{Na}_2\text{HPO}_4$ (molar ratio 1:2, pH 7.1) in 1.54 mmol/l NaN_3 against 500 ml 1.54 mmol/l NaN_3 .

§ 2.6.1.4 Regeneration of the column.

After each run, the Bio-Gel A/Cibacron Blue gel was regenerated using 1.54 mmol/l NaN_3 until absorbance reached the original baseline level. After each 6th run the gel was regenerated more rigorously, using 400 ml 0.5 mol/l KCNS. Afterwards the column was equilibrated as described in an earlier section.

§ 2.6.2 Isolation of porcine hemopexin.

Porcine serum hemopexin was isolated according to a method adapted from Noiva (17) and Spencer (27). Fresh pooled porcine blood was obtained from the local abattoir. Citrate was added to prevent clotting during transport to our laboratory. Upon arrival, blood was immediately centrifuged (1000 g, 10 min). Fibrin was removed as outlined above (§ 2.6.1.1). This solution was brought to 50% saturation with $(\text{NH}_4)_2\text{SO}_4$, left to stand for 1 h at 4 °C and centrifuged (4000 g, 20 min, 4 °C). The supernatant was dialyzed overnight against running tap water, followed by dialysis for 48 h at 4 °C against 0.01 mol/l sodium citrate buffer (pH 5.7), containing 0.02% (w/v) NaN_3 . Aliquots (150 ml) of this dialyzed solution were applied to a CM-Sephacrose CL-6B column (100 x 2.2 cm) and the column was rinsed with 0.01 mol/l sodium citrate buffer (pH 5.7) until a stable baseline was reached. Next, a 800 ml linear gradient of sodium citrate (0.01 to 0.06 M) was developed to elute hemopexin and transferrin. Hemopexin containing fractions were concentrated and loaded on a column (150 x 2.4 cm) packed with Sephadex G 100 to remove hemoglobin and hemopexin di- and polymers. Degraded hemopexin fragments and other low molecular

Materials and methods.

weight proteins were removed applying hemopexin containing fractions to a Sephadex G 75 column (100 x 1.4 cm).

§ 2.6.3 Isolation and subfractionation of porcine spleen ferritin.

§ 2.6.3.1 Ferritin isolation method 1.

Porcine spleen ferritin was isolated according to a method adapted from Penders (18). Briefly, after removal of fat and connective tissue, the spleen was rinsed in 0.15 M NaCl (4 °C) and homogenized (Ultra-turrax, Janke & Kunkel). The homogenate was heated (80 °C, 5 min), rapidly cooled and centrifuged (3000 g, 45 min). The supernatant was centrifuged (78,000 g, 1 h) and the resulting pellet resuspended in 0.15 M NaCl and centrifuged (7000 g, 1 h). The ferritin containing supernatant was then centrifuged at 78,000 g for 1 hour. The last two centrifugation steps were repeated and finally the pellet was resuspended in 0.15 M NaCl containing 0.01% NaN₃ and centrifuged again (78,000 g, 1 h). All centrifugation steps were performed at 4 °C.

§ 2.6.3.2 Ferritin isolation method 2.

Human placental ferritin and porcine spleen ferritin were isolated according to Konijn et al (14). Briefly, tissue was homogenized and then centrifuged (10,000 g, 20 min). Supernatant fractions were heated to 80 °C (5 min), cooled on ice and centrifuged (10,000 g, 20 min). The supernatant was adjusted to pH 4.2 with acetic acid, left to stand for 24 hours at 4° C and then centrifuged (10,000 g, 20 min). Following adjustment of the pH to 5.5 with sodium acetate, the supernatant was brought to 50% saturation with ammonium sulfate, left to stand for 1 hour at 4° C and centrifuged (10,000 g, 25 min). The pellet was resuspended in water, brought to 75% saturation with ammonium sulfate and centrifuged (10,000 g, 25 min). The clear supernatant was dialyzed against 0.15 mol/l NaCl for 24 hours and centrifuged (120,000 g, 4 h).

§ 2.6.3.3 Separation of isoferritins.

Porcine spleen ferritin was separated by ion-exchange chromatography on a DEAE-Sephadex A-25 column into acid, intermediate and basic fractions according to Konijn et al (14).

Chapter 2

§ 2.6.3.4 Preparation and operation of the combined Sepharose 4B and Sepharose 6B columns.

Two columns were packed with Sepharose 4B (207 * 2 cm) and Sepharose 6B (200 * 1.8 cm) respectively. Column dimensions required the level of the column outlet tubing to be adjusted during packing of the gel in order to prevent packing pressure exceeding 80 cm H₂O. Samples were loaded on the Sepharose 6B column, eluted with a 0.05 M Tris-HCL buffer (pH 8.0) and fed directly into the Sepharose 4B column. Both columns were serially linked with small diameter tubing (0.7 mm diameter) to prevent remixing of the already partially separated proteins. Pure ferritin fractions were collected and concentrated by ultracentrifugation (78,000 g, 1 h).

§ 2.6.4 Isolation and purification of TfR's from porcine liver (to test TfR recovery efficiency).

Fresh porcine liver tissue was cut into small fragments, washed 3 times in PBS (4°C) containing 0.01% PMSF, and homogenized in 1 mM NaHCO₃/0.5 mM CaCl₂ buffer (pH 7.5, 4°C). The homogenate was filtered through a 150 µm nylon mesh and centrifuged (2000 g, 30 min, 4°C). The pellet was resuspended in the same buffer and washed twice (= crude vesicle prepare). The pellet was then dissolved in PBS containing 0.5% Triton X-100 and 0.25% (w/v) Trypsine and placed in a waterbath (37°C, 2.5 h). This solution was dialyzed overnight against running tap water, concentrated by ultrafiltration with a 30 kDa filter and centrifuged (25,000 g, 4°C, 2 h). Supernatant samples were loaded on a Sephadex G100 (Pharmacia) column and the 70 kDa fraction was collected, concentrated and dialyzed against a start buffer (containing 0.25 M NaCl, 174 mM Na₂HPO₄·2H₂O and 13 mM sodium citrate, pH 7.2). Samples were then loaded on a column packed with porcine Tf coupled to CNBr-Sepharose 4B (Pharmacia, Sweden). Prior to loading, the column had been incubated overnight with a 0.02M Tris buffer (pH 8.2) containing 50 mM NTA, 2 mM Fe(III)-citrate, 20 mM NaHCO₃ and 0.02% NaN₃, to saturate all Tf iron binding sites. After loading, the column was washed with start buffer until a stable baseline was reached. The 70 kDa TfR subunit was eluted with a buffer (pH 2.8) containing 0.25 M NaCl, 32 mM Na₂HPO₄·2H₂O and 84 mM sodium citrate. Purity was checked with sodium dodecyl sulfate (SDS) polyacrylamide gel electrophoresis on a PhastSystem (see § 2.5.1.1).

Materials and methods.

§ 2.6.5 Isolation of granulocytes.

Granulocytes were isolated from citrated porcine blood, freshly obtained from a local slaughterhouse according to Pietersma et al (19). Briefly, blood cells were diluted and centrifuged over Lymphoprep (Nycomed, The Netherlands). Following isotonic lysis of erythrocytes in a mixture of 155 mM NH₄Cl, 10 mM NaHCO₃ and 0.1 mM EDTA (pH = 7.4) at 4 °C, granulocytes were washed and resuspended in PBS containing 5% (w/v) bovine serum albumin (Sigma Chemical, St. Louis, MO). Granulocytes were stored at 4 °C until use.

§ 2.7 Statistical analyses and curve fitting.

§ 2.7.1 Statistical analyses ferritin data sets.

Ferritin data sets were analyzed with a Bonferroni *t* test following a "repeated-measures analysis of variance" to test differences in amino acid and carbohydrate composition between the three ferritin fractions.

§ 2.7.2 Mathematical analysis of the surface and total TfR binding experiments.

In each individual experiment the percentage nonspecific binding was calculated using 6 wells incubated with different concentrations of ¹²⁵I-Tf in the presence of a 100-fold excess of non-labeled Tf. Furthermore, the results from each binding experiment were fitted using the following equation in a nonlinear curvefit program (Statgraphics, Statistical Graphics Corporation, USA).

$$f(x) = \frac{a*x}{b+x} + c*x$$

In this equation "f(x)" represents the amount of bound Tf, "x" free Tf, "a" the total TfR concentration, "b" the concentration at 50% receptor saturation (Kd) and "c" represents the slope of the linear part of this curve fit (= nonspecific binding). Parameters a, b and c were calculated in an iterative process using the Marquardt algorithm.

Chapter 2

§ 2.7.3 Mathematical analyses of the experimental data on TfR endocytosis and exocytosis.

TfR internalization was assumed to follow first order kinetics and experimental data were therefore fitted to the equation $Y(t) = B_{tot} * (1 - e^{-k*t})$, using a nonlinear curve fit program. "k" represents the TfR internalization rate constant K_{in} in min^{-1} . "Btot" represents the maximal amount of ^{59}Fe bound to the cell surface at $t=0$ min that can take part in the endocytic cycle (see *Fig. 6.3*). This correction is necessary to compensate for variations in the number of surface TfR's due to different culture conditions (see chapter 6).

TfR externalization was also assumed to follow first order kinetics and data were fitted to the equation $Y(t) = C_1 * e^{-k*t} + C_2$, in which the first term represents the first order exocytosis of TfR's. C_2 is a constant, introduced to compensate for the fact that even after 1 hour cycle time a considerable percentage of ^{125}I labeled transferrin remains within the cell.

§ 2.8 Transferrin receptor quantitation and kinetics.

§ 2.8.1 Radio-labeling of transferrin.

Porcine Tf was radio-labeled according to adapted from a method described by Starreveld (28). Porcine transferrin was dialyzed for 24 h against an acetate buffer (pH 5.0), containing 0.04 mol/l EDTA, to remove all iron. Following dialyses against distilled water and a Tris/HCl buffer (pH 8.2), apo-transferrin was incubated with $^{59}\text{FeCl}_3$ (Amersham, The Netherlands), NTA (nitrilotriacetate) and NaHCO_3 (30 min, 37 °C). Excess $^{59}\text{FeCl}_3$ was removed using a Sephadex PD-10 column (Pharmacia, Sweden). Next, $^{59}\text{Fe}_2\text{-Tf}$ was incubated with Na^{125}I in a Iodogen coated glass tube. Unbound ^{125}I was removed with a Sephadex PD-10 column, followed by extensive dialyses (3 x 24 h) against a Tris/HCl buffer (pH 8.2). Radioactivity was counted in a Packard 500C autogamma spectrometer. Specific activity (^{125}I) ranged from 0.8 - 1.2 x 10^9 counts/min/mg Tf.

§ 2.8.2 Surface TfR measurements.

Blood-brain barrier endothelial cells were used when reaching confluency. Prior to the

Materials and methods.

experiment, cells were pre-incubated for 1 to 2 h at 37 °C with M 199, supplemented with HEPES (20 mmol/L) and L-Glutamine (4 mmol/L) to deplete all TfR's from Tf. Surface TfR measurements were performed as described by Ciechanover (6).

Briefly: following pre-incubation cells were washed with PBS (4 °C) and incubated (for 1 h 45 min at 4 °C) with specific amounts of ^{125}I -Tf in M199 up to 100 times Kd to reach complete saturation of the TfR's (4). Next, the incubation medium was collected and cells were washed 4 times with PBS to remove unbound ^{125}I -Tf. Surface TfR bound ^{125}I -Tf was collected in a series of wash steps with acidic and neutral buffers. Cells were then harvested for protein assessment as described in § 2.5.2.2. Surface bound Tf is expressed in ng/ μg cell protein.

§ 2.8.3 Total TfR measurements.

To assess the total amount of TfR's present in the endothelial cells, a procedure as described by Rao (21) was used. Briefly: cells were pre-incubated with M199 to deplete all TfR's (see § 2.8.2), harvested and lysed as described in § 2.5.2.2. Duplicate samples were taken from each dish for protein measurements and cell lysates were then incubated (for 2 h at 4°C) with specific amounts of ^{125}I -Tf in M199 up to 100 times Kd. Following precipitation with 30% ammonium sulfate, the solution was filtered through a 1.2 μm glass microfiber filter. Filters were washed 8 times with 30% ammonium sulfate and the remaining radioactivity was counted.

The TfR recovery efficiency of this procedure was checked in a separate series of experiments (see § 2.8.4). Total TfR bound Tf is expressed in ng/ μg protein.

§ 2.8.4 TfR recovery efficiency assessment in total TfR measurements.

To test the recovery efficiency of TfR's in cell lysates, the TfR recovery procedure as described by Rao (21; see also § 2.8.3), was performed either on (a) ^{125}I -Tf in M 199, (b) known amounts of purified half TfR's incubated with ^{125}I -Tf, or (c) crude vesicle preparations (see § 2.6.4) incubated overnight at 4 °C with ^{125}I -Tf with or without 0.1% Triton X-100. To remove unbound Tf, the vesicle suspension was centrifuged (2000 g, 30 min) and the pellet redissolved in 10 vol PBS. This procedure was repeated 5 times, at which point radioactivity in the supernatant was less than 5% of that in the pellet.

Chapter 2

§ 2.8.5 Quantitation of TfR's participating in the endocytic cycle.

Cells were pre-incubated for 1.5 h at 37 °C with M 199, supplemented with 2% BSA (w/v), HEPES (20 mmol/L) and L-Glutamine (4 mmol/L). Cells were washed once with PBS and then incubated for 1.5 to 40 h with 1500 ng (≥ 50 times Kd) ^{125}I -Tf at 37 °C. Next, cells were placed on ice and rinsed 4 times with PBS (4°C). Surface TfR concentrations were assessed as described before (see § 2.8.2). Cells were harvested, duplo samples taken for protein measurements (see § 2.5.2.2) and radioactivity of the cell suspension was measured.

§ 2.8.6 Transferrin receptor endocytosis rate measurements.

Following pre-incubation with serum free medium to deplete TfR's, cells were placed on ice and washed with icecold PBS. Next, cells were incubated with 1.6 $\mu\text{g/ml}$ diferric ^{59}Fe -Tf at 4 °C for 1 h 45 min. Prior to the actual experiment, cells were washed 4 times with icecold PBS to remove all unbound ^{59}Fe -Tf. Endocytosis was started by rapidly heating petri dishes to 37 °C, at the same time adding 2 ml of prewarmed (37 °C) medium containing 1.6 $\mu\text{g/ml}$ unlabeled diferric transferrin. Endocytosis was allowed to continue at 37 °C for fixed time periods, and stopped by rinsing the cells 4 times with icecold PBS. Following 3 wash cycles with acid and neutral buffers respectively (see § 2.8.2) to collect surface bound Tf, cells were harvested and intracellular ^{59}Fe was measured.

§ 2.8.7 Transferrin receptor exocytosis rate measurements.

Cells were first pre-incubated with serum free medium for 1.5 hours at 37 °C, rinsed twice with PBS and then incubated with 1.6 $\mu\text{g/ml}$ ^{125}I labeled diferric transferrin at 37 °C for 1 h 45 min. To deplete all surface TfR's prior to the actual experiment, cells were placed on ice and washed 3 times with acid and neutral buffers. Exocytosis was started by rapid heating to 37 °C, at the same time adding 2 ml of prewarmed (37 °C) medium containing 1.6 $\mu\text{g/ml}$ unlabeled diferric transferrin. The experiment was stopped at fixed intervals by rinsing cells 4 times with icecold PBS. Surface and intracellular TfR bound ^{125}I -Tf were measured separately at each interval.

Materials and methods.

§ 2.8.8 Quantification of cellular iron accumulation and release.

Following pre-incubation at 37 °C with serum free medium, cells were washed twice with PBS and incubated for different time periods up to 24 h with 4.8 µg/ml diferric ⁵⁹Fe-Tf at 37 °C. At those intervals, cells were placed on ice and washed 4 times with icecold PBS to remove unbound ⁵⁹Fe-Tf. Next, cells were subjected to 3 washes with acid and neutral buffers to assess surface TfR bound ⁵⁹Fe-Tf and then harvested for both protein and intracellular iron (⁵⁹Fe) measurements. The ⁵⁹Fe/protein ratio represents the net intracellular iron accumulation (= iron uptake minus iron release).

A parallel experiment was set up to measure iron release only. In a number of dishes, cells were allowed to accumulate ⁵⁹Fe for three hours as described above. After three hours, medium containing ⁵⁹Fe was removed, cells were washed with icecold PBS to remove unbound ⁵⁹Fe and subjected to three cycles of acid and neutral washes at 4 °C to deplete surface TfR's (see § 2.8.2). Following this washing procedure, cells were incubated with standard medium at 37 °C and after another 3 hours the excreted amount of ⁵⁹Fe was measured.

§ 2.9 Rat brain dissection.

Rats were anesthetized with an intramuscular injection of a mixture of ketamine (25 mg/ml), xylazine (1.3 mg/ml) and acepromazine (0.25 mg/ml). Next, the animals were perfused with icecold PBS until the effluent was clear (≥ 5 min). Following decapitation, the brain was removed and microdissected with the aid of a coronal brain matrix (Harvard Apparatus, South Natick, MA), according to the method of Cuello and Carson (9). Briefly, the frontal cortex was obtained from a coronal slice of the brain, rostral to a cut made at the caudal end of the lateral olfactory tract. Under a dissecting microscope, a razor blade was used to hemisect the slice, and the olfactory tract and tubercle were dissected away from the frontal cortex. Next, a 4 mm coronal slice was cut using the caudal edge of the optic chiasm as a landmark. From the hemisection of this slice, both the medial septum/diagonal band of Broca, and a sample of the striatum was dissected as described by Williams et al (32). The remaining brain was hemisected and the cerebral cortex overlying the right hippocampus was removed. An approximately 2 mm² sample of parietal cortex was taken

Chapter 2

from the tissue overlying the septal pole of the hippocampus, and a 2 mm² sample of the temporal/enthorinal cortex was taken from the tissue surrounding the temporal pole of the hippocampus by the method of Zellis and Wree (33). The entire hippocampus was then removed and the underlying thalamus pinched off. The dissection was completed by separating the cerebellum from the brain stem. All brain regions were frozen on dry ice immediately upon dissection, and stored at -70 °C until processed.

§ 2.10 Fixation, embedding and transmission electron microscopy.

§ 2.10.1 Tissue fixation.

Membrane-grown cells were fixed overnight at 4 °C in a mixture of glutaraldehyde 4% (v/v) and formaldehyde 4% (v/v) in sodium phosphate buffer (pH = 7.2). The following day, membranes were rinsed 3 times (10 min each) in PBS at room temperature and postfixed in a mixture of OsO₄ 1% (w/v) and K₄Fe(CN)₆ in PBS (pH = 7.4) at 4 °C. Subsequently, cells were rinsed in PBS, distilled water (room temperature), and then dehydrated in alcohol (50 to 96% , 4 steps, 10 min per step).

§ 2.10.2 Embedding.

First, membrane-grown cells were placed in a mixture (1:1) of ethanol and Epon for 1 h at room temperature, followed by 1 h at 37 °C in pure Epon. Polymerization took place overnight at 60 °C.

The Epon embedding fluid consisted of a mixture of LX-112 (38 ml), DDSA (26 ml), MNA (20 ml), and DMP 30 (1.5 ml).

§ 2.10.3 Sectioning.

Ultrathin sections of the Epon embedded membranes were made on an Ultratome V (LKB, Sweden), equipped with Diatome 1.5 mm diamant knives. Sections were collected on unfilmed 200 mesh copper grids.

Materials and methods.

§ 2.10.4 Staining.

Uranylacetate was used as the only contrast enhancer, whereas leadcitrate was omitted to improve visibility of the gold particles.

§ 2.10.5 Transmission electron microscopy.

Sections were studied in a Zeiss EM 902 (Zeiss, Oberkochen, FRG) transmission electron microscope. This instrument was equipped with an integrated electron spectrometer allowing high-resolution imaging with energy-filtered electrons (= electron spectroscopic imaging (ESI)). For the technical details, see Sorber et al (25,26)

Chapter 2

References.

- (1) Ames B.N. (1966) Assay of inorganic phosphate, total phosphate and phosphatases. *Meth. Enzymol.* 8: 115-118.
- (2) Baumstark J.S. (1987) A simple one-column procedure for the separation of swine and human serum transferrins. *J. Biochem. Biophys. Meth.* 14: 59-70.
- (3) Bradford M.M. (1976) A rapid and sensitive method for the quantification of microgram quantities of proteins utilizing the principles of protein-dye binding. *Anal. Biochem.* 72: 248-251.
- (4) Bürgisser E. (1984) Radioligand-receptor binding studies: what's wrong with the Scatchard analysis. *Trends Pharmacol. Sci.* 142-144.
- (5) Chung M.C.-M. (1985) A specific iron stain for iron-binding proteins in polyacrylamide gels: Application to transferrin and lactoferrin. *Analyt. Biochem.* 148: 498-502.
- (6) Ciechanover A., Schwartz A.L., Dautry-Varsat A. and Lodish H.F. (1983) Kinetics of internalization and recycling of transferrin and the transferrin receptor in a human hepatoma cell line. *J. Biol. Chem.* 258: 9681-9689.
- (7) Clarke M.H.G and Freeman T. (1968) Quantitative immuno-electrophoresis of human serum proteins. *Clin. Sci.* 35: 403.
- (8) Cleton M.I., Frenkel E.J., de Bruin W.C. & Marx J.M. (1986) Determination of iron to phosphorus ratios of iron storage compounds in patients with iron overload: a chemical and electron probe X-ray microanalysis. *Hepatol.* 5: 848-851.
- (9) Cuello A.C. and Carson S. (1983) Microdissection of fresh rat brain tissue slices. In: *Methods of Neurosciences.* (Ed: Cuello A.C.), Vol. 2, pp 37-125. John Wiley and Sons, publishers.
- (10) Harris D.C. (1978) Iron exchange between ferritin and transferrin in vitro. *Biochem.* 17: 3071-3078.
- (11) Hatton M.W.C. and Berry L.R. (1984) Location of bi- and tri-antennary N-glycans among heterogeneous forms of human serum transferrin: a topological study. *Biochem. Soc. Trans.* 12: 293-294.
- (12) Heyns W. and De Moor P. (1974) A3(17) β -Hydroxysteroid Dehydrogenase in rat erythrocytes. *Biochim. Biophys. Acta* 358: 1-13.
- (13) Horgan I.E. (1981) A modified spectrophotometric method for determination of nanogram quantities of sialic acid. *Clin. Chim. Acta* 116: 409-415.

Materials and methods.

- (14) Konijn A.M., Tal R., Levy R. & Matzner Y. (1985) Isolation and fractionation of ferritin from human placenta- A source for human isoferritins. *Analyt. Biochem.* 144: 423-428.
- (15) Méresse S., Dehouck M.P., Delorme P., Bensaïd M., Tauber J.P., Delbart C, Fruchart J.C. and Cecchelli R. (1989) Bovine brain endothelial cells express tight junctions and monoamine oxidase activity in long-term culture. *J. Neurochem.* 53: 1363-1371.
- (16) Mischeck U., Meyer J. and Galla H.J. (1989) Characterization of γ -glutamyl transpeptidase activity of cultured endothelial cells from porcine brain capillaries. *Tissue Res.* 256: 221-226.
- (17) Noiva R., Pete M.J. and Babin D.R. (1987) Bovine serum hemopexin: properties of the protein from a single animal. *Comp. Biochem. Physiol.* 88B: 341-347.
- (18) Penders T.J., de Rooy-Dijk H.H. and Leijnse B. (1968) Rapid isolation of ferritin by means of ultracentrifugation. *Biochem. Biophys. Acta* 168: 588-590.
- (19) Pietersma A, de Jong N, Sluiter w. and Koster J.F. (1992) Studies on the interaction of leucocytes and the myocardial vasculature. I. Adherence of granulocytes under hypoxic conditions. *Mol. Cell. Biochem.* 116: 197-202.
- (20) Pietersma A, de Jong N, Koster J.F. and Sluiter W. (1994) Effect of hypoxia on adherence of granulocytes to endothelial cells in vitro. *Am. J. Physiol.* 267 (Heart circ. Physiol. 36): H874-879.
- (21) Rao K.K., Shapiro D., Mattia E., Bridges K. and Klausner R. (1985) Effects of alterations in cellular iron on biosynthesis of the transferrin receptor in K 562 cells. *Molec. Cell. Biol.* 5: 595-600.
- (22) Roskams A.J.I. and Connor J.R. (1994) Iron, transferrin, and ferritin in the rat brain during development and aging. *J. Neurochem.* 63: 709-716.
- (23) Schägger H. & von Jagow G. (1987) Tricine - sodium dodecyl sulfate polyacrylamide gel electrophoresis for the separation of proteins in the range from 1 to 100 kDa. *Analytical Biochemistry* 166: 368-379.
- (24) Smith C.D., Carney J.M., Starke-Reed P.E., Oliver C.N., Stadtman E.R., Floyd R.A. and Markesbery W.R. (1991) Excess brain protein oxidation and enzyme dysfunction in normal and Alzheimer disease. *Proc. Natl. Acad. Sci. USA* 88: 10540-10543.
- (25) Sorber C.W.J., de Jong A.A.W., den Breejen N.J. and de Bruijn W.C. (1990) Quantitative energy-filtered image analysis in cytochemistry I. Morphometric analysis of contrast-related images. *Ultramicroscopy* 32: 55-68.
- (26) Sorber C.W.J., van Dort J.B., Ringeling P.C., Cleton-Soeteman M.I. and de Bruijn W.C. (1990) Quantitative energy-filtered image analysis in cytochemistry II. Morphometric

Chapter 2

W.C. (1990) Quantitative energy-filtered image analysis in cytochemistry II. Morphometric analysis of element-distribution images. *Ultramicroscopy* 32: 69-79.

(27) Spencer H.T., Pete M.J. and Babin D.R. (1990) Structural studies on porcine hemopexin. *Int. J. Biochem.* 22: 367-377.

(28) Starreveld J.S., Dijk J.P., Kroos M.J. and van Eijk H.G. (1993) Regulation of transferrin receptor expression and distribution in in vitro cultured human cytotrophoblasts. *Clin. Chim. Acta* 220: 47-60.

(29) Van Eijk H.G. and van Noort W.L. (1986) The reliability of the use of para toluene sulfonic acid for simultaneous hydrolysis and quantitation of both N-acetyl-glucosamine and amino acids in human transferrins. *Clin. Chim. Acta* 157: 305-310.

(30) Van Eijk H.G. and van Noort W.L. (1992) The analysis of human serum transferrins with the PhastSystem: quantitation of microheterogeneity. *Electrophoresis* 13: 354-358.

(31) Van Noort W.L. and van Eijk H.G. (1990) Quantification of monosaccharides occurring in glycoproteins at subnanomole levels using an automated LC analyser. *LC-GC Int* 3: 50-52.

(32) Williams L.R., Jodelis K.S. and Donald M.R. (1989) Axotomy-dependent stimulation of choline acetyltransferase by exogenous mouse nerve growth factor in the rat basal forebrain. *Brain Res.* 498: 243-256.

(33) Zellis K. and Wree A. (1985) Cortex: areal and laminar structure. In: *The rat nervous system.* (ed: Paxinos G.), Vol. 1, pp 375-415. Academic Press Inc., New York, USA.

CHAPTER 3

Isolation, purification and characterization
of porcine serum transferrin and hemopexin.

This chapter is based on:

W. van Gelder, M.I.E. Huijskes-Heins, C.J.
Hukshorn, C.M.H. de Jeu-Jaspars, W.L. van
Noort and H.G. van Eijk

(1995) Isolation, purification and characteri-
zation of porcine serum transferrin and hemo-
pexin. *Comp. Biochem. Physiol.* 111B; 171-179.

Chapter 3

§ 3.0 Contents.

§ 3.1: Summary.

§ 3.2: Introduction.

§ 3.3: Materials and methods:

§ 3.3.1: Chemicals.

§ 3.3.2: Isolation of porcine transferrin:

§ 3.3.2.1: Serum pretreatment.

§ 3.3.2.2: Column preparation.

§ 3.3.2.3: Separation procedure.

§ 3.3.2.4: Regeneration of the column.

§ 3.3.3: Isolation of porcine hemopexin.

§ 3.3.4: Analytical techniques.

§ 3.4: Results:

§ 3.4.1: Porcine transferrin.

§ 3.4.2: Porcine hemopexin.

§ 3.5: Discussion:

§ 3.5.1: Porcine transferrin.

§ 3.5.2: Porcine hemopexin.

§ 3.1 Summary.

Two techniques are described for the isolation of porcine serum transferrin and hemopexin respectively, yielding nearly pure proteins (>99%) as tested with crossed immunoelectrophoresis. Porcine transferrin has an estimated mass of 79 kDa and porcine hemopexin a mass of 62 kDa.

Both purified proteins were subjected to amino acid and carbohydrate analyses. Based on carbohydrate and sialic acid analyses, it is proposed that porcine transferrin contains one bi-antennary glycan chain, whereas porcine hemopexin contains two bi-antennary and one tri-antennary glycan chains.

§ 3.2. Introduction.

Research on the metabolism of iron in mammalian species has mainly been focussed on peripheral tissues. The presence of iron in brain tissue was already described by Spatz early this century (15). However, for decades only a few studies were available on this subject.

Iron metabolism of the brain (reviewed in 3) came in view again with the discovery of excess iron in certain areas of the brain, associated with neurological disorders e.g. Parkin-

Porcine transferrin and hemopexin isolation.

son's disease (10). Accumulated iron can have deleterious effects on tissues due to its catalytic role in the formation of oxygen free radical species (6,7).

Transferrin is an iron carrier protein present in a wide range of species in the animal kingdom (23). Although its function is not completely elucidated, transferrin is held responsible for a major part of intracorporal iron transportation (4). Contrary to peripheral iron metabolism, mechanism and regulation of iron uptake into the brain are largely unknown (20). However, large numbers of transferrin receptors have been found on the luminal side of blood-brain barrier endothelial cells (9), suggesting their involvement in this process.

Hemopexin is a serum glycoprotein with a single high affinity binding site for free heme. Due to this high affinity for free heme, hemopexin will scavenge heme molecules nonspecifically bound to other serum proteins (12). Endothelial cells can take up free heme, thereby rendering these cells more susceptible to oxidative damage (1). Since hemopexin prevents the heme uptake by endothelial cells, it may affect both iron metabolism and susceptibility to oxidative stress in these cells.

Our investigations on regulatory aspects of iron metabolism in porcine brain require porcine transferrin and hemopexin of a high purity ($\geq 99\%$). These proteins will be used for receptor-binding and transport experiments, in which the accuracy of the kinetic data greatly depends on the purity of these proteins (8). Furthermore, antibodies directed against these proteins had to be raised for histochemical purposes, again requiring a high purity standard.

To our knowledge, neither of these proteins is commercially available and literature on the purification of porcine transferrin and hemopexin is sparse (2,16). In our hands, none of the existing techniques yielded the required purity, as checked with crossed immunoelectrophoresis. We therefore developed modifications to existing techniques to reach our objectives.

Following purification, both proteins were further characterized by the amino acid composition and number and structure of N-linked carbohydrates.

Chapter 3

§ 3.3 Materials and methods.

§ 3.3.1 Chemicals.

Bovine serum albumin (BSA), Cibacron Blue 3GA and N-acetylneuraminic acid were obtained from Sigma (Sigma, USA). CM-Sepharose CL-6B, Sephadex G 100, Sephadex G 75 and Agarose IEF were purchased from Pharmacia/LKB (Pharmacia, Sweden). Bio-Gel A 1.5m (coarse) was obtained from Bio-Rad (Bio-Rad, The Netherlands). Goat anti-Swine total serum protein antibodies were purchased from Nordic (Nordic, The Netherlands). LMW-marker for PAGE was obtained from Pharmacia (Pharmacia, Sweden). All other chemicals used, were of the highest purity commercially available.

§ 3.3.2 Isolation of porcine transferrin.

§ 3.3.2.1 Serum pretreatment.

A detailed description of this procedure can be found in § 2.6.1.1. Briefly: fresh porcine plasma was saturated with excess iron, and dialyzed against a solution consisting of NaCl (0.14 mol/l) and CaCl₂ (0.01 mol/l), to precipitate fibrin. Following two precipitation steps with (NH₄)₂SO₄, the solution was dialyzed and stored at -20 °C until further use.

§ 3.3.2.2 Column preparation.

Briefly: BioGel A 1.5m was coupled to Cibacron Blue 3GA at 45 °C in the presence of Na₂CO₃ and loaded on a column. The gel was equilibrated with start-, gradient- and regeneration buffer (see below) before sealing the column. Details of this procedure can be found in § 2.6.1.2.

§ 3.3.2.3 Separation procedure.

This procedure is described in § 2.6.1.3. Briefly: a sample of the pretreated serum was loaded onto the column, followed by circa 3 column volumes 1.54 mmol/l NaN₃ (startbuffer). Porcine transferrin was eluted with a linear phosphate buffer gradient.

Porcine transferrin and hemopexin isolation.

§ 3.3.2.4 Regeneration of the column.

The procedure for the regeneration of the column is described in § 2.6.1.4.

§ 3.3.3 Isolation of porcine hemopexin.

A detailed description of this isolation procedure can be found in § 2.6.2. Briefly: fresh pooled porcine serum was treated as outlined above to remove fibrin, precipitated with 50 % $(\text{NH}_4)_2\text{SO}_4$ and the supernatant dialyzed against 0.01 mol/l sodium citrate buffer. Aliquots were applied to a CM-Sepharose CL-6B column, and the column was then rinsed with 0.01 mol/l sodium citrate buffer. Next, a linear (0.01 to 0.08 mol/l) gradient of sodium citrate was developed to elute hemopexin and transferrin. Hemopexin containing fractions were concentrated and loaded on a Sephadex G 100 column, followed by a Sephadex G 75 column to remove contaminants.

§ 3.3.4 Analytical techniques.

Several techniques were used to assess the purity of the isolated porcine transferrin and hemopexin. A detailed description of these techniques can be found in chapter 2.

Transferrin and hemopexin containing samples obtained in either isolation procedure were subjected to the following analytical procedures:

- Native polyacrylamide gel electrophoresis (PAGE)
- Sodium dodecyl sulfate polyacrylamide gel electrophoresis - (SDS)-PAGE
- Isoelectric focussing
- Crossed immunoelectrophoresis
- Sepharose-concanavalin A chromatography:
- Protein concentration measurements:
- Carbohydrate analyses:
- Analyses of N-acetylglucosamine and amino acids
- Sialic acid quantification

§ 3.4 Results.

§ 3.4.1 Porcine transferrin.

Applying pretreated porcine serum to a BioGel-Cibacron Blue column resulted in chromatograms as depicted in *Fig. 3.1^A*. The number of peaks that could be discriminated

during development of the phosphate buffer gradient usually varied from 4 to 6.

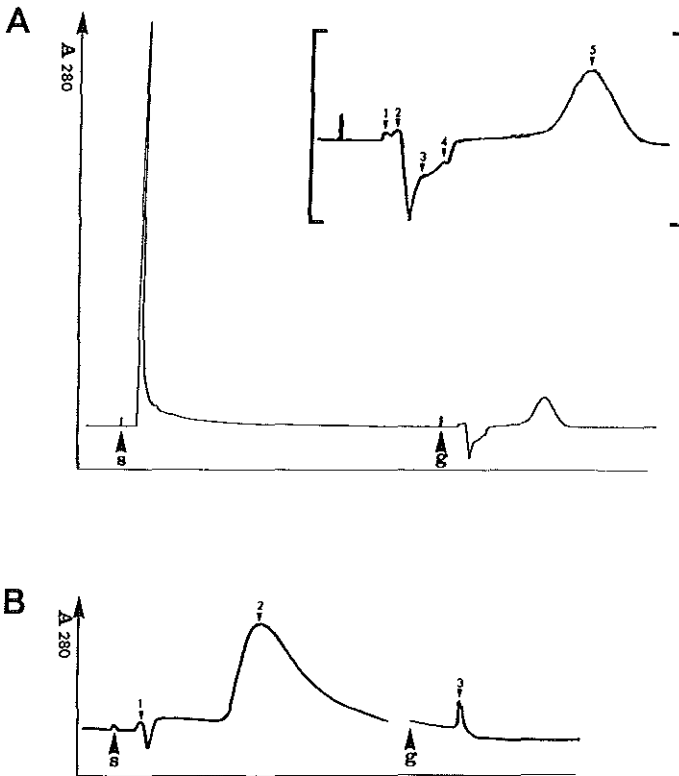


Fig. 3.1:

A:
Serum, subjected to a number of precipitation steps was loaded on a Cibacron Blue 3GA linked to BioGel A 1.5m column. A typical elution profile is shown in A. S: sample application; G: start of the phosphate gradient.

The insert (between brackets) shows a magnification of the chromatogram upon developing the phosphate gradient. 1 - 5 indicate the separate transferrin containing peaks that could be discerned. Peak 5 contained transferrin in a nearly pure (> 99.5%) form.

Porcine transferrin and hemopexin isolation.

B:

Purified porcine transferrin was applied to a Sepharose-linked concanavalin A column. Three peaks could be detected (1-3). Peak 2 (97%) was used for further analysis. S: sample application; G: start α -methyl glucopyranoside buffer.

A sample of each peak was applied to native gradient (8-25%) PAGE (Fig. 3.2^A) and SDS-PAGE (Fig. 3.2^B), showing that only transferrin was present in the last peak. The double transferrin band present in native gradient gels appeared as a single band when samples were applied to SDS-PAGE (Figs. 3.2^A and 3.2^B).

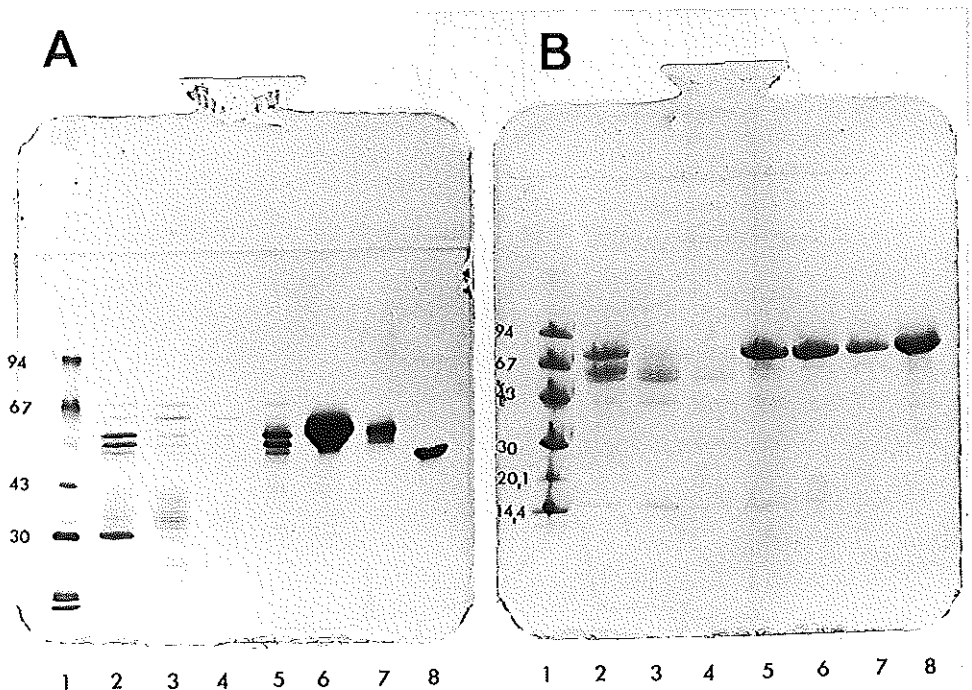


Fig. 3.2:

A:

Samples from transferrin containing fractions resulting from the BioGel/Cibacron Blue column (peak 1-5, Fig. 1) were applied to native gradient (8-25%) PAGE. Lane 1: LMW marker in kDa; lane 2: peak 1; lane 3: peak 2; lane 4: peak 3; lane 5: peak 4; lane 6: peak 5, 10 times concentrated; lane 7: peak 5; lane 8: human 4 sialo transferrin.

Chapter 3

B:

Identical samples were also applied to SDS-PAGE (8-25% gradient). Lane 1-8: see legends to A.

Samples from this last transferrin peak were subjected to crossed immunoelectrophoresis to assess its purity (*Fig. 3.3*). Repeated experiments with this technique, varying the transferrin/antibody ratio, showed transferrin to be over 99.5% pure.

Isoelectric focussing of purified transferrin yielded 3 major diferric and two monoferric bands (*Fig. 3.4*) ranging from pH 5.60 to 6.30.

Purified transferrin was fractionated on a Sepharose-linked concanavalin A column in three separate fractions (*Fig. 3.1^B*). About 97% was located within the second fraction and samples from this fraction were used for amino acid and carbohydrate analyses. Results of transferrin amino acid analyses are summarized in *table 3.1* and compared to porcine transferrin data described by Welch (22) and human transferrin amino acid sequence data from MacGillivray et al (11). Data on carbohydrate and sialic acid residue analyses are summarized in *table 3.2*.

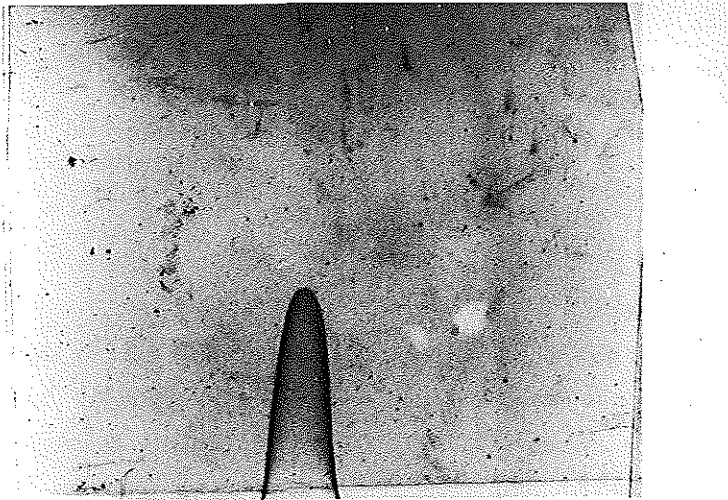


Fig. 3.3: Purified transferrin (peak 5, *Fig. 1*) was subjected to crossed immunoelectrophoresis. Electrophoresis in the first direction was performed in a 1% agarose gel. Electrophoresis in the second direction was performed in a gel containing rabbit anti pig serum protein antibodies. Only one precipitation arc could be detected.

Porcine transferrin and hemopexin isolation.

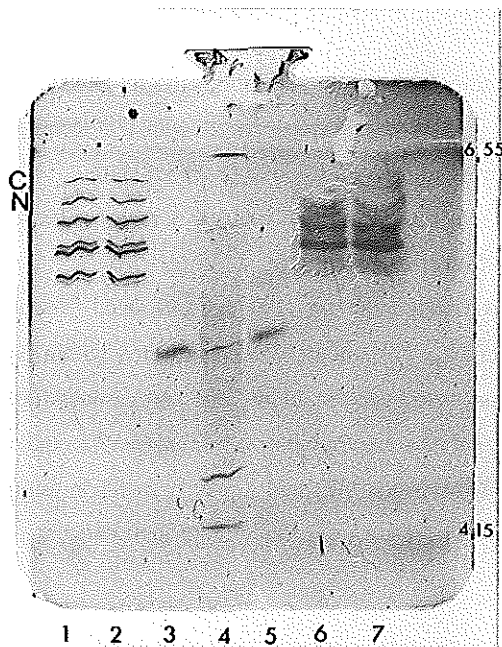


Fig. 3.4:

Purified porcine transferrin and hemopexin were applied to a PhastGel IEF (pH 4-6.5) for isoelectric focussing. Lane 1 and 2: purified transferrin; lane 3 and 5: human 4 sialo transferrin, pI= 5.25; lane 4: pI marker; lane 6 and 7: purified hemopexin. C: Monoferric transferrin with Fe bound to the C-terminal binding site. N: Monoferric transferrin with Fe bound to the N-terminal binding site.

§ 3.4.2 *Porcine hemopexin.*

Hemopexin, isolated according to the procedure described (see § 3.3.3), showed a single band when subjected to native gradient PAGE (*Fig. 3.5*). Purity of hemopexin was confirmed, subjecting samples to crossed immuno-electrophoresis. Electrophoresis in the second dimension was performed against porcine serum protein antibodies. Repeated runs showed that impurities were less than 1% of the total protein concentration (*Fig. 3.6*).

Isoelectric focussing of purified hemopexin yielded at least 4 discernible bands (*Fig. 3.4*) in the range of pH 5.60 to 6.45.

Chapter 3

Data on porcine hemopexin amino acid analyses are summarized in *table 3.1* and compared to values from Spencer (16). The data on carbohydrate and sialic acid analyses are summarized in *table 3.2*.

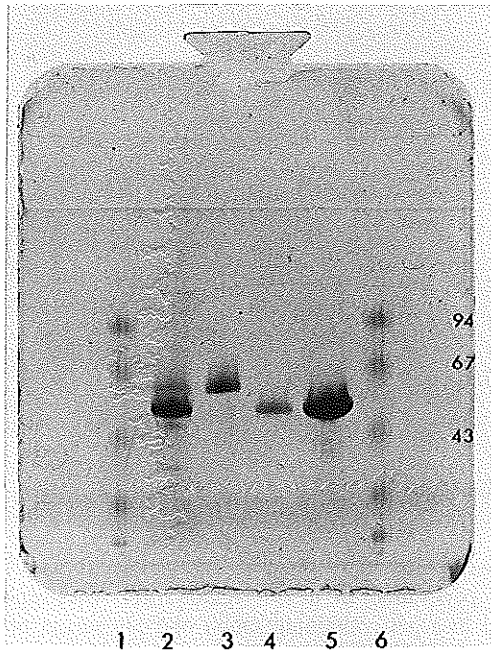


Fig. 3.5:

A hemopexin containing sample from the ion-exchange column and purified hemopexin were subjected to native gradient PAGE (8-25% gradient). Lane 1 and 6: LMW-marker in kDa; lane 2: hemopexin containing sample resulting from the CM-Sepharose CL-6B column; lane 3: purified porcine transferrin; lane 4: purified hemopexin; lane 5: purified hemopexin, 10 times concentrated.

Porcine transferrin and hemopexin isolation.

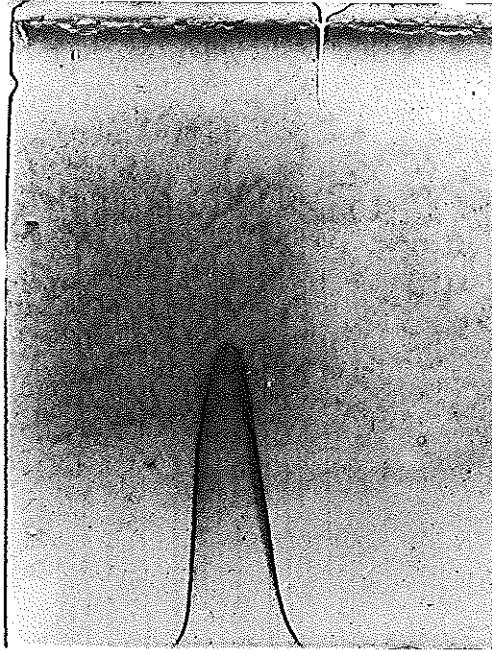


Fig. 3.6:

Purified hemopexin was subjected to crossed immunoelectrophoresis. Electrophoresis in the first direction was performed in a 1% agarose gel. Electrophoresis in the second direction was performed in a gel containing rabbit anti pig serum protein antibodies. Only one precipitation arc could be detected.

§ 3.5 Discussion.

§ 3.5.1 Porcine transferrin.

Our research on iron metabolism in porcine brain required transferrin with a high degree of purity (> 99%). Extensive series of experiments were performed in an attempt to purify porcine transferrin. However, various combinations of ammonium sulfate precipitation, preparative isoelectric focussing, gel-filtration and ion-exchange chromatography (as

Chapter 3

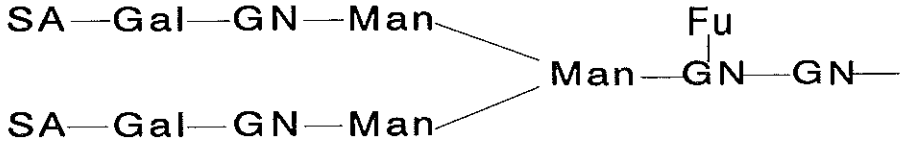
described in 23) never yielded transferrin with the desired degree of purity.

Of all existing techniques, isolation of porcine transferrin by means of a BioGel/Cibacron Blue column according to Baumstark (2), in our hands yielded the highest purity (about 80-85%). A number of modifications were tried and checked with crossed immunoelectrophoresis, resulting in an isolation procedure as described in chapter 2. The purity of the resulting transferrin fraction improved upon modification of the phosphate gradient, especially if a less steep gradient (0 to 0.1 mol/l) was applied. Based on the results of electrophoresis (*Fig. 3.2^A and 3.2^B*), all peaks except for the last (*Fig. 3.1^A*) were discarded. Because of this, a considerable amount of transferrin was lost (serum transferrin yield: \pm 35%), but the remaining transferrin fraction was nearly 100% pure. Purity was checked subjecting samples to crossed immunoelectrophoresis, which is a very sensitive technique to analyze proteins with a (near) identical electrophoretic behaviour (21). Moreover, in crossed immunoelectrophoresis the area underneath a peak is proportional to the protein concentration. Impurities could only be detected, if the top of the transferrin peak exceeded the upper edge of the gel. Peak area measurements indicated that transferrin in this fraction was over 99.5% pure.

Prior to amino acid and carbohydrate analyses, porcine transferrin was applied to a Sepharose-linked concanavalin A column. This enabled assessment of transferrin heterogeneity due to structural variations in the N-linked glycan chain(s). In this way, porcine transferrin could be separated in three fractions. Carbohydrate analysis of the second con A fraction (*table 3.2*) suggests that a major part of porcine transferrin (97%) contains one N-linked biantennary glycan chain. This is in agreement with the finding of 2 sialic acid residues per molecule porcine transferrin, both in our experiments and by Welch (22). Based on these findings and considering known outer chain sequence variations (4,17) we therefore propose a glycan chain structure in porcine transferrin as depicted in *Fig. 3.7^A*. Rhamnose as well as human 4-sialo transferrin (with two bi-antennary glycans) were used as an internal standard in this procedure.

The amino acid composition of porcine transferrin (con A II) is shown in *table 3.1* and compared to the results obtained by Welch (22). Results of both analyses were not identical, which could either be due to differences in analytical techniques or to differences in the isolation procedure.

A: Bi-antennary chain



B: Tri-antennary chain

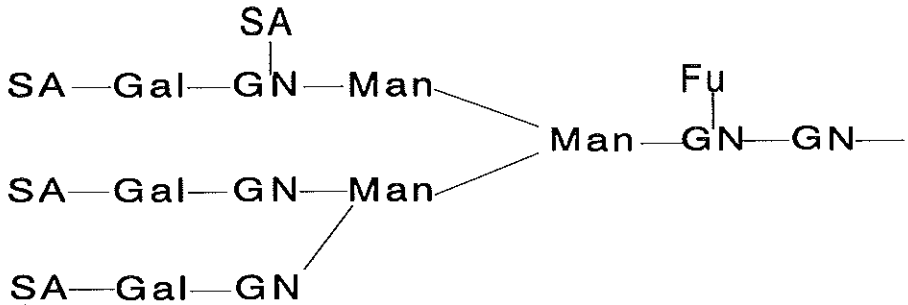


Fig. 3.7:

Proposed glycan chain structures for porcine transferrin and hemopexin (see text). Adapted from De Jong et al (3.07 De Jong 1990). A: proposed structure of a bi-antennary glycan chain. B: proposed structure of a tri-antennary glycan chain. SA: sialic acid; Gal: galactose; GN: N-acetyl glucosamine; Man: mannose; Fu: fucose.

In our procedure however, pure human 4 sialo transferrin (prepared according to 5) was used as an internal standard in each run and analyzed according to the same technique. Results of these analyses were compared to known amino acid sequence data (11) and were found to vary less than 2%.

Isoelectric focussing of porcine transferrin resulted in 5 bands (Fig. 3.4). The upper two bands (marked C and N) are most likely monoferric bands, as they disappeared upon additional iron loading of transferrin. The next three major bands are probably due to a

Chapter 3

variation in the number of sialic acid residues in the N-linked glycans, better known as the microheterogeneity pattern of transferrin (4). The minor bands visible, are probably due to genetic variation, as transferrin was isolated from pooled serum.

§ 3.5.2 Porcine hemopexin.

Hemopexin is a specific serum β -glycoprotein present in mammalian species, with a single high affinity binding site for heme (12). To date, only limited knowledge exists as to the mechanism of transport and internalization of heme (13). A receptor-mediated transport system is proposed in human Hep G2 cells (14), where hemopexin re-enters the circulation after releasing heme. Upon degradation, heme iron is recovered for further use. This would therefore implicate a second transmembrane iron transport mechanism (besides transferrin). In this respect, Taketani et al (18) found evidence that iron released from heme reduces transferrin mediated iron uptake. The binding of the heme-hemopexin complex to blood-brain barrier derived endothelial cells is currently under investigation.

The isolation of porcine hemopexin consisted of a combination of an ion-exchange and several gel filtration chromatography steps, modified from a technique described by Spencer et al (16). Adaptations included changes in pH and gradient of the ion-exchange column buffer, and application of both a Sephadex G 100 and a Sephadex G 75 column to optimize purification of hemopexin. Hemopexin containing fractions from each isolation step were routinely checked for contaminating proteins, by applying samples to native gradient PAGE (*Fig. 3.5*). A more accurate estimate of purity (discussed above) was obtained subjecting samples to crossed immunoelectrophoresis (*Fig. 3.6*). Repeated experiments, varying both the amount of hemopexin and antibodies, indicated that hemopexin obtained in this manner was over 99% pure.

Data on amino acid analyses of purified porcine hemopexin are summarized in *table 3.1*. On average, our analyses yielded somewhat higher results when compared to data presented by Spencer et al (16). This is possibly due to a milder protein hydrolysis step prior to amino acid analysis (19). Pure human 4 sialo transferrin (5) with 2 biantennary glycan chains was used as an internal standard for both carbohydrate and amino acid analyses.

Carbohydrate analyses on porcine hemopexin (data summarized in *table 3.2*) suggest it to contain 2 biantennary and 1 triantennary glycan chains (*Fig. 3.7^A and 3.7^B*).

Porcine transferrin and hemopexin isolation.

Amino acid residues	Tf ConA II	Pig Tf Welch	Hu-Tf sequence	Hpx	Hpx Spencer
Asp	84	78	79	51	42
Thr	29	23	30	22	25
Ser	50	50	41	40	31
Glu	70	73	60	41	36
Gly	46	42	49	47	35
Ala	61	56	57	31	29
Val	45	40	45	30	26
1/2 Cys	28*	28	38	29*	29
Met	7	6	9	4	4
Ile	19	23	15	9	10
Leu	49	58	58	41	39
Tyr	24	24	25	16	22
Phe	25	26	29	20	18
Lys	54	62	58	25	26
His	13	26	19	19	19
Arg	26	30	26	32	26
Trp	7	3	8	16*	16
Pro	17*	17	17*	12*	12
Total no of residues.	654	665	663	485	454

Table 3.1:

Results on amino acid analyses of purified porcine transferrin and hemopexin are summarized in this table. Both are compared to known values from literature. For porcine transferrin: Welch (3.13 Welch 1990) and for hemopexin: Spencer et al (3.12 Spencer 1990). Human transferrin amino acid sequence data are shown as reference. Results shown are an average of duplo analyses of 3 separately obtained purified protein fractions. * data obtained from literature.

Residues:	Transferrin	Hemopexin
N-acetyl glucosamine	4	n.d.
Mannose	3	9
Galactose	2	7
Fucose	1	3
Sialic acid	2	8

Table 3.2:

Results on carbohydrate and sialic acid analyses of purified porcine transferrin and hemopexin are summarized in this table.

Results shown are an average of duplo analyses of 3 separately obtained purified protein fractions.

n.d.: analyses not performed.

Based on the results of these analyses, the molecular weight of porcine hemopexin (including glycan chains) is estimated to be 62.2 kDa.

In summary, we describe two techniques for the purification of porcine transferrin and hemopexin, respectively. Both transferrin and hemopexin could be isolated in nearly pure form, which was checked with both SDS- and crossed immunoelectrophoresis. Carbohydrate analyses suggest that transferrin carries one biantennary glycan chain, whereas hemopexin contains 2 biantennary and one triantennary glycan chains. Based on both amino acid and carbohydrate analyses, the molecular weight of hemopexin is estimated to be 62.2 kDa. Based on SDS-electrophoresis, the molecular weight of transferrin is estimated to be nearly equal to that of human transferrin (± 79 kDa).

Porcine transferrin and hemopexin isolation.

References.

- (1) Balla G., Vercellotti G.M., Muller-Eberhard, Eaton J. and Jacob H.S. (1991) Exposure of endothelial cells to free heme potentiates damage mediated by granulocytes and toxic oxygen species. *Lab. Invest.* 64: 648-655.
- (2) Baumstark J.S. (1987) A simple one-column procedure for the separation of swine and human serum transferrins. *J. Biochem. Biophys. Meth.* 14: 59-70.
- (3) Connor J.R. (1993) Cellular and regional maintenance of iron homeostasis in the brain: normal and diseased states. In: *Iron in central nervous system disorders.* (Eds: Riederer P. and Youdim M.B.H.), pp. 1-18. Springer-Verlag, New York.
- (4) De Jong G., van Dijk J.P. and van Eijk H.G. (1990) The biology of transferrin. *Clin. Chim. Acta* 190: 1-46.
- (5) De Jong G., van Noort W.L. and van Eijk H.G. (1992) Carbohydrate analysis of transferrin subfractions isolated by preparative isoelectric focusing in immobilized pH gradients. *Electrophoresis* 13: 225-228.
- (6) Floyd R.A. and Carney J.M. (1992) Free radical damage to protein and DNA: Mechanisms involved and relevant observations on brain undergoing oxidative stress. *Ann. Neurol.* 32: S22-27.
- (7) Gutteridge J.M.C. and Halliwell B. (1989) *Baillière's Clinical Haematology*, Vol 2 (2): 195-256.
- (8) Hulme E.C. and Birdsall J.M. (1992) Strategy and tactics in receptor-binding studies. In: *Receptor-ligand interactions. A practical approach.* (Ed: Hulme E.C.), pp. 63-176. Oxford University Press, New York.
- (9) Jefferies W.A., Brandon M.R., Hunt S.V., Williams A.F., Gatter K.C. and Mason D.Y. (1984) Transferrin receptor on endothelium of brain capillaries. *Nature* 312: 162-163.
- (10) Jellinger K. and Kienzl E. (1993) Iron deposits in brain disorders. In: *Iron in central nervous system disorders.* (Eds: Riederer P. and Youdim M.B.H.), pp. 19-36. Springer-Verlag, New York.
- (11) MacGillivray R.T.A., Mendez E., Sinha S.K., Sutton M.R., Lineback-Zins J. and Brew K. (1982) The complete amino acid sequence of human serum transferrin. *Proc. Natl. Acad. Sci. USA* 79: 2504-2508.
- (12) Muller-Eberhard U. (1988) Hemopexin. *Meth. Enzymol.* 163: 536-565.
- (13) Muller-Eberhard U. and Fraig M. (1993) Bioactivity of heme and its containment. *Am. J. Hematol.* 42: 59-62.

Chapter 3

- (14) Smith A. and Hunt R.C. (1990) Hemopexin joins transferrin as representative members of a distinct class of receptor-mediated endocytic transport systems. *Eur. J. Cell Biol.* 53: 234-245.
- (15) Spatz H. (1922) Über den Eisennachweis im Gehirn, besonders in Zentren des extrapyramidal-motorischen systems. *Z. Ges. Neurol. Psychiat. Berl.* 77: 261-290.
- (16) Spencer H.T., Pete M.J. and Babin D.R. (1990) Structural studies on porcine hemopexin. *Int. J. Biochem.* 22 (4): 367-377.
- (17) Spik G., Coddeville B., Legrand D., Mazurier J., Leger D., Goavec M. and Montreuil J. (1985) A comparative study of the primary structure of glycans from various sero-, lacto- and ovotransferrins. Role of human lactotransferrin glycans. In: *Proteins of iron storage and transport.* (Eds: Spik G., Montreuil J., Crighton R.R. and Mazurier J.), pp. 47-51. Elsevier Science Publishing Company Inc., New York, USA.
- (18) Taketani S., Kohno H., Sawamura T. and Tokunaga R. (1990) Hemopexin-dependent down-regulation of expression of the human transferrin receptor. *J. Biol. Chem.* 265: 13981-13985.
- (19) Van Eijk H.G. and van Noort W.L. (1986) The reliability of the use of para toluene sulfonic acid for simultaneous hydrolysis and quantitation of both N-acetyl-glucosamine and amino acids in human transferrins. *Clin. Chim. Acta* 157: 305-310.
- (20) Van Gelder W., Huijskes-Heins M.I.E., van Dijk J.P., Cleton-Soeteman M.I. and van Eijk H.G. (1995) Quantification of different transferrin receptor pools in primary cultures of porcine blood-brain barrier endothelial cells. *J. Neurochem.* 64: 2708-2715.
- (21) Weeke B. (1973) Crossed immunoelectrophoresis. In: *Quantitative immunoelectrophoresis.* (Eds: Axelsen N.H., Kroll J. and Weeke B.), pp 47-56. Universitetsforlaget, Oslo, Norway.
- (22) Welch S.A. (1990) Comparison of the structure and properties of serum transferrin from 17 animal species. *Comp. Biochem. Physiol.* 97B (3): 417-427.
- (23) Welch S.A. (1992) Transferrin structure and iron binding. In: *Transferrin : the iron carrier.* (Ed: Welch S.A.), pp. 61-108. CRC Press, Boca Raton, USA.

CHAPTER 4

Isolation and partial characterization of a 440 kDa and a 660 kDa porcine spleen ferritin fraction.

This chapter is based on:

W. van Gelder, M.I.E. Huijskes-Heins, D. Klepper, W.L. van Noort, M.I. Cleton-Soeteman and H.G. van Eijk

*(1995) Isolation and partial characterization of a 440 kDa and a 660 kDa porcine spleen ferritin fraction.
Submitted.*

Chapter 4

§ 4.0 Contents.

§ 4.1: Summary.

§ 4.2: Introduction.

§ 4.3: Materials and methods:

§ 4.3.1: Materials.

§ 4.3.2: Isolation and subfractionation of porcine spleen ferritin.

§ 4.3.2.1: Ferritin isolation method 1.

§ 4.3.2.2: Ferritin isolation method 2.

§ 4.3.3: Separation of isoferritins.

§ 4.3.4: Preparation and operation of the combined Sepharose 4B and Sepharose 6B columns.

§ 4.3.5: Analytical techniques.

§ 4.3.6: Quantitative techniques.

§ 4.3.7: Statistical analyses.

§ 4.4: Results.

§ 4.5: Discussion.

§ 4.1 Summary.

Ferritin isolated from different organs, obtained from three different mammalian species, could routinely be separated in a 440 and 660 kDa fraction on non-denaturing gradient gels. Both fractions could be isolated with a purity of 96% when applied to two serially linked columns, each 200 cm in length, packed respectively with Sepharose 4B and Sepharose 6B. Both fractions were equal with respect to subunit composition, iron and phosphorus content, as well as amino acid composition, with the exception of N-acetylglucosamine. Carbohydrate analysis showed that the 440 kDa fraction contained 1.8% (w/w) glycans, whereas the 660 kDa fraction contained nearly 5 times as much (neutral) sugar residues (8.9%, w/w) and 10 times as much sialic acid. Although not explanatory for the apparent difference in mass, the difference in amount of charged side chains can at least partially explain the dissimilarity in electrophoretic mobility of the two fractions.

§ 4.2 Introduction.

Prokaryotic and eukaryotic cells all contain ferritin as their major iron storage protein. According to the "classical" idea ferritin protein is composed of 24 subunits of two types:

440 and 660 kDa spleen ferritin.

the H-type of circa 21 kDa and the L-type of circa 19 kDa amounting to a total mass of circa 450 kDa. Inter- and intraspecies heterogeneity was explained by the various proportions in which the subunits assemble. Arranged with 4:3:2 symmetry the subunits form a hollow shell, in which up to 5000 iron atoms can be stored (10,11, reviewed 1 and 4).

Although it was accepted that serum ferritins were glycosylated and tissue ferritins were not (5), the existence of a small amount of associated carbohydrates in horse spleen (21), and in human spleen, liver and heart have been reported (3,14,18). The amount however, is still a subject for discussion.

Refinement in biochemical research resulted from 1980 onwards in reports on ferritins of different molecular weights due to either assembly of more than 24 subunits (15) or to attachment of a non-ferritin component (19). Passaniti et al (16) report on ferritin intermediates of lower molecular weight next to the common ferritin of around 440 kDa. Moreover, other authors describe either a subunit of different amino acid composition (2), or different classes of subunits besides the well known H and L subunits (6).

Our current research on porcine brain iron metabolism requires ferritin of a high purity. After improvement of a standard method for the isolation of porcine ferritin, we found next to the expected 440 kDa a substantial portion of this ferritin (30%) to consist of an iron-containing protein of 660 kDa. Testing horse spleen ferritin as a reference we also found the two components in about the same ratio. We decided to further explore these findings and to report on the composition of subunits, amino acids and carbohydrates of the two acquired porcine spleen isoferritins.

§ 4.3 Materials and methods.

§ 4.3.1 Materials.

Fresh porcine spleens were obtained from the local slaughterhouse, transported and kept on ice until further processing. Horse spleen ferritin, BSA (bovine serum albumin) and PMSF (Phenylmethylsulfonylfluoride) were obtained from Sigma (USA). Sepharose 4B, Sepharose 6B and Sephadex G 200 were purchased from Pharmacia/LKB (Pharmacia, Sweden). All other chemicals were of the highest purity commercially available.

Polyacrylamide gel electrophoresis were performed on both Mini protean system 2 (BioRad,

Chapter 4

the Netherlands), and Phastsystem (Pharmacia/LKB, Sweden).

§ 4.3.2 *Isolation and subfractionation of porcine spleen ferritin.*

§ 4.3.2.1 *Ferritin isolation method 1.*

A detailed description of this isolation procedure can be found in § 2.6.3.1. Briefly: porcine spleen ferritin was isolated according to a method adapted from Penders (17). Fresh spleen tissue was homogenized, heated (80 °C, 5 min) and then rapidly cooled and centrifuged (3000 g, 45 min). The supernatant was then subjected to a number of centrifugation steps to yield ferritin with a high purity as confirmed by native and Tricine-SDS PAGE.

§ 4.3.2.2 *Ferritin isolation method 2.*

Ferritin was also isolated according to a precipitation technique described by Konijn (13). This procedure yielded ferritin with a degree of purity comparable to that of ferritin obtained by method 1. A description of this isolation procedure can be found in § 2.6.3.2.

§ 4.3.3 *Separation of isoferritins.*

Porcine spleen ferritin was separated into acid, intermediate and basic fractions by ion-exchange chromatography on a DEAE-Sephadex A-25 column. This procedure was described by Konijn et al (13).

§ 4.3.4 *Preparation and operation of the combined Sepharose 4B and Sepharose 6B columns.*

Ferritin, purified according to either method 1 or 2, could be separated in a 440 and 660 kDa fraction (see discussion) when applied to two serially linked sepharose 4B and 6B columns. A description of the preparation and operation of these columns can be found in § 2.6.3.4.

§ 4.3.5 *Analytical techniques.*

Detailed descriptions of the analytical techniques can be found in chapter 2.

440 and 660 kDa spleen ferritin.

On a Mini protean system 2, samples were subjected to:

- Native polyacrylamide gel electrophoresis (PAGE).
- Sodium dodecyl sulfate polyacrylamide gel electrophoresis (SDS-PAGE).
- Tricine-SDS Polyacrylamide gel electrophoresis (L and H subunit ratio's).

On a Phastsystem, samples were subjected to:

- Native polyacrylamide gel electrophoresis (PAGE).
- Sodium dodecyl sulfate polyacrylamide gel electrophoresis (SDS-PAGE).
- Isoelectric focussing.

Ouchterlony double immuno diffusion assays were used in:

- Alpha-2-macroglobulin assay.
- Ferritin / anti-440 kDa and anti 660 kDa ferritin assays.

§ 4.3.6 *Quantitative techniques.*

Detailed descriptions of these techniques can be found in chapter 2.

- Protein, iron and phosphorus assays.
- Determination of the iron to phosphorus ratio with electron probe microanalysis (EPMA).
- Carbohydrate analyses.
- Amino acid analyses.
- Sialic acid quantification.

§ 4.3.7 *Statistical analysis.*

Data sets were analyzed with a Bonferroni *t* test following a "repeated-measures analysis of variance" to test differences in amino acid and carbohydrate composition between the "crude" (see § 4.4), 440 kDa and 660 kDa ferritin fractions.

§ 4.4 Results.

Porcine spleen ferritin isolated according to the two procedures described and henceforward referred to as "crude" ferritin, always yielded two distinct bands when applied to a native 4-15% gradient gel (*Fig. 1, lane 4*) on the Phastsystem. A vague third band (*Fig. 1, lane 3*) with an estimated mass of around 850 kDa, appeared more clearly when the ferritin solution was left to stand for a number of weeks.

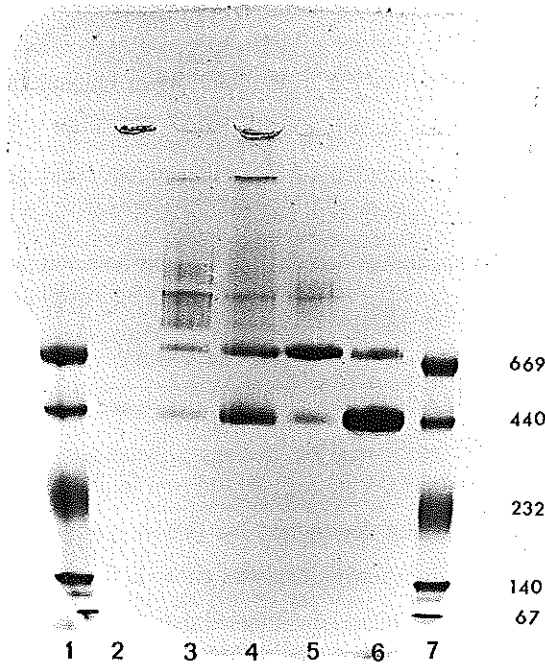


Fig. 4.1:

Native polyacrylamide gel, 4-15% gradient. Samples were obtained after separation on two linked Sepharose 4B and 6B columns. Lane 1: high molecular weight marker (in kDa). Lane 2: first ferritin peak to appear in gel-filtration, consisting of ferritin aggregates. Lane 3: second ferritin peak to appear in gel-filtration, consisting of ferritin aggregates. Lane 4: "crude" ferritin fraction. Lane 5: 660 kDa fraction after 2nd run. Lane 6: 440 kDa fraction after 2nd run, purity is 89%. Lane 7: high molecular weight marker (in kDa).

The marker proteins (Fig. 1, lane 1 & 7) defined the largest band to be located around 440 kDa and the second band around 660 kDa. The two large dark spots at the top of lane 4 (Fig. 1) are ferritins with a molecular weight over 1000 kDa, that did not penetrate the separating gel. Similar results were obtained with native gradient gels (8-25%) on a mini protean system (BioRad). Surprisingly, both major bands were also distinctly present in commercially available horse spleen and human placental ferritin (courtesy Dr J.P. van Dijk). In all cases both bands stained positively for protein and iron. Densitometric analyses showed that about 30% of fresh porcine spleen ferritin was located in the 660 kDa

440 and 660 kDa spleen ferritin.

band (*Fig. 1, lane 4*). "Crude" ferritin from either isolation procedure was separated on a DEAE column with a NaCl-gradient (13). At least 4 subspecies could be separated, which each showed a 440 kDa and 660 kDa band when applied to a native gradient gel. Isoelectric focussing of "crude" ferritin resulted in multiple bands ranging from pH 4.8 to 5.2. Applying "crude" ferritin samples to two serially linked Sepharose columns (see § 4.3.4) resulted in a nearly complete separation of the 440 and 660 kDa bands. Densitometric analysis of native gradient gels showed each band to be over 96% pure after three runs.

The L- and H-subunit composition of "crude" ferritin and both the purified 660 and 440 kDa fractions was assessed using both SDS-PAGE and Tricine SDS-PAGE. Results of the 16.5% Tricine SDS-PAGE are shown in *Fig. 2*. Densitometric analysis confirmed a predominance of L-subunits (60%) in each of the samples. The L to H ratios in the three samples were not significantly different.

In *Table I* biochemically obtained iron to protein and iron to phosphorus ratios are shown. The latter are compared to results determined by EPMA. As no difference was found between EPMA data acquired from ferritin analyses either in the pyroform holes or on the film itself, the ratios given are the mean of combined data sets.

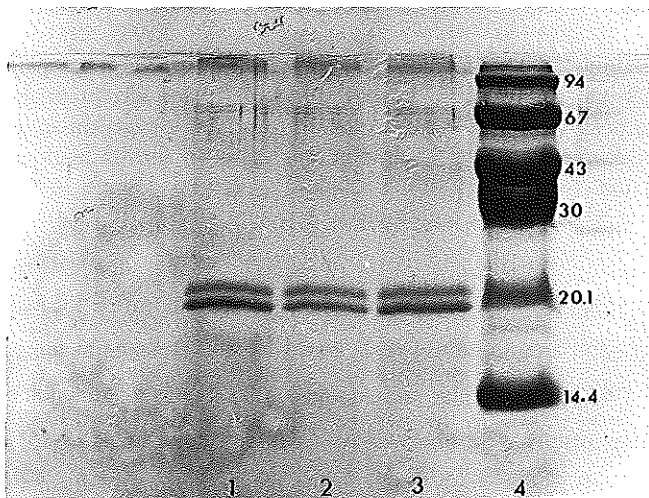


Fig. 4.2:

Tricine-SDS polyacrylamide gel (16.5% T; 3% C). Samples were obtained after separation on a Sephadex G 200 column. Lane 1: 440 kDa fraction after 4th run. Lane 2: 660 kDa fraction after 3rd run. Lane 3: crude ferritin. Lane 4: low molecular weight marker in kDa.

Chapter 4

Porcine spleen ferritins	mol Fe/mol ferritin (n = 6)	Fe/P ratio (biochem.) (n = 6)	Fe/P ratio (EPMA) (n = 30)
"crude" ferritin	1700 ± 219	# 8.3 ± 1.1	# 17.5 ± 4.9
660 kDa fraction	1675 ± 244	23.5 ± 11.5	31.9 ± 13.3
440 kDa fraction	1638 ± 132	30.3 ± 21.2	33.6 ± 14.4

Table 4.1:

Data were obtained from three individual isolation procedures in duplo. A # indicates a significant difference ($p < 0.05$) from the other values in that column.

The means of 6 individual amino acid analyses of three batches of "crude" porcine spleen ferritin and both fractions are summarized in *Table II*. Only the N-acetyl glucosamine content of the 440 and 660 kDa fractions was significantly different ($p < 0.02$) as shown by repeated-measures analysis of variance, followed by a Bonferroni *t* test.

Carbohydrate and sialic acid analyses of all fractions are shown in *Table III*. Despite considerable variation in glucose content between batches, a consistent 5:1 ratio in total carbohydrate content (a 10:1 ratio for sialic acid) was found between 660 and 440 kDa fractions, respectively.

440 and 660 kDa spleen ferritin.

rel. % amino acids	"crude" ferritin	660 kDa fraction	440 kDa fraction
Asp	11.6	12.6	12.8
Thr	4.8	4.2	3.9
Ser	9.3	7.0	6.6
Glu	14.1	15.0	16.0
Gly	8.4	8.3	7.5
Ala	8.3	8.3	7.5
Val	4.5	4.1	3.8
Met	2.2	2.0	2.2
Ile	2.4	2.1	1.6
Leu	11.0	11.6	12.8
Trp	n.d.	n.d.	n.d.
Tyr	3.2	3.2	3.3
Phe	3.9	3.9	4.2
GlcNH ₂ *	0.6	1.0	0.4
His	3.7	3.9	4.3
Lys	5.4	5.7	5.7
Arg	5.2	5.4	5.9
.5 Cys	n.d.	n.d.	n.d.
total	98.6%	98.3%	98.5%

Table 4.2:

Data obtained (in duplo) from three individual isolation procedures. Results were expressed as means of 6 data sets. An * indicates a significant difference between the 440 and 660 kDa fractions.

Carbohydrate residues (mol/mol)	residues	"crude" ferritin	660 kDa fraction	440 kDa fraction
Mannose		14	20	5
Glucose		39	100	25
Galactose		48	80	11
Sialic acid		3	10	1
% carbohydrates/ferritin (w/w)		4.3%	8.9%	1.8%

Table 4.3:

Carbohydrate and sialic acid residues are expressed in mol/mol protein. Data were obtained in duplo from three individual isolation procedures. Results were significantly different within the three fractions ($p < 0.01$).

§ 4.5 Discussion.

To obtain a porcine spleen ferritin of high purity we used two modified standard procedures, which yielded in each case two distinct bands, appearing at 440 and 660 kDa respectively in non-denaturing gradient gel electrophoresis. To exclude the possibility that either band was in fact an artifact, native gradient electrophoresis was repeated on another system with gels from another manufacturer, yielding identical results. Moreover, we obtained similar bands in horse spleen, human placental and porcine heart ferritin, and also, contrary to the findings of Linder et al (15), in porcine liver ferritin.

Molecular weight estimates of proteins based on the results in non-denaturing gel electrophoresis are at best unreliable, for electrophoretic mobility of a protein in this type of analysis is not only affected by its mass, but also by its size, shape and number of charged side chains. We therefore decided to perform a series of experiments to further elucidate the nature of these two ferritins of different electrophoretic mobility.

(1) Gel filtration chromatography was applied to separate both fractions. Based on the results in non-denaturing gel electrophoresis, there appeared to be a 50% difference in molecular weight between both fractions. However, considerable column dimensions (4m) and repeated runs (up to five times) were necessary to accomplish separation with an acceptable degree of purity. On the one hand these results would suggest that the difference

440 and 660 kDa spleen ferritin.

in mass between both fractions was less than expected, on the other hand K_{av} values of Sephadex and Sepharose separating gels are nearly equal for two fractions this size (7).

(II) We could exclude that the apparent difference in mass between both fractions was due to a difference in iron load. First, both bands stained for iron, which excluded the possibility that one fraction was in fact apoferritin. Second, the absence of a smear between both bands (*Fig. 1, lane 4*) suggested against a variation in iron content. Biochemical assays, quantitating the amount of iron per molecule ferritin in "crude" ferritin and the purified fractions (*Table I*) confirmed that the iron load of the 440 and 660 kDa fractions was not significantly different. Moreover, electron micrographs did not show any difference in iron core diameter between both fractions (*Fig. 4*).

The iron to phosphorus ratio assessed both biochemically and with electron probe micro analysis (*Table I*) showed no significant difference between both 440 and 660 kDa fractions. However, compared to "crude" ferritin there is either a loss of phosphorus or an increase in iron in both fractions (compare: 9). According to our data (*Table I*), the amount of iron per molecule of ferritin is equal in all fractions. Therefore, we have to assume a loss of phosphorus in both fractions for which we have no explanation.

(III) A difference in subunit composition between both fractions was ruled out when "crude" ferritin was applied to a DEAE column (13). Each of the 4 ferritin subspecies (acid, intermediate 1 and 2, basic) yielded a 440 and 660 kDa band on a non-denaturing gel. Also, samples of "crude" ferritin and purified 440 and 660 kDa fractions showed only minor differences in subunit composition when applied to a SDS- or a Tricine SDS-PAGE (*Fig. 2*).

(IV) Up till now, a band appearing above 440 kD has been considered as a ferritin dimer, and our results sofar indicated that the 660 kDa fraction might in fact be a dimer of 440 kDa ferritin, showing a different electrophoretic mobility due to loss of its spherical structure (7). Therefore, to facilitate dimer formation, purified 440 and 660 kDa fractions were left to stand for a number of weeks at 4 °C and then subjected again to non-denaturing gradient gel electrophoresis (4-15%). In the stacking gel above the 660 kDa lane a new band appeared. According to manufacturer's information, the 4-15% gel will exclude molecules above 1000 kDa and this band could therefore be a 660 kDa dimer or polymer. In the 440 kDa fraction lane on the other hand, no extra bands appeared. In our hands, the

440 kDa fraction showed no tendency at all to form aggregates.

(IVa) Purified 440 and 660 kDa fractions were dialyzed for 60 h against 8 M urea at 4 °C. According to Harrison (11) this could lead to dissociation of ferritin di- and polymers, although Yang (22) recently stated that ferritin dimers are not affected by these conditions. In our experiments, neither fraction showed any change in electrophoretic mobility in non-denaturing gradient gel electrophoresis following dialysis against 8 M urea. Together, these findings suggest against a 660 kDa ferritin fraction consisting of aggregates (or dimers) of 440 kDa ferritin, or other nonspecifically attached proteins.

(V) Santambrogio and Massover (19,20) discovered on non-denaturing gels an additional band in rabbit liver ferritin, consisting of ferritin associated to alpha-2-macroglobulin. Although this finding would seem to fit the description of our 660 kDa fraction, our experimental results indicated otherwise, as in both fractions: (i) SDS-PAGE and Tricine SDS-PAGE showed only 19 and 21 kDa bands, (ii) Amino acid analyses (see below) revealed no significant differences, (iii) Ouchterlony double immunodiffusion against rabbit anti-porcine-serum protein antibodies showed no precipitation.

(VI) Antibodies generated against each of the purified ferritin fractions cross-reacted with samples of both fractions in an Ouchterlony. However, small precipitation arcs deviating from the larger "ring" (*Fig. 3*) suggest against complete homology. As mentioned before, contamination of either fraction with other proteins was ruled out (see V), and it would therefore appear that the two fractions are not completely identical.

(VII) Finally, averaged amino acid analyses of the purified 440 and 660 kDa fractions showed no significant differences, with the exception of N-acetylglucosamine (*Table II*). This carbohydrate residue is an essential element in the core structure of N-linked glycans (8). We assumed a difference in ferritin glycosylation and therefore subjected each fraction to carbohydrate analysis. These analyses showed a circa 5 to 1 carbohydrate ratio (w/w) between the 660 and 440 kDa fractions. The difference in sialic acid composition was even more pronounced (*Table III*). In all analyses, the results of "crude" ferritin fitted in between (*Table III*).

This difference in carbohydrate content will not explain the apparent difference in mass (\pm 220 kDa) between both fractions, as shown in non-denaturing gel electrophoresis. However, electrophoretic mobility of a protein in non-denaturing gel electrophoresis will

440 and 660 kDa spleen ferritin.

be influenced by differences in the number of charged side chains (e.g. sialic acid).

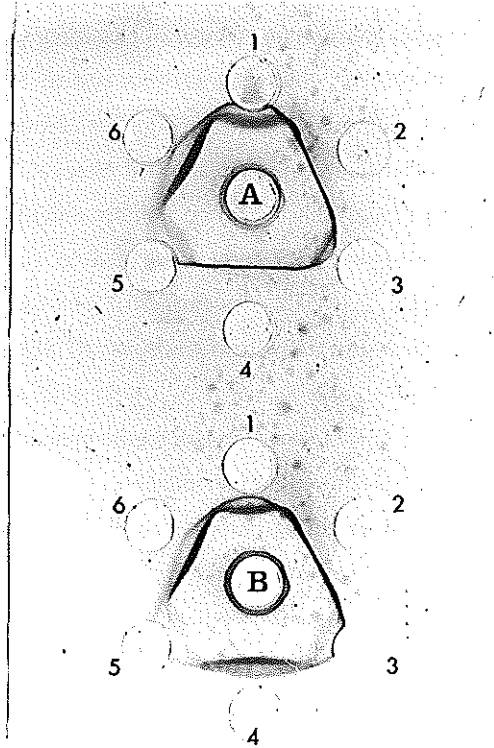


Fig. 4.3:

Polyclonal antibodies generated against each of the two purified ferritin fractions were tested against both fractions in an Ouchterlony double immunodiffusion assay. A: anti-440 kDa ferritin antibodies; B: anti-660 kDa ferritin antibodies. 1: 440 kDa ferritin (undiluted); 2: 660 kDa ferritin (undiluted). 3: 440 kDa ferritin (diluted 1:2); 4: 660 kDa ferritin (diluted 1:2). 5: 440 kDa ferritin (diluted 1:5); 6: 660 kDa ferritin (diluted 1:5).

In summary: porcine spleen ferritin isolated according to different standard procedures routinely showed two distinct bands in non-denaturing gradient gel electrophoresis. Both fractions are equal in subunit composition, iron load and amino acid composition (except for N-acetylglucosamine), but differ in carbohydrate content. Moreover, both fractions show incomplete homology when cross-reacted with antibodies generated against both

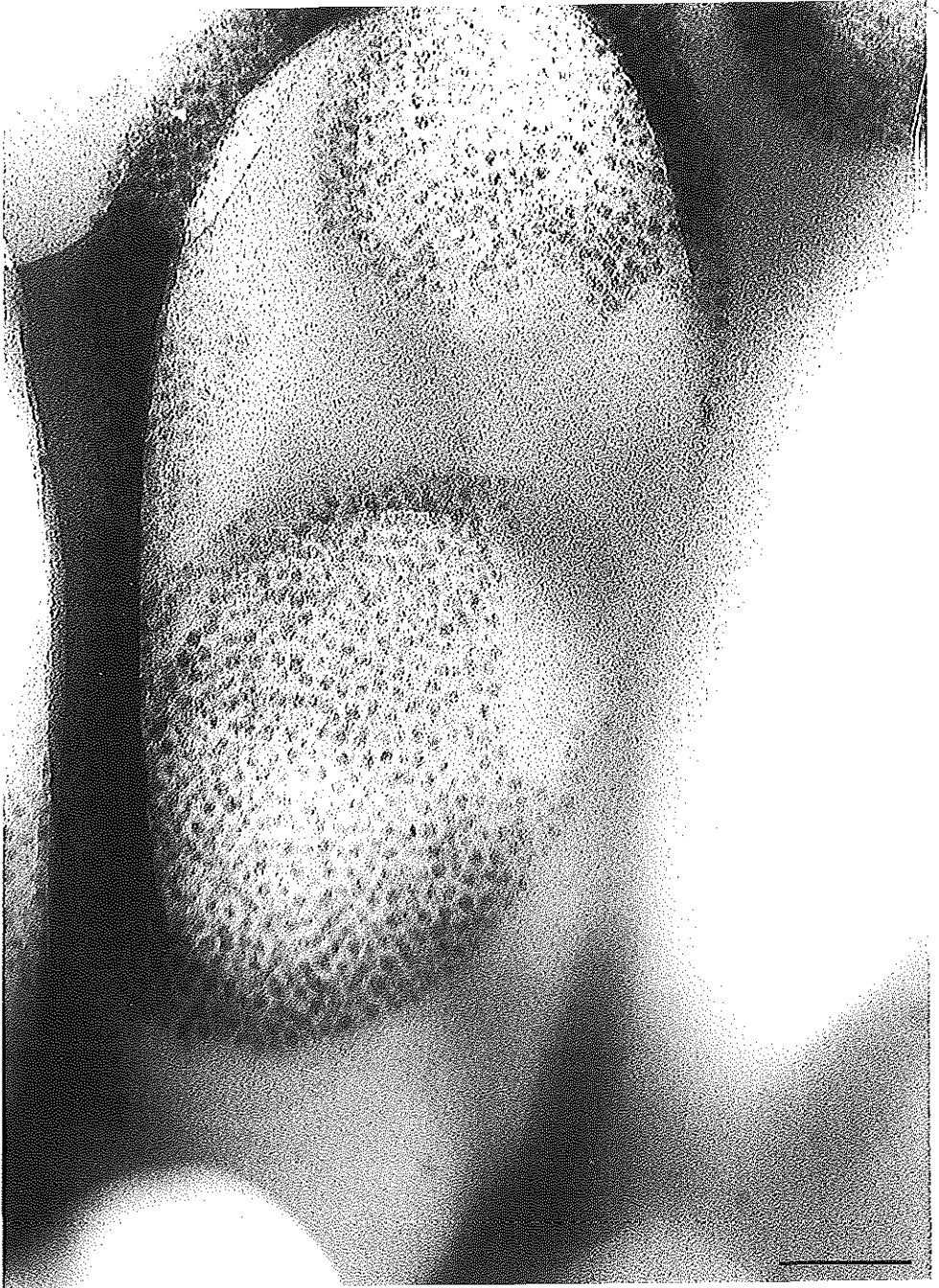
Chapter 4

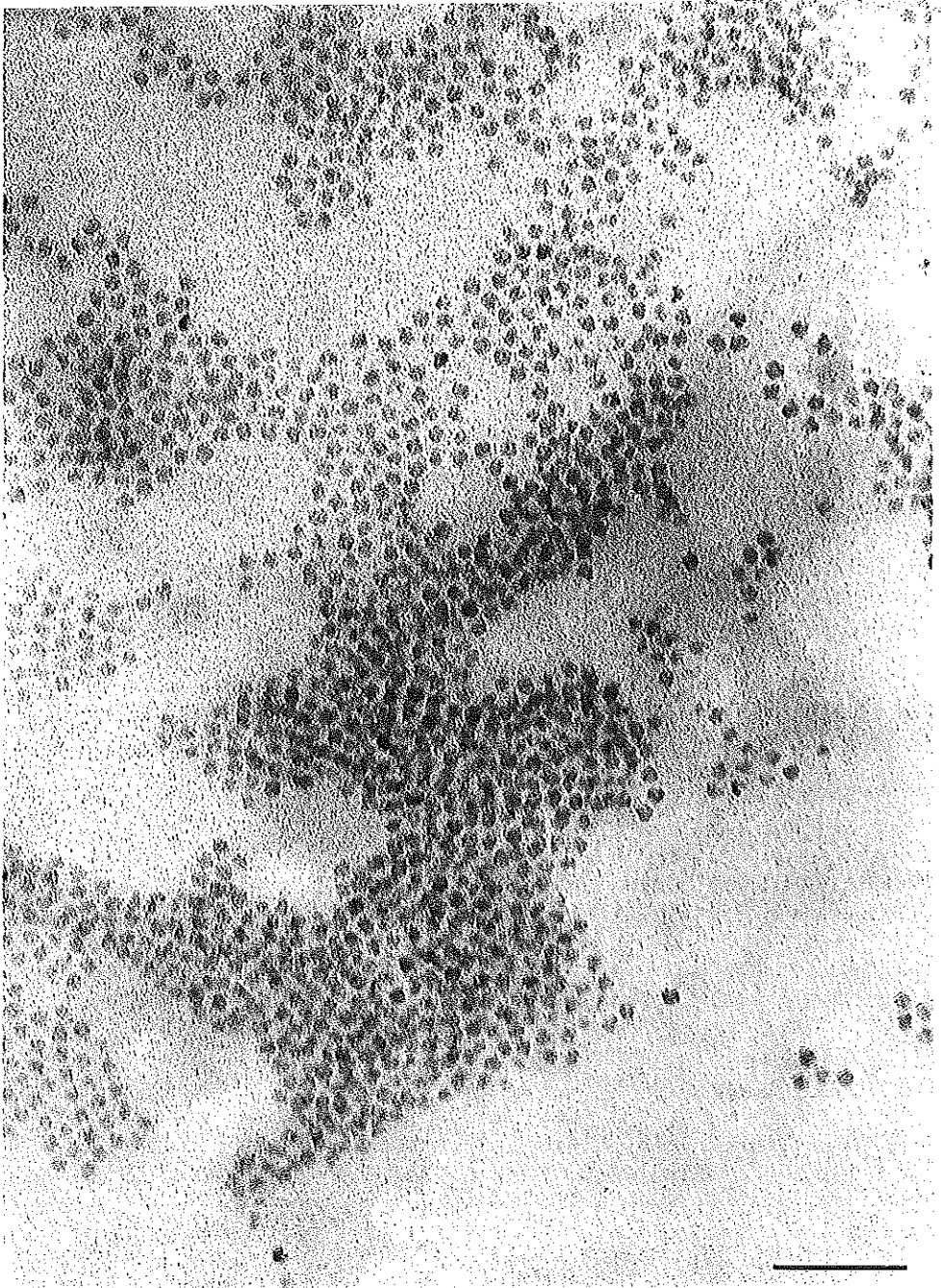
fractions. Together, these findings militate against, but cannot completely rule out the possibility that the "660 kDa" fraction is in fact a ferritin dimer. However, results indicate definitely that the "660 kDa" fraction is in fact a more glycosylated type of tissue ferritin. Whether this difference in glycosylation reflects a difference in cellular function remains as yet unknown.

Fig. 4.4^a and 4^b:

Electron micrographs of 440 kDa (Fig. 4^a) and 660 kDa (Fig. 4^b) ferritin fractions. Bar represents 50 nm.

440 and 660 kDa spleen ferritin.





440 and 660 kDa spleen ferritin.

References:

- (1) Aisen Ph. (1980) Iron transport and storage proteins. *Ann. Rev. Biochem.* 49: 357-393.
- (2) Andrews S.C. (1987) A new form of ferritin heterogeneity explained. Isolation and identification of a nineteen-amino-acid residue fragment from siderosomal ferritin of rat liver. *Biochem. J.* 245: 447-453.
- (3) Cynkin M.A. and Knowlton J. (1977) Studies on the carbohydrate components of ferritin. *Proteins of iron metabolism.* (ed. by Brown E.B., Aisen Ph., Fielding J. and Crichton R.R.), pp. 115-120. Grune and Stratton, New York.
- (4) Crichton R.R. (1983) Primary structure of horse and human apoferritins. *Structure and Function of Iron Storage and Transport Proteins.* (ed. by Urushizaki I., Aisen P., Listowski J. and Drysdale J.W.), pp. 3-10. Elsevier Science, Amsterdam.
- (5) Collawn J.F., Lau P.Y., Morgan S.L., Fox A. and Fish W.W. (1984) A chemical and physical comparison of ferritin subunit species fractionated by high-performance liquid chromatography. *Arch. Biochem. Biophys.* 233: 260-266.
- (6) Collawn J.F., Gowan L.K., Crow H., Schwabe C. and Fish W.W. (1987) Isolation and partial amino acid sequence of three subunit species of porcine spleen ferritin: evidence of multiple H subunits. *Arch. Biochem. Biophys.* 259: 105-113.
- (7) De Haën C. (1987) Molecular weight standards for calibration of gel filtration and sodium dodecyl sulfate-polyacrylamide gel electrophoresis: ferritin and apoferritin. *Analyt. Biochem.* 166: 235-245.
- (8) De Jong G., van Dijk J.P. and van Eijk H.G. (1990) The biology of transferrin. *Clin. Chim. Acta* 190: 1-46.
- (9) De Silva D., Guo J.H. and Aust S.D. (1993) Relationship between iron and phosphate in mammalian ferritins. *Arch. Biochem. Biophys.* 303: 451-455.
- (10) Drysdale JW (1977) Ferritin phenotypes: structure and metabolism. *Ciba Foundation Symposium* 71. *Iron Metabolism.* pp 41-57.
- (11) Harrison P.M. and Gregory D.W. (1965) Evidence for the existence of stable "aggregates" in horse spleen ferritin and apoferritin. *J. Mol. Biol* 14: 626-629.
- (12) Harrison P.M., Hoare R.J., Hoy T.G. and Macara I.G. (1974) Ferritin and haemosiderin: structure and function. *Iron in biochemistry and medicine.* (ed. by Jacobs A. and Worwood M.), pp. 73-114. Academic Press, London.
- (13) Konijn A.M., Tal R., Levy R. & Matzner Y. (1985) Isolation and fractionation of ferritin from human placenta- A source for human isoferritins. *Analyt. Biochem.* 144: 423-428.

Chapter 4

- (14) Lavoie D.J., Marcus D.M., Ishikawa K. and Listowski I. (1977) Ferritin and apoferritin from human liver: aspects of heterogeneity. *Proteins of iron metabolism*. (ed. by Brown E.B., Aisen P., Fielding J. and Crichton JJ), pp. 71-78. Grune and Stratton, New York.
- (15) Linder M., Goode C.A., Gonzalez R., Gottschling C., Gray J. and Nagel G.M. (1989) Heart tissue contains small and large aggregates of ferritin subunits. *Arch. Biochem. Biophys.* 273: 34-41.
- (16) Passaniti A. and Roth T.F. (1989) Purification of chicken liver ferritin by two novel methods and structural comparison with horse spleen ferritin. *Biochem. J.* 258: 413-419.
- (17) Penders T.J., de Rooij-Dijk H.H. and Leijnse B. (1968) Rapid isolation of ferritin by means of ultracentrifugation. *Biochim. Biophys. Acta* 168: 588-590.
- (18) Sala G., Worwood M. and Jacobs A. (1986) The effect of isoferritins on granulopoiesis. *Blood* 67: 436-443.
- (19) Santambrogio P. and Massover W.H. (1987) Protein heterogeneity in rabbit liver ferritin: two types of molecular dimers. *Biochem. Biophys. Res. Comm.* 148: 1363-1369.
- (20) Santambrogio P. and Massover W.H. (1989) Rabbit serum alpha-2- macroglobulin binds to liver ferritin: association causes a heterogeneity of ferritin molecules. *Brit. J. Haematol.* 71: 281-290.
- (21) Shinjyo S., Abe H. and Masuda M. (1975) Carbohydrate composition of horse spleen ferritin. *Biochim. Biophys. Acta* 411: 165-167.
- (22) Yang D., Matsubara K., Yamaki M., Ebina S. and Nagayama K. (1994) Heterogeneities in ferritin dimers as characterized by gel filtration, nuclear magnetic resonance, electrophoresis, transmission electron microscopy, and gene engineering techniques. *Biochim Biophys Acta* 1206: 173-179.

CHAPTER 5

Quantification of different transferrin receptor pools in primary cultures of porcine blood-brain barrier endothelial cells.

This chapter is based on:

W. van Gelder, M.I.E. Huiskes-Heins, J.P. van Dijk, M.I. Cleton-Soeteman and H.G. van Eijk

(1995) Quantification of different transferrin receptor pools in primary cultures of porcine blood-brain barrier endothelial cells.
J. Neurochem 64: 2708-2715.

Chapter 5

§ 5.0 Contents.

§ 5.1: Summary.

§ 5.2: Introduction.

§ 5.3: Materials and methods:

§ 5.3.1: Materials.

§ 5.3.2: Methods:

§ 5.3.2.1: Blood-brain barrier microvessel endothelial cell isolation and culturing.

§ 5.3.2.2: Isolation and purification of porcine serum transferrin.

§ 5.3.2.3: Isolation and purification of transferrin receptors from porcine liver.

§ 5.3.2.4: Radio-labeling of transferrin.

§ 5.3.2.5: Surface transferrin receptor measurements.

§ 5.3.2.6: Total transferrin receptor measurements.

§ 5.3.2.7: Transferrin receptor recovery efficiency assessment in total TfR measurements.

§ 5.3.2.8: Quantification of transferrin receptors participating in the endocytic cycle.

§ 5.3.2.9: Protein measurements.

§ 5.3.2.10: DNA measurements.

§ 5.3.2.11: Mathematical analysis of the receptor binding experiments.

§ 5.3.2.12: Anti-Von Willebrand immunocytochemistry.

§ 5.4: Results:

§ 5.4.1: Isolation procedure.

§ 5.4.2: Quantification of surface and total TfR pools.

§ 5.4.3: Assessment of TfR amounts, actively participating in the endocytic cycle.

§ 5.4.4: Control experiments.

§ 5.4.5: Nonlinear curve fit analyses of binding assays.

§ 5.5: Discussion.

§ 5.1 Summary.

Distribution of iron in the brain varies with region, cell type and age. Furthermore, some neurological diseases are accompanied by an abnormal accumulation of iron in specific areas of the CNS. These findings implicate a mobile intracerebral iron pool; however, transport of iron across the blood-brain barrier and its regulation are largely unknown.

We separately quantified surface bound and total cellular transferrin receptor pools in primary cultures of porcine blood-brain barrier endothelial cells. Although 90% of all transferrin receptors were located inside the cell, only 10% of these intracellular receptors actively took part in the endocytic cycle. This large "inactive" intracellular transferrin

Different BBB transferrin receptor pools.

receptor pool could either function as a storage site for spare receptors, or be activated by the cell to increase its capacity for iron transport.

Data were corrected for nonspecific binding by: (i) separate biochemical assessment using a 100-fold excess of unlabeled ligand, (ii) analyzed in a nonlinear curve fit program, which resulted in a less elaborate and less biased estimate of nonspecific binding.

§ 5.2 Introduction.

As early as 1922, Spatz (35) showed iron to be present in the brain. This finding received only little attention for a number of decades (18). Recently however, research in this field gained momentum when it became clear that (accumulated) iron could have deleterious effects by acting as a catalyst in the formation of reactive oxygen species (25,19). These reactive oxygen species can damage or modify lipids, proteins and DNA (17,10). Brain tissue is very rich in lipids and therefore more vulnerable to oxidative stress than most other tissues (13,15,19).

The overall distribution of iron, transferrin and ferritin in the brain has recently been re-examined (7,27). These studies (reviewed in 8) show that iron levels in the brain vary with region and cell type. Moreover, the pattern of iron distribution in the brain changes with age (8,11) and in certain (neurological) diseases. For instance, Alzheimer's and Parkinson's disease are accompanied by an abnormal accumulation of iron in specific areas of the central nervous system (7,22). On the other hand, iron deficiency leads to a reduction in cerebral iron as well as cerebral function (39). These studies implicate a mobile intracellular iron pool, but the mechanism by which iron enters or leaves the brain is still unclear (14). The discovery of transferrin receptors (TfR's) on the luminal side of blood-brain barrier endothelial cells (21) clarifies a route by which transferrin (Tf) enters the endothelial cell. However, conflicting evidence exists as to the fate of Tf after uptake (14,28,32). Either Tf is returned to the luminal surface (30,33) by an endocytic cycle (9,38), or Tf enters the brain by transcytosis (12,14). Factors regulating transport of iron across the blood-brain barrier are as yet unknown (4).

The purpose of this study is to quantify the amount of TfR's on the cell surface, the total cellular TfR pool in primary cultures of porcine blood-brain barrier endothelial cells (BBB-EC's) and the number of TfR's that actually take part in the transport of iron. The results

Chapter 5

will be used as a basis for future experiments in search for factors regulating iron transport across the blood-brain barrier.

§ 5.3 Materials and methods.

§ 5.3.1 *Materials.*

Fresh porcine brain was obtained from the local slaughterhouse. Hanks' Balanced Salt solution (HBSS), M 199 with Earle's salts, Fungizone (Amphotericin B), Fetal Calf Serum (FCS) were obtained from ICN Biomedicals (ICN Biomedicals Ltd, UK). L-Glutamine was obtained from Merck (Merck, Germany). Dispase Neutral protease from *Bacillus Polymyxa* Grade II, mouse anti-human Von Willebrand Factor and fluorescein labeled goat anti-mouse IgG were purchased from Boehringer Mannheim (Boehringer Mannheim, Germany). Trypsin from beef pancreas was obtained from BDH (BDH Biochemicals, UK). All other chemicals used were of the highest purity.

§ 5.3.2 *Methods.*

§ 5.3.2.1 *Blood-brain barrier microvessel endothelial cell isolation and culturing.*

A detailed description of this procedure can be found in § 2.2.1. Briefly: microvascular endothelial cells were isolated from fresh porcine brain using a method adapted from Mischeck (26) and Méresse (24). Brain tissue was homogenized after careful removal of cerebellum, meninges and choroid plexus. The homogenate was resuspended in brain culture medium. Dispase was added and the homogenate was gently shaken for 3 hrs, then filtered and centrifuged. The bottom layer of the pellet was resuspended and the procedure was repeated (3x). Cells were plated on gelatine coated petri dishes. After 30 min culture medium was replaced. Culture medium was changed every other day.

§ 5.3.2.2 *Isolation and purification of porcine serum transferrin.*

A detailed description of this procedure can be found in § 2.6.1. Briefly: fresh porcine plasma was saturated with iron and fibrins were removed. Following two precipitation steps

Different BBB transferrin receptor pools.

with ammonium sulfate, the pellet was redissolved and dialyzed. Aliquots were loaded on a column packed with Cibacron 3GA coupled to BioGel A 1.5m and porcine transferrin was eluted with a linear (0 to 0.1 M) sodium phosphate gradient.

§ 5.3.2.3 Isolation and purification of transferrin receptors from porcine liver.

A detailed description of this procedure can be found in § 2.6.4. Briefly: porcine liver tissue was homogenized in buffer, filtered and centrifuged. The pellet was resuspended and washed (= crude vesicle preparate), then dissolved in PBS containing Triton X-100 and Trypsin and placed in a waterbath at 37 °C. This solution was dialyzed, concentrated and then centrifuged. Supernatant samples were fractionated on a Sephadex G100 column and a column packed with porcine 2Fe-Tf coupled to CNBr-Sepharose 4B. The 70 kDa TfR subunit was eluted with a buffer (pH 2.8). Purity was checked with SDS-PAGE (see § 2.5.1.1).

§ 5.3.2.4 Radio-labeling of transferrin.

A description can be found in § 2.8.1.

§ 5.3.2.5 Surface transferrin receptor measurements.

Surface TfR measurements were performed as described by Ciechanover (6). Blood-brain barrier endothelial cells were incubated with ¹²⁵I-Tf at 4 °C, rinsed with PBS and receptor bound ¹²⁵I-Tf was measured. A detailed description of this procedure can be found in § 2.8.2.

§ 5.3.2.6 Total transferrin receptor measurements.

To assess the total amount of TfR's present in the endothelial cells, a procedure as described by Rao (29) was used (see § 2.8.3). Blood-brain barrier endothelial cells were homogenized, incubated with ¹²⁵I-Tf at 4 °C and precipitated with ammonium sulfate. ¹²⁵I-Tf-TfR complexes were collected on filters and measured. The TfR recovery efficiency of this procedure was checked in a separate series of experiments (see § 5.3.2.7).

Chapter 5

§ 5.3.2.7 *Transferrin receptor recovery efficiency assessment in total TfR measurements.*

Known amounts of partially purified and purified TfR's were subjected to the procedure as described in § 5.3.2.6 to test the recovery efficiency of this procedure. A detailed description of this procedure can be found in § 2.8.4.

§ 5.3.2.8 *Quantification of transferrin receptors participating in the endocytic cycle.*

A detailed description of this technique can be found in § 2.8.5. Briefly; blood-brain barrier endothelial cells were washed once with PBS and then incubated for 1.5 to 40 h with 1500 ng (≥ 50 times Kd) ^{125}I -Tf at 37 °C. Surface and intracellular TfR concentrations were assessed separately.

§ 5.3.2.9 *Protein measurements.*

Cellular protein measurements were performed as described in § 2.5.2.2.

§ 5.3.2.10 *DNA measurements.*

Cellular DNA content of each sample was assessed using a NucleoSpin DNA kit (Sanbio, the Netherlands) according to manufacturers instructions (see § 2.5.2.3).

§ 5.3.2.11 *Mathematical analysis of the receptor binding experiments.*

A detailed description can be found in § 2.7.2. Briefly; the percentage nonspecific binding was calculated using wells incubated with different concentrations of ^{125}I -Tf in the presence of a 100-fold excess of non-labeled Tf. Furthermore, the results from each binding experiment were fitted using the following equation in a nonlinear curvefit program

$$f(x) = \frac{a*x}{b+x} + c*x$$

§ 5.3.2.12 *Anti-Von Willebrand immunocytochemistry.*

Blood-brain barrier endothelial cells grown on gelatin coated coverslides were incubated with mouse anti-human von Willebrand factor immunoglobulins. A detailed description of

Different BBB transferrin receptor pools.

this technique can be found in § 2.3.1.

§ 5.4 Results.

§ 5.4.1 *Isolation procedure.*

The isolation procedure (as described in § 5.3.2.1), resulted in a more than 95% pure blood brain-barrier microvascular endothelial cell culture. Purity was checked in phase contrast light microscopy (*Fig. 1b*) and in immunocytochemistry with antibodies against human Von Willebrand Factor (*Fig. 1a*). Cells were used upon reaching confluency and cell counts at that time yielded an average of $4.1 (\pm 0.4) \times 10^4$ cells/cm² (mean \pm SD). Repeated DNA measurements ($n = 6$) resulted in an estimate of 10.8 pg DNA/cell.

§ 5.4.2 *Quantification of surface and total TfR pools.*

The amount of TfR's on the cell surface was assessed in 8 separate experiments. Each individual binding plot was the result of 12 to 15 (duplicate) measuring points and 3 (duplicate) measuring points to estimate nonspecific binding. In *Fig. 2* the combined results of these experiments are summarized. Nonlinear curve fit analysis yielded a B_{\max} value of 0.031 ± 0.013 ng Tf/ μ g protein (mean \pm SD) which equals $3.6 (\pm 2.8) \times 10^{11}$ Tf binding sites/mg protein (mean \pm SD).

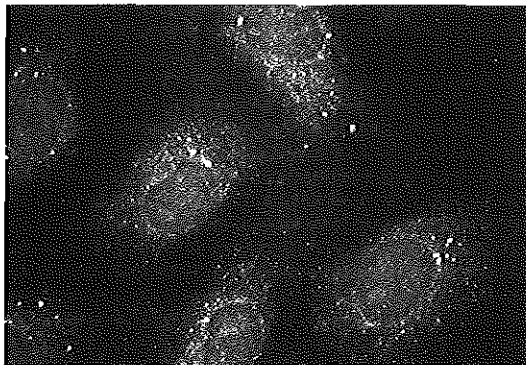


Fig. 1a:

Immunofluorescence micrograph of a primary culture of porcine blood-brain barrier endothelial cells incubated with mouse anti-human Von Willebrand Factor. (M = 1000x).

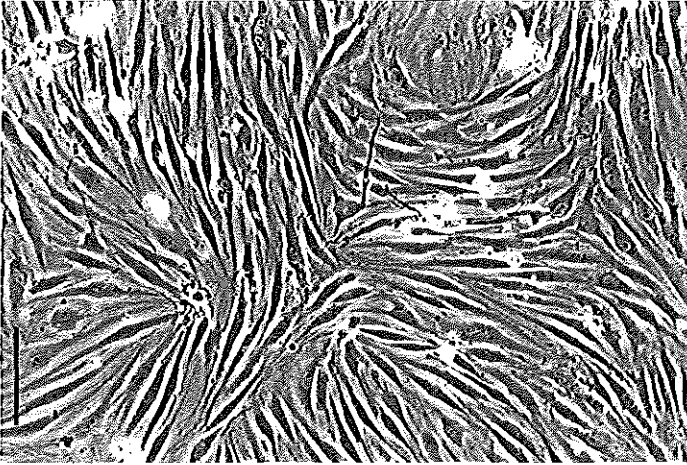


Fig. 1b:

Phase-contrast micrograph of a primary culture of porcine blood-brain barrier endothelial cells. (Bar: 100 μm)

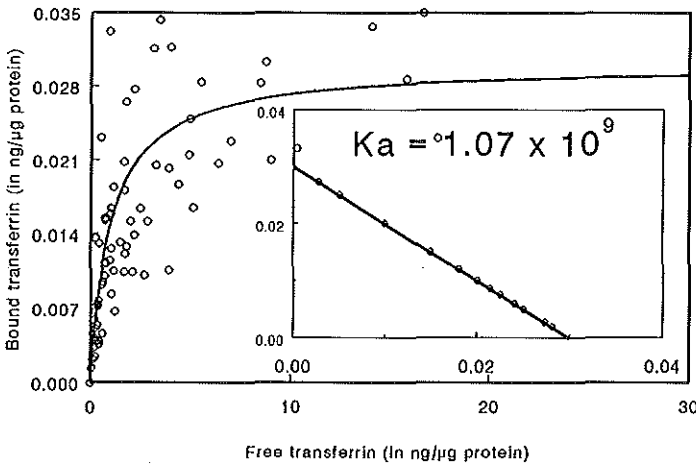


Fig. 2: The results of 8 separate experiments ($n = 12$, in duplicate) are summarized in this figure. Blood-brain barrier endothelial cells were incubated with ^{125}I -Tf at 4 $^{\circ}\text{C}$ and surface TfR bound ^{125}I -Tf was measured. Each open circle represents the average of a result in duplicate. The binding plot (solid line) was obtained in a nonlinear curve fit program. The insert shows the scatchard plot derived from the nonlinear curve fit data. The Y-axis represents bound/free Tf, the X-axis represents bound Tf (in $\text{ng}/\mu\text{g}$ protein). The TfR affinity constant derived from this analysis is shown at the top of the insert.

Different BBB transferrin receptor pools.

The insert in Fig. 2 shows the scatchard plot and affinity constant derived from the nonlinear curve fit data. The number of total TfR's is derived from the results of 8 individual experiments, each consisting of 10 (duplo) experimental data and 3 (duplo) experimental data for correction of nonspecific binding. The binding plot resulting from the nonlinear curve fit is depicted in Fig. 3. The insert shows the scatchard plot and affinity constant derived from the analysis.

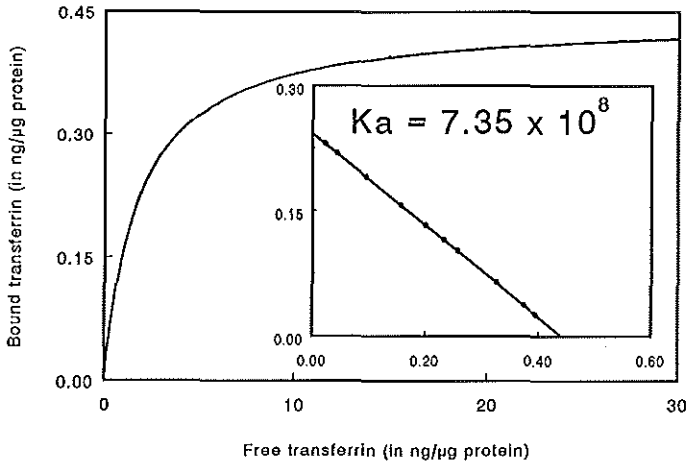


Fig. 3:

The results of 8 separate experiments ($n = 10$, in duplo) are summarized in this figure. Lysed blood-brain barrier endothelial cells were incubated with ^{125}I -Tf at 4°C , precipitated and ^{125}I -Tf-TfR complexes were collected. (Individual data are shown in Fig. 5). The binding plot was obtained in a nonlinear curve fit program. The insert shows the scatchard plot derived from the nonlinear curve fit data. The Y-axis represents bound/free Tf, the X-axis represents bound Tf (in $\text{ng}/\mu\text{g}$ protein). The TfR affinity constant derived from this analysis is shown at the top of the insert.

The B_{\max} value is 0.442 ± 0.180 ng Tf/ μg protein (mean \pm SD) which equals $4.1 (\pm 1.8) \times 10^{12}$ Tf binding sites/mg protein (mean \pm SD).

§ 5.4.3 *Assessment of TfR amounts, actively participating in the endocytic cycle.*

Data on the amount of TfR's actively participating in the endocytic cycle, are summarized in Table 1. Data are derived from 3 separate experiments ($n = 12$) expressed as mean \pm SD.

Chapter 5

incubation time with ^{125}I -Tf (in hrs)	surface TfR bound Tf (ng Tf/ μg prot)	intracell TfR bound Tf (ng Tf/ μg prot)	ratio of surface TfR's to intracellular TfR's
1.5	0.023 ± 0.005	0.029 ± 0.002	0.79
3.0	0.020 ± 0.001	0.029 ± 0.003	0.68
6.0	0.018 ± 0.002	0.029 ± 0.003	0.62
20	0.031 ± 0.004	0.029 ± 0.005	1.07
40	0.041 ± 0.011	0.041 ± 0.005	1.0

Table 1:

Results of 3 separate experiments (12 wells per incubation time in each experiment) on the quantification of TfR's actively participating in the endocytic cycle. Cells were incubated for 1.5 to 40 hrs at 37 °C with ^{125}I -Tf, followed by separate assessment of surface bound and intracellular TfR's. Results are expressed as mean \pm SD. The ratio of surface to "active" intracellular TfR's is shown in the last column.

§ 5.4.4 Control experiments.

Separate series of experiments were performed to estimate the total TfR recovery efficiency of our technique. Each set of data points is the mean result (\pm S.D.) of 4 individual experiments performed in duplo. Fig. 4 shows that at 30% saturation with ammonium sulfate only 2% of the incubated Tf is precipitated, whereas $15 \pm 5\%$ (mean \pm SD) of the purified half TfR is recovered (data corrected for nonspecific precipitation of Tf). These experiments further show that $72 \pm 2\%$ (mean \pm SD) of the vesicle membrane bound TfR's is recovered, when incubated with ^{125}I -Tf in the presence of 0.1% Triton X-100. When Triton X-100 was left out, TfR recovery rate decreased to $58 \pm 1\%$ (mean \pm SD).

§ 5.4.5 Nonlinear curve fit analyses of binding assays.

As an example of the nonlinear curvefit analyses, individual data points from 8 separate experiments quantifying the total amount of TfR's, are presented in Fig. 5. Together with these data, the curve fit based on the nonlinear analysis is presented, both in its complete form and split in its nonlinear and linear part. The linear part is an estimate of the amount of nonspecific binding, $9.7 \pm 1.5\%$ (mean \pm SD).

Different BBB transferrin receptor pools.

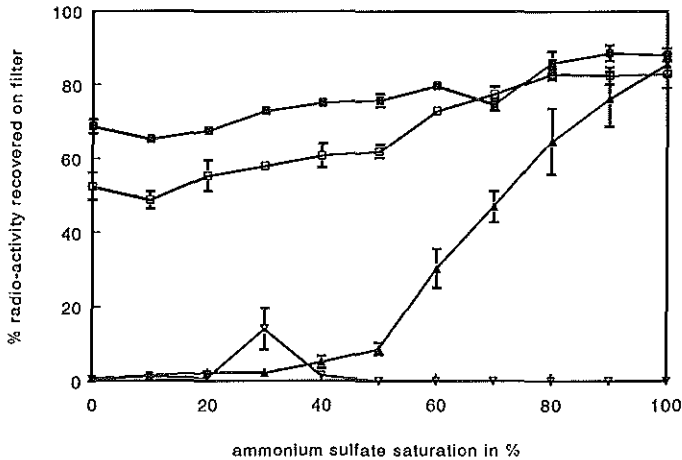


Fig. 4:

Experimental results on the quantification of ¹²⁵I-Tf-TfR complex recovery rate are summarized in this figure. Standard amounts of ¹²⁵I-Tf, purified half TfR-¹²⁵I-Tf complexes and complexes of ¹²⁵I-Tf linked to membrane bound TfR's (crude vesicles; see §.....) were precipitated with ammonium sulfate in various concentrations up to 100% saturation. Each data point represents the mean of 4 separate experiments performed in duplo. Results are expressed as the percentage of recovered radio-activity and error bars represent 1 SD. Open triangles: purified half TfR-¹²⁵I-Tf complexes; closed triangles: ¹²⁵I-Tf. Open squares: complexes of membrane bound TfR's and ¹²⁵I-Tf, without Triton X-100. Closed squares: complexes of membrane bound TfR's and ¹²⁵I-Tf, with Triton X-100.

§ 5.5 Discussion.

The endothelial cells lining the brain microvasculature are held responsible for the selective barrier that exists between the circulatory system and central nervous system (16). Three major features distinguish the brain microvascular endothelial cells from their periferal counterparts: (i) tight junctions connecting adjacent endothelial cells, (ii) a low rate of pinocytosis (31) and (iii) membrane bound receptors (14) serving as highly specific and selective transport mechanisms across the blood-brain barrier.

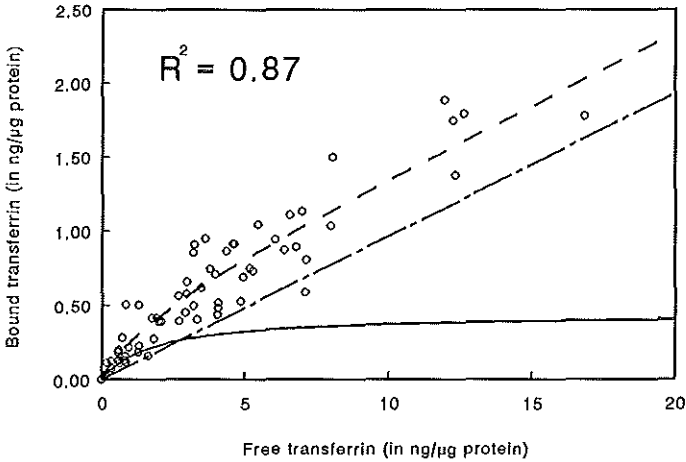


Fig. 5:

Combined data of 8 separate experiments (10 duplo points each) to measure total cellular TfR amounts are shown (open circles). Nonlinear curve fit analysis, based on the equation $f(x)=((a * x)/(b+x))+c * x$, yields the top curve (- - -) with an R^2 of 0.87.

The equation can be separated in the Langmuir isotherm, predicting a saturable binding between receptor and ligand (solid line; see also fig 3) and a linear term, compensating for nonspecific binding (- . . - line).

Several techniques have been described to isolate and culture brain microvascular endothelial cells with a high degree of purity (23). Although each of these techniques has been tested for one or more blood-brain barrier endothelium specific characteristics, e.g. von Willebrand factor (factor VIII related antigen), problems may still arise. First, dedifferentiation due to repeated passaging can affect highly specific cell functions (1,30). Secondly, isolated endothelial cells show polymorfism (34) and selection of one subtype could yield limited information. Thirdly, astrocytes (5) and pericytes (2) affect growth and structure of endothelial cell cultures and could modulate cell specific function characteristics. We therefore performed all our experiments on primary culture endothelial cells (Fig. 1) with a purity of $\geq 95\%$, other cells mainly being pericytes and some astrocytes.

A separate series of experiments was performed to estimate porcine TfR recovery efficiency in our total-TfR experiments. TfR has two identical (70 KDa) subunits (37), each capable of binding one Tf molecule. Treating TfR containing vesicles (crude vesicle

Different BBB transferrin receptor pools.

prepare, see § 5.3.2.3) with trypsin will free this hydrophilic 70 kDa subunit from its transmembrane segment. The recovery rates of Tf and the 70 kDa TfR subunit-Tf complex were low (*Fig. 4*). Crude vesicles however, contain complete TfR's still anchored in lipid membranes and precipitated more readily (*Fig. 4*). Adding Triton X-100 increased the TfR recovery rate (72%), most likely due to an increased accessibility of the intravesicular TfR's for ^{125}I -Tf. The TfR recovery was not complete, probably because vesicle bound TfR's are an already partly purified substrate. Results in cell lysates were not corrected for this loss in recovery, because these lysates consist of even larger membrane fragments than vesicles. This will most likely enhance precipitation and therefore increase the TfR recovery rate above 72%.

Experimental data were analyzed with a nonlinear curve fit program for two reasons. First of all, a mathematical analysis of the raw data set will give the least biased response (20). Secondly, an adequate mathematical analysis of nonspecific binding will reduce the need for a series of wells reserved for a biochemical estimate of nonspecific binding and therefore increase the number of experimental data in the actual experiment.

The equation used (see § 5.3.2.11) consists of a nonlinear and a linear term. The nonlinear (Langmuir) isotherm predicts a saturable interaction between receptor and ligand (20), whereas the linear term is introduced to compensate for nonspecific binding. The pooled data on surface and total TfR's were analyzed mathematically, yielding an estimate of nonspecific binding which was in good agreement with the biochemical assessment of nonspecific binding. The mathematical estimation of nonspecific binding in the surface TfR experiments was nearly zero and on average less than 1% when assessed biochemically. As shown in *Fig. 5*, nonspecific binding in the pooled data of total TfR experiments is $9.7 \pm 1.5\%$ (mean \pm SD). The averaged nonspecific binding assessed biochemically was $15 \pm 7\%$ (mean \pm SD).

Computing the amount of internal TfR's from the results on surface and total TfR numbers, we found circa 90% of all TfR's to be located inside the cell, in agreement with Raub et al (30). In the individual datasets, however, the number of internal receptors varied between 78 and 98%. Nonlinear curvefit analyses on the combined datasets of the total-TfR experiments resulted in an R^2 of 0.88 (*Fig. 3*), indicating that the total number of TfR's is rather consistent throughout experiments. Mathematical analysis on the combined datasets

Chapter 5

of surface TfR experiments only yielded an R^2 of 0.57 (*Fig. 2*), whereas in similar analyses on results of individual surface TfR binding experiments R^2 ranged from 0.85 to 0.99. This indicates a substantial variation in the number of surface TfR's between different experiments, which cannot be explained by nonspecific binding as shown both biochemically and mathematically ($< 1\%$). Moreover, TfR affinity constants of both surface and total TfR data sets were not significantly different ($p < 0.05$). These results suggest that the total TfR concentration is more or less constant, while the amount of TfR's on the surface can be modulated by the cell, for instance to regulate its iron uptake.

The number of TfR's actively participating in the endocytic cycle was assessed (*Table 1*) by incubating cells with an excess of ^{125}I -Tf. Based on an estimated recycling time of 90 min for TfR's (30) incubations were performed up to 40 h (over 25 cycles) to label all active TfR's. The number of labeled surface TfR's was not significantly different ($p < 0.05$) from that found in the experiments on surface TfR quantification. However, only circa 10% of all intracellular TfR's could be labeled in this way. These results suggest that there are at least two separate intracellular TfR pools. One of these pools, roughly equal to the amount of surface TfR's (*Table 1*), is active in the endocytic cycle, whereas circa 90% of all intracellular TfR's seem to be inactive. This inactive pool could function as a storage site to replace those TfR's damaged or lost during the endocytic cycle. On the other hand, if TfR's stored in this inactive pool could be "activated" to participate in the endocytic cycle, the inactive pool would serve as a regulatory mechanism for iron transport across the blood-brain barrier. Variation in the amount of surface bound TfR's (discussed earlier) could be the result of minor changes in the ratio of active to inactive TfR's.

Bérczi et al (3) found that a significant amount of ^{125}I -labeled ligand remained in the K562 cell and suggested a third TfR-pathway next to the two described by Stein and Sussmann (36). In our experiments however, 40 hrs of incubation with excess ^{125}I -Tf could only reach 10% of all internal TfR's (active pool). It would seem that the proposed third TfR-pathway (3) is not connected to the inactive TfR pool as described above.

To gain further insight in mechanisms regulating iron uptake and transport across the blood-brain barrier, we are currently conducting similar experiments on endothelial cells cultured in iron poor and iron enriched media.

Different BBB transferrin receptor pools.

References:

- (1) Abbott N.J., Hughes C.C.W., Revest P.A. and Greenwood J. (1992) Development and characterisation of a rat brain capillary endothelial culture: towards an *in vitro* blood-brain barrier. *J. Cell Science* 103, 23-37.
- (2) Antonelli-Orlidge A., Saunders K.B., Smith S.R. and D'Amore P.A. (1989) An activated form of transforming growth factor β is produced by cocultures of endothelial cells and pericytes. *Proc. Natl. Acad. Sci. USA* 86, 4544-4548.
- (3) Bérczi A., Ruthner M., Szuts V., Schweinzer E. and Golderbergh H. (1993) Influence of conjugation of doxorubicin to transferrin on the ironuptake by K562 cells via receptor-mediated endocytosis. *Eur. J. Biochem* 213, 427-436.
- (4) Broadwell R.D. and Banks W.A. (1993) Cell biological perspective for the transcytosis of peptides and proteins through the mammalian blood-brain fluid barrier, in: *The blood-brain barrier. Cellular and molecular biology.* (Pardridge W.M., ed), pp. 165-199. Raven Press, New York.
- (5) Cancilla P.A., Bready J. and Berliner J. (1993) Brain endothelial-astrocyte interactions, in: *The blood-brain barrier. Cellular and molecular biology.* (Pardridge W.M., ed), pp. 25-46. Raven Press, New York.
- (6) Ciechanover A., Schwartz A.L., Dautry-Varsat A. and Lodish H.F. (1983) Kinetics of internalization and recycling of transferrin and the transferrin receptor in a human hepatoma cell line. *J. Biol. Chem.* 258, 9681-9689.
- (7) Connor J.R., Snyder B.S., Beard J.L., Fine R.E. and Mufson E.J. (1992) Regional distribution of iron and iron-regulatory proteins in the brain in aging and Alzheimer's disease. *J. Neurosci. Res.* 31, 327-335.
- (8) Connor J.R. (1993) Cellular and regional maintenance of iron homeostasis in the brain: normal and diseased states, in: *Iron in central nervous system disorders.* (Riederer P. and Youdim M.B.H., eds), pp. 1-18. Springer-Verlag, New York.
- (9) Dautry-Varsat A., Ciechanover A., Lodish H.F. (1983) pH and recycling of transferrin during receptor-mediated endocytosis. *Proc. Natl. Acad. Sci. USA* 80, 2258-2262.
- (10) Davies K.J.A. (1987) Protein damage and degradation by oxygen radicals. I. General aspects. *J. Biol. Chem.* 262, 9895-9901.
- (11) Dwork A.J., Lawler G., Zybert P.A., Durkin M., Osman M., Wilson N. and Barkai A.I. (1990) An autoradiographic study of the uptake and distribution of iron by the brain of the young rat. *Brain. Res.* 518, 31-39.

Chapter 5

- (12) Fishman J.B., Rubin J.B., Handrahan J.V., Connor J.R. and Fine R.E. (1987) Receptor-mediated transcytosis of transferrin across the blood-brain barrier. *J. Neurosci. Res.* 18, 299-304.
- (13) Floyd R.A. and Carney J.M. (1992) Free radical damage to protein and DNA: Mechanisms involved and relevant observations on brain undergoing oxidative stress. *Ann. Neurol.* 32, S22-27.
- (14) Friden P.M. (1993) Receptor-mediated transport of peptides and proteins across the blood-brain barrier, in: *The blood-brain barrier. Cellular and molecular biology.* (Pardridge W.M., ed), pp. 229-247. Raven Press, New York.
- (15) Götz M.E., Dirr A., Gsell W., Burger R., Freyberger A. and Riederer P. (1993) Some reflections on iron dependent free radical damage in the central nervous system, in: *Iron in central nervous system disorders.* (Riederer P. and Youdim M.B.H., eds), pp. 45-54. Springer-Verlag, New York.
- (16) Goldstein G.W. and Betz A.L. (1986) The blood-brain barrier. *Sci. Am.* 255, 74-83.
- (17) Gutteridge J.M.C. and Halliwell B. (1989) Iron toxicity and oxygen radicals. *Baillière's Clinical Hematology* 2(2), 195-256.
- (18) Hallgren B. and Sourander P. (1958) The effect of age on the nonhaem iron in the human brain. *J. Neurochem.* 3, 41-51.
- (19) Halliwell B. (1992) Reactive oxygen species and the central nervous system. *J. Neurochem.* 59, 1609-1623.
- (20) Hulme E.C. and Birdsall J.M. (1992) Strategy and tactics in receptor-binding studies, in: *Receptor-ligand interactions. A practical approach.* (Hulme E.C., ed), pp. 63-176. Oxford University Press, New York.
- (21) Jefferies W.A., Brandon M.R., Hunt S.V., Williams A.F., Gatter K.C. and Mason D.Y. (1984) Transferrin receptor on endothelium of brain capillaries. *Nature* 312, 162-163.
- (22) Jellinger K. and Kienzl E. (1993) Iron deposits in brain disorders, in: *Iron in central nervous system disorders.* (Riederer P. and Youdim M.B.H., eds), pp. 19-36. Springer-Verlag, New York.
- (23) Joó F. (1992) The cerebral microvessels in culture, an update. *J. Neurochem.* 58, 1-17.
- (24) Méresse S., Dehouck M.P., Delorme P., Bensaïd M., Tauber J.P., Delbart C, Fruchart J.C. and Cecchelli R. (1989) Bovine brain endothelial cells express tight junctions and monoamine oxidase activity in long-term culture. *J. Neurochem.* 53, 1363-1371.
- (25) Minotti G. and Aust S.D. (1992) Redox cycling of iron and lipid peroxidation. *Lipids*

Different BBB transferrin receptor pools.

27, 219-226.

(26) Mischeck U., Meyer J. and Galla H.J. (1989) Characterization of γ -glutamyl transpeptidase activity of cultured endothelial cells from porcine brain capillaries. *Tissue Res.* 256, 221-226.

(27) Morris C.M., Candy J.M., Oakley A.E., Bloxham C.A. and Edwardson J.A. (1992) Histochemical distribution of non-haem iron in the human brain. *Acta Anatomica* 144, 235-257.

(28) Morris C.M., Keith A.B., Edwardson J.A. and Pullen R.G.L. (1992) Uptake and distribution of iron and transferrin in the adult rat brain. *J. Neurochem.* 59, 300-306.

(29) Rao K.K., Shapiro D., Mattia E., Bridges K. and Klausner R. (1985) Effects of alterations in cellular iron on biosynthesis of the transferrin receptor in K 562 cells. *Molec. Cell. Biol.* 5, 595-600.

(30) Raub T.J. and Newton C.R. (1991) Recycling kinetics and transcytosis of transferrin in primary cultures of bovine brain microvessel endothelial cells. *J. Cell. Physiol.* 149, 141-151.

(31) Reese T.S. and Karnovsky M.J. (1967) Fine structural localization of a blood-brain barrier to exogenous peroxidase, *J. Cell. Biol.* 34, 207-217.

(32) Roberts R., Sandra A., Siek G.C., Lucas J.J. and Fine R.E. (1992) Studies of the mechanism of iron transport across the blood-brain barrier. *Ann. Neurol.* 32, S42-S50

(33) Roberts R.L., Fine R.E. and Sandra A. (1993) Receptor-mediated endocytosis of transferrin at the blood-brain barrier. *J. Cell Science* 104, 521-532.

(34) Rupnick M.A., Carey A. and Williams S.K. (1988) Phenotypic diversity in cultured cerebral microvascular endothelial cells. *In Vitro Cell Dev. Biol.* 24 (5), 435-444.

(35) Spatz H. (1922) *Über den Eisennachweis im Gehirn, besonders in Zentren des extrapyramidal-motorischen systems.* *Z. Gesamte Neurol. Psych. (Berl)* 77, 261-290.

(36) Stein B.S. and Sussmann H.H. (1986) Demonstration of two distinct transferrin receptor recycling pathways and transferrin-independent receptor internalization in K562 cells. *J. Biol. Chem.* 261, 10319-10331.

(37) Testa U., Pelosi E. and Peschle C. (1993) The transferrin receptor. *Crit. Rev. Oncogen.* 4 (3), 241-276.

(38) van Renswoude J., Bridges K.R., Harford J.B., Klausner R.D. (1982) Receptor mediated endocytosis of transferrin and uptake of iron in K562 cells. Identification of a non-lysosomal compartment. *Proc. Natl. Acad. Sci. USA* 79, 6186-6190.

Chapter 5

(39) Youdim M.B.H. and Ben-Shachar D. (1987) Minimal brain damage induced by early iron deficiency: modified dopaminergic neurotransmission. *Isr. J. Med. Sci.* 23, 19-25.

CHAPTER 6

Regulatory aspects of iron uptake in blood-brain barrier endothelial cells cultured in either iron-depleted or iron-enriched media.

This chapter is based on:

van Gelder W., Huijskes-Heins M.I.E., Cleton-Soeteman M.I., van Dijk J.P. and van Eijk H.G.

(1995) Regulatory aspects of iron uptake in blood-brain barrier endothelial cells cultured in either iron-depleted or iron-enriched media
Submitted.

Chapter 6

§ 6.0 Contents.

§ 6.1: Summary.

§ 6.2: Introduction.

§ 6.3: Materials and methods:

§ 6.3.1: Materials.

§ 6.3.2: Methods:

§ 6.3.2.1: Blood-brain barrier microvessel endothelial cell isolation and culturing.

§ 6.3.2.2: Radio-labeling of transferrin.

§ 6.3.2.3: Surface TfR measurements.

§ 6.3.2.4: Total TfR measurements.

§ 6.3.2.5: Quantitation of intracellular TfR's participating in the endocytic cycle.

§ 6.3.2.6: Transferrin receptor endocytosis rate measurements.

§ 6.3.2.7: Transferrin receptor exocytosis rate measurements.

§ 6.3.2.8: Quantification of cellular iron uptake and release.

§ 6.3.2.9: Protein measurements.

§ 6.3.2.10: Mathematical analyses of the experimental data on TfR binding, TfR endocytosis and TfR exocytosis.

§ 6.4: Results:

§ 6.4.1: Quantification of surface TfR's, total TfR's and active intracellular TfR's.

§ 6.4.2: Transferrin receptor kinetics: estimates of endocytosis and exocytosis rates.

§ 6.4.3: Quantification of iron uptake and release.

§ 6.5: Discussion.

§ 6.1 Summary.

Iron is an essential element in the cellular metabolism of all mammalian tissues including the brain. Intracerebral iron concentrations have been shown to vary with age and in a number of (neurological) diseases. To date however, factors governing the regulation of intracerebral iron concentration are unknown, although there is some evidence to suggest that the endothelial cells lining the capillaries in the brain (BBB-EC's) are of major importance in this process. To further investigate the role of these BBB-EC's in cerebral iron regulation, primary cultures of porcine BBB-EC's were grown in either iron-enriched (Fe^+) or iron-depleted (Fe^-) culture medium. Fe^+ cultured BBB-EC's showed a reduction in surface bound and total transferrin receptor (TfR) numbers compared to Fe^- cultured cells. Experiments on the endocytic cycle of TfR's showed that the TfR internalization rate of

Regulatory aspects of iron uptake.

Fe⁺ BBB-EC's ($K_{in} = 0.62$) was twice that of Fe⁻ cultured cells, whereas the TfR externalization rate of Fe⁺ was lower than that of Fe⁻ cultures. Our findings indicate that TfR endocytosis rates in BBB-EC's are in agreement with those found in other cell types. Moreover, Fe⁺ cultured BBB-EC's were able to accumulate more iron intracellularly than Fe⁻ cells. These results are in agreement with both the kinetic data on TfR's and clinical findings in hemochromatosis and suggest that at high peripheral iron concentrations, the rate of iron transport across the BBB-EC's is to some extent proportional to this peripheral iron concentration.

§ 6.2 Introduction.

Iron is an essential element in a large number of enzymes required for proper cellular functioning (1,16). In brain tissue cells, iron can be found in various enzymes involved in oxidative phosphorylation, neurotransmitter synthesis and degradation, and myelin formation (2,20,27). Both iron deficiency and iron overload change the normal distribution pattern of intracerebral iron, resulting in neurological dysfunction and sometimes even in overt cellular damage (10,14,15,30,34).

Contrary to what is known about the distribution of iron in peripheral tissues, only limited information is available on the distribution of iron in the brain (2,6). Recently, morphological and biochemical studies determined the overall distribution of iron, transferrin and ferritin in human brain tissue (7,20). However, as discussed in chapter 1 and 5, the cerebral iron pool is subject to changes due to ageing, iron deficiency or overload, and a number of neurological diseases (e.g. Alzheimer's disease). The finding of elevated iron concentrations in areas prone to damage in Parkinson's and Alzheimer's disease, suggests that iron is involved in the pathogenesis of these diseases (see chapter 8). Indeed, some (although indirect) evidence for an involvement of oxygen radical species in those diseases has been described (9,12,21).

Regulatory factors governing the uptake and distribution of iron in the brain are as yet unknown (3,7). With the discovery of transferrin receptors on the luminal side of the blood-brain barrier endothelial cells (13), it became evident that iron might cross the blood-brain barrier, although most aspects of this pathway are still unclear (3,19,26,32). Considering the large surface area of the blood-brain barrier ($\pm 240 \text{ cm}^2/\text{g}$ brain tissue), it can be

Chapter 6

assumed that the BBB is of major importance in the uptake of iron into the brain (23). In earlier work (see chapter 5), experiments were performed to quantify both intracellular and surface bound transferrin receptors in primary cultures of BBB-EC's. To further elucidate the role of BBB-ECs in the regulation of iron transport, we have grown primary isolates of porcine BBB-ECs in either iron-enriched or iron-depleted medium, thus mimicking iron overload and iron deficiency. Data will be presented on the quantification, distribution and kinetics of transferrin receptors on these endothelial cells.

§ 6.3 Materials and methods.

§ 6.3.1 *Materials.*

Fresh porcine brain was obtained from the local slaughterhouse. Specific chemicals used for the isolation and culturing of BBB-EC's are listed in chapter 5.

§ 6.3.2 *Methods.*

§ 6.3.2.1 *Blood-brain barrier microvessel endothelial cell isolation and culturing.*

A detailed description of this procedure can be found in § 2.2.1 and § 2.2.2. Following isolation, all cells were cultured according to the standard procedure for 3 days. Subsequently, cells designated to be "iron loaded", were incubated with culture medium containing 300 μM diferric transferrin (= Fe^+ medium). Fe^+ medium was changed every other day and experiments were performed when cultures were nearly confluent.

Cells designated to be "iron deficient" were treated according to the standard procedure until two days before the actual experiment. At that time, Deferrioxamine (50 $\mu\text{g}/\text{ml}$) was added to the culture medium (= Fe^- medium) and this was repeated on the day before the experiment.

§ 6.3.2.2 *Radio-labeling of transferrin.*

Experiments were performed with either ^{125}I and/or ^{59}Fe labeled Tf. A description of the radio-labeling procedure can be found in § 2.8.1.

Regulatory aspects of iron uptake.

§ 6.3.2.3 *Surface transferrin receptor measurements.*

Surface TfR measurements were performed as described by Ciechanover (5). Blood-brain barrier endothelial cells were incubated with ^{125}I -Tf at 4 °C, rinsed with PBS and receptor bound ^{125}I -Tf was measured. A detailed description of this procedure can be found in § 2.8.2.

§ 6.3.2.4 *Total transferrin receptor measurements.*

To assess the total amount of TfR's present in the endothelial cells, a procedure as described by Rao (22) was used (see § 2.8.3). Blood-brain barrier endothelial cells were homogenized, incubated with ^{125}I -Tf at 4 °C and precipitated with ammonium sulfate. ^{125}I -Tf-TfR complexes were collected on filters and measured. The TfR recovery efficiency of this procedure was checked in a separate series of experiments (see § 5.3.2.7).

§ 6.3.2.5 *Quantification of intracellular transferrin receptors participating in the endocytic cycle.*

A detailed description of this technique can be found in § 2.8.5. Briefly: cells were washed once with PBS and then incubated for 1 to 3 h with 1500 ng (≥ 50 times Kd) ^{125}I -Tf-2Fe at 37 °C. Cells were then harvested and intracellular TfR bound ^{125}I -Tf was measured.

§ 6.3.2.6 *Transferrin receptor endocytosis rate measurements.*

A detailed description of these single cycle experiments can be found in § 2.8.6. Briefly, cells were incubated with 1.6 $\mu\text{g}/\text{ml}$ diferric ^{59}Fe -Tf at 4 °C. Endocytosis was started by rapidly heating cells to 37 °C, at the same time adding 2 ml of prewarmed (37 °C) medium containing 1.6 $\mu\text{g}/\text{ml}$ unlabeled diferric transferrin. Endocytosis was stopped at fixed time periods by rinsing the cells with icecold PBS. Intracellular ^{59}Fe (as a marker for endocytosis) was measured at those time periods. Data sets were analyzed in a nonlinear curve fit program according to the equation $Y(t) = B_{\text{tot}} * (1 - e^{-k^*t})$, to yield an estimate of the internalization rate constant K_{in} .

Chapter 6

§ 6.3.2.7 *Transferrin receptor exocytosis rate measurements.*

A detailed description of these single cycle experiments can be found in § 2.8.7. Briefly, cells were incubated with 1.6 µg/ml ¹²⁵I labeled diferric transferrin at 37 °C for 1 h 45 min and then placed on ice and washed repeatedly with acid and neutral buffers. Exocytosis was started by rapid heating to 37 °C, and stopped at fixed intervals by rinsing cells with icecold PBS. Remaining intracellular ¹²⁵I-Tf (as a marker for exocytosis) was measured at those intervals. Data sets were analyzed in a nonlinear curve fit program according to the equation $Y(t) = C_1 * e^{-k^*t} + C_2$, to yield an estimate of the externalization rate constant K_{out} .

§ 6.3.2.8 *Quantification of cellular iron accumulation and release.*

This procedure is described in detail in § 2.8.8. Briefly, following pre-incubation with serum free medium, cells were incubated for different time periods up to 24 h with 4.8 µg/ml diferric ⁵⁹Fe-Tf at 37 °C. At those intervals, cells were placed on ice, washed and harvested for both protein and intracellular iron (⁵⁹Fe) measurements. The ⁵⁹Fe/protein ratio represents the net iron accumulation (= uptake minus release).

A parallel experiment was set up to measure iron release only. In a number of dishes, medium containing ⁵⁹Fe was replaced at t = 3 h by standard medium. After another 3 h the excreted amount of ⁵⁹Fe was measured.

§ 6.3.2.9 *Protein measurements.*

Cell protein measurements were performed as described in §2.5.2.2.

§ 6.3.2.10 *Mathematical analyses of the experimental data on transferrin receptor binding, endocytosis and exocytosis.*

Detailed descriptions can be found in § 2.7.2 and § 2.7.3.

§ 6.4 Results.

§ 6.4.1 *Quantification of surface bound, total, and active intracellular transferrin receptors.*

Surface bound TfR's were assessed in primary cultures of BBB-EC's grown either in Fe⁺

Regulatory aspects of iron uptake.

or Fe⁻ medium. Cells subjected to either of the culture conditions originated from the same isolate. In this way, possible variations due to differences between separate batches could be avoided.

Each individual binding experiment consisted of 10 (duplicate) measuring points and the combined results of 4 separate experiments are depicted in *Fig. 1*. The inserts show the result of the nonlinear curve fit program applied to the pooled data sets for Fe⁺ and Fe⁻ cultures. The two curves in the large graph are the result of nonlinear curve fits (see chapter 5) corrected for nonspecific binding. The differences in surface TfR bound Tf between Fe⁺ and Fe⁻ are considered significant, since data differed more than twice the standard deviation (Fe⁻: Bmax = 0.037 ± 0.003; Fe⁺: Bmax = 0.029 ± 0.003).

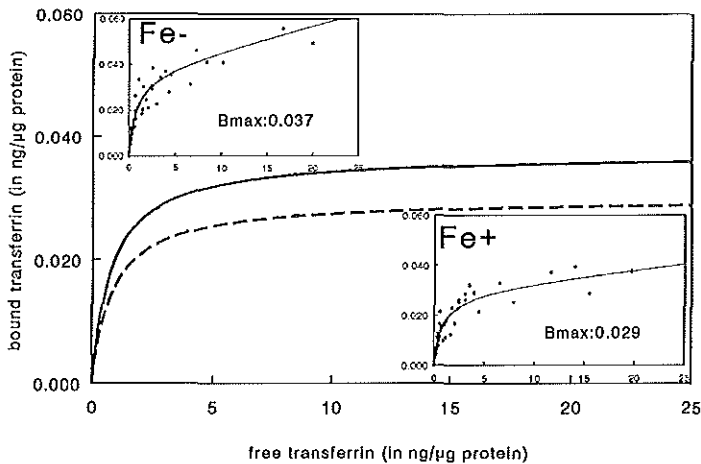


Fig. 1:

The results of 4 separate experiments (n = 10, in duplicate) are summarized in this figure. Blood-brain barrier endothelial cells, either cultured in iron-enriched (Fe⁺) or iron-depleted (Fe⁻) medium, were incubated with ¹²⁵I-Tf at 4 °C and surface bound ¹²⁵I-Tf was measured. The binding plots in the large graph were obtained using a nonlinear curve fit program and are corrected for nonspecific binding. The solid line represents the fitted binding plot of Fe⁻ cultured cells, the interrupted line represents the binding plot of the Fe⁺ cultured cells. The inserts show the original data points of both the Fe⁺ and Fe⁻ cultured cells. Each data point is the average of a result in duplicate. X-axis and Y-axis scalings in the inserts are identical to those in the large graph.

Bmax, R², Scatchard analysis derived TfR affinity constants Ka, and other data are summarized in *Table 1*.

Chapter 6

Total transferrin receptor assessments were obtained and displayed in a similar way. Results are summarized in Fig. 2 and Table 1.

	Surface Tfr's		Total Tfr's	
	Fe +	Fe -	Fe +	Fe -
Bmax in ng Tf/ μ g prot	0.029	0.037	0.072	0.090
Ka (* 10^9)	1.25	1.32	0.36	0.28
R ² (nonlin curve fit)	0.85	0.85	0.77	0.88
no of binding sites/mg prot (* 10^{11})	2.25	2.79	5.45	6.80
% nonspec. binding	1.6%	2.8%	9.3%	7.8%

Table 1:

This table summarizes the experimental results on surface and total Tfr quantification in primary cultures of BBB-EC's.

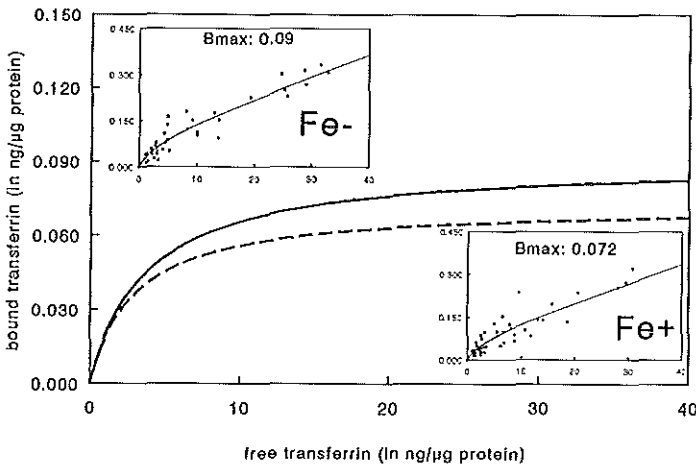


Fig. 2: The results of 4 separate experiments (n = 10, in duplicate) are summarized in this figure. Lysed blood-brain barrier endothelial cells, either cultured in iron-enriched (Fe⁺) or iron-depleted (Fe⁻) medium, were incubated with ¹²⁵I-Tf at 4 °C, precipitated and ¹²⁵I-Tf-TfR complexes were collected. The binding plots in the large graph were obtained using a nonlinear curve fit program and are corrected for nonspecific binding. The solid line represents the fitted binding plot of Fe⁻ cultured cells, the interrupted line represents the binding

Regulatory aspects of iron uptake.

plot of the Fe^+ cultured cells.

The inserts show the original data points of both the Fe^+ and Fe^- cultured cells. Each data point is the average of a result in duplicate. The X-axis represents free Tf (in $\text{ng}/\mu\text{g}$ protein) and the Y-axis represents bound Tf (in $\text{ng}/\mu\text{g}$ protein).

The number of intracellular TfR's actively participating in the endocytic cycle of BBB-EC's cultured in Fe^+ or Fe^- medium was assessed in three separate experiments. Each experiment was performed in sixfold with three different incubation times up to 3 hours. Since earlier experiments had made clear that the number of active intracellular TfR's is independent of the incubation time (see chapter 5), results of all obtained data were averaged. BBB-EC's cultured in Fe^+ medium contained 0.089 ± 0.004 ng bound Tf/ μg protein (mean \pm SD). BBB-EC's cultured in Fe^- medium contained 0.107 ± 0.005 ng bound Tf/ μg protein (mean \pm SD), which means a significant difference ($p < 0.05$).

§ 6.4.2 Transferrin receptor kinetics: estimates of endocytosis and exocytosis rates.

A series of single cycle experiments were performed to study the effects of iron overload and iron depletion on the rate of transferrin receptor endocytosis in primary cultures of BBB-EC's. Each series consisted of four separate experiments, with 8 measuring points (time intervals) per experiment. The rate of endocytosis was estimated by measuring ^{59}Fe uptake in the first few minutes. Results are summarized in *Fig. 3* and *Table 2*. Correlation coefficients of the nonlinear curve fits were better than 92%.

	endocytosis		exocytosis	
	Fe^-	Fe^+	Fe^-	Fe^+
K_{in} resp. K_{out} in min^{-1}	0.30	0.62	0.06	0.05
$T_{1/2}$ in min	2.3	1.1	11.6	14.6

Table 2:

This table summarizes the experimental results on TfR internalization and externalization in BBB-EC's. ($T_{1/2} = \ln 2/K_{\text{in}}$ resp. K_{out})

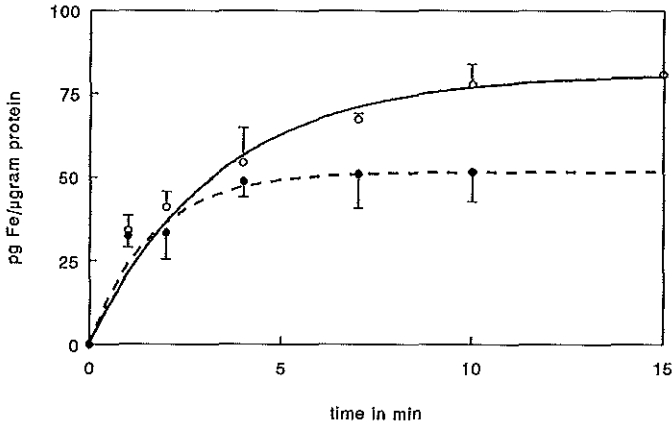


Fig. 3:

Results of four separate single cycle experiments with 8 time intervals per experiment were performed to assess the TfR internalization rate. Intracellular ⁵⁹Fe was measured: each open circle represents the mean ± SD of 4 experiments with Fe⁻ cultured cells; closed circles represent the mean ± SD of 4 experiments with Fe⁺ cultured cells. The solid (Fe⁻) and interrupted (Fe⁺) lines represent the plots derived from the nonlinear curve fit analyses, using the equation $Y(t) = B_{tot} * (1 - e^{-k*t})$.

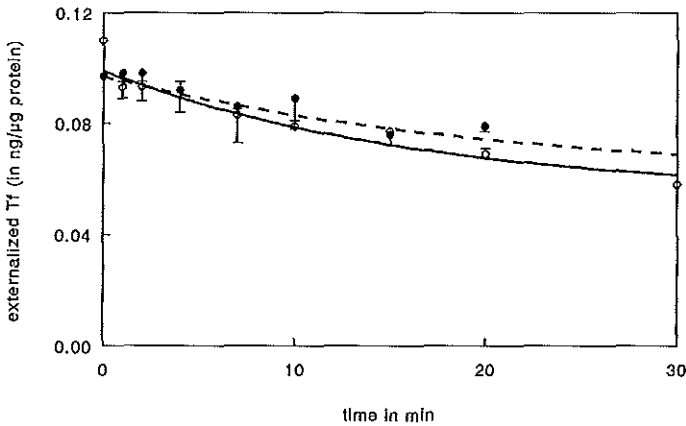


Fig. 4:

Results of four separate single cycle experiments with 10 time intervals per experiment were performed to assess the TfR externalization rate. Excreted ¹²⁵I-Tf was measured: each

Regulatory aspects of iron uptake.

open circle represents the mean \pm SD of 4 experiments with Fe^- cultured cells; closed circles represent the mean \pm SD of 4 experiments with Fe^+ cultured cells. The solid (Fe^-) and interrupted (Fe^+) lines represent the plots derived from the nonlinear curve fit analyses, using the equation $Y(t) = C_1 * e^{-k*t} + C_2$.

Transferrin receptor exocytosis was studied in a similar fashion, measuring the amount of ^{125}I labeled TF that re-entered the medium in a specific time interval at 37 °C. Again, each series consisted of four separate experiments, with 8 measuring points per experiment. Results are displayed in Fig. 4 and Table 2. Correlation coefficients of the nonlinear curve fits averaged 97%.

§ 6.4.3 Quantification of iron accumulation.

Cells, cultured in Fe^+ or Fe^- medium, were incubated for 0.5 to 24 hours with diferric (^{59}Fe) transferrin to quantify iron accumulation (= iron uptake minus release). The averaged results of 4 separate experiments are depicted in Fig. 5.

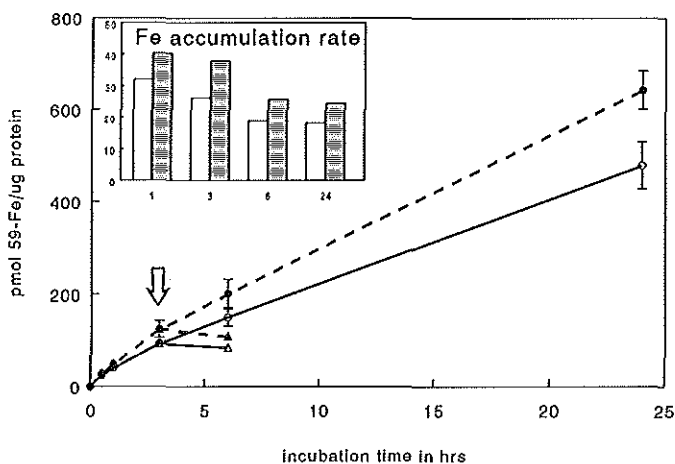


Fig. 5:

Results of three separate experiments with 5 time intervals per experiment were performed to quantify iron accumulation. Each open circle (and solid line) represents the mean \pm SD of 3 experiments with Fe^- cultured cells; closed circles (and interrupted line) represent the mean \pm SD of 3 experiments with Fe^+ cultured cells.

A parallel experiment was set up to measure iron release only. The two open triangles represent the mean \pm SD of 2 experiments with Fe^- cultured cells; closed triangles represent

Chapter 6

the mean \pm SD of 2 experiments with Fe^+ cultured cells.

The insert shows the averaged iron accumulation rate in $\text{pmol Fe}/\mu\text{g protein/h}$ (Y-axis) between each two experimental time points (X-axis). Solid bars represent the iron accumulation rate in Fe^- cultured cells; dotted bars represent the iron accumulation rate in Fe^+ cultured cells.

The insert in *Fig. 5* shows the net decrease in iron accumulation rate with prolonged incubation times.

After 3 h of iron uptake, iron release during the next 3 h was quantified in 2 separate experiments. These results are also displayed in *Fig. 5*. Iron release in Fe^+ cultures was 4.8 $\text{pmol Fe}/\mu\text{g protein/hour}$, and 2.9 $\text{pmol Fe}/\mu\text{g protein/hour}$ in Fe^- cultures.

§ 6.5 Discussion.

The total amount of iron in the brain, and the distribution of iron over different brain regions are subject to changes throughout life. Alterations in the peripheral iron status (e.g. hemochromatosis) affect the intracerebral iron concentration, suggesting that iron traffics between peripheral tissues and the brain. This raises two questions: (i) where does iron enter or leave the brain, and (ii) which factors modulate this iron trafficking.

Brain tissue is isolated from the peripheral circulation by the blood-brain barrier, a monolayer of non-fenestrated endothelial cells interconnected by tight junctions (25,28). The large BBB microvascular surface area and the presence of transferrin receptors on the luminal side of the BBB-EC's suggest that the BBB-EC's are of major importance to iron transport. If so, it is conceivable that iron transport is regulated through a modulation of TfR quantity, TfR distribution and/or TfR kinetics in these BBB-EC's (31).

The results in *Figs. 1 and 2* and *Table 1* show that there is a significant increase in surface TfR's, total TfR's and active intracellular TfR's in those cells that were cultured in Fe^- medium as compared to the cells cultured in Fe^+ medium. This increase in the number of TfR's in Fe^- cultures can easily be explained assuming that low intracellular concentrations of iron induce TfR synthesis (see chapter 1) through the IRE-IRF system (17).

TfR internalization and externalization constants (K_{in} and K_{out}), as determined in single cycle experiments (see *Fig. 3*, *Fig. 4* and *Table 2*), show that cells cultured in Fe^- medium internalize their TfR's twice as slow as Fe^+ cultured cells. On the other hand, Fe^- cultured

Regulatory aspects of iron uptake.

cells externalize their TfR's more rapidly than Fe⁺ cultured cells (see *Fig. 4* and *Table 2*). A high K_{in} and low K_{out}, as in Fe⁺ cultured cells, will result in a low number of surface bound TfR's, and is in accordance with results shown in *Fig. 1*.

Our data disagree with the results of Raub et al (24) on TfR receptor kinetics in BBB-EC's. They found considerably lower values for K_{in} (0.03 min⁻¹) and K_{out} (0.017 min⁻¹). However, the results are not fully comparable due to differences in experimental techniques and data interpretation. Our experimental data yield estimates of K_{in} and K_{out} that are in good agreement with those found in other cell types (29,33). Moreover, we performed experiments (see chapter 7) in which we studied endocytosis of Au-labeled Tf in BBB-EC's and found a number of clathrin coated pits and vesicles containing Au-labeled Tf after 1 min incubation.

We are also faced with the problem that assessment of the externalization rate is based on measuring the amount of ¹²⁵I-Tf that remains within the cell after incubation at 37 °C. In this way, one cannot discern between ¹²⁵I-Tf that is released from the cell through the endocytic cycle, or released otherwise (e.g. transcytosis). To date, the issue of transcytosis of Tf through the BBB-EC is still a matter of debate (3, see also chapter 7). However, should transcytosis of Tf through the BBB-EC indeed exist, our experimental procedure would yield an overestimation of the exocytosis rate, thereby not affecting our conclusion as such.

Studies have shown that ⁵⁹Fe, when administered peripherally, can be detected within the brain after some time (8,11,19). There was also some evidence that BBB-EC's can accumulate iron (18,24). Our results as summarized in *Fig. 5*, confirm that BBB-EC's accumulate iron. Since the BBB is a selective barrier that regulates the transport of substances to and from the brain (i.e. iron), it is possible that iron accumulation in BBB-EC's is in fact an artifact due to in vitro culturing. There is evidence that BBB-EC's function differently when co-cultured with astrocytes (4) and nearly pure BBB-EC cultures (as in our experiments) are devoid of those cells. In vivo, astrocytes are in close contact with BBB-EC's and they could therefore affect or participate in the process of iron transport.

In our experiments, Fe⁺ cultured cells accumulate iron more rapidly than Fe⁻ cultured cells. This finding is in agreement with the kinetic data on TfR internalization (see *Table 2*), since Fe⁺ cultured cells show higher K_{in}'s than Fe⁻ cultured cells.

Chapter 6

Based on the difference found in K_m 's between Fe^- and Fe^+ cultured cells (Table 2), one would expect iron to accumulate twice as fast in Fe^+ cultured cells. However, iron accumulation in the BBB-EC is the net result of uptake and release. And although Fe^- cultured cells internalize their surface bound TfR's at a slower rate, this is at least partially compensated as Fe^- cells have more TfR's on their cell surface than Fe^+ cultured cells (Fig. 1 and Fig. 3). Moreover, Fe^+ cultured cells also show a more rapid release of iron (see Fig. 5), namely 4.8 pmol/h (Fe^+) and 3.9 pmol Fe/h (Fe^-) (data corrected for differences in intracellular iron concentration between both cultures). Together, this will diminish the difference in iron accumulation between Fe^+ and Fe^- cultured cells. Interestingly, the insert in Fig. 5 shows that, although the iron accumulation rate decreases with prolonged incubation times, this decrease is not linear. In fact, the accumulation rates seem to stabilize within 24 hours, suggesting that iron uptake and excretion (= accumulation) in the BBB-EC reached equilibrium. Furthermore, experiments with BBB-EC's cultured on porous filters (Falcon, Costar) show that these cells also accumulate iron, independent of the presence of either diferric Tf or apo-Tf in the lower chamber (results not shown).

Since Fe^+ cultured cells accumulate and release iron more rapidly than Fe^- cultured cells, it would seem that iron transport across the blood-brain barrier is (partly) iron concentration dependent. This is in agreement with clinical studies in patients with hemochromatosis, showing that elevated peripheral iron concentrations will lead to an increase in intracerebral iron. These findings also imply that besides brain tissue, BBB-EC's can also accumulate iron, rendering these cells more susceptible to oxidative damage. On the other hand, since iron depletion results in increased TfR numbers, higher TfR externalization rates and less accumulated iron, it would appear that in these circumstances the BBB-EC's promote transport over accumulation.

In summary we conclude that: (i) variations in peripheral iron concentration affect both the TfR quantity and TfR kinetics of BBB-EC's. (ii) BBB-EC's are capable of iron excretion and accumulation at the same time, and future research in this field should therefore include studies on the vulnerability of BBB-EC's to oxidative stress. (iii) The rate of iron transport across the BBB-EC's at high peripheral iron concentrations, is to some extent proportional to this peripheral iron concentration. (iv) Iron depletion will promote iron transport over iron accumulation.

Regulatory aspects of iron uptake.

References:

- (1) Aisen P. (1994) Iron metabolism: an evolutionary perspective. In: Iron metabolism in health and disease (eds: Brock J.H., Halliday J.W., Pippard M.J. and Powell L.W.), pp 1-30. Saunders company Ltd, London, Uk.
- (2) Beard J.L., Connor J.R. and Jones B.C. (1993) Iron in the brain. *Nutr. Rev.* 51: 157-179.
- (3) Broadwell R.D. and Banks W.A. (1993) Cell biological perspective for the transcytosis of peptides and proteins through the mammalian blood-brain fluid barrier. In: The blood-brain barrier. Cellular and molecular biology. (Ed: Pardridge W.M.), pp 165-199. Raven Press, New York.
- (4) Cancilla P.A., Bready J. and Berliner J. (1993) Brain endothelial-astrocyte interactions. In: The blood-brain barrier. Cellular and molecular biology. (Ed: Pardridge W.M.), pp. 25-46. Raven Press, New York.
- (5) Ciechanover A., Schwartz A.L., Dautry-Varsat A. and Lodish H.F. (1983) Kinetics of internalization and recycling of transferrin and the transferrin receptor in a human hepatoma cell line. *J. Biol. Chem.* 258, 9681-9689.
- (6) Connor J.R. and Benkovic S.A. (1992) Iron regulation in the brain: histochemical, biochemical, and molecular considerations. *Ann. Neurol.* 32: S51-61.
- (7) Connor J.R. (1993) Cellular and regional maintenance of iron homeostasis in the brain: normal and diseased states. In: Iron in central nervous system disorders. (Eds: Riederer P. and Youdim M.B.H.), pp. 1-18. Springer-Verlag, New York.
- (8) Crowe A. and Morgan E.H. (1992) Iron and transferrin uptake by brain and cerebrospinal fluid in the rat. *Brain Res.* 592: 8-16.
- (9) Dexter D.T., Carter C.J., Wells F.R., Javoy-Agid F., Agid Y., Lees A., Jenner P. and Marsden C.D. (1989) Basal lipid peroxidation in substantia nigra is increased in Parkinson's disease. *J. Neurochem.* 52: 381-389.
- (10) Dexter D.T., Jenner P., Schapira A.H.V. and Marsden C.D. (1992) Alterations in levels of iron, ferritin, and other trace metals in neurodegenerative diseases affecting the basal ganglia. *Ann. Neurol.* 32 (Suppl): S94-100.
- (11) Dwork A.J., Lawler G., Zybert P.A., Durkin M., Osman M., Willson N. and Barkai A.I. (1990) An autoradiographic study of the uptake and distribution of iron by the brain of the young rat. *Brain Res.* 518: 31-39.
- (12) Evans P.H. (1993) Free radicals in brain metabolism and pathology. *Brit. Med. Bull.* 49: 577-587

Chapter 6

- (13) Jefferies W.A., Brandon M.R., Hunt S.V., Williams A.F., Gatter K.C. and Mason D.Y. (1984) Transferrin receptor on endothelium of brain capillaries. *Nature* 312, 162-163.
- (14) Jellinger K. and Kiendl E. Iron deposits in brain disorders. In: Iron in central nervous system disorders. (Eds: Riederer P. and Youdim M.B.H.), pp 19-36. Springer-Verlag, New York.
- (15) Koeppen A.H. and Dentinger M.P. (1988) Brain hemosiderin and superficial siderosis of the central nervous system. *J. Neuropathol. Exp. Neurol.* 47: 249-270.
- (16) Matzanke B.F., Müller-Matzanke G. and Raymond K.N. (1989) Siderophore-mediated iron transport. In: Iron carriers and iron proteins (ed: Loehr T.M.), pp 1-121. VCH Publishers, Inc, New York, USA.
- (17) Melefors Ö and Hentze M.W. (1993) Iron regulatory factor - the conductor of cellular iron regulation. *Blood Rev.* 7: 251-258.
- (18) Moos T. and Mollgård K. (1993) A sensitive post-DAB enhancement technique for demonstration of iron in the central nervous system. *Histochem.* 99: 471-475.
- (19) Morris C.M., Keith A.B., Edwardson J.A. and Pullen R.G.L. (1992) Uptake and distribution of iron and transferrin in the adult rat brain. *J. Neurochem.* 59: 300-306.
- (20) Morris C.M., Candy J.M., Oakley A.E., Bloxham C.A. and Edwardson J.A. (1992) Histochemical distribution of non-haem iron in the human brain. *Acta Anat.* 144: 235-257.
- (21) Olanow C.W. (1990) Oxidation reactions in Parkinson's disease. *Neurol.* 40 (suppl.): 32-37.
- (22) Rao K.K., Shapiro D., Mattia E., Bridges K. and Klausner R. (1985) Effects of alterations in cellular iron on biosynthesis of the transferrin receptor in K 562 cells. *Molec. Cell. Biol.* 5, 595-600.
- (23) Rapoport S.I. (1976) Blood-brain barrier in physiology and medicine. Raven Press, New York, USA.
- (24) Raub T.J. and Newton C.R. (1991) Recycling kinetics and transcytosis of transferrin in primary cultures of bovine brain microvessel endothelial cells. *J. Cell. Physiol.* 149: 141-151.
- (25) Reese T.S. and Karnovsky M.J. (1967) Fine structural localization of a blood-brain barrier to exogenous peroxidase, *J. Cell. Biol.* 34, 207-217.
- (26) Roberts R., Sandra A., Siek G.C., Lucas J.J. and Fine R.E. (1992) Studies of the mechanism of iron transport across the blood-brain barrier. *Ann. Neurol.* 32: S43-50.

Regulatory aspects of iron uptake.

- (27) Roskams A.J.I. and Connor J.R. (1994) Iron, transferrin, and ferritin in the rat brain during development and aging. *J. Neurochem.* 63: 709-716.
- (28) Rubin L.L., Hall D.E., Porter S., Barbu K., Cannon C., Horner H.C., Janatpour M., Liaw C.W., Manning K., Morales J., Tanner L.I., Tomaselli K.J. and Bard F. (1991) A cell culture model of the blood-brain barrier. *J. Cell Biol.* 115 (6), 1725-1735.
- (29) Schonhorn J.E. and Wessling-Resnick M. (1994) Brefeldin A down-regulates the transferrin receptor in K562 cells. *Molec. Cell. Biochem.* 135:159-169.
- (30) Sofic E., Paulus W., Jellinger K., Riederer P. and Youdim M.B.H. (1991) Selective increase of iron in substantia nigra zona compacta of parkinsonian brains. *J. Neurochem.* 56: 978-982.
- (31) Starreveld J.S., van Dijk J.P., Kroos M.J. and van Eijk H.G. (1993) Regulation of transferrin receptor distribution in in vitro cultured human cytotrophoblasts. *Clin. Chim. Acta* 220: 47-60.
- (32) Taylor E.M., Crowe A. and Morgan E.H. (1991) Transferrin and iron uptake by the brain: effects of altered iron status. *J. Neurochem.* 57: 1584-1592.
- (33) van Dijk J.P., van Noort W.L., Kroos M.J., Starreveld J.S. and van Eijk H.G. (1991) Isotransferrins and pregnancy: a study in the guinea pig. *Clin. Chim. Acta* 203: 1-16.
- (34) Youdim M.B.H. (1988) Iron in the brain: implications for Parkinson's and Alzheimer's diseases. *Mount Sinai J. Med.* 55: 97-101.

CHAPTER 7

Transcytosis of 6.6 nm gold-labeled transferrin: an ultrastructural study in blood-brain barrier endothelial cells.

This chapter is based on:

van Gelder W., Huijskes-Heins M.I.E., Cleton-Soeteman M.L., van Run P.R.W.A. and van Eijk H.G.

(1995) Transcytosis of 6.6 nm gold-labeled transferrin: an ultrastructural study in blood-brain barrier endothelial cells.
Submitted.

Transcytosis and ultrastructural morphology.

§ 7.0 Contents.

§ 7.1: Summary.

§ 7.2: Introduction.

§ 7.3: Materials and methods:

§ 7.3.1: Materials.

§ 7.3.2: Methods:

§ 7.3.2.1: Isolation and culturing of blood-brain barrier endothelial cells on semiporous membranes.

§ 7.3.2.2: Isolation and purification of porcine serum transferrin.

§ 7.3.2.3: Coupling of 6.6 nm gold to transferrin.

§ 7.3.2.4: Incubation procedure of membrane-grown endothelial cells with gold-labeled transferrin.

§ 7.3.2.5: Fixation, embedding and transmission electron microscopy.

§ 7.4: Results:

§ 7.4.1: Choice of semi-porous membrane type.

§ 7.4.2: Morphology of membrane-grown P₀ and P₁ blood-brain barrier endothelial cells.

§ 7.4.3: Ultrastructural study of gold-labeled transferrin endocytosis in P₁ blood-brain barrier endothelial cells.

§ 7.5: Discussion.

§ 7.1 Summary.

The mechanism and regulation of iron transport to the brain are largely unknown. The large surface area of the blood-brain barrier capillaries and the presence of transferrin receptors on the luminal plasma membranes of the blood-brain barrier endothelial cells (BBB-EC's) suggest that these cells actively participate in the transport of iron into the brain.

In this chapter we describe the ultrastructural morphology of primary and first passage cultures of BBB-EC's grown on various porous membranes. To investigate the mechanism of iron transport into and across the BBB-EC's, membrane grown first passage cells were incubated with gold-labeled transferrin and studied with electron microscopy. Results will be presented, suggestive for a transcytosis of transferrin through the BBB-EC's.

§ 7.2 Introduction.

Iron is an absolute requirement for proper neuronal functioning (1,2), but high concentrati

Chapter 7

ons of intracerebral iron may cause neurodegenerative disorders (e.g. Parkinson's disease) (11,13,26). Fortunately, these potentially noxious effects of iron are restrained as the distribution and storage of this trace element are tightly regulated (6). The exact nature of the intracerebral iron regulation is still largely unknown (see chapter 6), although discovery of transferrin receptors on the blood-brain barrier endothelial cells (17) indicated that the BBB might be involved in the transport of iron into and/or out of the brain. Recent studies ((14,21,23,25) and chapter 6) clearly demonstrated that BBB-EC's actively take up iron by means of receptor mediated endocytosis. The subsequent part of the pathway of iron through these cells and into the brain is, however, still subject to discussion (5,7,15).

In previous experiments (see chapter 6) we demonstrated that BBB-EC's grown on petri dishes can take up, accumulate, and excrete iron. Since BBB-EC's (in vivo) have a barrier function, it was decided to pursue transport of iron (with gold labeled Tf) in BBB-EC's grown on semi-porous membranes. These membranes allow culturing of cells leaving both cell sides accessible to compounds under study (compare Ussing chamber (18,36)).

We describe in this chapter the results of an electron microscopical study of primary and first passage cultures of porcine BBB-EC's grown on different membrane types. Furthermore, we report on the results of an ultrastructural study of the (endocytic) pathway of 6.6 nm gold-labeled transferrin in BBB-EC's.

§ 7.3 Materials and methods.

§ 7.3.1 *Materials.*

Fresh porcine brain tissue was obtained from a local slaughterhouse. Specific chemicals used in the isolation and culturing of BBB-EC's are listed in chapter 5.

Various membrane types were used in the present study, namely: transparent Costar Transwell-col culture chamber inserts (6.5 and 24.5 mm diameter) with a 0.4 μm pore size (Costar, Badhoevedorp, The Netherlands), transparent Falcon Cyclopore cell culture inserts (24.1 mm diameter) with 1 μm pore size, and translucent Falcon Cyclopore cell culture inserts (24.1 mm diameter) with 0.45 μm pore size (Becton Dickinson, Franklin lakes, NJ, USA). Gold sol (6.6 nm \pm 10%) was obtained from Aurion (Aurion, Wageningen, The

Transcytosis and ultrastructural morphology.

Netherlands). Epon embedding fluid consisted of a mixture of LX-112 (LADD Research Industries Inc., Burlington, USA), dodecylsuccinic anhydride (DDSA) (Merck, Darmstadt, FRG), methyl norbonene 2,3 dicarboxylic anhydride (MNA) (Merck, Darmstadt, FRG), and 2,4,6 tris (dimethyl aminomethyl)-phenol (DMP 30) (Merck, Darmstadt, FRG).

§ 7.3.2 Methods.

§ 7.3.2.1 Isolation and culturing of blood-brain barrier endothelial cells on semiporous membranes.

A detailed description of the BBB-EC isolation procedure can be found in § 2.2.1 and § 2.2.3. Briefly, brain tissue was homogenized after careful removal of cerebellum, meninges and choroid plexus. The homogenate was resuspended in culture medium containing dispase and gently shaken for 3 hours. Following filtration and centrifugation (4x), cells were resuspended in culture medium containing penicilline/ streptomycine.

Cells designated to be "primary cultures" (P₀) were then plated on membranes and culture medium was replaced after 1 hour. "First passage cells" (P₁) were first seeded in gelatin coated plastic culture flasks, grown to confluency and then harvested with trypsin/EDTA in PBS. Following resuspension in culture medium and centrifugation, cells were plated on various membranes. Before plating, membranes were preconditioned for 2 hours at 37 °C in culture medium containing 20% fetal calf serum.

§ 7.3.2.2 Isolation and purification of porcine serum transferrin.

This procedure is described in detail in § 2.6.1.

§ 7.3.2.3 Coupling of 6.6 nm gold to transferrin.

A detailed description of this procedure can be found in § 2.3.2. Briefly, diferric porcine transferrin was dialyzed against 0.5 mM NaHCO₃ (pH = 6.4) and mixed (under continuous stirring) with the 6.6 nm gold suspension of similar pH. This solution was left to stand for 15 min, when BSA was added to a final concentration of 1% (w/v). To remove both unbound transferrin and gold-aggregates, the transferrin-gold (Au-Tf) suspension was centrifuged, loaded on a linear sucrose gradient and centrifuged again. The end product

Chapter 7

was checked on homogeneity under the electron microscope (see § 7.3.2.5).

§ 7.3.2.4 *Incubation procedure of membrane-grown endothelial cells with gold-labeled transferrin.*

This procedure is described in detail in § 2.3.3. Briefly, P₀ and P₁ cells were grown on membranes until confluent, washed with PBS and the luminal sides of the cells (upper chamber) were incubated with $\pm 1 \mu\text{g/ml}$ Au-Tf for 2 h at 4 °C. Membranes were then washed with icecold PBS and heated to 37 °C to start the endocytic cycle. Endocytosis was stopped at 1, 5 or 10 min by rapidly placing the membranes on ice, rinsing the cells with icecold PBS and submerging the membranes in fixation fluid.

§ 7.3.2.5 *Fixation, embedding, staining and transmission electron microscopy.*

These procedures are described in detail in § 2.10.

Fixation:

Membrane-grown cells were fixed overnight at 4 °C in a mixture of glutaraldehyde and formaldehyde in sodium phosphate buffer. The following day, samples were rinsed in PBS at room temperature and postfixed in a mixture of OsO₄ and K₄Fe(CN)₆ in PBS.

Embedding:

Following fixation, membrane-grown cells together with the membranes were embedded in Epon, and allowed to polymerize overnight at 60 °C.

Sectioning:

Ultrathin sections of the Epon embedded membranes were made on an Ultratome V (LKB, Sweden), equipped with Diatome 1.5 mm diamant knives. Sections were collected on unfilmed 200 mesh copper grids.

Staining:

Uranyl magnesium acetate was used as the only contrast enhancer, lead citrate was omitted.

Transmission electron microscopy:

Sections were studied in a Zeiss EM 902 (Zeiss, Oberkochen, FRG) transmission electron microscope. This instrument was equipped with an integrated electron spectrometer allowing high-resolution imaging of stained and unstained sections with energy-filtered electrons (= electron spectroscopic imaging (ESI)).

Transcytosis and ultrastructural morphology.

§ 7.4 Results.

§ 7.4.1 Choice of semi-porous membrane type.

We were able to grow both P_0 and P_1 blood-brain barrier endothelial cells (BBB-EC's) on all three membrane types (see § 7.3.1), although it took P_0 cultures considerably longer to reach confluency on membranes (± 14 days) than on petri dishes (± 8 days) of the same diameter.

We experienced considerably more difficulties growing BBB-EC's on Costar Transwell-Col membranes, especially with P_0 cells, than on Falcon Cyclopore membranes. As Costar membranes are very thin (25-50 μm), they tend to sag in the middle when there is culture medium in the upper chamber. Since our BBB-EC isolation procedure mainly yields small clumps of endothelial cells (i.e. fragments of capillaries), sagging results in an assembling of the BBB-EC clumps in the middle of the membrane. As new BBB-EC's mainly originate from these capillary fragments, cells in the center part of the membrane will already reach confluency while the rim of the membrane is still rather empty. Continuation of the culture then leads to post-confluent phenomena in the center of the membrane, such as: formation of "holes" in the monolayer (i.e. neovascularization), and loosening of parts of the monolayer with concomitant cell death. Moreover, mechanical deformation of these membranes also occurs when changing culture medium. This has a negative effect on the attachment of BBB-EC's on the membrane, and cells easily come loose when these membranes are rinsed.

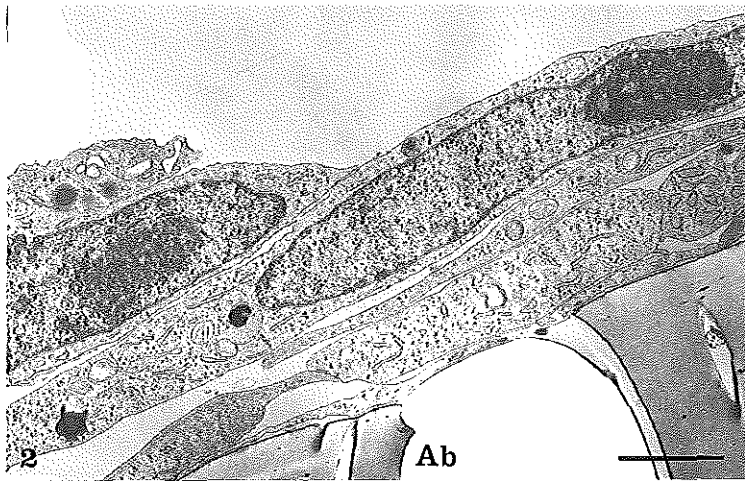
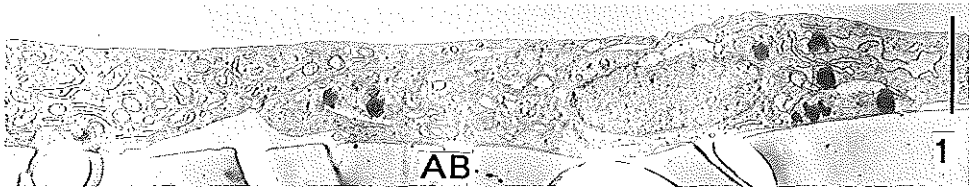
Falcon Cyclopore membranes display a more rigid mechanical behaviour and hardly sag. As a result, P_0 cells plated on these membranes show a more homogenous distribution pattern throughout the membrane surface. Since all membranes could rather easily be sectioned, we chose for the Falcon Cyclopore membranes as the membrane with the best mechanical properties.

§ 7.4.2 Morphology of membrane-grown P_0 and P_1 blood-brain barrier endothelial cells.

Both P_0 and P_1 cultured BBB-EC's were virtually devoid of other cell types. The BBB-EC is an elongated cell with a thickness of about 2.5 to 3 μm (*Fig. 1*), retaining its form on all membrane types. P_0 cells grow in monolayers with an occasional cell on top of this layer,

Chapter 7

whereas P_1 cells more often show two or more cell layers on top of each other (Fig. 2).



Figs. 1 and 2:

Figs. 1 (P_0) and 2 (P_1) are electronmicrographs of stained sections of BBB-EC's on translucent Falcon cyclopore culture inserts. Note the morphological similarity of the cell organelles of P_0 and P_1 , and the tendency of P_1 to grow in multiple layers. Ab = abluminal (filter side). Bar represents 2.5 μ m.

Both P_0 and P_1 cells synthesize basal membrane-like material, although it is our impression that the material made by P_0 cells is thicker and more regular than that of P_1 cells (compare *Figs. 3 and 4*).

Both P_0 and P_1 cells are interconnected by tight junctions (*Figs. 5 and 6*), regardless of arrangement in monolayers or multilayers. Coated pits and vesicles as well as caveolae are a common finding in P_0 and P_1 cells. The coated pits are mainly located in the luminal membrane, although they are also present in the abluminal membrane of P_0 and P_1 cells

Transcytosis and ultrastructural morphology.

(Figs. 3 and 5). There is also suggestion of pinocytosis at both sides of the cell.

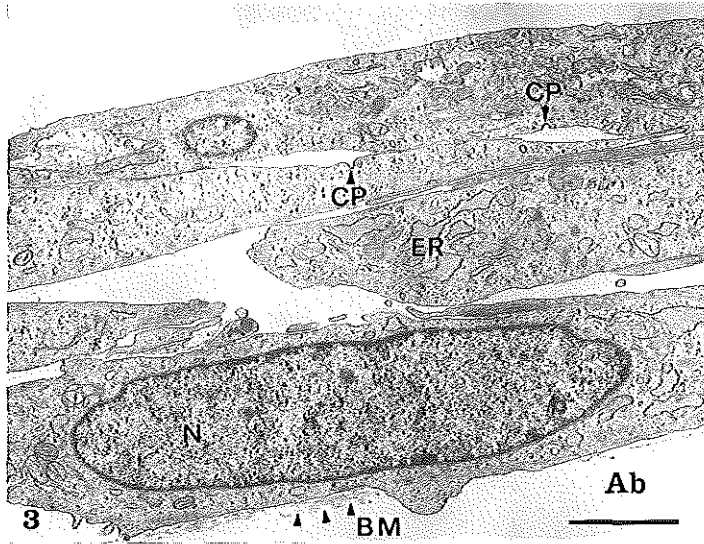
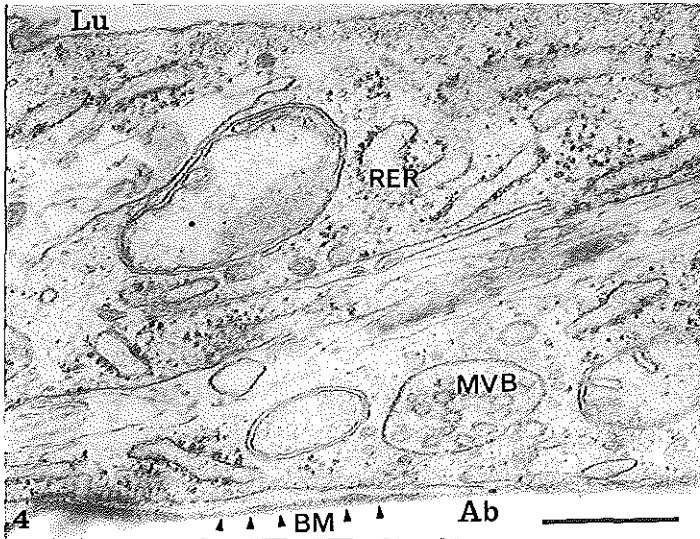


Fig. 3:

Electronmicrograph of stained section of P₁ BBB-EC's. Note the basal membrane-like material (BM); coated pits (CP) on the luminal and abluminal (Ab) side, and the active endoplasmic reticulum (ER). N = nucleus. Bar represents 2.5 μ m.



Chapter 7

Fig. 4:

Electronmicrograph of stained section of P_0 BBB-EC at higher magnification. Note the electron-dense basal membrane-like material (BM) in the abluminal (Ab) side and the swollen rough endoplasmic reticulum (RER). MVB = multivesicular body, Lu = luminal side. Bar represents $0.5 \mu\text{m}$.

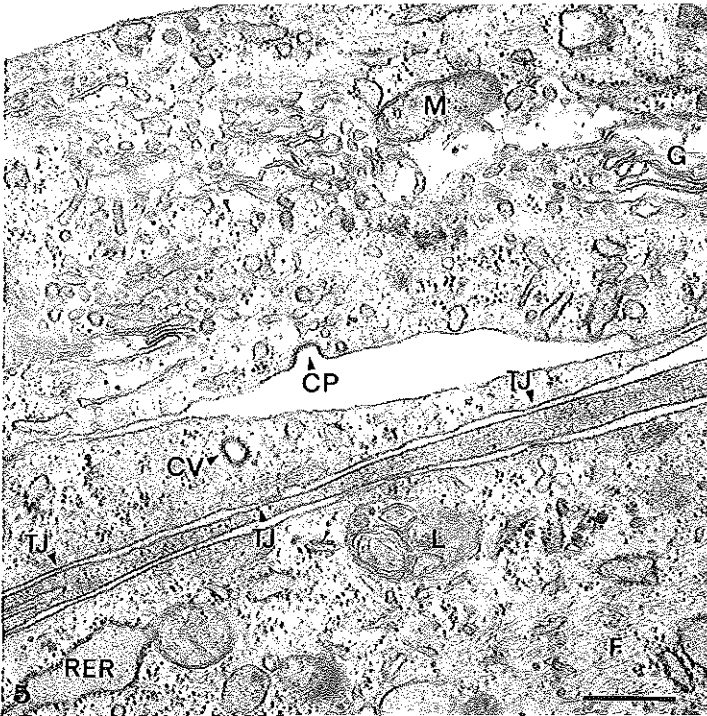


Fig. 5:

Electronmicrograph of P_1 BBB-EC's (stained section) at higher magnification. Note the coated pits (CP) and vesicles (CV). TJ = tight junction, L = lysosome, G = Golgi, F = fibrils, Lu = luminal side, M = mitochondrion. Bar represents $0.5 \mu\text{m}$.

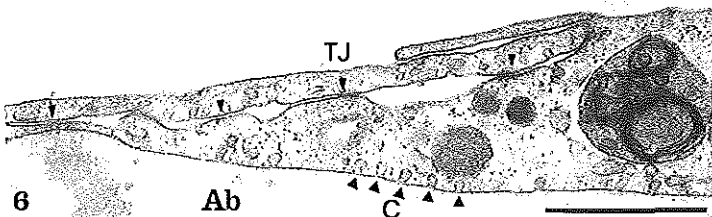


Fig. 6:

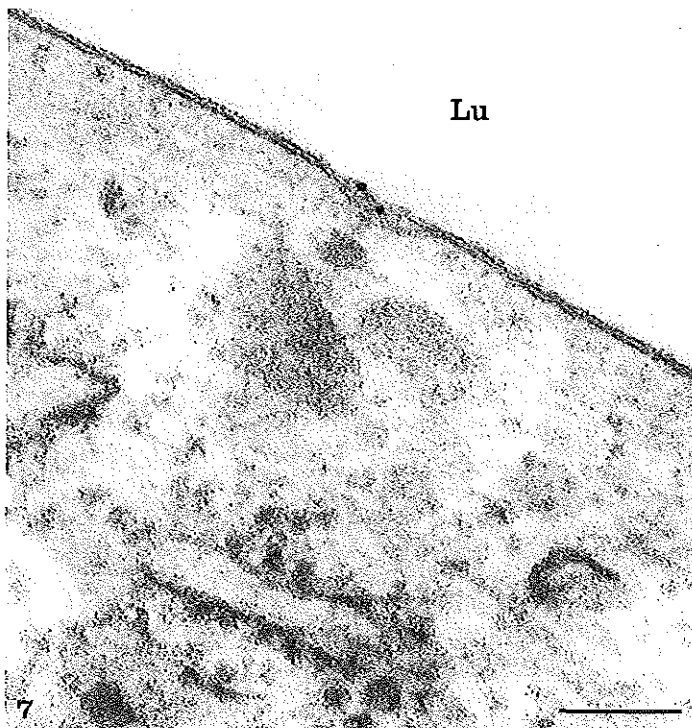
Electronmicrograph of P_1 BBB-EC's (stained section). Note the metabolic activity of the cell as judged by a row of caveolae (C) and a lysosome with whorls. TJ = tight junction. Bar represents $1 \mu\text{m}$.

Transcytosis and ultrastructural morphology.

In *Fig. 4* and *Fig. 5* a multitude of cellular organelles can be discerned in both P_0 and P_1 cells: rough and smooth endoplasmic reticulum, mitochondria, Golgi, lysosomes, multivesicular bodies, and a large number of fibrils. The general morphological appearance is suggestive for an active cellular metabolism.

§ 7.4.3 Ultrastructural study of gold-labeled transferrin endocytosis in P_1 blood-brain barrier endothelial cells.

Endocytosis of Au-Tf was allowed to continue for either 1, 5 or 10 min at 37 °C. Unstained sections of the 1 min incubations show gold particles in various stages of the endocytic cycle (*Figs. 7 through 10*). *Fig. 7* shows two Au-Tf particles attached to the luminal membrane of the BBB-EC. The indentation of the cell membrane at this Au-Tf binding site shows processing of the membrane. Note the organisation of the lipid bilayer around the two gold particles.



Chapter 7

Fig. 7:

ESI micrograph of unstained section of P₁ BBB-EC. Note the lipid bilayer being processed around the 6.6 nm gold particles. The gold particles indicate the presence of Tf. Lu = luminal side. Bar represents 0.1 μm.

In *Fig. 8* two coated pits, each containing multiple Au-Tf particles, can be observed. One of these coated pits seems to be closing to form a coated vesicle (see inserts *Fig. 8*).

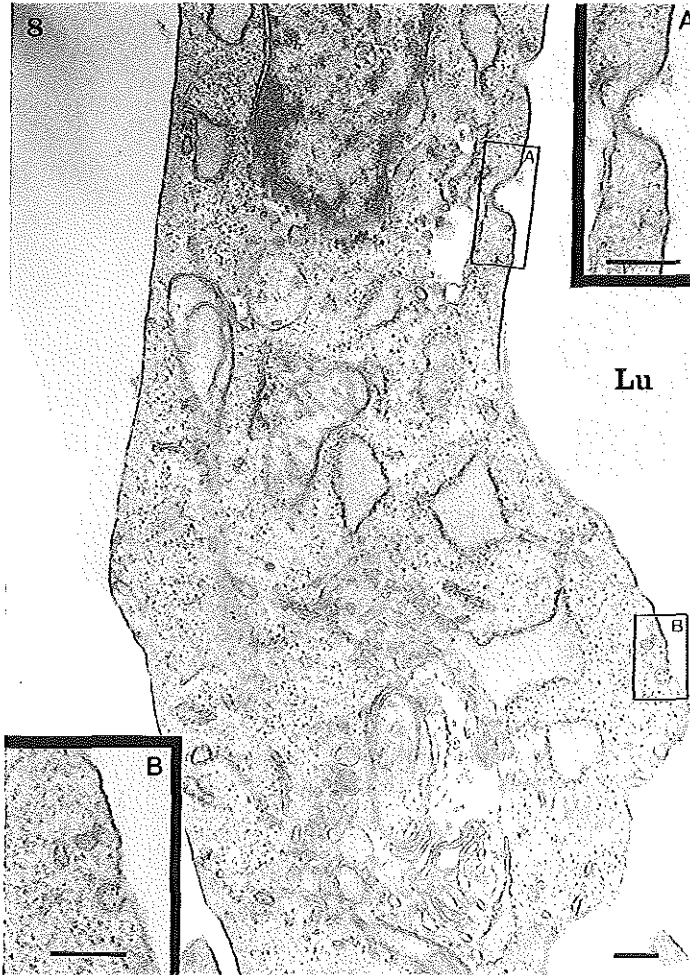


Fig. 8:

ESI micrograph of unstained section of P₁ BBB-EC. Two subsequent stages of internalization of Tf (marked by 6.6 nm gold particles) at the luminal (Lu) side after 1 min incubation time. Insets A and B show this process at higher magnification. Bar represents 0.25 μm.

Transcytosis and ultrastructural morphology.

Fig. 9 shows a group of Au-Tf particles located in an organelle, probably representing an early endosome. Note the single gold particle on the outer (luminal) membrane and the cisterns of the Golgi apparatus. Interestingly, in these 1 min incubations, we also found intracellular Au-Tf particles at the abluminal (membrane) side of the BBB-EC (*Fig. 10*).

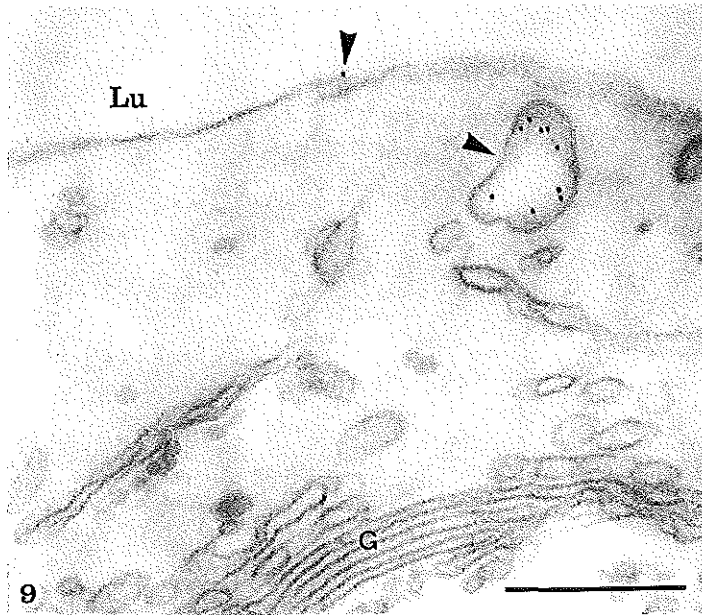


Fig. 9:

ESI micrograph of unstained section of P₁ BBB-EC after 1 min incubation time, showing a 6.6 nm gold particle (marked Tf) on the verge of being internalized (arrowhead). Note several gold particles in an organelle probably representing an early endosome (arrowhead). Lu = luminal side, G = Golgi. Bar represents 0.25 μ m.

Micrographs of BBB-EC's incubated for 5 min with Au-Tf confirmed the finding of Au-Tf particles at the abluminal side. A number of vesicles with Au-Tf particles can be seen in *Fig. 11*. The localization of these vesicles is suggestive for a transcytotic pathway of Au-Tf

Chapter 7

through the BBB-EC. Moreover, *Fig. 12* shows a detailed photomicrograph of the abluminal cell membrane, with two Au-Tf particles probably on the brink of being released.

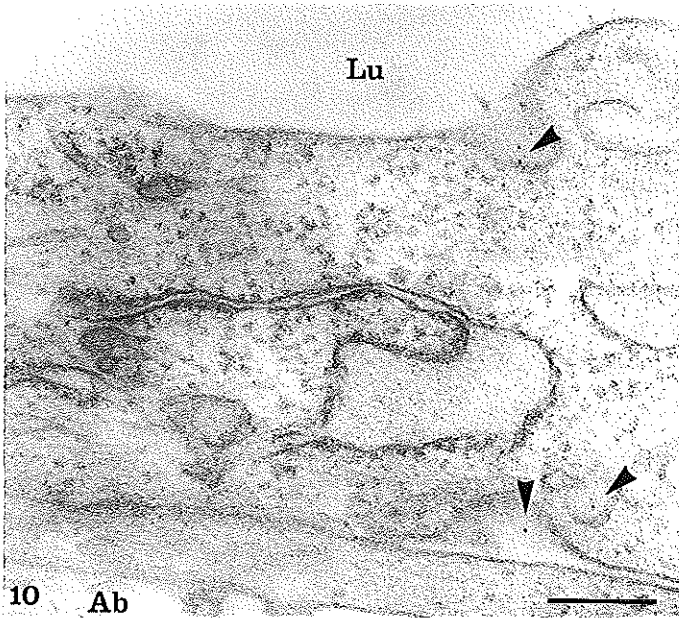


Fig. 10:

ESI micrograph of unstained section of P₁ BBB-EC. An example of possible transcytotic process after 1 min incubation time. Note 6.6 nm gold particles (marked Tf) at the luminal (Lu) and abluminal (Ab) side of the cell (arrowheads). Bar represents 0.25 μ m.

Transcytosis and ultrastructural morphology.

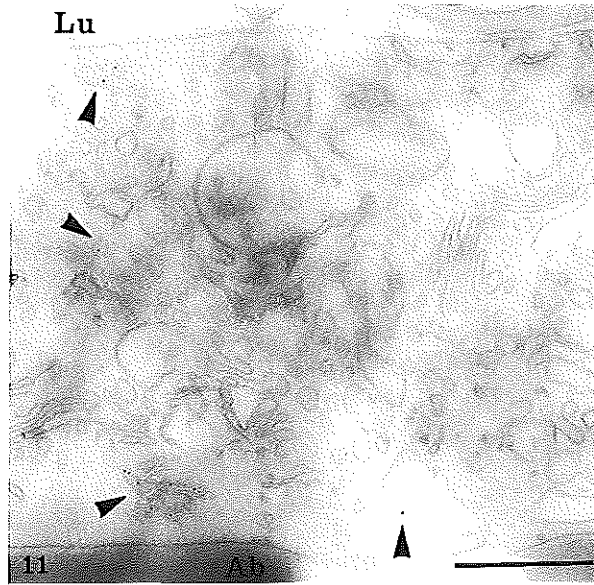


Fig. 11:

ESI micrograph of unstained section of P₁ BBB-EC after 5 min incubation time. Overview of possible transcytotic process. Note the 6.6 nm gold particles (marked Tf) in tubulovesicular structures at the luminal (Lu) and abluminal (Ab) side (arrowheads). Bar represents 0.25 μ m.

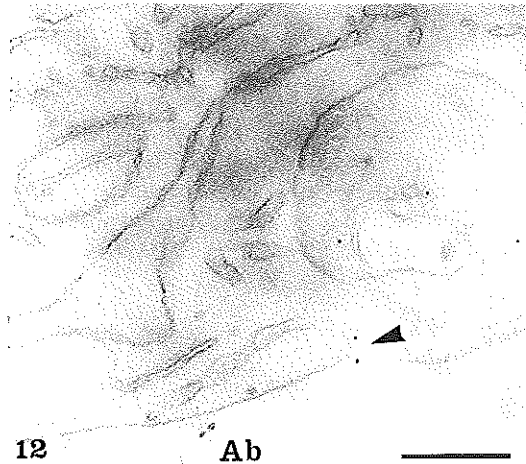


Fig. 12:

ESI micrograph of unstained section of P₁ BBB-EC after 5 min incubation time. Note the 6.6 nm gold particles (marked Tf) on both sides of the abluminal (Ab) membrane (arrowhead). Bar represents 0.25 μ m.

Chapter 7

§ 7.5 Discussion.

BBB-EC's display, like all endothelial cells, a certain polarity i.e. a luminal and an abluminal side (3). The procedure of culturing cells on membranes and co-sectioning them with the cells allows the observer to differentiate between luminal and abluminal side. Moreover, culturing of BBB-EC's on porous membranes offers interesting perspectives for e.g. transport studies. There are relatively few studies on the latter subject (10,18,29,37) and even less on the ultrastructural morphology of BBB-EC's grown on membranes (9,21). It is our experience that BBB-EC's do not readily attach to just any surface (e.g. glass, membranes), and this may have contributed to the paucity of studies on this subject. Our first attempts to grow BBB-EC's on Costar filters completely failed and results did not improve until we exchanged the Gentamycine in our culture medium for penicilline/streptomycine (see § 2.2.3), a phenomenon for which we have no valid explanation.

P_0 and P_1 cells are typical endothelial cells showing evidence of a very active metabolism. This is in line with results of biochemical studies reported earlier (4,18,20). P_1 compared to P_0 cell may display less contact inhibition, as they show an increased tendency to grow in multiple layers upon reaching confluency.

Several studies have shown that iron can enter and (presumably) leave the brain (8,14,27,-34,35). Although there are some areas devoid of a blood-brain barrier that may allow free passage of solutes (see chapter 1), the BBB-EC is still the most likely site for the transport of iron. The presence of high affinity TfR's on the luminal BBB-EC membrane in combination with a large capillary surface area are in support of this view (17,24). Recent biochemical investigations have demonstrated that: (i) ^{125}I -Tf can enter the BBB-EC by receptor mediated endocytosis (15,25,27), and (ii) a major part ($\geq 60\%$) of this ^{125}I -Tf is recycled to the luminal surface (see chapter 6). There are however, also some biochemical studies indicating that transcytosis of Tf through the BBB-EC does occur (14,15,19). The issue of Tf transcytosis and the quantitative extent of this process are still under debate (15).

One of the aims of the present study was to visualize the endocytic cycle of TfR's at an ultrastructural level. Much to our surprise our experimental results are suggestive for a transcytosis of at least part of the Au-Tf through the BBB-EC.

Experiments on TfR endocytosis were performed with P_1 cells cultured on Falcon cyclopore membranes. This membrane was chosen for reasons as stated in § 7.4.1.

Transcytosis and ultrastructural morphology.

Although we would have preferred to use P₀ cells, P₁ BBB-EC's were chosen for a practical reason. Since porous membranes require a much higher (3 to 4 fold) plating density than petri dishes of the same diameter, sufficient quantities of cells from a single batch of BBB-EC's for a TfR endocytosis experiment could only be obtained from a first passage (P₁) culture. In our opinion, the observed tendency of P₁ BBB-EC's to grow in multiple layers in some areas of the porous membrane will not be of major influence on the behaviour of Tf. Even in those areas where P₁ cells grow in multiple layers, the formation of tight junctions apparently is not affected (*Fig. 5*). Moreover, we found no evidence of Au-Tf particles in intercellular clefts, suggesting that the intercellular barriers remain intact in P₁.

In order to visualize the endocytic cycle, we had to choose a compound to label Tf. Horse radish peroxidase was unsuitable, as the DAB-deposit obscures the fine ultrastructural localization of Tf (31). We therefore decided to use gold particles, in spite of earlier reports (22) showing that gold labeled Tf was directed to lysosomes after receptor mediated endocytosis. From literature we conceived that two factors can affect the final destination of the Au-Tf molecule: (i) size of the gold particle, and (ii) the type of cell involved (16,30). In Hep G2 cells, 8 and 20 nm Au labeled Tf was eventually found in lysosome-like structures and not recycled to the cell surface (22). In the same cell type however, Woods (38) reported that 5 nm Au labeled Tf trafficked through the same endosomes as native Tf and eventually left the cell, suggesting that Au-Tf was recycled to the cell surface. These conflicting results may be explained by the difference in Au particle surface area. For example, 10 nm gold can bind 7 to 12 immunoglobulin molecules, whereas 6 nm Au particles can only bind 1 or 2 (manufacturer's information). A 10 nm gold particle, loaded with Tf molecules, can therefore simultaneously interact with more than one transferrin receptor (TfR). Once bound to more than one TfR, a 10 nm Au-Tf particle would rigidly fixate a membrane segment of the endosome. This may obstruct sorting of the Tf-TfR complexes (32,33), thereby interrupting the endocytic pathway, possibly with subsequent lysosomal degradation (22). Based on these data, we chose for 6.6 nm Au as a compromise between visibility in the electron microscope and capacity to bind Tf molecules. In fact, we found Au-Tf in tubulovesicular structures and did not detect any Au-Tf particles in lysosomes.

Chapter 7

Our experimental results (see § 7.4.3) with Au-Tf are suggestive for the existence of a receptor mediated transcytotic transport of Tf through the BBB-EC, as Au-Tf appears at the abluminal side of the cell (see *Fig. 10 through 12*). The alternative, an uptake of Au-Tf via the abluminal membrane is less likely, as: (i) Au-Tf was administered to the luminal side of the cells and access to the abluminal side was hampered because of the tight junctions, (ii) TfR's have never been demonstrated on the abluminal membrane (17,15), and (iii) we found no morphological evidence in support of Au-Tf uptake (by coated pits) at the abluminal side of BBB-EC's. Our experimental results also indicate that transcytosis of Au-Tf is a receptor mediated process, as: (i) Au-Tf at the luminal membrane was located within coated pits, and (ii) addition of unlabeled diferric Tf to the Au-Tf incubation mixture completely blocked the binding and uptake of Au-Tf. Recent experiments conducted by Kang et al (19), showing that OX-26 (anti-TfR antibody) coupled compounds could be retrieved within the brain, are in support of this view.

Roberts et al were unable to show transcytosis (in vivo) of horse radish peroxidase labeled Tf (27,28). However, according to the author's description, the coupling of horse radish peroxidase to diferric Tf included lowering of the pH to 6.0 and addition of dithiothreitol. These reaction conditions might affect Tf-iron binding and lower Tf-iron saturation. Subsequently, a low Tf-iron saturation may affect the pathway of Tf through the BBB-EC in vivo.

Several biochemical reports show that there is indeed transcytosis of Tf through the BBB (8,15,19,35). These studies comprise several techniques and report the transport of either ^{59}Fe , ^{125}I -Tf, or OX-26 coupled peptides through the BBB. Our morphological results underline these biochemical findings. Moreover, the rapid uptake of Au-Tf as shown *Fig. 8*, is also in good agreement with internalization rates derived from our biochemical experiments on TfR mediated endocytosis (as described in chapter 6) and data from literature (5).

Transcytosis and ultrastructural morphology.

References:

- (1) Baynes R.D. (1994) Iron deficiency. In: Iron metabolism in health and disease (Eds: Brock J.H., Halliday J.W., Pippard M.J. and Powell L.W.), pp 152-187. Saunders company Ltd, London, UK.
- (2) Beard J.L., Connor J.R. and Jones B.C. (1993) Iron in the brain. *Nutr. Rev.* 51, 157-170.
- (3) Betz D.W., Firth J.A. and Goldstein G.W. (1980) Polarity of the blood-brain barrier, distribution of enzymes between the luminal and antiluminal membranes of brain capillary endothelial cells. *Brain Res.* 192: 17-28.
- (4) Betz A.L. (1993) Oxygen free radicals and the brain microvasculature. In: The blood-brain barrier. Cellular and molecular biology. (Ed: Pardridge W.M.), pp 303-321, Raven Press, New York, USA.
- (5) Broadwell R.D. and Banks W.A. (1993) Cell biological perspective for the transcytosis of peptides and proteins through the mammalian blood-brain fluid barrier. In: The blood-brain barrier. Cellular and molecular biology. (Ed: Pardridge W.M.), pp 165-199, Raven Press, New York, USA.
- (6) Connor J.R. and Benkovic S.A. (1992) Iron regulation in the brain: histochemical, biochemical, and molecular considerations. *Ann. Neurol.* 32: S51-61.
- (7) Connor J.R. (1993) Cellular and regional maintenance of iron homeostasis in the brain: normal and diseased states. In: Iron in central nervous system disorders. (Eds: Riederer P. and Youdim M.B.H.), pp 1-18. Springer-Verlag, New York, USA.
- (8) Crowe A. and Morgan E.H. (1992) Iron and transferrin uptake by brain and cerebrospinal fluid in the rat. *Brain Res.* 592: 8-16.
- (9) Dehouck M.P., Méresse S., Delorme P., Fruchart J.C. and Cecchelli R. (1990) An easier, reproducible, and mass-production method to study the blood-brain barrier in vitro. *J. Neurochem.* 54: 1798-1801.
- (10) Dehouck M.P., Jolliet-Riant P., Brée F., Fruchart J.C., Cecchelli R. and Tillement J.P. (1992) Drug transfer across the blood-brain barrier: correlation between in vitro and in vivo models. *J. Neurochem.* 58: 1790-1797.
- (11) Dexter D.T., Jenner P., Schapira A.H.V. and Marsden C.D. (1992) Alterations in levels of iron, ferritin, and other trace metals in neurodegenerative diseases affecting the basal ganglia. *Ann. Neurol.* 32: S94-100.
- (12) Dorovini-Zis K., Bowman P.D. and Prameya R. (1992) Adhesion and migration of human polymorphonuclear leucocytes across cultured bovine brain microvessel endothelial cells. *J. Neuropathol. Exp. Neurol.* 51: 194-205.

Chapter 7

- (13) Evans P.H. (1993) Free radicals in brain metabolism and pathology. *Brit. Med. Bull.* 49: 577-587.
- (14) Fishman J.B., Rubin J.B., Handrahan J.V., Connor J.R. and Fine R.E. (1987) Receptor-mediated transcytosis of transferrin across the blood-brain barrier. *J. Neurosci. Res.* 18:299-304
- (15) Friden P.M. (1993) Receptor-mediated transport of peptides and proteins across the blood-brain barrier. In: *The blood-brain barrier. Cellular and molecular biology.* (Ed: Pardridge W.M.), pp 229-247, Raven Press, New York, USA.
- (16) Ghitescu L., Fixman A., Simionescu M. and Simionescu N. (1986) Specific binding sites for albumin restricted to plasmalemmal vesicles of continuous capillary endothelium: receptor-mediated transcytosis. *J. Cell Biol.* 102: 1304-1311.
- (17) Jefferies W.A., Brandon M.R., Hunt S.V., Williams A.F., Gatter K.C. and Mason D.Y. (1984) Transferrin receptor on endothelium of brain capillaries. *Nature* 312: 162-163.
- (18) Joó F. (1992) The cerebral microvessels in culture, an update. *J. Neurochem.* 58: 1-17.
- (19) Kang Y.S., Bickel U. and Pardridge W.M. (1994) Pharmacokinetics and saturable blood-brain barrier transport of biotin bound to a conjugate of avidin and a monoclonal antibody to the transferrin receptor. *Drug Metab. Disp.* 22: 99-105.
- (20) Méresse S., Dehouck M.P., Delorme P., Besaid M., Tauber J.P., Delbart C., Fruchart J.C. and Cecchelli R. (1989) Bovine brain endothelial cells express tight junctions and monoamine oxidase activity in long-term culture. *J. Neurochem.* 53: 1363-1371.
- (21) Moos T. and Mollgård K. (1993) A sensitive post-DAB enhancement technique for demonstration of iron in central nervous system. *Histochemistry* 99: 471-475.
- (22) Neutra M.R., Ciechanover A., Owen L.S. and Lodish H.F. (1985) Intracellular transport of transferrin- and asialoorosomucoid-colloidal gold conjugates to lysosomes after receptor-mediated endocytosis. *J. Histochem. Cytochem.* 33: 1134-1144.
- (23) Pardridge W.M., Eisenberg J. and Yang J. (1987) Human blood-brain barrier transferrin receptor. *Metabolism* 36: 892-895.
- (24) Rapoport S.I. (1976) *Blood-brain barrier in physiology and medicine.* Raven Press, New York, USA.
- (25) Raub T.J. and Newton C.R. (1991) Recycling kinetics and transcytosis of transferrin in primary cultures of bovine brain microvessel endothelial cells. *J. Cell. Physiol.* 149: 141-151.
- (26) Richardson J.S., Subbarao K.V. and Ang L.C. (1992) On the possible role of iron-

Transcytosis and ultrastructural morphology.

induced free radical peroxidation in neuronal degeneration in Alzheimer's disease. *Ann. N.Y. Acad. Sci.* 648: 326-327.

(27) Roberts R., Sandra A., Siek G.C., Lucas J.J. and Fine R.E. (1992) Studies of the mechanism of iron transport across the blood-brain barrier. *Ann. Neurol.* 32: S43-50.

(28) Roberts R.L., Fine R.E. and Sandra A. (1993) Receptor-mediated endocytosis of transferrin at the blood-brain barrier. *J. Cell Sci.* 104: 521-532.

(29) Rubin L.L., Hall D.E., Porter S., Barbu K., Cannon C., Horner H.C., Janatpour M., Liaw C.W., Manning K., Morales J., Tanner L.I., Tomaselli K.J. and Bard F. (1991) A cell culture model of the blood-brain barrier. *J. Cell Biol.* 115: 1725-1735.

(30) Seddiki T., Delpal S. and Ollivier-Bousquet M. (1992) Endocytosis and intracellular transport of transferrin across the lactating rabbit mammary epithelial cell. *J. Histochem. Cytochem.* 40: 1501-1510.

(31) Snelting-Havinga I., Mommaas M., van Hinsbergh V.W.M., Daha M.R., Daems W.Th. and Vermeer B.J. (1989) Immunoelectron microscopic visualization of the transcytosis of low density lipoproteins in perfused rat arteries. *Eur. J. Cell Biol.* 48: 27-36.

(32) Stoorvogel W., Geuze H.J., Griffith J.M. and Strous G.J. (1988) The pathway of endocytosed transferrin and secretory protein are connected in the trans-Golgi reticulum. *J. Cell Biol.* 106: 1821-1829.

(33) Stoorvogel W., Strous G.J., Ciechanover A. and Schwartz A.L. (1991) Trafficking of the transferrin receptor. In: *Liver diseases. Targeted diagnosis and therapy using specific receptors and ligands.* (Eds: Wu G.Y. and Wu C.H.), pp 267-304.

(34) Taylor E.M., Crowe A. and Morgan E.H. (1991) Transferrin and iron uptake by the brain: effects of altered iron status. *J. Neurochem.* 57: 1584-1592.

(35) Ueda F., Raja K.B., Simpson R.J., Trowbridge I.S. and Bradbury M.W.B. (1993) Rate of ⁵⁹Fe uptake into brain and cerebrospinal fluid and the influence thereon of antibodies against the transferrin receptor. *J. Neurochem.* 60: 106-113.

(36) Ussing H.H. (1971) A discussion on active transport of salts and water in living tissues. *Introductory remarks.* *Philos. Trans R. Soc. Lond.* 262: 85-90.

(37) van Bree J.B.M.M., de Boer A.G., Verhoef J.C., Danhof M. and Breimer D.D. (1989) Transport of vasopressin fragments across the blood-brain barrier: in vitro studies using monolayer cultures of bovine brain endothelial cells. *J. Pharmacol. Exp. Ther.* 249: 901-905.

(38) Woods J.W., Goodhouse J. and Farquhar M.G. (1989) Transferrin receptors and cation-independent mannose-6-phosphate receptors deliver their ligands to two distinct

Chapter 7

subpopulations of multivesicular endosomes. *Eur. J. Cell Biol.* 50: 132-143.

CHAPTER 8

A new approach to visualize and quantify the susceptibility to oxidative stress in cultured blood-brain barrier endothelial cells. A 2,4 dinitrophenyl hydrazine assay in iron-enriched and iron-depleted cultures.

This chapter is based on:

van Gelder W., Huijskes-Heins M.I.E., Cleton-Soeteman M.I., Connor J.R. and van Eijk H.G.

(1995) A new approach to visualize and quantify the susceptibility to oxidative stress in cultured blood-brain barrier endothelial cells. A 2,4 dinitrophenyl hydrazine assay in iron-enriched and iron-depleted cultures. Submitted.

Chapter 8

§ 8.0 Contents.

§ 8.1: Summary.

§ 8.2: Introduction.

§ 8.3: Materials and methods:

§ 8.3.1: Materials.

§ 8.3.2: Methods:

§ 8.3.2.1: Isolation and culturing of blood-brain barrier endothelial cells in iron-enriched and iron-depleted medium.

§ 8.3.2.2: Protein carbonyl measurements.

§ 8.3.2.3: Protein measurements.

§ 8.3.2.4: Oxidizing system.

§ 8.3.2.5: 2,4 Dinitrophenol hydrazine immunocytochemistry.

§ 8.3.2.6: Granulocyte adherence assay.

§ 8.3.2.7: Statistical analysis of the granulocyte adherence assay data.

§ 8.4: Results:

§ 8.4.1: Protein carbonyl concentration measurements.

§ 8.4.2: Dinitrophenyl immunocytochemistry.

§ 8.4.3: Granulocyte adherence to blood-brain barrier endothelial cells.

§ 8.5: Discussion.

§ 8.1 Summary.

Oxidative stress is thought to be involved in the pathophysiology of aging and a number of diseases, e.g. Parkinson's and Alzheimer's disease. These diseases are accompanied by alterations in the intracerebral concentration of iron, a transition metal capable of catalyzing the formation of reactive oxygen species. Blood-brain barrier endothelial cells (BBB-EC's) are probably involved in the regulation of the iron flux into the brain and may therefore contribute to the cause of these diseases. In this chapter we show both biochemically and morphologically that BBB-EC's grown under iron-enriched culture conditions are more susceptible to oxidative stress than cells grown under iron-depleted conditions.

In vivo, hypoxia and subsequent reoxygenation of tissue may lead to a surge of reactive oxygen species and concomitant oxidative damage. Granulocytes, that show an increased adherence to damaged tissues, are also involved in these events. We investigated the effects of 2 hrs of hypoxia followed by a brief (5 min) period of reoxygenation on granulocyte adherence to BBB-EC's, and show that this adherence is reduced in cells cultured in iron-enriched conditions. We hypothesize on the role of iron herein, possibly through a suppression of phospholipase A₂ activity.

§ 8.2 Introduction.

Reactive oxygen species are implicated as a key factor in a wide variety of diseases (14,31,39) and the effects of reactive oxygen species on DNA, RNA, proteins, and lipids are well documented (1,4,9,15). Transition metals (e.g. iron) are considered essential in oxidative damage, either acting as catalysts in the formation of highly reactive oxygen species like the hydroxyl radical (OH) (11,25,32) or alternatively, participating in the formation of reactive iron-oxygen complexes known as perferryl ions (Fe_3O_2) (8,51). In fact, the list of diseases in which an involvement of transition metals is suspected, is still expanding (31,39).

One of the tissues containing considerable concentrations of iron, is brain tissue. As already noted by Hallgren (27) and confirmed more recently (reviewed in 13), certain areas in the brain (e.g. globus pallidus) display iron concentrations equal to that of liver (per gram wet weight). Besides, brain iron concentration is subject to changes and increases with age (13,50) and in certain neurological disorders (e.g. Parkinson's disease) (13,17,57). In addition, recent studies show that brain tissue is highly susceptible to oxidative damage, as a result of: (i) high concentrations of poly unsaturated fatty acids (PUFA's), and (ii) relatively low concentrations of antioxidants (e.g. catalase) (19,29).

In chapter 9, results will be presented on the relationship between iron concentration and oxidative damage in different brain regions. The present study focusses on the "porte d'entree" of iron into the brain. Iron transport to the brain is mediated by the endothelial cells lining the capillaries in the brain (BBB-EC). We previously showed (see chapter 6) that, in response to an increase in peripheral iron concentration, BBB-EC's accumulate more iron despite a down-regulation in the number of surface bound and total TfR's. Since BBB-EC's (i) contain enzymes like monoamine oxidase and xanthine oxidase, (ii) have a close proximity to ample oxygen (bloodstream), and (iii) display an active intracellular metabolism with abundant mitochondria, iron accumulation may render these cells more susceptible to oxidative damage (6,7,37).

We report in this chapter on the effects of an oxidizing system (vitamin C and H_2O_2) on BBB-EC's, cultured in either iron-enriched or iron-depleted culture medium. The susceptibility of BBB-EC's to oxidative damage is assessed measuring the increase in protein carbonyl groups following exposure to the oxidizing system. Carbonyl groups are the

Chapter 8

principal product of metal-catalyzed oxidation of proteins and can be quantified using 2,4 dinitrophenyl hydrazine (DNPH) (40,56). Based on the reaction of DNPH with protein carbonyl groups, we also developed a novel technique to visualize oxidative damage in cell cultures.

In addition, we report on the effects of hypoxia/reoxygenation on the adherence of granulocytes to primary cultures of BBB-EC's, in relation to the intracellular iron concentration.

§ 8.3 Materials and methods.

§ 8.3.1 *Materials.*

Fresh porcine brain tissue was obtained from a local slaughterhouse. Specific chemicals used in the isolation and culturing procedure of BBB-EC's are listed in chapter 5. Rabbit anti dinitrophenyl and swine anti-rabbit immunoglobulins (fluorescein labeled) were purchased from DAKO (DAKO A/S, Denmark). Bovine non-fat dried milk powder (Blotto), 3-aminopropyltriethoxysilane (Sigma), and 2,4 dinitrophenyl hydrazine were obtained from Sigma (Sigma, St. Louis, MO, USA). Hexadecyltrimethylammonium bromide was purchased from Merck (Merck, FRG).

§ 8.3.2 *Methods.*

§ 8.3.2.1 *Isolation and culturing of blood-brain barrier endothelial cells in iron-enriched and iron-depleted medium.*

A detailed description of the BBB-EC isolation procedure can be found in § 2.2.1. Briefly, brain tissue was homogenized after careful removal of cerebellum, meninges and choroid plexus. The homogenate was resuspended in culture medium containing dispase and gently shaken for 3 hours. Following filtration and centrifugation (4x), cells were resuspended in culture medium and plated on 5 cm petri dishes. After 3 days, cells were subjected iron-enriched (Fe^+) or iron-depleted (Fe^-) culture conditions as described in § 2.2.2. To avoid possible differences between separate batches of BBB-EC's, Fe^+ and Fe^- grown cells within one experiment always originated from the same isolation batch.

Oxidative damage in BBB endothelial cells.

§ 8.3.2.2 *Protein carbonyl measurements.*

A detailed description of this procedure can be found in § 2.5.2.10. Briefly, blood-brain barrier endothelial cells were grown to near confluency under standard (see § 2.2.1), iron-enriched or iron-depleted conditions (see § 2.2.2), washed and harvested. Following sonication and centrifugation, supernatant was incubated with 2,4 DNPH and left to stand. An additional aliquot of each sample was incubated with 2 M HCl instead of DNPH (blank). Following precipitation of the proteins, pellets were washed to remove unbound DNPH and redissolved in 6 M guanidine hydrochloride. Aliquots of this solution were taken for protein measurements (see § 8.3.2.3). Carbonyl concentrations were measured directly by reading samples spectrophotometrically at 367 nm, after correction for blanks and guanidine HCl. Protein carbonyl concentrations were expressed in nmol/mg protein.

§ 8.3.2.3 *Protein measurements.*

Protein concentrations of the sonicated cell suspensions were measured according to the procedure described in § 2.5.2.1.

§ 8.3.2.4 *Oxidizing system.*

To test the relative susceptibility of BBB-EC's to oxidative damage and the effect thereon of iron-enriched and iron-depleted culturing, cells were exposed to an oxidizing system composed of vitamin C and H₂O₂. A detailed description of this procedure can be found in § 2.2.5. Briefly, cells (culture dishes and cover slides alike) were rinsed with PBS and incubated with M199 culture medium containing 2 mM vitamin C. After 15 min 2 mM H₂O₂ was added to the medium and cells were kept at 37 °C for the duration of the experiment.

§ 8.3.2.5 *2,4 Dinitrophenyl hydrazine immunocytochemistry.*

A detailed description of this procedure can be found in § 2.3.4. Briefly, primary isolates of BBB-EC's were grown on glass cover slides coated with 3-aminopropyltriethoxysilane. From day 3 on, 50% of the cultures were exposed to iron-enriched medium as described in § 2.2.2, whereas the remaining 50% were grown under normal culture conditions (see § 2.2.1). To avoid possible differences between separate batches of BBB-EC's, Fe⁺ and

Chapter 8

standard grown cells within one experiment always originated from the same isolation batch.

After 10 days, cells were rinsed with PBS, fixed in methanol, and incubated with a mixture of 2,4 DNP_H, methanol and sodium phosphate buffer. Following removal of unbound DNP_H with ethyl acetate/ethanol, cells were incubated in 5% (w/v) Blotto to block nonspecific binding. Cells were then rinsed with PBS, incubated for 1 h with rabbit anti-dinitrophenol (1:100), rinsed again and incubated for 1 h with Swine anti-rabbit immunoglobulins Fluorescein (1:200). Coverslides were washed, mounted on glass slides and viewed with a Zeiss Axioskop fluorescence microscope. This microscope was equipped with a triple pass filter set for simultaneous viewing of FITC, Texas Red, and DAPI. Images were taken with Fugicolor Super G400 ASA film.

§ 8.3.2.6 Granulocyte adherence assay.

The adherence of granulocytes to primary cultures of BBB-EC's was tested in a procedure described by Pietersma (47). Details of this technique can be found in § 2.5.2.12. Briefly, primary cultures of BBB-EC's, grown in either Fe⁺ or Fe⁻ culture medium were incubated for 2 h under hypoxic conditions (pO₂ ≈ 7.5 mm Hg). Control cultures (both Fe⁺ and Fe⁻) were kept under normoxic conditions. Meanwhile, granulocytes were isolated from fresh porcine blood as described in § 2.6.5, suspended in PBS and stored at 4 °C until use.

The adherence of granulocytes was studied 5 min after reoxygenation of the BBB-EC's. Hypoxic medium overlying the cells was removed and replaced by normoxic Hanks' balanced salt solution. This medium was removed after 5 min and replaced by the granulocyte suspension. After another 5 min at 37 °C, cells were washed and incubated with 5% hexadecyltrimethylammonium bromide to extract myeloperoxidase. The myeloperoxidase activity was used to assess the number of adherent granulocytes (procedure described in § 2.5.2.11).

§ 8.3.2.7 Statistical analysis of the granulocyte adherence assay data.

Data derived from the granulocyte adherence assays were analyzed by means of the Wilcoxon's signed rank test for paired data. This approach yields slightly less effective (± 96%) predictions when results follow a normal (Gaussian) distribution pattern. However, it

Oxidative damage in BBB endothelial cells.

warrants a correct interpretation of results that are not normally distributed or have a unknown distribution pattern. Results were considered significant if $p < 0.05$.

§ 8.4 Results.

§ 8.4.1 Protein carbonyl concentration measurements.

Primary cultures of BBB-EC's, grown in either Fe^+ or Fe^- culture conditions, were either exposed to an oxidizing system consisting of vitamin C and H_2O_2 or left untreated (§ 8.3.2.4). Protein carbonyl concentration was detected by incubation with 2,4 dinitrophenyl hydrazine (§ 8.3.2.2). As tested separately, we found that varying DNPH-protein incubation times (between 5 and 60 min) did not notably affect the final concentration of protein-DNP derivatives (results not shown). On the other hand, prolonged incubation time (hours) will promote nonspecific binding of DNPH to the substrate (22). Sonicates were therefore allowed to react for 15 min before proteins were precipitated with trichloroacetic acid.

Averaged results of separate experiments, expressed in nmoles of carbonyls/mg protein, are summarized in *Fig. 1*.

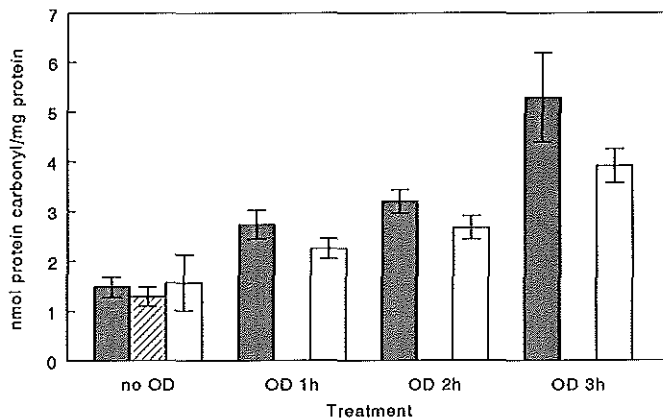


Fig. 1

Cells grown in either Fe^+ (gray bars) or Fe^- (white bars) culture conditions were incubated with 2,4 DNPH to measure protein carbonyl concentrations under basic conditions (no

Chapter 8

OD), or upon exposure to an oxidizing system for either 1 h (OD 1h), 2 hrs (OD 2h), or 3 hrs (OD 3h). The striped bar represents protein carbonyl concentrations in cells cultured according to standard procedures and without oxidative damage. Results are expressed in nmol carbonyls/mg protein. Bars represent means \pm SEM of 4 separate experiments.

Basic levels of protein carbonyl concentrations are not significantly affected by Fe^+ or Fe^- culture conditions when compared to cells grown under standard culture procedures. Both Fe^+ and Fe^- cultured BBB-EC's show a significant increase in protein carbonyl concentration with prolonged exposure (up to 3 h) to the oxidizing system. Moreover, results show that Fe^+ cultured cells are significantly more susceptible to oxidative damage than Fe^- cultured cells.

§ 8.4.2 Dinitrophenyl immunocytochemistry.

Oxidative damage in BBB-EC's as a result of exposure to vitamin C and H_2O_2 was visualized in a novel immunocytochemical assay (*Fig. 2 to 5*). These cells originated from the same isolation batch and were maintained under identical circumstances, with the exception of the iron concentration in the culture medium. Fe^- culturings were not performed to exclude the possible contribution of carbonyl groups in deferoxamine. All cover slides were photographed in one session using the same film and exposure time for all cover slides.

Fig. 2 (standard culturing) shows that a background level of fluorescence due to a number of carbonyl groups always present in cultured BBB-EC's. It was our impression that Fe^+ cultures (*Fig. 4*) on average show a somewhat more intense background fluorescence. In *Fig. 3* standard cultures exposed for 1 h to an oxidizing system show an increase in fluorescence, especially in the cytoplasm and at the rim of the cells. Maximum fluorescence is found in Fe^+ cultured cells exposed to oxidative stress (compare *Fig. 5* to *Fig. 3*). Interestingly, next to an intense fluorescence in the cytoplasm and plasma membrane, Fe^+ grown BBB-EC's under these conditions also show a marked increase in fluorescence in their nuclei (*Fig. 5*).

Oxidative damage in BBB endothelial cells.

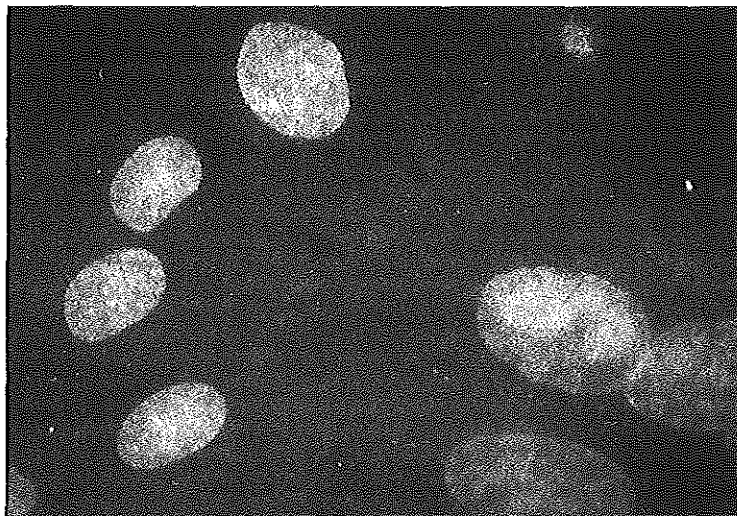


Fig. 2

Primary isolates of BBB-EC's were plated on cover slides and grown in standard culture medium. After 10 days, cells were fixed and incubated with DNPH to detect protein carbonyl groups. Bound DNPH was made visible with anti DNPH immunoglobulins and a fluorescent secondary antibody. This photograph shows the basic fluorescence pattern, due to carbonyl groups always present in these cells.

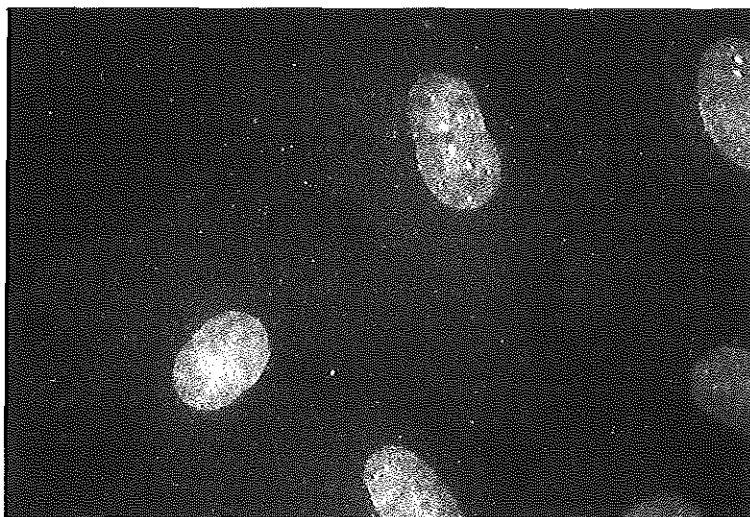


Fig. 3

Primary isolates of BBB-EC's were plated on glass cover slides and grown in standard culture medium. After 10 days cells were exposed for 1 h to an oxidizing system. Further treatment was as described in *Fig. 2*.

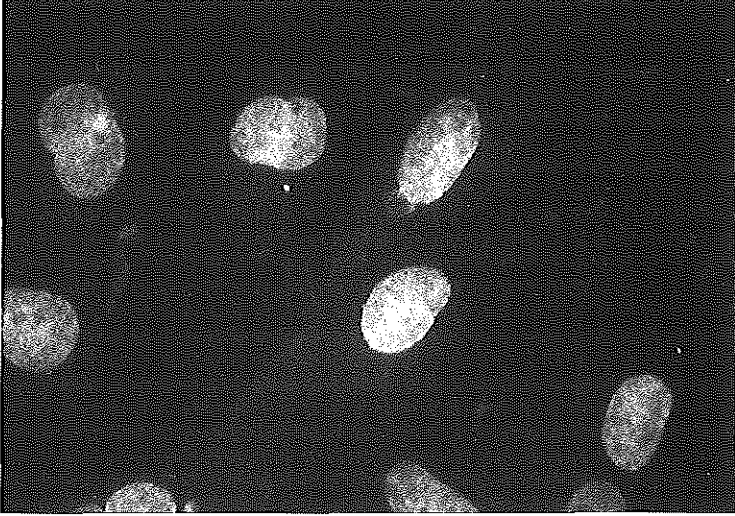


Fig. 4

Primary isolates of BBB-EC's were plated on cover slides and grown in iron-enriched culture medium. After 10 days, cells were fixed and incubated with DNPH to detect protein carbonyl groups. Bound DNPH was made visible with anti DNPH immunoglobulins and a fluorescent secondary antibody. Note the difference in fluorescent staining when compared to *Fig. 2*.



Oxidative damage in BBB endothelial cells.

Fig. 5

Primary isolates of BBB-EC's were plated on glass cover slides and grown in iron-enriched culture medium. After 10 days cells were exposed for 1 h to an oxidizing system, fixed and incubated with DNPH to detect protein carbonyl groups. Bound DNPH was made visible with anti DNPH immunoglobulins and a fluorescent secondary antibody. This photograph clearly shows the intense fluorescence as a result of an increase in carbonyl groups.

§ 8.4.3 Granulocyte adherence to blood-brain barrier endothelial cells.

Results on the adherence of granulocytes to Fe⁺ and Fe⁻ cultured BBB-EC's, either under normoxic conditions or subjected to hypoxia, are depicted in *Fig. 6*. Data are the averaged results of two separate experiments in twelve fold and expressed as percentage of increase or decrease in adherent granulocytes. Adherence of granulocytes in Fe⁺ and Fe⁻ cultured BBB-EC's maintained at normoxic conditions are set to 100%. As shown in *Fig. 6*, Fe⁺ cultured cells show a significant decrease in granulocyte adherence during hypoxia, whereas Fe⁻ cultured cells show a slight, although not significant, increase in adherence.

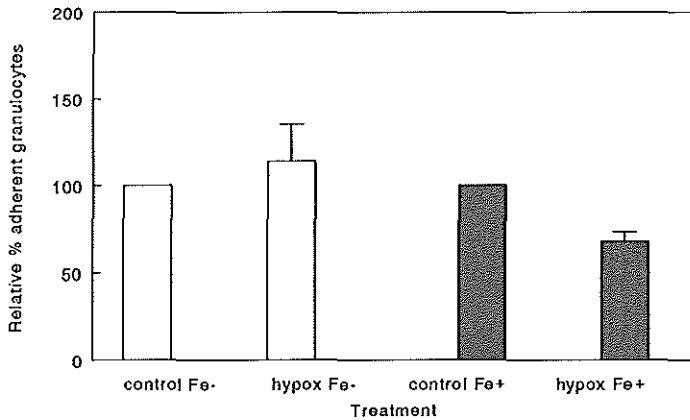


Fig. 6

Cells grown in either Fe⁺ (gray bars) or Fe⁻ (white bars) culture conditions were incubated with granulocytes to quantify adherence following hypoxia + reoxygenation (hypox Fe⁻ and hypox Fe⁺). Results are compared to identical cultures kept at normoxic conditions (control Fe⁻ and control Fe⁺). Results are expressed as mean percentage adherence of granulocytes relative to results found in normoxic conditions (set to 100%). Error bars represent SEM of two separate experiments in twelve fold.

Chapter 8

In a parallel experiment we tested whether the number of adherent granulocytes was affected by the amount of granulocytes that were added to the cultures. Results are displayed in Fig. 7 and show that the number of adherent granulocytes is lineary related to the amount of incubated granulocytes, irrespective of culture conditions. Since results in Fig. 7 were obtained from BBB-EC's originating from one isolation batch, adherent granulocytes could be expressed in numerical values.

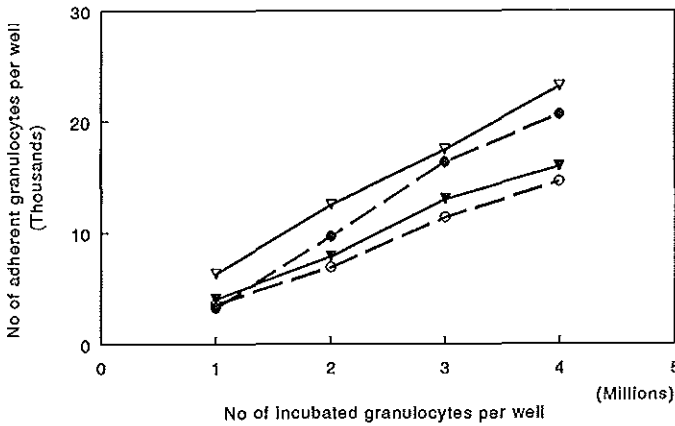


Fig. 7

Cells grown in either Fe⁺ (triangles) or Fe⁻ (circles) culture conditions were incubated with various quantities of granulocytes (X-axis, in millions) following hypoxia + reoxygenation (filled circles and triangles), and compared to BBB-EC's kept at normoxic conditions (open circles and triangles). Since results were obtained from BBB-EC's originating from one isolation batch, adherent granulocytes could be expressed in absolute numbers (Y-axis, in thousands).

§ 8.5 Discussion.

Oxidative damage is thought to be involved in the pathophysiology of aging and a large number of diseases, although in most cases it remains unclear whether this oxidative damage is a cause or a result of disease (28,33,42,45,48,52). The question of "post or proper" is inherent in the fact that reactive oxygen species have a very limited life span, as they readily interact with other compounds (18,25,48). Assessment of oxidative damage is

Oxidative damage in BBB endothelial cells.

therefore mainly based on indirect techniques, measuring the reaction products generated in the oxidation of biomolecules (48). To this purpose, the detection of lipid peroxidation products, e.g. malondialdehyde and 4-hydroxynonenal, have been widely used (18,25,48).

In recent years oxidative modification of another major group of biomolecules, namely proteins, came to attention (2,16,59). As already described by Garrison et al in 1962 (22) and investigated in more detail by Amici and others (2,35,58), radiation-induced as well as metal catalyzed oxidation of proteins result in the formation of carbonyl derivatives (C=O) due to conversion of the side chains of certain amino acids. Histidine, arginine, lysine and proline appear to be particularly sensitive to this type of oxidation (2).

Oxidative modification of proteins results in conformational changes and promotes fragmentation and cross-linking (36). This may cause loss of biological function and will usually enhance degradation (16,54), although some oxidized proteins become in fact more resistant to degradation (23). Moreover -analogous to the generation of radical intermediates (e.g. alkoxy radicals) in the process of lipid peroxidation (12,34)- exposure of proteins to reactive oxygen species may also result in the formation of reactive protein compounds i.e. "protein peroxides" and "protein bound reducing moieties" (16,54). The latter compounds are capable of reducing transition metals (e.g. iron), and could therefore promote the generation of reactive oxygen species via the iron-catalyzed Haber-Weiss cycle (11,16,30) (see also chapter 1). In general, oxidative inactivation and/or modification of proteins have been implicated in the process of aging (16,45,59). Of particular interest in this respect are the results of Oliver et al (43) on cultured fibroblasts of patients with progeria (premature aging). These cells show a significantly higher percentage of oxidatively modified proteins than age-matched controls.

In our experiments, protein carbonyl groups are detected by incubation with 2,4 dinitrophenyl hydrazine to form hydrazone derivatives (technique previously described by Levine and others (40,43,53,55)). Based on the experiments of Keller et al (38), who described an Western immunoblot assay with anti dinitrophenyl immunoglobulins to detect oxidatively modified proteins, we developed a novel immunofluorescence staining technique to visualize these oxidative modifications, i.e. carbonyl groups, in cell cultures. As a first step, the procedure involves fixation with methanol, being a mild fixative without carbonyl groups. In this way, the staining will merely detect carbonyl groups formed as a result of

exposure to oxidative stress.

Our quantitative data on protein carbonyl concentration and the results of the immunochemical experiments with anti dinitrophenyl hydrazine are in good agreement with each other. *Fig. 1 to 5* clearly show that, as was hypothesized before, Fe^+ cultured BBB-EC's are more susceptible to oxidative stress. Judging from the fluorescence pattern, oxidative damage is revealed by a general increase in protein carbonyl groups throughout the cytoplasm (*Fig. 5*), possibly somewhat stronger at the plasma membrane (*Fig. 4 and 5*). Results in *Fig. 1* show that the basic (= no oxidative stress) protein carbonyl concentration was not significantly affected by culture conditions. However, there appears to be a slight increase in fluorescence in Fe^+ grown BBB-EC's as compared to cells cultured in normal conditions (compare *Fig. 2 and 4*). Since cells within a single immunochemical experiment originated from the same isolation batch (see § 8.3.2.5) and were treated identically, the difference in iron concentration in these cultures is the only parameter that could bring about this variation in fluorescence. This suggests that even without exposure to an explicit oxidizing system, Fe^+ cultured cells are more susceptible to this type of stress.

In vivo, a surge of reactive oxygen species and concomitant oxidative damage may occur as a result of: (i) reoxygenation of hypoxic tissue (10,26,63), (ii) activation of granulocytes (5,44), or (iii) a combination of both (7,47). Previous studies in peripheral tissue derived endothelial cells showed that hypoxia increased intracellular xanthine oxidase activity (60). Reoxygenation of these cells resulted in an outburst of toxic reactive oxygen species (e.g. H_2O_2) (41), and was accompanied by an increased permeability of the endothelial monolayer to albumin, and an increased adherence of granulocytes to these endothelial cells (41,60). Since the increase in xanthine oxidase activity is a likely source of these reactive oxygen species (7,10,24), it would appear that endothelial cells are both source and target of reactive oxygen species (7,41). As for granulocytes, (ischemic) tissue damage will lead to the generation of inflammatory mediators, promoting the adherence of granulocytes to endothelial cells by stimulating the expression of adhesion molecules and platelet-activating factor (PAF) of both endothelial cells and granulocytes (46,47). Endothelial cell damage is attributed to the reactive oxygen species released by stimulated granulocytes (46,47,62) and this damage markedly increases with elevated iron concentrations within the endothelial cells (5,62).

Oxidative damage in BBB endothelial cells.

Our biochemical experiments confirm that Fe^+ cultured BBB-EC's are more easily damaged by exposure to an oxidizing system than Fe^- cultured cells. However, after a brief (5 min) period of reoxygenation of hypoxic BBB-EC's we found a decreased adherence of granulocytes to Fe^+ cultured cells, whereas adherence to Fe^- BBB-EC's did not differ from that in normoxic controls (*Fig. 6*). Although this finding is in contrast to what we expected, previous studies on granulocyte adherence to endothelial cells exposed to hypoxia (and reoxygenation) also yielded conflicting results (47,60).

In line with our results, Pietersma et al (22) found a decreased adherence of granulocytes to umbilical vene endothelial cells exposed to hypoxia. They showed that soluble factors which could reduce granulocyte adherence (e.g. NO, adenosine) were not elevated and hypothetically attributed their results to the absence of inflammatory mediators that are normally released from tissue surrounding the endothelial cells.

On the other hand, Terada et al (60) show that ischemia/reperfusion indeed increases granulocyte adherence to endothelial cells. However, they exposed cells for 48 h to hypoxia and 4 h of reoxygenation prior to their tests. As shown in *Fig. 1*, increase in protein carbonyl groups is directly related to the duration of the exposure. In our opinion, 5 min of reoxygenation will only yield minor changes, whereas 4 hrs of reoxygenation will probably result in more -if not extensive- cellular damage and concomitant granulocyte adherence. In fact, our results indicate that an increase in granulocyte adherence to BBB-EC's may not occur until sufficient oxidative damage has been inflicted upon the cell (compare 46). This implies that both Fe^- and Fe^+ cultured cells in our experiments were not expected to show any change in granulocyte adherence. Interestingly, Fe^+ cultured BBB-EC's show a significant decrease in granulocyte adherence. This may be explained by the direct inhibitory effects of Fe^{2+} and Fe^{3+} on phospholipase A_2 (20,21). This enzyme releases arachidonic acid from phospholipids for the biosynthesis of leukotriene B_4 and PAF, which are potent activators of the inflammatory process (3,49,61). A reduction in PAF could concomitantly result in a decreased adherence of granulocytes (3). An elevated intracellular iron content could therefore initially suppress granulocyte adherence by inhibition of PAF synthesis. Prolonged reoxygenation however, might cause cellular damage with subsequent increase in granulocyte adherence. Further research will be necessary to gain more insight in the mechanisms underlying the adherence of granulocytes to BBB-EC's.

Chapter 8

References:

- (1) Ames B.N. (1989) Endogenous DNA damage as related to cancer and aging. *Mutat. Res.* 214: 41-46.
- (2) Amici A., Levine R.L., Tsai L. and Stadtman E.R. (1989) Conversion of amino acid residues in proteins and amino acids homopolymers to carbonyl derivatives by metal-catalyzed oxidation reactions. *J. Biol. Chem.* 264: 3341-3346.
- (3) Arndt H., Russell J.B., Kurose I., Kubes P. and Granger D.N. (1993) Mediators of leukocyte adhesion in rat mesenteric venules elicited by inhibition of nitric oxide synthesis. *Gastroenterology* 105: 675-680.
- (4) Aruoma O.I., Halliwell B., Gajewski E. and Dizdaroglu M. (1989) Damage to the bases in DNA induced by hydrogen peroxide and ferric ion chelates. *J. Biol. Chem.* 264: 20509-20512.
- (5) Balla G., Vercellotti G.M., Muller-Eberhard U., Eaton J. and Jacob H.S. (1991) Exposure of endothelial cells to free heme potentiates damage mediated by granulocytes and toxic oxygen species. *Lab. Invest.* 64: 648-655.
- (6) Betz A.L., Firth J.A. and Goldstein G.W. (1980) Polarity of the blood-brain barrier: distribution of enzymes between the luminal and antiluminal membranes of brain capillary endothelial cells. *Brain Res.* 192: 17-28.
- (7) Betz A.L. (1993) Oxygen free radicals and the brain microvasculature. In: *Iron in central nervous system disorders.* (Eds: Riederer P and Youdim M.B.H.), pp 303-321. Springer-Verlag Wien, Austria.
- (8) Bielski B.H.J. (1992) Reactivity of hypervalent iron with biological compounds. *Ann. Neurol.* 32: S28-32.
- (9) Braugher J.M., Chase R.L. and Pregoner J.F. (1987) Oxidation of ferrous iron during the oxidation of lipid substrates. *Biochim. Biophys. Acta* 921: 457-464.
- (10) Braugher J.M. and Hall E.D. (1989) Central nervous system trauma and stroke. I. Biochemical considerations for oxygen radical formation and lipid peroxidation. *Free Rad. Biol. Med.* 6: 289-301.
- (11) Burkitt M.J. and Gilbert B.C. (1990) Model studies of the iron-catalysed Haber-Weiss cycle and the ascorbate-driven Fenton reaction. *Free Rad. Res. Comms.* 10: 265-280.
- (12) Cadenas E. (1989) Biochemistry of oxygen toxicity. *Ann. Rev. Biochem.* 58: 79-110.
- (13) Connor J.R. (1993) Cellular and regional maintenance of iron homeostasis in the brain: normal and disease states. In: *Iron in central nervous system disorders.* (Eds: Riederer P and Youdim M.B.H.), pp 1-18. Springer-Verlag Wien, Austria.

Oxidative damage in BBB endothelial cells.

- (14) Cross C.E., Halliwell B., Borish E.T., Pryor W.A., Ames B.N., Saul R.L., McCord J.M. and Harman D. (1987) Oxygen radicals and human disease. (Davis Conference) *Ann. Int. Med.* 107: 526-545.
- (15) Davies K.J.A. (1987) Protein damage and degradation by oxygen radicals. I. General aspects. *J. Biol. Chem.* 262: 9895-9901.
- (16) Dean R.T., Gebicki J., Gieseg S., Grant A.J. and Simpson J.A. (1992) Hypothesis: a damaging role in aging for reactive protein oxidation products. *Mut. Res.* 275: 387-393.
- (17) Dexter D.T., Carter C., Wells F.R., Javoy-Agid F., Agid Y., Lees A., Jenner P. and Marsden C.D. (1989) Basal lipid peroxidation in substantia nigra is increased in Parkinson's disease. *J. neurochem.* 52: 881-889.
- (18) Esterbauer H., Schaur R.J. and Zollner H. (1991) Chemistry and biochemistry of 4-hydroxynonenal, malonaldehyde and related aldehydes. *Free Rad. Biol. Med.* 11:81-128.
- (19) Evans P.H. (1993) Free radicals in brain metabolism and pathology. *Brit. Med. Bull.* 49: 577-587.
- (20) Fawzy A.A., Dobrow R. and Franson R.C. (1987) Modulation of phospholipase A₂ activity in human synovial fluid by cations. *Inflammation* 11: 389-400.
- (21) Ferrer X. and Moreno J.J. (1992) Effects of copper, iron and zinc on oedema formation induced by phospholipase A₂. *Comp. Biochem. Physiol.* 102C: 325-327.
- (22) Garrison W.M., Jayko M.E. and Bennett W. (1962) Radiation-induced oxidation of protein in aqueous solution. *Rad. Res.* 16: 483-502.
- (23) Grant A.J., Jessup W. and Dean R.T. (1993) Inefficient degradation of oxidized regions of protein molecules. *Free Rad. Res. Comms.* 18: 259-267.
- (24) Grune T., Siems W.G. and Schneider W. (1993) Accumulation of aldehydic lipid peroxidation products during postanoxic reoxygenation of isolated rat hepatocytes. *Free Rad. Biol. Med.* 15: 125-132.
- (25) Gutteridge J.M.C. and Halliwell B. (1989) Iron toxicity and oxygen radicals. *Baillière's Clinical Haematology*, Vol. 2: 195-256.
- (26) Hall E.D. and Braughler J.M. (1989) Central nervous system trauma and stroke. II. Physiological and pharmacological evidence for involvement of oxygen radicals and lipid peroxidation. *Free Rad. Biol. Med.* 6: 303-313.
- (27) Hallgren B. and Sourander P. (1958) The effect of age on non-haem iron in the human brain. *J. Neurochem.* 3: 41-51.

Chapter 8

- (28) Halliwell B. (1987) Oxidants and human disease: some new concepts. *FASEB J.* 1: 358-364.
- (29) Halliwell B. (1989) Oxidants and the central nervous system: some fundamental questions. *Acta Neurol. Scand.* 126: 23-33.
- (30) Halliwell B. and Gutteridge J.M.C. (1992) Biologically relevant metal ion-dependent hydroxyl radical generation. An update. *FEBS* 307: 108-112.
- (31) Halliwell B., Gutteridge J.M.C. and Cross C.E. (1992) Free radicals, antioxidants, and human disease: where are we now? *J. Lab. Clin. Med.* 119: 598-620.
- (32) Halliwell B and Gutteridge J.M.C. (1992) Biologically relevant metal ion-dependent hydroxyl radical generation. An update. *FEBS* 307: 108-112.
- (33) Halliwell B. (1992) Oxygen radicals as key mediators in neurological disease: fact or fiction? *Ann. Neurol.* 32: S10-15.
- (34) Halliwell B. (1992) Free radicals, antioxidants, and human disease: where are we now? *J. Lab. Clin. Med.* 119: 598-620.
- (35) Haris P.I., Rice-Evans C., Ahmad J., Khan R. and Chapman D. (1989) Application of Fourier transform infrared spectroscopy to the study of free radical interactions with biomolecules in aqueous media. In: *Free radicals, diseased states and anti-radical interventions.* (Ed: Rice-Evans C.), pp 307-353. Richelieu Press, London, UK.
- (36) Hunt J.V., Simpson J.A. and Dean R.T. (1988) Hydroperoxide-mediated fragmentation of proteins. *Biochem. J.* 250: 87-93.
- (37) Joó F. (1992) The cerebral microvessels in culture, an update. *J. Neurochem.* 58: 1-17.
- (38) Keller R.J., Halmes N.C., Hinson J.A. and Pumford N.R. (1993) Immunochemical detection of oxidized proteins. *Chem. Res. Toxicol.* 6:430-433
- (39) Lauffer R.B. (1992) Iron in human diseases. Ed: Lauffer R.B. CRC Press Inc., Boca Raton, Florida, USA.
- (40) Levine R.L., Garland D., Oliver C.N., Amici A., Climent I., Lenz A.G., Ahn B.W., Shaltiel S. and Stadtman E.R. (1990) Determination of carbonyl content in oxidatively modified proteins. *Meth. Enzymol.* 186: 464-478.
- (41) Lum H., Barr D.A., Shaffer J.R., Gordon R.J., Ezrin A.M. and Malik A.B. (1992) Reoxygenation of endothelial cells increases permeability by oxidant-dependent mechanisms. *Circ. Res.* 70: 991-998.
- (42) Mizuno Y. and Ohta K. (1986) Regional distributions of thiobarbituric acid-reactive products, activities of enzymes regulating the metabolism of oxygen free radicals, and

Oxidative damage in BBB endothelial cells.

some of the related enzymes in adult and aged rat brains. *J. Neurochem.* 46: 1344-1352.

(43) Oliver C.N., Ahn B.W., Moerman E.J., Goldstein S. and Stadtman E.R. (1987) Age-related changes in oxidized proteins. *J. Biol. Chem.* 262: 5488-5491.

(44) Oliver C.N. (1987) Inactivation of enzymes and oxidative modification of proteins by stimulated neutrophils. *Arch. Biochem. Biophys.* 253: 62-72.

(45) Pacifici R.E. and Davies K.J.A. (1991) Protein, lipid and DNA repair systems in oxidative stress: the free-radical theory of aging revisited. *Gerontology* 37: 166-180.

(46) Patel K.D., Zimmerman G.A., Prescott S.M. and McIntyre T.M. (1992) Novel leukocyte agonists are released by endothelial cells exposed to peroxide. *J. Biol. Chem.* 267: 15168-15175.

(47) Pietersma A., de Jong N., Koster J.F. and Sluiter W. (1994) Effect of hypoxia on adherence of granulocytes to endothelial cells in vitro. *Am. J. Physiol.* 267: H874-879.

(48) Pryor W.A. and Shipley Godber S.S. (1991) Noninvasive measures of oxidative stress status in humans. *Free Rad. Biol. Med.* 10: 177-184.

(49) Rae D., Porter J., Beechey-Newman N., Sumar N., Bennett D. and Hermon-Taylor J. (1994) Type 1 phospholipase A₂ propeptide in acute lung injury. *Lancet* 344: 1472-1473.

(50) Roskams A.J.I. and Connor J.R. (1994) Iron, transferrin, and ferritin in the rat brain during development and aging. *J. Neurochem.* 63: 709-716.

(51) Rush J.D., Maskos Z. and Koppenol W.H. (1990) Reactions of iron(II) nucleotide complexes with hydrogenperoxide. *FEBS* 261: 121-123.

(52) Sawada M., Sester U. and Carlson J.C. (1992) Superoxide radical formation and associated biochemical alterations in the plasma membrane of brain, heart, and liver during the lifetime of the rat. *J. Cell. Biochem.* 48: 296-304.

(53) Schauenstein E. (1977) Aldehydes in biological systems. Their natural occurrence and biological activities. Eds: Schauenstein E., Esterbauer H. and Zollner H. Pion Limited, London, UK.

(54) Simpson J.A., Gieseg S.P. and Dean R.T. (1993) Free radical and enzymatic mechanisms for the generation of protein bound reducing moieties. *Biochim. Biophys. Acta* 1156: 190-196.

(55) Smith C.D., Carney J.M., Starke-Reed P.E., Oliver C.N., Stadtman E.R., Floyd R.A. and Markesbery W.R. (1991) Excess brain protein oxidation and enzyme dysfunction in normal and Alzheimer disease. *Proc. Natl. Acad. Sci. USA* 88: 10540-10543.

Chapter 8


- (56) Smith C.D., Carney J.M., Tatsumo T., Stadtman E.R., Floyd R.A. and Markesbery W.R. (1992) *Ann. N.Y. Acad. Sci.* 663: 110-119.
- (57) Sofic E., Paulus W., Jellinger K., Riederer P. and Youdim M.B.H. (1991) Selective increase of iron in substantia nigra zona compacta of Parkinsonian brains. *J. Neurochem.* 56: 978-982.
- (58) Stadtman E.R. (1990) Metal ion-catalyzed oxidation of proteins: biochemical mechanism and biological consequences. *Free Rad. Biol. Med.* 9: 315-325.
- (59) Starke-Reed P.E. and Oliver C.N. (1989) Protein oxidation and proteolysis during aging and oxidative stress. *Arch. Biochem. Biophys.* 275: 559-567.
- (60) Terada L.S., Guidot D.M., Leff J.A., Willingham I.R., Hanley M.E., Piermattei D. and Repine J.E. (1992) Hypoxia injures endothelial cells by increasing endogenous xanthine oxidase activity. *Proc. Natl. Acad. Sci. USA* 89: 3362-3366.
- (61) Tjoelker L.W., Wilder C., Eberhardt C., Stafforini D.M., Dietsch G., Schimpf B., Hooper S., Trong H.L., Cousens L.S., Zimmerman G.A., Yamada Y., McIntyre T.M., Prescott S.M. and Gray P.W. (1995) Anti-inflammatory properties of a platelet-activating factor acetylhydrolase. *Nature* 374: 549-553.
- (62) Varani J., Dame M.K., Gibbs D.F., Taylor C.G., Weinberg J.M., Shayevitz J. and Ward P.A. (1992) Human umbilical vein endothelial cell killing by activated neutrophils. *Lab. Invest.* 66: 708-714.
- (63) Watson B.D., Busto R., Goldberg W.J., Santiso M., Yoshida S. and Ginsberg M.D. (1984) Lipid peroxidation in vivo induced by reversible global ischemia in rat brain. *J. Neurochem.* 42: 268-274.

CHAPTER 9

Effects of aging on the regional distribution of iron, transferrin, ferritin, and oxidatively modified proteins in rat brains.

This chapter is based on:

Focht S.J., Snijder B.S., Beard J.L., van Gelder W., Williams L.R. and Connor J.R..

(1995) Regional distribution of iron, transferrin, ferritin, and oxidatively modified proteins in young and aged Fischer 344 rat brains. 

Submitted.

Chapter 9

§ 9.0 Contents.

§ 9.1: Summary.

§ 9.2: Introduction.

§ 9.3: Materials and methods:

§ 9.3.1: Materials.

§ 9.3.2: Methods:

§ 9.3.2.1: Brain dissection.

§ 9.3.2.2: Brain tissue preparation.

§ 9.3.2.3: Transferrin and ferritin immunosorbent assays.

§ 9.3.2.4: Total iron determinations.

§ 9.3.2.5: Carbonyl determinations: biochemical assays and Western blots.

§ 9.3.2.6: Data analyses.

§ 9.4: Results:

§ 9.4.1: Iron.

§ 9.4.2: Ferritin

§ 9.4.3: Transferrin.

§ 9.4.4: Protein carbonyls.

§ 9.5: Discussion.

§ 9.1 Summary.

Iron dysregulation is thought to contribute to the oxidative damage seen in neurodegenerative processes like Alzheimer's and Parkinson's disease. Oxidative stress may also contribute to the process of normal aging, but the role of iron in this process is less clear. To better characterize the role of iron in normal aging, the concentrations of iron, transferrin, ferritin, and protein carbonyl groups are measured in nine separate regions of Fisher 344 rat brains. The largest ($\pm 30\%$) age-related increase in brain iron concentration is seen in the temporal cortex, medial septum, and cerebellum. Ferritin concentration in the same brain regions increases 50 to 250% with age, while increase in protein carbonyl concentration is only -27 to +4% of that of young rats. These results indicate that an increase in the major iron-binding protein ferritin compensates for any age-related increase in iron concentration, and that the increased ferritin is cytoprotective and prevents the accumulation of protein carbonyl groups (the principal product of metal-catalyzed oxidation of proteins).

Iron and oxidative damage in aging in rat brain.

§ 9.2 Introduction.

Iron is the most abundant trace element in the brain, essential in cellular metabolism (e.g. fatty acid synthesis and DNA synthesis) and neurotransmitter synthesis and degradation (2) (chapter 1). Iron transport and storage are tightly regulated processes, involving proteins (e.g. transferrin) with a high affinity for iron. It is thought that these proteins (at physiological pH) prevent iron from acting as a catalyst in the formation of reactive oxygen species (13,15), whereas unbound (LMW) iron can readily promote the production of reactive oxygen species (5,11).

Brain tissue is prone to oxidative damage due to its high concentration of poly unsaturated fatty acids (PUFA's) and reduced concentration of catalase (10,18) (discussed in chapter 1). Oxidative damage occurs in specific brain regions in neurodegenerative diseases (19,23), but also nonspecifically in normal aging (4,16). Concomitantly, aging rat and human brains also display changes in the concentration and distribution of iron and iron binding proteins (7,17).

In this study, experiments were performed to test the hypothesis that in rats specific brain regions display an altered iron status due to aging. For this purpose, the levels of iron, transferrin and ferritin were measured in nine separate brain regions of young and aged rats. Furthermore, protein carbonyl groups (the principal product of metal-catalyzed oxidations of proteins) were quantified in each region, to monitor possible changes in oxidative damage due to alterations in the regional iron status.

§ 9.3 Materials and methods.

§ 9.3.1 Materials.

Young (4 month) and aged (24 month) Fischer 344 male rats were obtained from the National Institute on Aging colony at Harlan/Sprague-Dawley (Indianapolis, IN). Rats were housed in small groups, at 22 °C, with a photoperiod of 12 h per day. All rats had *ad libitum* access to water and Purina Laboratory Chow 5001 (Richman, IN).

Materials:

Chapter 9

§ 9.3.2 *Methods.*

§ 9.3.2.1 *Brain dissection.*

A detailed description of this technique can be found in § 2.9. Briefly, rats were anesthetized, perfused with icecold PBS for ≥ 5 min and then decapitated. Brains were microdissected according to Cuello and Carson (8). Samples were obtained from the frontal cortex, medial septum, striatum, parietal and temporal cortex, hippocampus, thalamus, cerebellum and brainstem. All sections were frozen immediately upon dissection and stored at -70 °C until further processing.

§ 9.3.2.2 *Brain tissue preparation.*

Brain regions were thawed on ice and homogenized in 0.25 M sucrose containing 10 mM PMSF at a total volume of 60 μ l/mg tissue weight. Aliquots were either kept on ice for immediate protein, transferrin, and ferritin determinations, or frozen at -20 °C for subsequent iron determinations.

Analogous brain regions were thawed on ice and sonicated in 0.01 M Sodium Phosphate buffer (pH = 7.4), containing 0.1% Triton X-100. The sonicate was centrifuged (10 min, 40000 x g, 4 °C) and supernatants were used for protein and protein carbonyl determinations.

§ 9.3.2.3 *Transferrin and ferritin immunosorbent assays.*

A detailed description can be found in § 2.4.3. Briefly, standards (transferrin and ferritin) and brain homogenates were applied to nitrocellulose membranes (in triplicate) as described by Roskams and Connor (21). Following incubation with the primary antibody (rabbit anti-rat transferrin or rabbit anti-horse ferritin), membranes were incubated with 125 I-goat anti-rabbit IgG. Membranes were then rinsed, dried and packed with film (15 h). Developed films were analyzed on a densitometer.

§ 9.3.2.4 *Total iron determinations.*

A detailed description can be found in § 2.5.2.8. Briefly, total iron concentrations in brain homogenate samples were determined using flame atomic absorption spectrophotometry

Iron and oxidative damage in aging in rat brain.

following digestion with nitric acid for one week at 37 °C.

§ 9.3.2.5 Carbonyl determinations: biochemical assays and Western blots.

Protein carbonyl concentration was determined as outlined by Smith et al (24). The procedure is described in detail in § 2.5.2.10. Briefly, protein carbonyl groups were allowed to form hydrazone derivatives with 2,4 dinitrophenylhydrazine (2,4 DNPH). Following precipitation with trichloroacetic acid, these hydrazone derivatives were rinsed to remove unbound 2,4 DNPH. Samples were redissolved and read spectrophotometrically at 367 nm.

For Western blots, brain sample homogenates of 4 rats had to be pooled, in order to obtain sufficient quantities of protein for analysis. Samples were treated as outlined above, redissolved in SDS buffer and loaded on a 10% polyacrylamide gel. Following electrophoresis, proteins were transferred to nitrocellulose and incubated with anti-dinitrophenyl antisera. Control lanes consisted of pooled samples that did not undergo derivitization with 2,4 DNPH, but otherwise treated in the same manner.

§ 9.3.2.6 Data analyses.

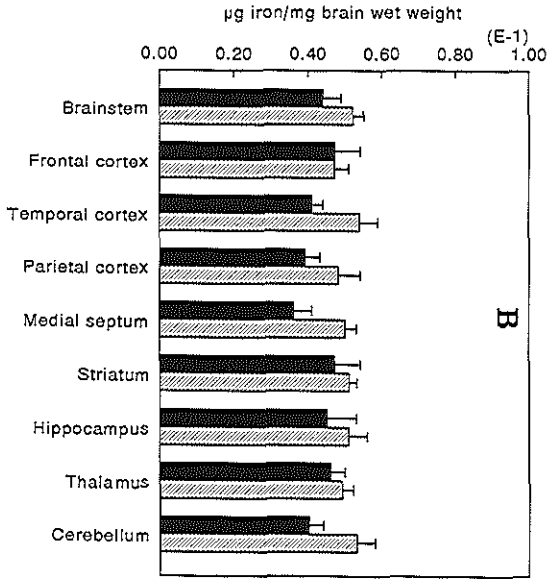
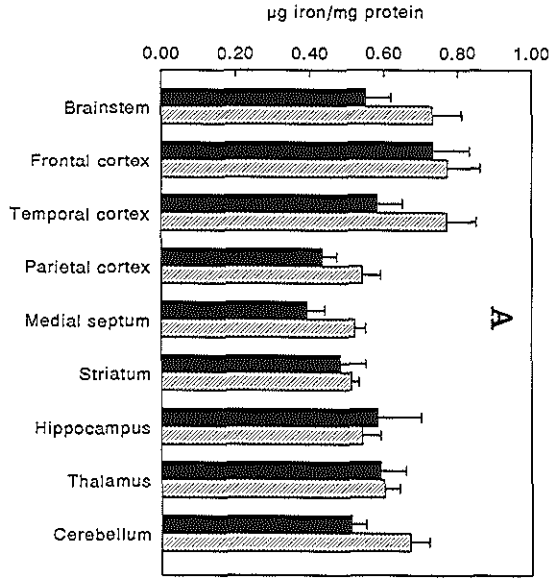
Data on regional concentrations of iron, transferrin, ferritin and protein carbonyl groups are expressed as mean \pm SEM in both young (4 month) and aged (24 month) rat brains. Statistical significance between age groups for individual brain regions was determined using an unpaired T-test, and statistical significance among brain areas within either age group was determined using the Scheffe F-test, with $p \leq 0.05$ considered significant.

§ 9.4 Results.

§ 9.4.1 Iron.

Regional brain iron concentration ranges between 0.39 ± 0.05 and 0.77 ± 0.09 Fe/mg protein (*Fig. 1A*). Within each age group, brain regions are divided into high, intermediate, and low iron concentration groups (*Table 1*). In the 4 month old group, iron concentration is highest in the frontal cortex and lowest in the medial septum, parietal cortex, striatum, and cerebellum. Intermediate iron concentrations, not significantly different from either the

high or the low iron regions, are found in brainstem, temporal cortex, hippocampus, and thalamus.



Iron and oxidative damage in aging in rat brain.

Fig. 1A and 1B

Levels of iron in nine separate brain regions of both young (black bars) and aged (gray bars) rats, expressed per mg protein (A), or per unit brain wet weight (B). Data are presented as mean \pm standard error of the mean, with $n = 6$ for young rats and $n = 8$ for aged rats. An asterisk above a given brain region indicates the level of iron is higher in the aged group; with $p \leq 0.05$ by an unpaired T-test.

In the 24 month old group, iron concentration is highest in the brainstem, frontal and temporal cortex, and lowest in the striatum, medial septum, parietal cortex and hippocampus. In this age group, intermediate iron concentrations (not significantly different from both the high and low iron group) are found in thalamus and cerebellum.

In general, levels of brain iron (per mg protein) tend to be higher in the 24 month old group (*Fig. 1A*), although this trend is significant only for the cerebellum and the medial septum. When expressed per unit wet weight (*Fig. 1B*), iron concentrations in the temporal cortex are also significantly different in the 4 and 24 month old groups.

§ 9.4.2 Ferritin.

Regional brain ferritin concentrations range between 0.060 ± 0.006 and 0.429 ± 0.032 μg ferritin/mg protein (*Fig. 2A*). Within each age group, brain regions have been divided into high, intermediate, and low ferritin concentration groups (*Table 1*). In the 4 month old group, ferritin concentration is highest in the frontal cortex, medial septum, and temporal cortex, and lowest in the striatum and cerebellum. Intermediate ferritin concentrations are found in the parietal cortex, thalamus, hippocampus and brainstem. Results in the intermediate group do not differ significantly from those in the high and low ferritin groups.

In the 24 month old group, ferritin concentration is highest in the medial septum, intermediate in the frontal cortex, brainstem, and temporal cortex, and lowest in the striatum, parietal cortex, hippocampus, cerebellum, and thalamus. Within the 24 month old group, the high, intermediate, and low ferritin concentration groups all differ significantly.

Within each brain region, ferritin concentration increases with age (*Fig. 2A*), and ferritin concentrations on the average are 1.7 times higher in the 24 month old group. This trend is significant in all brain regions except the hippocampus.

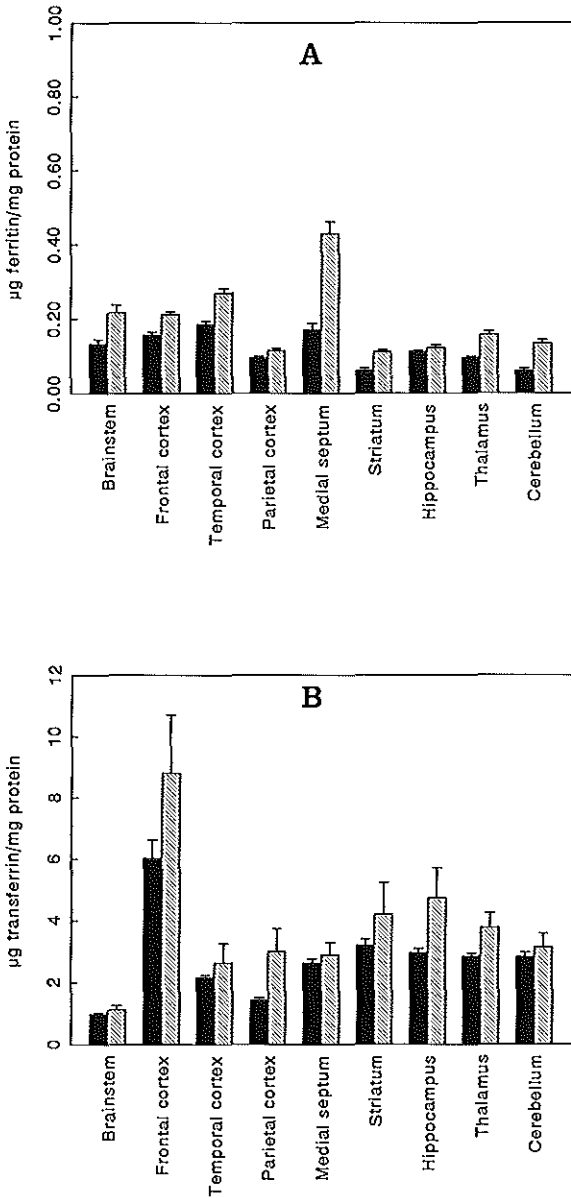


Fig. 2A and 2B

Levels of iron-binding protein ferritin (A) and transferrin (B) in nine separate brain regions of both young (black bars) and aged (gray bars) rats. Data are presented as mean \pm

Iron and oxidative damage in aging in rat brain.

standard error of the mean, with $n = 6$ for young rats and $n = 8$ for aged rats. An asterisk above a given brain region indicates the level of iron-binding protein is higher in the aged group; with $p \leq 0.05$ by an unpaired T-test.

§ 9.4.3 Transferrin.

Regional brain transferrin concentrations range between 0.96 ± 0.05 and 8.80 ± 1.90 μg transferrin/mg protein (*Fig. 2B*). Within each age group, brain regions have been divided into high, intermediate, and low transferrin concentration groups (*Table 1*). In the 4 month old group, transferrin concentration is highest in the frontal cortex, and lowest in the brainstem and parietal cortex. The transferrin concentration is intermediate in the temporal cortex, medial septum, cerebellum, thalamus, hippocampus, and striatum, and does not differ significantly from either the high or the low transferrin groups.

In the 24 month old group, transferrin concentration is highest in the frontal cortex and lowest in the brainstem. Due to a large intra-regional variability, brainstem transferrin concentration is significantly lower only in comparison with the frontal cortex, striatum, hippocampus, and thalamus. Among the 24 month old group, transferrin concentration is considered intermediate in the temporal cortex, medial septum, parietal cortex, cerebellum, thalamus, striatum, and hippocampus.

Within each brain region, there is no significant effect of age on transferrin concentration (*Fig. 2B*). Although transferrin concentration tends to be slightly higher in 24 month old group than in 4 month old group, this trend is not significant in any brain region.

§ 9.4.4 Protein carbonyls.

Regional brain protein carbonyl concentration ranges between 1.88 ± 0.16 and 8.21 ± 0.49 nmol/mg protein (*Fig. 3*). Within each age group, brain regions have been divided into high and low protein carbonyl concentration groups (*Table 1*). In the 4 month old group, protein carbonyl concentration is high in the parietal cortex, cerebellum and frontal cortex, and low in temporal cortex, brainstem, thalamus, medial septum, hippocampus, and striatum.

In the 24 month old group, protein carbonyl concentration is high for the parietal cortex and cerebellum, and low in the temporal cortex, brainstem, thalamus, striatum, frontal cor-

Chapter 9

tex, medial septum, and hippocampus. The effect of age on protein carbonyl concentration within each brain region is presented in *Fig. 3*. When compared to the 4 month old group, there is a 40% decrease in carbonyl concentration in the frontal cortex of the 24 month old group, while the carbonyl concentration of both the temporal cortex and brainstem is slightly but still significantly decreased in this group. The trend for decreased carbonyl concentration in parietal cortex is not significant ($p \leq 0.08$).

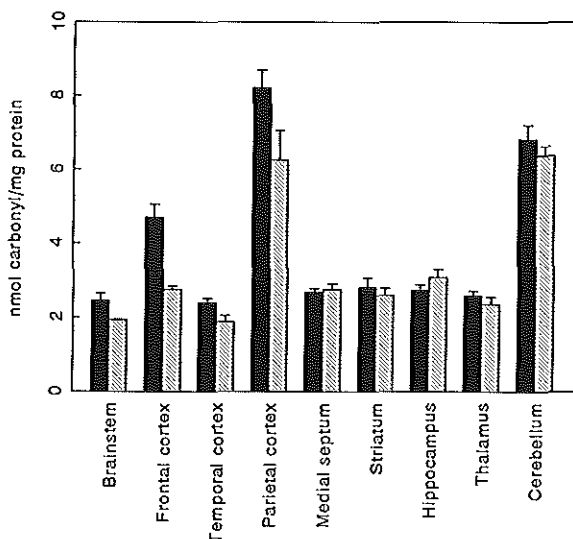


Fig. 3

Levels of protein carbonyl groups in nine separate brain regions of both young (black bars) and aged (gray bars) rats. Data are presented as mean \pm standard error of the mean, with $n = 6$ for young rats and $n = 8$ for aged rats. An asterisk above a given brain region indicates the level of protein carbonyl groups are lower in the aged group; with $p \leq 0.05$ by an unpaired T-test.

Representative Western blots of hippocampus, parietal cortex and cerebellum are shown in *Fig. 4*. A lack of nonspecific binding by the anti-dinitrophenyl antibody is clearly shown in the even numbered lanes, that contain brain samples not reacted with 2,4 DNP (see § 9.3.2.5). The protein carbonyl staining pattern shows only minor changes between different regions and both age groups.

Iron and oxidative damage in aging in rat brain.

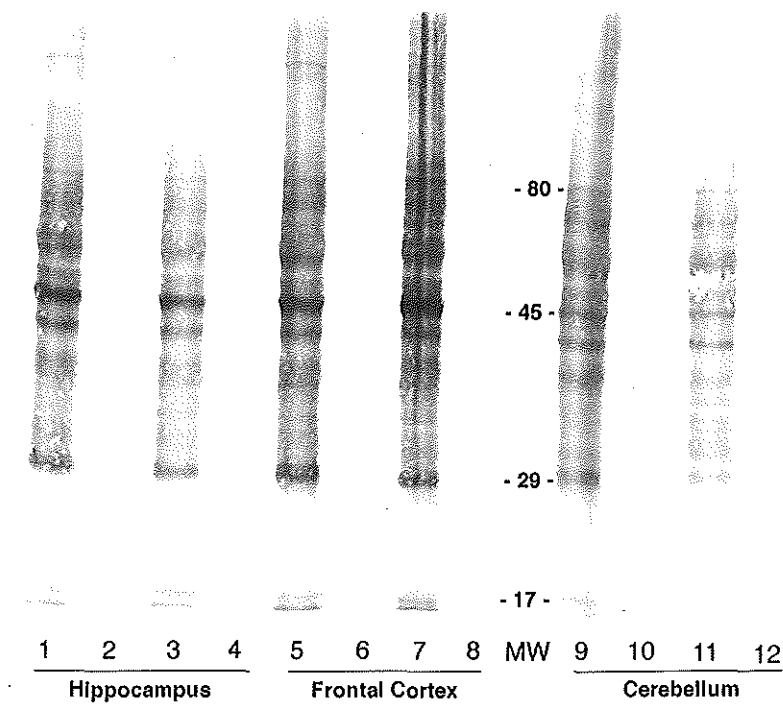


Fig. 4

Western blot staining protein carbonyl groups of sonicates of hippocampus (lanes 1, 2, 3, 4), frontal cortex (lanes 5, 6, 7, 8), and cerebellum (lanes 9, 10, 11, 12). Lanes were loaded with 50 μ g protein, pooled from 4 rats. Lanes 1, 2, 5, 6, 9, 10 are sonicates from young rats, while lanes 3, 4, 7, 8, 11, 12 are sonicates from aged rats. Even numbered lanes are control lanes containing pooled samples that did not undergo initial hydrazone derivitization, as outlined in materials and methods. Numbers in MW lane (between lanes 8 and 9) are apparent molecular weights expressed in kD.

§ 9.5 Discussion.

In the present study, regional rat brain iron concentrations as determined by flame atomic absorption spectrophotometry, are in agreement with results in earlier studies (22,26). The highest brain iron concentration in young Fisher rats is found in the frontal cortex, while in aged rats iron concentration is highest in frontal cortex, brainstem and cerebellum. These findings do not correlate with prior colorimetric and histochemical studies in which the

Chapter 9

basal ganglia, substantia nigra, deep cerebellar nuclei, and circumventricular organs have the highest staining intensity (3,12,14). This lack of correspondance may reflect an averaging effect in the spectrophotometric (atomic absorption) method, where iron-rich cells are homogenized with iron-poor cells in a gross regional brain dissection. On the other hand, the disagreement could be the result of intrinsic differences in the various detection methods. Iron compounds visualized histochemically by the Perls' reaction include ferritin and other major iron storage compounds, whereas flame atomic absorption spectrophotometry of acid digested tissue homogenates detects total tissue iron. These quantitative data suggest that many brain regions may contain significant levels of iron that is tightly bound to enzymes and heme-containing compounds, and therefore undetectable with histochemical techniques.

Results show an age-related increase in the iron concentration in several brain regions (*Fig. 1A*), especially in the temporal cortex, medial septum and cerebellum. This finding is consistent with previous work (21) reporting a 33% increase in total cortical iron in rats between the ages of 2.5 and 24 months. In that same study however, the highest brain iron concentration in aged rats as measured colorimetrically, was found in the cerebellum-pons region. This age-related increase in cerebellar iron concentration was correlated to the intense iron staining seen in oligodendrocytes and fibers of the deep cerebellar nuclei, and the increased iron staining of Purkinje cells and microglia in aged rats (3).

Since the age-related increase in iron concentration does not appear to be unique to the cerebellum, the mechanisms of iron accumulation may also be more widespread within the brain. Indeed, in humans non-heme iron has been shown to increase from birth up to the age of thirty in several areas of the basal ganglia and cortex (12). Further iron increases (up to 80%) are seen in the substantia nigra, caudate and putamen of normal elderly humans, and excess iron depositions can be found in the globus pallidus in humans with Alzheimer's and Parkinson's disease (17).

Next to an initial difference in iron concentration between the frontal, parietal and temporal lobe of the cortex in the young rat (*Fig. 1A*) there is also a difference in age-related changes in iron concentration in these regions. These findings suggest that cortical iron is differentially regulated at the regional level, as has been proposed for subcortical brain regions (6).

Iron and oxidative damage in aging in rat brain.

In the present study, certain areas (e.g. hippocampus) show no age-related changes in total iron concentration. However, in prior studies of rat hippocampal sections, histochemical staining showed that neurons throughout the granular and pyramidal layers contained iron in small vesicles that became more abundant in aged animals (3). It would therefore appear that although the hippocampal regions show no increase in iron with age biochemically, there may be a shift in neuronal iron stores in histochemically stainable iron. This possible shift in neuronal iron stores may be significant. If loosely bound iron is more cytotoxic, aging neurons may be more susceptible to oxidative damage. A more detailed cellular analysis is needed to assess the significance to hippocampal neuronal vulnerability to oxidative damage.

Ferritin concentrations in the present study (*Fig. 2A*) are lower than those reported previously in rats (21). This difference may be a result of using ^{125}I -conjugated secondary antibody in the present study (instead of HRP-conjugated secondary antibody). The iodinated secondary antibody extends the linearity of the standard curve and increases the assay sensitivity at lower ferritin concentrations.

Earlier semi-quantitative studies in rats have shown that ferritin concentrations decrease in all brain regions from birth until weanling, after which ferritin concentrations begin to rise with no significant regional differences in concentration (21). The 1.1 to 2.5 fold increase in regional brain ferritin concentration in the aged rats of this study is in agreement with reports on the two fold increase in ferritin concentration seen in all rat brain regions (21), and with the 1.7 to 10 fold increase in both heavy and light chain isoforms of ferritin seen in regions of human brain (7).

The age-related increase in brain ferritin concentrations could not be detected in postmortem brain samples of patients with Alzheimer's or Parkinson's disease (7). Since oxidative damage (probably) contributes to the neurodegenerative changes seen in the latter disease (9), this finding supports the theory that ferritin is protective against iron-induced oxidative damage (1).

Both young and aged rats show regional differences in brain transferrin concentration, and results show a consistent (but not significant) increase in regional transferrin concentration with age (*Fig. 2B*). Previous quantitative data on regional differences in rat brain transferrin levels are limited, but similar to those in the present study (21).

Chapter 9

Regional differences in transferrin concentration may reflect variations in iron requirement. A minor increase in transferrin concentration over a prolonged period of time may therefore be of biological significance, contributing to the increase in total brain iron. However, because the age-related increase in transferrin is only a fraction of that in total iron, it appears that there is a general decrease in brain iron mobility with increasing age.

Carbonyl groups (C=O) are normally present in proteins at a low level. Recent studies suggest that metal-catalyzed oxidation can induce the formation of carbonyls in proline, arginine, lysine, and histidine residues (24). Protein carbonyl concentrations may therefore indicate to what extent of oxidative stress proteins have been exposed.

In the present study, protein carbonyl concentrations in the brain are of the same magnitude as those reported previously in Mongolian gerbil brainstem and cortex (20) and human parietal and occipital cortex (23). In the 4 month old rats, highest levels of protein carbonyl concentration were found in cerebellum, frontal and parietal cortex (*Fig. 3*). We found no publications on this subject with which to compare our results. On the other hand, Zaleska and Floyd (27) showed that lipid peroxidation was highest in the rat cerebellum and cortex. Likewise, Subbarao and Richardson (25) demonstrated that rat cerebellum and amygdala have the highest endogenous peroxidative activity of eight brain regions. These data in combination with our results suggest that the cerebellum and cortical regions have the highest oxidative activity, and may represent regions with increased susceptibility to oxidative damage.

Contrary to prior studies in aged humans and gerbils (4,23), the present study in rats shows a significant decrease in protein carbonyl concentration in brainstem, frontal and temporal cortex. Possibly, these conflicting results represent a species-specific difference in susceptibility to oxidative stress. Another possibility is, that this discrepancy is caused by a difference in mode of storage of age related iron. As discussed before, a difference in mode of storage may lead to more or less oxidative damage.

In summary, our results clearly show that different brain regions regulate iron concentrations independently. Moreover, regional increase in iron is accompanied by a concomitant increase in ferritin. The decrease in protein carbonyl concentration with age in cerebellum and temporal cortex, despite a significant increase in total iron, supports the notion that ferritin is protective against oxidative stress.

Iron and oxidative damage in aging in rat brain.

Future studies on the mode of cerebral iron accumulation, e.g. iron increase with or without concomitant increase in (iso)ferritin, may contribute to a better understanding of certain neurological disorders, e.g. Parkinson's and Alzheimer's disease.

Table 1

Brain regions organized according to relative concentrations of iron, ferritin, transferrin, and protein carbonyl groups, for both young (4 months) and aged (24 month) rats.

(a) Brain regions in the high concentration group are significantly greater than those of the low concentration group ($p \leq 0.05$; Scheffe F-test); while those in the intermediate concentration group do not differ significantly from either the high or low concentration groups.

(b) Brain regions in the high concentration group are significantly greater than those of the intermediate concentration group, which are significantly greater than those of the low concentration group ($p \leq 0.05$; Scheffe F-test).

(*) In the low concentration group of 24 month old transferrin, the brainstem is also significantly lower than the striatum, hippocampus, and thalamus of the intermediate concentration group ($p \leq 0.05$; Scheffe F-test).

(#) In the high concentration group of 4 month old protein carbonyl rats, the parietal cortex is significantly greater than the cerebellum, which is significantly greater than the frontal cortex ($p \leq 0.05$; Scheffe F-test).

Chapter 9

	Age	Relative concentration		
		low	intermediate	high
Iron	4 ^a	Cerebellum Striatum Medial Sept. Parietal ctx	Thalamus Hippocampus Temporal ctx Brainstem	Frontal ctx
	24 ^a	Hippocampus Parietal ctx Medial Sept. Striatum	Cerebellum Thalamus	Temporal ctx Frontal ctx Brainstem
Ferritin	4 ^a	Cerebellum Striatum	Brainstem Hippocampus Thalamus Parietal ctx	Temporal ctx Medial Sept. Frontal ctx
	24 ^b	Thalamus Cerebellum Hippocampus Parietal ctx Striatum	Temporal ctx Brainstem Frontal ctx	Medial Sept.
Transferrin	4 ^a	Parietal ctx Brainstem	Striatum Hippocampus Thalamus Cerebellum Medial Sept. Temporal ctx	Frontal ctx
	24 ^a	Brainstem *	Striatum Hippocampus Thalamus Cerebellum Medial Sept. Temporal ctx Parietal ctx	Frontal ctx
protein carbonyls	4 ^a	Striatum Hippocampus Medial Sept. Thalamus Brainstem Temporal ctx		Parietal ctx # Cerebellum Frontal ctx
	24 ^a	Striatum Hippocampus Medial Sept. Frontal ctx Thalamus Brainstem Temporal ctx		Cerebellum Parietal ctx

Iron and oxidative damage in aging in rat brain.

References:

- (1) Balla G., Jacob H.S., Balla J., Rosenberg M., Nath K., Apple F., Eaton J.W. and Vercellotti G.M. (1992) Ferritin: a cytoprotective antioxidant strategem of endothelium. *J. Biol. Chem.* 267: 18148-18153.
- (2) Beard J.L., Connor J.R. and Jones B.C. (1993) Iron in the brain. *Nutr. Rev.* 51, 157-170.
- (3) Benkovic S.A. and Connor J.R. (1993) Ferritin, transferrin and iron in selected regions of adult and aged rat brain. *J. Comp. Neurol.* 338: 97-113.
- (4) Carney J.M., Starke-Reed P.E., Oliver C.N., Landrum R.W., Cheng M.S. and Wu J.F. (1991) Reversal of age-related increase in brain protein oxidation, decrease in enzyme activity, and loss in temporal and spatial memory by chronic administration of spin-trapping compound N-tert-butyl-alpha-phenylnitron. *Proc. Natl. Acad. Sci. USA* 88, 3633-3636.
- (5) Connor J.R. and Benkovic S.A. (1992) Iron regulation in the brain: histochemical, biochemical, and molecular considerations. *Ann. Neurol.* 32 (suppl.), S51-61.
- (6) Connor J.R. (1993) Cellular and regional maintenance of iron homeostasis in the brain: normal and disease states. In: *Iron in central nervous system disorders.* (Eds: Riederer P. and Youdim M.B.H.), pp 1-18. Springer-Verlag Wien, Austria.
- (7) Connor J.R., Snijder B.S., Arosio P., Loeffler D.A. and LeWitt P. (1995) A quantitative analysis of isoferritins in select regions of aged, Parkinsonian, and Alzheimer's diseased brains. *J. Neurochem.* In press.
- (8) Cuello A.C. and Carson S. (1983) Microdissection of fresh rat brain tissue slices. In: *Methods of Neurosciences* (Ed: Cuello A.C.), Vol. 2, pp 37-125. John Wiley and Sons, Publishers.
- (9) Dexter D.T., Carter C., Wells F.R., Javoy-Agid F., Agid Y., Lees A., Jenner P. and Marsden C.D. (1989) Basal lipid peroxidation in substantia nigra is increased in Parkinson's disease. *J. Neurochem.* 52: 881-889.
- (10) Evans P.H. (1993) Free radicals in brain metabolism and pathology. *Brit. Med. Bull.* 49: 577-587.
- (11) Gutteridge J.M.C. (1992) Iron and oxygen radicals in brain. *Ann. Neurol.* 32: S16-21.
- (12) Hallgren B. and Sourander P. (1958) The effect of age on non-haem iron in the human brain. *J. Neurochem.* 3: 41-51.

Chapter 9

- (13) Halliwell B. (1993) Iron and damage to biomolecules. In: Iron and human disease (Ed: Lauffer R.B.), pp 209-236. CRC Press, Inc, Florida, Usa.
- (14) Hill J.M. and Switzer R.C. (1984) The regional distribution and cellular localization of iron in the rat brain. *Neurosci.* 11: 595-603.
- (15) Lamb D.J. and Leake D.S. (1994) Iron released from transferrin at acidic pH can catalyze the oxidation of low density lipoprotein. *FEBS Lett.* 352: 15-18.
- (16) LeBel C.P. and Bondy S.C. (1992) Oxidative damage and cerebral aging. *Prog. Neurobiol.* 38, 601-609.
- (17) Loeffler D.A., Connor J.R., Juneau P.A., Snijder B.S., Kanaley L., DeMaggio A.J., Nguyen H., Brickman C.M. and LeWitt P.A. (1995) Transferrin and iron in normal, Alzheimer's disease and Parkinson's disease brain regions. *J. Neurochem.* In Press.
- (18) Lohr J.B. (1991) Oxygen radicals and neuropsychiatric illness. *Arch. Gen. Psychiatry* 48: 1097-1106
- (19) Olanow C.W. (1990) Oxidation reactions in Parkinson's disease. *Neurology* 40, 32-37.
- (20) Oliver C.N., Starke-Reed P.E., Stadtman E.R., Liu G.J., Carney J.M. and Floyd R.A. (1990) Oxidative damage to brain proteins, loss of glutamine synthetase activity, and production of free radicals during ischemia/reperfusion-induced injury to gerbil brain. *Proc. Natl. Acad. Sci. USA* 87: 5144-5147.
- (21) Roskams A.J.I. and Connor J.R. (1994) Iron, transferrin, and ferritin in the rat brain during development and aging. *J. Neurochem.* 63: 709-716.
- (22) Saguaro N., Ikeda T., Saguaro C., Kohgo Y., Kato J. and Takeichi N. (1992) Regional distribution of copper, zinc and iron in the brain in Long-Evans Cinnamon rats with a new mutation causing hereditary hepatitis. *Brain Res.* 588: 278-290.
- (23) Smith C.D., Carney J.M., Starke-Reed P.E., Oliver C.N., Stadtman E.R., Floyd R.A. and Markesbery W.R. (1991) Excess brain protein oxidation and enzyme dysfunction in normal and Alzheimer's disease. *Proc. Natl. Acad. Sci. USA* 88, 10540-10543.
- (24) Smith C.D., Carney J.M., Tatsumo T., Stadtman E.R., Floyd R.A. and Markesbery W.R. (1992) Protein oxidation in aging brain. *Ann. N.Y. Acad. Sci.* 663: 110-119.
- (25) Subbarao K.V. and Richardson J.S. (1990) Iron-dependent peroxidation of rat brain: a regional study. *J. Neurosci. Res.* 26: 224-232.
- (26) Wallwork J.C., Milne D.B., Sims R.L. and Sandstead (1983) Severe zinc deficiency: effects on the distribution of nine elements (potassium, phosphorus, sodium, magnesium, calcium, iron, zinc, copper and manganese) in regions of the rat brain. *J. Nutr.* 113: 1895-

Iron and oxidative damage in aging in rat brain.

1905.

(27) Zaleska M.M. and Floyd R.A. (1985) Regional lipid peroxidation in rat brain in vitro: possible role of endogenous iron. *Neurochem. Res.* 10: 397-410.

CHAPTER 10

General discussion and conclusions.

Discussion and conclusions.

§ 10.0 Contents.

§ 10.1: Introduction.

§ 10.2: Experimental model.

§ 10.3: Isolation and culturing techniques.

§ 10.4: Transferrin receptor distribution.

§ 10.5: Endocytosis and transcytosis.

§ 10.6: Iron accumulation and susceptibility to oxidative stress.

§ 10.7: Conclusions.

§ 10.8: Future research.

§ 10.1 Introduction.

Iron is an essential element in the cellular metabolism and depletion will result in malfunction and eventually cell death. Under certain circumstances, however, iron may also have deleterious effects on the cell. As a transition metal, free or low molecular weight iron (see § 1.6) is capable of catalyzing the formation of reactive oxygen species, causing damage to cellular DNA, proteins and lipids alike. Due to a tightly regulated system of transport and storage, these noxious effects of iron are largely prevented.

In brain tissue, the margins between iron deficiency and iron overload are rather narrow. Although separated from the peripheral circulation by a highly selective barrier, brain tissue can be affected by both iron depletion and iron overload. Certain neurological diseases (e.g. Parkinson's disease) probably result from inappropriate intracerebral iron concentrations. Moreover, due to a high concentration of PUFA's and relatively low concentration of catalase, brain tissue is more susceptible to oxidative damage than most other tissues.

Although recent investigations have established the regional distribution of iron in the central nervous system, both mechanism and regulation of iron transport into the brain are to a large extent unknown. Considering the presence of transferrin receptors on the luminal surface of brain capillary endothelial cells, and the large surface area of the brain capillaries, it was assumed that these cells constitute the "porte d'entree" of iron into the brain. It was the purpose of this thesis to further investigate the mechanism and regulatory factors underlying this transport.

§ 10.2 Experimental model.

The first and most important limitation to this study was the availability of fresh brain tissue. Ideally, we would have liked to conduct our experiments on freshly isolated human blood-brain barrier endothelial cells. However, as there is - for obvious reasons - only a limited availability of fresh human brain tissue, our experimental aims would have been severely restricted. Based on the expert opinion of Professor Voogd from the department of Neuroanatomy and Professor Stefanko from the department of Pathological Anatomy, it was decided to use porcine brain tissue as an alternative. This choice was mainly based on the gross anatomical similarity between the human and porcine brain. Moreover, by courtesy of Mr van der Zon and co-workers of the Rotterdamse Varkensslachterij, we had a nearly endless supply of fresh porcine brain and other tissues at our disposal.

§ 10.3 Isolation and culturing techniques.

A number of techniques have been described to isolate blood-brain barrier endothelial cells (BBB-EC's). Most of these techniques yield very limited quantities of BBB-EC's and require repeated passaging of cells to obtain sufficient material for experimental purposes. However, with each cell division the odds of functional dedifferentiation in culture will increase (1). Since BBB-EC's are highly specialized barrier cells with a variety of selective transport mechanisms (e.g. transferrin receptors), it is conceivable that repeated passaging and concomitant dedifferentiation will affect or alter these mechanisms. In order to prevent (as much as possible) these effects, we only used primary cultures of BBB-EC's in our experiments with the exception of our morphological studies, in which we used first passage cells.

Moreover, BBB-EC's are a heterogeneous population of cells (8) and we observed that repeated passaging altered the appearance of the cultures. This is probably due to differences in growth pattern and division rate between the different subtypes of BBB-EC's. Since the BBB-EC subtypes found *in vitro* are a reflection of the heterogeneity of these cells *in vivo* (4), all subtypes should be included when investigating typical BBB-EC functions (e.g. transport). Our primary cultures of BBB-EC's fulfilled this requirement.

In general, working with living organisms and primary cultures increases the variability in

Discussion and conclusions.

experimental results. To minimize these adverse effects: (i) we performed all experiments in the same growth phase of the cultures, and (ii) we increased the number of measuring points per experiment (§ 5.5). Since none of the existing isolation techniques yielded sufficient quantities of BBB-EC's, we developed an isolation technique with a sufficient yield of viable BBB-EC's to meet our experimental requirements.

§ 10.4 Transferrin receptor distribution.

As shown in chapter 5, BBB-EC's grown under standard culture conditions display two distinct populations of transferrin receptors (TfR's): (i) those located on the outer cell membrane, and (ii) TfR's located within the cell. The latter group can be subdivided into a group of TfR's that actively participate in the endocytic cycle, and another group that appears to be quiescent (inactive TfR pool). We hypothesized that this quiescent group of TfR's constituted in fact a reserve pool of TfR's that could be activated if the intracellular iron requirements increased. Results in chapter 6 confirm this hypothesis inasmuch that the BBB-EC's grown under iron-depleted (Fe^-) conditions have significantly more surface bound and intracellular TfR's than cells grown under iron-enriched (Fe^+) conditions.

In neither Fe^+ nor Fe^- cultured BBB-EC's quiescent TfR's could be detected. In case of the Fe^- cultured cells it seemed that all TfR's from the quiescent pool were mobilized to participate in the endocytic cycle, thereby increasing the iron uptake capacity of the cell. However, the total amount of TfR's in the Fe^- cultured cells (i.e. culturing in deferoxamine-enriched medium) is far less than that of BBB-EC's grown under standard culture conditions (see chapter 5). Since neither the isolation procedure nor the total TfR quantitation assay were changed, we have no explanation for this discrepancy other than a possible (toxic) effect of deferoxamine. The decrease in total TfR's as found in the Fe^+ cultured cells can easily be explained in the light of the IRE-model (see § 1.3.1.5.1). Assuming that the IRE-regulatory mechanism is valid for BBB-EC's, high intracellular concentrations would suppress TfR synthesis and reduce the total number of TfR's.

However, we doubt whether the IRE-model is applicable to the BBB-EC iron metabolism. The IRE-model describes the interaction of a number of processes involved in the regulation of iron uptake and storage. The intracellular iron concentration has a pivotal role in this

process, basically steering the system by negative feedback. However, as discussed before, BBB-EC's probably participate in the transport of iron into the brain. Iron uptake by the BBB-EC may therefore fulfill the intracellular iron requirements of the BBB-EC itself, or those of other cell types in the brain. In the current concept of the IRE-model, a high intracellular iron concentration in BBB-EC's would reduce iron uptake and block iron transport to the brain, which might be in contrast with their main function. Our findings as described in chapter 6 and reports from *in vivo* observations (i.e. hemochromatosis), show that iron transport across the blood-brain barrier is at least partially iron concentration dependent.

§ 10.5 Endocytosis and transcytosis.

How does iron reach the brain? The limited number of studies on this subject have not yet elucidated the issue (3). On the contrary, although some investigators were able to trace peripherally administered transferrin (Tf) into the brain, others could not show transcytosis of Tf across the BBB-EC. This contradiction may result from differences in techniques applied in these investigations. Basically, three different techniques were used:

(i) *In vivo* experiments in which ^{125}I -labeled Tf was administered peripherally. Transferrin was indeed detected in the brain. However, these studies cannot exclude the possible "leakage" of Tf across those vesicles in the brain that lack a blood-brain barrier (see § 1.4).

(ii) An *in vitro* experiment in which BBB-EC's were grown on a porous membrane. Raub et al (6) used ^{125}I -labeled Tf to show that only a small percentage of Tf crossed the BBB-EC's. Again, intercellular leakage cannot be ruled out.

(iii) An experiment by Roberts et al (7) who used horse radish peroxidase labeled Tf. Once administered peripherally, it was traced within the BBB-EC's, although no evidence of transcytosis was found. In our opinion, the horse radish peroxidase-Tf coupling procedure might have yielded a high percentage of apo-Tf (discussed in chapter 7).

Our experiments, as described in chapter 6, show that BBB-EC's recycle Tf through receptor mediated endocytosis with recycling kinetics that are in agreement with those found in other cell types. However, up to 40% of the internalized Tf was not returned to the luminal surface within 1 hour ($\pm 4 \times T_{\text{out}}$), indicating that some Tf molecules may be routed differently (i.e. may be transcytosed). In support of this view, our morphological

Discussion and conclusions.

experiments with gold-labeled Tf are suggestive for a transcytotic pathway through the BBB-EC. Electron micrographs revealed that: (i) gold-labeled Tf at the luminal membrane was located within coated pits, and (ii) addition of unlabeled diferric Tf completely blocked the binding and uptake of gold-labeled Tf. Combining (i) and (ii) we presume that nonspecific fluid phase endocytosis of gold labeled Tf is not a major mechanism (see chapter 7).

We also showed that BBB-EC's can take up as well as release iron, even though iron uptake was considerably faster than iron release (see chapter 6).

Together, these findings suggest that both receptor mediated endocytosis and receptor mediated transcytosis occur within the BBB-EC, although we are not sure if and to what extent these processes are coupled. Indirect evidence of the transcytotic process was provided by Pardridge (see chapter 7), who showed that small pharmaceutical compounds coupled to OX-26 (anti-TfR immunoglobulins) could be retrieved within the brain compartment.

However, the issue of iron transport into the brain has not been solved yet. We still have to quantify Tf transcytosis through the BBB-EC. Based on the results of iron accumulation versus iron release, we estimate that transcytosis of Tf is relatively low when compared to receptor mediated endocytosis. Since the pathway of iron becomes obscure once it is released from Tf in the endosome, we cannot exclude the possibility of yet another iron transport mechanism in the BBB-EC. On the other hand, we may have underestimated the release of iron from the BBB-EC. Our BBB-EC cultures are devoid of astrocytes, with which they are closely related *in vivo*. Recent studies with co-cultures of BBB-EC's and astrocytes showed that these astrocytes affect the barrier characteristics of BBB-EC's. It is therefore conceivable that astrocytes influence or even participate in the iron transport process.

§ 10.6 Iron accumulation and susceptibility to oxidative stress.

The prevalence of neurological diseases in which iron is implicated (e.g. Parkinson's disease), increases with age. As shown in chapter 9, the intracerebral iron concentration increases with age. The question is: are these two phenomena related? One might speculate

Chapter 10

that certain neurological diseases are caused by a disturbance in the storage of iron, or that once a threshold level has been reached cells become intoxicated by iron. However, even more important is the question why the intracerebral iron concentration increases with age. It seems unlikely that an aged brain would require more iron, considering that both metabolic rates and absolute cell number decrease with age. In our opinion, the age related increase in cerebral iron concentration is a result of an increased blood-brain barrier permeability, if not an increase in blood-brain barrier damage.

In general, age related changes have been attributed to an increase in oxidative damage and there is no reason to assume the blood-brain barrier would be spared. On the contrary, as argued by Betz (2) (see also chapter 8) the BBB-EC is in fact a likely site for oxidative damage to occur. Oxidative damage may occur if two conditions are met: (i) the presence of reactive oxygen species (e.g. superoxide), and (ii) the presence of transition metals (e.g. iron). Xanthine oxidase, monoamine oxidase and mitochondria have been implied in the synthesis of reactive oxygen species, and all are abundantly present in the BBB-EC. As for transition metals i.c. iron, most intracellular iron is stored in transferrin and ferritin and therefore unable to exert its catalytic role in the formation of reactive oxygen species (e.g. hydroxyl radical). On the other hand, free (or LMW) iron can readily participate in the formation of reactive oxygen species. It would therefore seem that the "mobile" LMW or free iron pool, rather than the total iron concentration, will increase the susceptibility of the BBB-EC's to oxidative stress.

It was Lauffer (5) who recently stated that people of the "Western worlds" are at risk to develop diseases related to an increased iron concentration. A high dietary intake of iron-rich animal proteins (see chapter 1) without a concomitant increase in iron loss would cause an elevated iron flux and could render us more susceptible to oxidative damage. As shown in chapter 8, BBB-EC's grown under Fe^+ conditions are more susceptible to oxidative stress than Fe^- cells. This is in support of our experiments in chapter 6, showing that Fe^+ BBB-EC's accumulate and release more iron than their Fe^- counterparts. It is conceivable that a prolonged high dietary intake iron intake would lead to an increase in iron metabolism in the BBB-EC's. This in turn would lead to a longlasting increase in oxidative stress which might affect these highly specialized barrier cells. This is in agreement with the histochemical results of chapter 8, showing that Fe^+ grown BBB-EC's -

Discussion and conclusions.

even without exposure to an oxidizing system- seem to have more protein carbonyl groups than their the Fe⁺ cultured cells. Moreover, this increase in protein carbonyl groups (as indicator for increased oxidative damage) appears to be focussed in the plasma membrane of these cells.

Experimental results in chapter 9 show that although there is a general increase in cerebral iron concentration with age, there is no concomitant increase in protein carbonyl groups. We attributed this to a protective effect of ferritin, which increased concomitantly with the iron concentration. On the other hand, it might also be a species (i.e. rat) related phenomenon, since other studies have shown that human brain tissue displays an increase in lipid peroxidation products with age.

Evidence of increased susceptibility to oxidative stress *in vitro* is not yet proof for an increased permeability of the blood-brain barrier to iron *in vivo*. Nevertheless, we suggest that *in vivo* an elevated peripheral iron concentration may contribute to an increase in cerebral iron concentration. This may be due either to blood-brain barrier leakage as a result of oxidative damage (chapter 8), or to an iron concentration dependent increase in iron uptake (as shown in chapter 6).

§ 10.7 Conclusions.

Based on the experimental results presented in this thesis, we conclude that:

- (i) BBB-EC's participate in the transport of iron to the brain, although the mechanism(s) have not yet been completely elucidated.
- (ii) Receptor mediated endocytosis of Tf takes places at the luminal membrane of the BBB-EC, and internalization as well as externalization rate constants are similar to those found in other cell types.
- (iii) BBB-EC's can both accumulate and release iron. This process partly depends on the peripheral iron concentration: Fe⁺ cultured BBB-EC's accumulate more iron than Fe⁻ cultured cells.
- (iv) Receptor mediated transcytosis of Tf -as based on ultrastructural evidence- may occur within the BBB-EC as part of the total iron transport mechanism.
- (v) BBB-EC's grown in iron-enriched culture medium are more susceptible to oxidative

stress compared to iron-depleted cells. In fact, even without being exposed to an oxidizing system, Fe⁺ grown BBB-EC's display minor histochemical changes.

(vi) Age related intracerebral iron increase will not always lead to an increase in oxidative damage. A protective effect of ferritin, or a species related difference in susceptibility might be of influence.

§ 10.8 Future research.

As always, experimental results yield more questions than answers. In general, this thesis describes certain aspects of the iron transport into -and possibly through- the BBB-EC. Unfortunately, we have not been able to elucidate the intracellular pathway of iron within these cells. Over the years, the issue of iron transport into the brain has been debated without reaching a conclusion and additional work will be needed to solve this enigma.

Based on our findings, we propose that future research in this field should include:

- (i) Confirmation and quantification of receptor mediated transcytosis of Tf through the BBB-EC.
- (ii) Studies on the iron uptake and release of BBB-EC's co-cultured with astrocytes.
- (iii) Further investigations into the regulation of iron metabolism in the BBB-EC. Is the IRE-model applicable to this process?
- (iv) In vivo quantification of oxidative modifications of BBB-EC's. What effects of prolonged increase in peripheral iron concentration (e.g. hemochromatosis) can be observed at the blood-brain barrier? Is age and/or disease related cerebral iron increase a cause or a result of changes in blood-brain barrier permeability?

Discussion and conclusions.

References.

- (1) Abbott N.J., Hughes C.C.W., Revest P.A. and Greenwood J. (1992) Development and characterization of a rat brain capillary endothelial culture: towards an in vitro blood-brain barrier. *J. Cell Sci.* 103: 23-37.
- (2) Betz A.L. (1993) Oxygen free radicals and the brain microvasculature. In: *The Blood-brain barrier. Cellular and molecular biology.* (Ed: Pardridge W.M.), pp 303-321. Raven Press, New York, USA.
- (3) Friden P.M. (1993) Receptor-mediated transport of peptides and proteins across the blood-brain barrier. In: *The Blood-brain barrier. Cellular and molecular biology.* (Ed: Pardridge W.M.), pp 229-247. Raven Press, New York, USA.
- (4) Joó F. (1992) The cerebral microvessels in culture, an update. *J. Neurochem.* 58: 1-17.
- (5) Lauffer R.B. Iron, aging, and human disease: historical background and new hypotheses. In: *Iron and human disease.* (Ed: Lauffer R.B.), pp 1-20. CRC Press, Inc, Boca Raton, FL, USA.
- (6) Raub T.J. and Newton C.R. (1991) Recycling kinetics and transcytosis of transferrin in primary cultures of bovine brain microvessel endothelial cells. *J. Cell. Physiol.* 149: 141-151.
- (7) Roberts R.L., Fine R.E. and Sandra A. (1993) Receptor-mediated endocytosis of transferrin at the blood-brain barrier. *J. Cell Sci.* 104: 521-532.
- (8) Rupnick M.A., Carey A. and Williams S.K. (1988) Phenotypic diversity in cultured cerebral microvascular endothelial cells. *In vitro Cell Dev. Biol.* 24: 435-444.

CHAPTER 11

Summary - samenvatting.

Summary - samenvatting.

§ 11.0 Contents.

§ 11.1: Summary.

§ 11.2: Samenvatting.

§ 11.1 Summary.

Iron is a trace element vital to nearly all living organisms. However, in certain circumstances iron may also have deleterious effects. This duality is clearly displayed in brain tissue. A decrease in cerebral iron concentration is associated with reduced cognitive functions, whereas an increase in iron concentration can be found with age and in a number of neurological diseases (e.g. Parkinson's disease). Although recent studies did establish the overall distribution of iron in the brain, the mechanism and regulation of iron transport into the brain are largely unknown.

Brain tissue is separated from the peripheral circulation by the blood-brain barrier, a highly selective barrier that controls the transport of most solutes into and out of the brain. The endothelial cells that constitute this barrier display a large number of transferrin receptors on their luminal cell surface, suggesting that these cells are involved in the transport of iron into the brain.

This thesis describes the results of a study on the mechanism and regulatory aspects of iron transport across the blood-brain barrier endothelial cells. During our investigations, the following issues were addressed:

- (i) Can iron enter the brain via the blood-brain barrier endothelial cells?
- (ii) Which mechanism is responsible for the transport of iron across the blood-brain barrier?
- (iii) Does the blood-brain barrier endothelial cell adjust its iron metabolism in response to changes in the extracellular iron concentration?
- (iv) To what extent will high iron concentrations affect the structure and function of the blood-brain barrier endothelial cell?

Chapter 11

Chapter 1:

This chapter summarizes the current views on:

- (i) Function and distribution of iron.
- (ii) Mechanisms of iron uptake and storage.
- (iii) Regulatory aspects of iron uptake.
- (iv) Structure and function of the blood-brain barrier.
- (v) Iron uptake, storage and distribution in the brain.
- (vi) Iron and oxidative damage.

Chapter 2:

All techniques that contributed to the experimental results presented in this thesis, are described in this chapter.

Chapter 3:

For our experiments, we required porcine transferrin with a high ($\geq 99\%$) degree of purity. This chapter describes the isolation, purification and structural characterization of porcine transferrin and hemopexin.

Chapter 4:

Ferritin is the major iron storage protein in mammalian tissues. In native polyacrylamide gel electrophoresis purified ferritins from different species all yielded two distinct bands, 440 and 660 kDa respectively. In this chapter we summarize the results of the isolation, purification and partial characterization of the two porcine ferritins.

Chapter 5:

In this chapter we describe a high yield isolation procedure to obtain from fresh porcine brain tissue nearly pure (as tested with anti Von Willebrand factor immunoglobulins) batches of blood-brain barrier endothelial cells. Furthermore, we investigated the distribution of transferrin receptors in primary cultures of these cells. Three different transferrin receptor pools were detected and quantified.

In addition, the results of a standard biochemical technique to assess nonspecific binding

Summary - samenvatting.

of transferrin were compared to estimates of nonspecific binding derived from a nonlinear curvefit analysis of the experimental data.

Chapter 6:

To test whether blood-brain barrier endothelial cells adjust their iron metabolism in response to variations in the extracellular iron concentrations, primary cultures were subjected to either iron-enriched or iron-depleted culture conditions. This chapter gives an overview of the effects of changes in extracellular iron concentration on: (i) numbers of surface bound and intracellular transferrin receptors, (ii) rate constants of transferrin receptor internalization and externalization, and (iii) rates of iron accumulation and release. It is shown that despite a down regulation of surface and total transferrin receptor numbers, the rates of iron accumulation and release are related to the extracellular iron concentration.

Chapter 7:

Primary and first passage cultures of blood-brain barrier endothelial cells were grown on various types of porous membranes. In this chapter we demonstrate that the ultrastructural appearance of these cells was similar on all membrane types. Minor differences were observed between cells derived from either primary or first passage cultures.

In addition we describe the results of histochemical experiments with first passage blood-brain barrier endothelial cells incubated with 6.6 nm gold-labeled transferrin. The pathway of these gold-transferrin conjugates within and through the cell is visualized by means of electron microscopy. Results are suggestive for a receptor mediated transcytosis of transferrin through the blood-brain barrier endothelial cell.

Chapter 8:

Since blood-brain barrier endothelial cells grown under iron-enriched conditions accumulate more iron than cells grown under iron-depleted conditions, we hypothesized that iron-enriched grown cells are more susceptible to oxidative stress. In this chapter, a new immunochemical technique is presented to visualize the amount of oxidative damage in cell cultures. As described, both biochemical and immunochemical experiments show that iron-enriched cultured cells are more susceptible to oxidative stress.

Chapter 11

In addition we measured the adherence of granulocytes to the blood-brain barrier endothelial cells following 2 hours of ischaemia and a 5 min period of reoxygenation. Results show that the adherence of granulocytes to cells grown in iron-enriched cultures is reduced. A suppressive effect of increased intracellular iron concentration on phospholipase A₂ is speculated.

Chapter 9:

As known from studies in human brain tissue, both the iron concentration and the concentration of products resulting from oxidative damage increase with age. In this chapter we show that 24 month old rats display a significant increase in total iron and ferritin concentration in several brain regions when compared to 4 month old rats. However, oxidative damage as assessed by the amount of protein carbonyl groups, did not increase concomitantly. This is attributed to a protective effect of the increase in ferritin and/or a species related difference in susceptibility to oxidative stress.

Chapter 10:

In this chapter we consider the results of previous chapters in relation to their significance in vivo. Although recent studies have shown that certain neurological diseases are accompanied by high intracerebral iron concentrations, to date there is only limited knowledge on the role of the blood-brain barrier in these processes. Our results indicate that high peripheral iron concentrations may affect the intracerebral iron concentration both directly (uptake and release related to the iron concentration) and indirectly (increased susceptibility to oxidative stress).

Summary - samenvatting.

§ 11.2 Samenvatting.

Ijzer is als spore-element van levensbelang voor bijna alle levende organismen. In bepaalde omstandigheden kan ijzer echter ook schadelijke effecten hebben. Dit dualisme komt duidelijk naar voren in de hersenen. Er is een associatie tussen een verlaagde ijzerconcentratie in de hersenen en afgenomen cognitieve functies, terwijl een verhoogde ijzerconcentratie gevonden kan worden bij veroudering en bij een aantal neurologische aandoeningen (bijv. ziekte van Parkinson).

Hoewel recente studies een duidelijk beeld hebben opgeleverd van de ijzerverdeling in de hersenen, is er nog niet veel bekend over het transport van ijzer naar de hersenen en de wijze waarop dit geregeld wordt. Hersenweefsel is van de perifere circulatie gescheiden door de bloed-hersen barrière. Deze zeer selectieve barrière regelt het transport van de meeste wateroplosbare stoffen van en naar het hersenweefsel. De feitelijke barrière wordt gevormd door endotheel cellen die de wanden van de capillairen in de hersenen bekleeden. Deze cellen bevatten een groot aantal transferrine receptoren op het lumenale celoppervlak, hetgeen erop zou kunnen duiden dat de bloed-hersen barrière endotheel cellen betrokken zijn bij het ijzer transport naar de hersenen.

Dit proefschrift beschrijft de resultaten van een onderzoek naar het mechanisme van het ijzertransport naar de hersenen via de bloed-hersen barrière endotheel cellen. In ons onderzoek komen de volgende vraagstukken aan de orde:

- (i) Kan ijzer de hersenen bereiken via de endotheel cellen van de bloed-hersen barrière?
- (ii) Welk mechanisme is verantwoordelijk voor het transport van ijzer over de bloed-hersen barrière?
- (iii) Past de bloed-hersen barrière endotheel cel zijn ijzermetabolisme aan onder invloed van veranderingen in de extracellulaire ijzerconcentratie?
- (iv) In hoeverre worden de structuur en functie van de bloed-hersen barrière endotheel cel aangetast door hoge ijzerconcentraties?

Hoofdstuk 1:

In dit hoofdstuk worden de huidige inzichten over de volgende onderwerpen samengevat:

- (i) Functie en verdeling van ijzer in het lichaam.
- (ii) Mechanismen voor ijzeropname en opslag.

Chapter 11

- (iii) Regulatie van ijzeropname.
- (iv) Structuur en functie van de bloed hersen barriere.
- (v) Opname, opslag en verdeling van ijzer in de hersenen.
- (vi) IJzer en oxidatieve schade.

Hoofdstuk 2:

In dit hoofdstuk worden alle technieken beschreven die een rol gespeeld hebben bij de totstandkoming van dit proefschrift.

Hoofdstuk 3:

Zeer zuiver ($\geq 99\%$) varkenstransferrine was voor onze experimenten een absolute noodzaak. Dit hoofdstuk beschrijft de isolatie, zuivering en karakterisering van de structuur van varkenstransferrine en -hemopexine.

Hoofdstuk 4:

Ferritine is het belangrijkste eiwit voor de ijzer opslag in zoogdieren. Gezuiverd ferritine van verschillende diersoorten bleek in natieve palyacrylamide gel electroforese twee aparte banden te geven, met een molecuul massa van respectievelijk 440 en 660 kDa. Dit hoofdstuk vat de resultaten samen van de isolatie, zuivering en gedeeltelijke karakterisering van de twee subtypen varkensferritine.

Hoofdstuk 5:

In dit hoofdstuk beschrijven we de isolatie van bloed-hersen barriere endotheel cellen uit vers hersenweefsel. De procedure zoals beschreven gaf een hoge opbrengst aan cellen van dit type. Verontreiniging met andere celtypen was miniem, zoals bleek uit testen met immunoglobulinen gericht tegen de Von Willebrand factor.

In primaire kweken van bloed-hersen barriere endotheel cellen onderzochten we voorts het voorkomen en de verdeling van transferrine receptoren. Drie verschillende transferrine receptor "pools" konden worden onderscheiden, die elk werden gekwantificeerd.

De resultaten van de receptor-bindingsexperimenten werden geanalyseerd met behulp van een wiskundig computerprogramma. De aldus verkregen schatting van de specifieke

Summary - samenvatting.

binding werd vergeleken met het resultaat verkregen uit standaard biochemische technieken.

Hoofdstuk 6:

Primaire cellijnen werden gekweekt in ijzerverrijkt of ijzerarm medium om te onderzoeken of bloed-hersen barrière endotheel cellen hun ijzermetabolisme aanpassen onder invloed van veranderingen in de ijzerconcentratie. Dit hoofdstuk geeft een overzicht van de effecten die veranderingen in de extracellulaire ijzerconcentratie hebben op: (i) het aantal transferrine receptoren in de cel en de aan het celoppervlak gebonden receptoren, (ii) de snelheid van endocytose en exocytose van de transferrine receptor en (iii) de snelheid waarmee en de mate waarin ijzer gestapeld en afgegeven wordt.

We laten zien dat, ondanks een afname zowel in het aantal oppervlakte receptoren als in het totaal aantal transferrine receptoren, de mate van ijzerstapeling en ijzerafgifte afhankelijk is van de extracellulaire ijzerconcentratie.

Hoofdstuk 7:

Primaire en eerste passage cultures van bloed-hersen barrière endotheel cellen werden gekweekt op verschillende soorten poreuze membranen. Zoals dit hoofdstuk laat zien, is de ultrastructurele morfologie van deze cellen onafhankelijk van het type membraan waarop gekweekt is. We zagen slechts kleine verschillen in ultrastructuur tussen cellen in primaire cultures en na één passage.

Verder beschrijven we de resultaten van experimenten met eerste passage bloed-hersen barrière endotheel cellen geïncubeerd met 6,6 nm goud gelabeld transferrine. Met behulp van het elektronenmicroscop werd de weg die dit goud-transferrine complex aflegt in de cel zichtbaar gemaakt. De resultaten suggereren dat receptor gemedieerde transcytose van transferrine door de bloed-hersen barrière endotheel cel kan plaats vinden.

Hoofdstuk 8:

We veronderstelden dat ijzerverrijkt gekweekte bloed-hersen barrière endotheel cellen gevoeliger zijn voor oxidatieve stress, omdat deze cellen meer ijzer stapelen dan cellen die in ijzerarme omstandigheden gekweekt werden. In dit hoofdstuk wordt een nieuwe

Chapter 11

immunochemische techniek beschreven om het verschil in oxidatieve schade in celkweken zichtbaar te maken. Zoals aangetoond in zowel biochemische als immunochemische experimenten blijken cellen gekweekt in ijzerverrijkte omstandigheden inderdaad gevoeliger voor oxidatieve stress.

Daarnaast werd de hechting van granulocyten aan de bloed-hersen barrière endotheel cellen gemeten. In deze experimenten werden de cellen gedurende twee uur aan ischaemie en vervolgens 5 minuten aan reoxygenatie blootgesteld. De resultaten laten zien dat de hechting van granulocyten aan die cellen, die gekweekt zijn in ijzerverrijkte omstandigheden, verlaagd is. Mogelijk is deze verminderde hechting te wijten aan het feit dat een hoge intracellulaire ijzerconcentratie de activiteit van het fosfolipase A₂ kan onderdrukken.

Hoofdstuk 9:

Onderzoeken in humaan hersenweefsel tonen aan dat de concentratie zowel van ijzer als van producten die ontstaan door oxidatieve schade toenemen met de leeftijd. In dit hoofdstuk vergelijken we 24 maanden oude ratten met 4 maanden oude soortgenoten. De oudere ratten vertonen een duidelijke toename van zowel de totaal ijzer als de ferritine concentratie in enkele gebieden in de hersenen. De mate van oxidatieve schade, vastgesteld aan de hand van de hoeveelheid carbonyl groepen in eiwitten, nam echter niet evenredig hiermee toe. Dit effect is mogelijk het gevolg van een beschermende werking van het ferritine, ofwel een species gerelateerd verschil in gevoeligheid voor oxidatieve stress.

Hoofdstuk 10:

In dit hoofdstuk overwegen we de implicaties van de resultaten van ons in vitro onderzoek voor de situatie in vivo. Hoewel recente onderzoeken hebben aangetoond, dat bepaalde neurologische aandoeningen gepaard gaan met hoge ijzerconcentraties in de hersenen, is er tot op heden slechts weinig bekend over de rol van de bloed-hersen barrière in dit verband. We concluderen uit onze resultaten dat hoge concentraties perifeer ijzer van invloed kunnen zijn op de ijzerconcentratie in de hersenen, zowel direct (opname en afgifte gerelateerd aan de ijzerconcentratie) als indirect (toegenomen gevoeligheid voor oxidatieve stress).

Summary - samenvatting.

Publications.

Articles:

Van Gelder W., Siersema P.D., Voogd A., de Jeu-Jaspars N.C.M., van Eik H.G., Koster J.F., de Rooy F.W.M. and Wilson J.H.P. (1993) The effect of desferrioxamine on iron metabolism and lipid peroxidation in hepatocytes of C57BL/10 mice in experimental uroporphyrin. *Biochem. Pharmacol.* 46: 221-228.

Segerer H., van Gelder W., Angenent F.W.M., van Woerkens L.J.P.M., Curstedt T., Obladen M. and Lachmann B. (1993) Pulmonary distribution and efficacy of exogenous surfactant in lung-lavaged rabbits are influenced by the instillation technique. *Pediat. Res.* 34: 490-494.

Van Gelder W., Huijskes-Heins M.I.E., Klepper D., van Noort W.L., Cleton-Soeteman M.I. and van Eijk H.G. (1994) Isolation and partial characterization of a 440 kDa and a 660 kDa porcine spleen ferritin fraction. Submitted.

Segerer H., van 't Veen A., van Gelder W., Gommers D., Robertson B., Obladen B. and Lachmann B. (1994) Pulmonary efficacy and distribution of multiple fractional doses of exogenous surfactant versus one bolus in an animal model of surfactant deficiency. Submitted.

Van Gelder W., Huijskes-Heins M.I.E., Hukshorn C.J., de Jeu-Jaspars C.M.H., van Noort W.L. and van Eijk H.G. (1995) Isolation, purification and characterization of porcine serum transferrin and hemopexin. *Comp. Biochem. Physiol.* 111B: 171-179.

Van Gelder W., Huijskes-Heins M.I.E., van Dijk J.P., Cleton-Soeteman M.I. and van Eijk H.G. (1995) Quantification of different transferrin receptor pools in primary cultures of porcine blood-brain barrier endothelial cells. *J. Neurochem.* 64: 2708-2715.

Van Gelder W., Huijskes-Heins M.I.E., Cleton-Soeteman M.I., van Dijk J.P. and van Eijk H.G. (1995) Regulatory aspects of iron uptake in blood-brain barrier endothelial cells cultured in either iron-depleted or iron-enriched media. Submitted.

Van Gelder W., Huijskes-Heins M.I.E., Cleton-Soeteman M.I., van Run P.r.W.A., de Bruijn W.C. and van Eijk H.G. (1995) Transcytosis of 6.6 nm gold-labeled transferrin: an ultrastructural study in blood-brain barrier endothelial cells. Submitted.

Van Gelder W., Huijskes-Heins M.I.E., Cleton-Soeteman M.I., Connor J.R. and van Eijk H.G. (1995) A new approach to visualize and quantify the susceptibility to oxidative stress in cultured blood-brain barrier endothelial cells. A 2,4 dinitrophenyl hydrazine assay in iron-enriched and iron-depleted cultures. Submitted.

Focht S.J., Snijder B.S., Beard J.L., van Gelder W., Williams L.R. and Connor J.R. (1995)

Chapter 11

Effects of aging on the regional distribution of iron, transferrin, ferritin, and oxidatively modified proteins in rat brains. Submitted.

Abstracts.

Van Gelder W., Siersema P.D., Voogd A., de Jeu-Jaspars C.M.H., Koster J.F., van Eijk H.G. and Wilson J.H.P. (1992) Iron induced porphyria in inbred mice: a possible role for lipid peroxidation. International meeting on porphyrin metabolism and iron metabolism. Papendal, The Netherlands.

Voogd A., van Gelder W., van Eijk H.G and Koster J.F. (1992) A novel approach to determine intracellular low molecular weight iron. International meeting on porphyrin metabolism and iron metabolism. Papendal, The Netherlands.

Seegerer H., van Gelder W., Curstedt T., Obladen M. and Lachmann B. (1992) Poor response after tracheal infusion of curosurf (CS) in rabbits. 7th International workshop on surfactant replacement. San Sebastian, Spain.

Hulet S.W., Snijder B.S., Powers S., van Gelder W. and Connor J.R. (1994) An in vitro model to study the relationship between iron and protein oxidative modification. Society for Neuroscience, 1994 Annual meeting. Miami Beach, Florida, USA.

Van Gelder W., Huijskes-Heins M.I.E., Cleton-Soeteman M.I. and van Eijk H.G. (1995) Regulatory aspects of iron transport across the blood-brain barrier. European Iron Club 1995. Hamburg, Germany.

Cleton-Soeteman M.I., van Gelder W., van Run P.R.W.A. and van Eijk H.G. (1995) Blood-brain barrier microvascular endothelial cells: ultrastructure and evidence of transcytosis of gold-labeled transferrin. European Iron Club 1995. Hamburg, Germany.

Summary - samenvatting.

Dankwoord.

Dit proefschrift kwam tot stand met de hulp van velen en ik wil op deze plaats dan ook graag iedereen bedanken die er zijn of haar steentje aan heeft bijgedragen. Zonder deze "velen" tekort te willen doen, zijn er een aantal mensen die ik met name wil bedanken voor hun inzet en steun.

Henk, hooggeleerde promotor, je stond altijd klaar met goede raad als een experiment niet wilde lukken, of de kinderen weer eens slecht geslapen hadden. Je inzet voor studenten en AIO's kent zijn weerga niet en krijgt -ten onrechte- niet de waardering die het verdient. Ik zie uit naar de concerten die we gezamenlijk nog zullen bezoeken.

Maud, je kritische blik en vermogen tot helder formuleren hebben dit proefschrift (hopelijk) tot een begrijpelijk geheel gemaakt. Met veel genoeg denk ik terug aan het "thuiswerken" in Stolwijk en ik hoop het nog vaak te bezoeken (maar dan niet om te werken).

Marja, zonder jou had ik al dit werk niet kunnen doen. Je onvermoeibare inzet -ook buiten kantooruren- je efficiënte werkwijze en oog voor details laten zich alleen met superlatieven beschrijven. Ik zal onze "ontbijten" missen, ook al liggen varkenshersenen soms wat zwaar op de maag.

Prof. Koster, Hans, om de een of andere reden liepen onze gesprekken altijd uit en was het eigenlijke onderwerp al snel uit het oog verloren. Je brede kennis en belangstelling, alsmede je kritische kijk op experimentele procedures en resultaten hebben me vaak op de goede weg geholpen, of de relativiteit van mijn inspanningen laten zien.

Hans van Dijk, aan jou dank ik mijn inzichten op het gebied van de receptor kinetiek en niet-lineaire curvefits. Nel (leerde mij pipetteren), Wim, Martin, Linda en Ben dank ik voor alle hulp en gezelligheid in de afgelopen jaren. Mijn collega-AIO's Peter en Christel wens ik veel sterkte en Peter, nu heb je eindelijk wat rust op het lab.

De leden van de lezerscommissie dank ik voor de snelle beoordeling van het manuscript. Ashraf en Chris dank ik voor al het werk wat ze voor mij gedaan hebben en ik wens ze succes met hun verdere carrière. Peter van Run, Tar van Os en Ann Langeveld dank ik voor de mooie "plaatjes" die dit proefschrift sieren.

Dhr van der Zon, John, Kees, Cor (Plukkie), Marcel, Hans en vele anderen van de

Chapter 11

Rotterdamse varkensslachterij dank ik voor al die keren dat ze mij vers varkenshersenweefsel gaven.

Dr Connor, Jim, I would like to thank you for your hospitality and support during my stay at your lab. Hopefully, we'll meet next year.

De meeste dank ben ik echter verschuldigd aan mijn vrouw Wilma. Je onvoorwaardelijke steun en begrip, als de cellen weer eens eten moesten hebben of een experiment wat uitliep, hebben het mij mogelijk gemaakt dit onderzoek te verrichten. Dit proefschrift draag ik dan ook op aan jou en onze beide zoons, Jasper en Bart.

Summary - samenvatting.

Curriculum vitae.

Warry van Gelder werd geboren op 23 September 1958 te Valkenburg-Houthem. Na het behalen van het diploma Gymnasium β in 1977 aan het Rooms Katholiek Gymnasium Juvenaat 't Heilig Hart te Bergen op Zoom, volgde een periode van zeven jaar waarin hij vijf keer "uitlootte" voor de studie geneeskunde. Vanaf 1984 studeerde hij geneeskunde aan de Erasmus Universiteit te Rotterdam, alwaar hij in 1991 zijn artsexamen haalde (cum laude). Keuze-onderzoek verrichtte hij op de afdeling Biomedische Technologie aan een computermodel dat de transportprocessen van elektrolyten over de dialysemembranen bij hemodialyse beschrijft en op de afdeling Chemische Pathologie aan de relatie tussen ijzer, oxydatieve schade en het ontstaan van porphyrie bij C57BL/10 muizen. Voor zijn studieresultaten ontving hij de studieprijz van het Bataafsch Genootschap der Proefondervindelijke Wijsbegeerte.

Direct na het behalen van zijn artsexamen trad hij als AIO in dienst bij Prof. Dr. H.G. van Eijk op de afdeling Chemische Pathologie en verrichtte onderzoek naar het transport van ijzer over de bloed-hersen barrière. Hij volgde cursussen op het gebied van cel- en weefselkweek (Boerhave cursus), transportprocessen over biomembranen (Masterclass Utrecht), wetenschapsfilosofie en engels (Rotterdam).

Naast zijn onderzoek was hij als docent verbonden aan de School voor Gezondheidszorg te Rotterdam, examinator bij het Oranje Kruis, vervulde hij het voorzitterschap van de MAIOR (medische Aio/Oio's Rotterdam), was hij lid van verschillende onderwijscommissies en bestuurslid van het Rode Kruis afdeling Dordrecht.

Vanaf 1 September 1995 volgt hij de opleiding tot laboratoriumarts bij Dr. R. B. Dinkelaar in het Drechtsteden Ziekenhuis te Dordrecht.

